STION ENGINES
AND THERMODYNAMICS

TUG
GRAZ UNIVERSITY
OF TECHNOLOGY
Erzherzog-Johann-Universität

Simulation of Real World Vehicle Exhaust Emissions

Submitted to obtain the postdoctoral qualification by

(eingereicht als Habilitationsschrift von)

Stefan Hausberger

December 2002

Preface

Impacts of the transport sector on the air quality and its share on the greenhouse gas emissions as well as methods for reducing negative environmental effects have been subject of research for decades. Main goals are the improvement of vehicles and engines - performed by the manufacturers - and the assessment of effects of different technological and political measures - usually performed by independent laboratories.

I elaborated several studies on these tasks during my career at the Institute for Internal Combustion Engines and Thermodynamics at the Technical University of Graz. In the course of my work I came to the conclusion that the quality of the results of this field of research very much depends on the quality of the basic data being available in the emission performance of vehicles. While emissions in the type approval tests are a well defined value, the assessment of the emission behaviour of vehicles in real world driving is more complex and does not follow standardized procedures.

Since I am leading different national and international projects related to this topic, I decided to write a paper which ought to give an overview on the actual status of measurement programmes and simulation tools for the calculation of the emission levels of vehicles in real world traffic situations. I hope this paper will give the colleagues working at this topic some new ideas and results and that readers who are mainly interested in the resulting emission values will get some insight into the methods used for emission simulation and into the related uncertainties.

The realisation of the projects on which this paper is based was supported by the very engaged work of the employees of the unit "Emissions" which I have been leading since 1998. For their assistance I especially want to thank Dieter Engler, Jürgen Blassnegger, Mario Ivanisin, Martin Rexeis, Micheal Zallinger, Thomas Vuckovic, Edim Bukvarevic and Gerald Mair. I also want to thank all employees of the Institute for Internal Combustion Engines and Thermodynamics as well as all partners from the international projects D.A.CH., ARTEMIS, PARTICULATE and COST 346 and from all the national projects we performed for the stimulating cooperation.

I want to address special thanks to Prof. Pischinger who always supported my work and allowed the very positive work climate at our institute and to Prof. Eichlseder who very successfully continues Prof. Pischinger´s work as head of the Institute.

Graz, December 2002 Stefan Hausberger

CONTENT

Abbreviations

a ..... Acceleration [m/s^2]

DPF..... Diesel particulate filter

EGR..... Exhaust gas recirculation

ESC..... European Stationary Cycle

ETC ..... European Transient Cycle

HDV ..... Heavy duty vehicle (> 3.5 t maximum allowed gross weight)

LGV..... Light gods vehicle (< 3.5 t maximum allowed gross weight)

M_d..... (Engine-) Torque [Nm]

n..... Engine speed [rpm]

n_norm ..... Normalized engine speed (idling = 0%, rated engine speed = 100%)

NEDC ..... New European Driving Cycle. Test cycle for cars

Pc..... Passenger car (< 3.5 t maximum allowed gross weight)

ppm..... Parts per million

rpm ..... Engine speed in revolutions per minute

SCR ..... Selective catalytic reduction

SI engine..... Spark ignition engine (Otto engine)

v..... velocity [m/s]

λ..... Lambda value [-]

1 Introduction

Transport emissions have been subject of health concerns for many years. While the traffic volume steadily increased the total traffic related toxic emissions were reduced or at least were kept stable over the last two decades within Europe.

Impressive reductions were achieved for CO and HC while particulate emissions and NO_x showed a rather stable trend in recent years (Figure 1). Energy consumption and CO_2 emissions increase approximately simultaneously with the passenger-km and ton-km performed. Improvements in the engine efficiencies and in the vehicle designs are compensated by changes in the modal split towards more energy intensive modes.

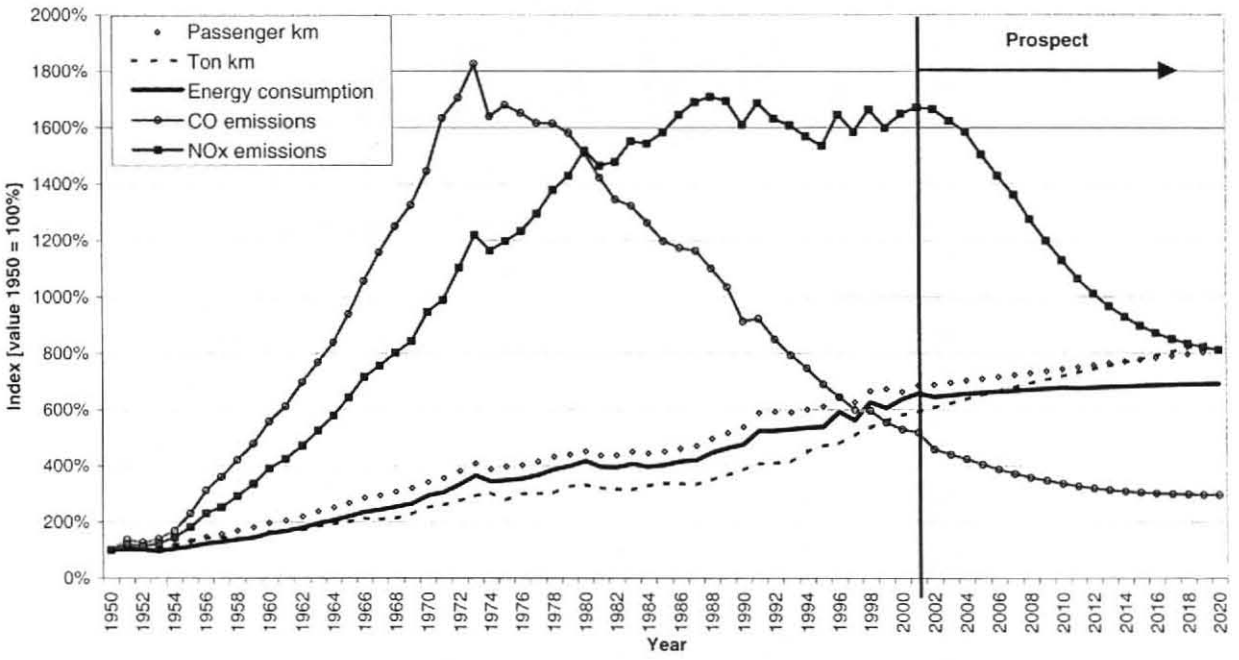

Figure 1: Development of the transport volume, the energy consumption and emissions of CO and NO_x from the transport sector in Austria (Hausberger, 2003)

Reductions in the emission level are nearly exclusively the merit of improved technologies for combustion and exhaust gas after treatment driven by reducing the exhaust gas limits. Figure 2 for example shows the development of the exhaust gas limits for passenger cars with Otto engines (SI engines) in the European Union where the emission limits have been decreased by more than 90% since 1975.

For heavy duty vehicles (HDV) a comparable limitation of exhaust gases was started later than for passenger cars (Figure 3). The main challenges for HDV will be the future legislation. EURO 4 prescribes a significant reduction of particulate emissions and NO_x, while EURO 5 drops the NO_x limits by another 43 %.

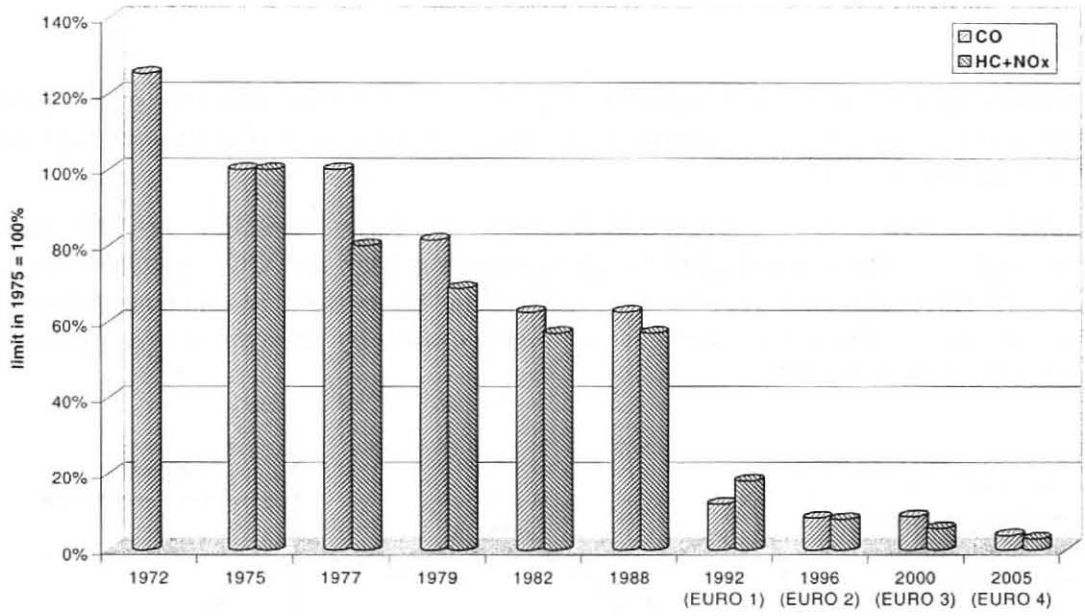

Figure 2: Development of the exhaust gas limits for passenger cars in Europe

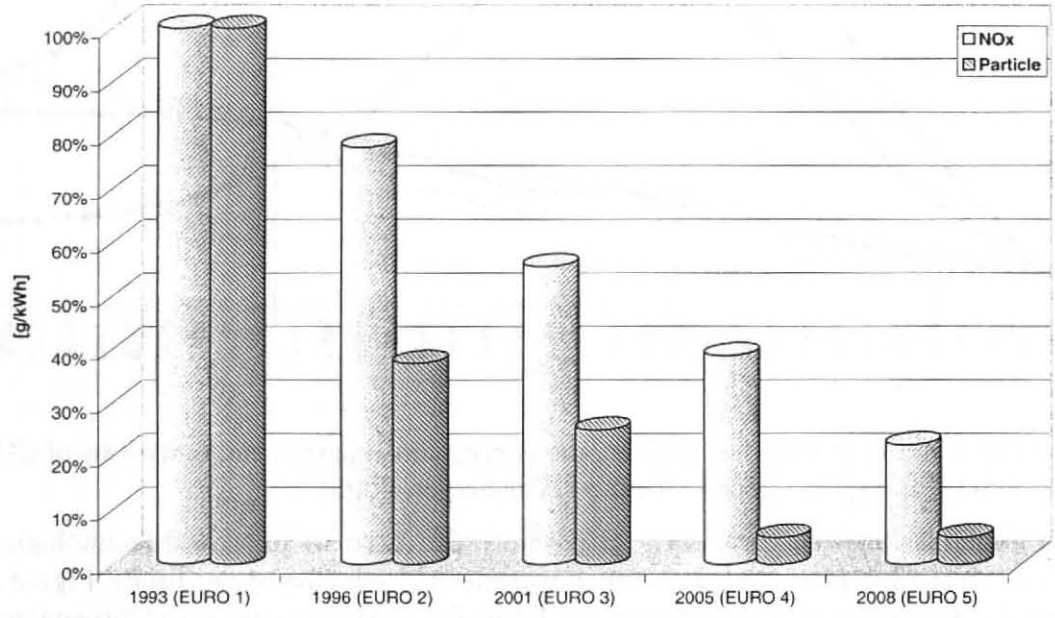

Figure 3: Development of the exhaust gas limits for NO_x and particulate matter for heavy duty vehicles in Europe

Fixing exhaust gas limits needs a proper planning since usually reduced limit values lead to additional costs for the vehicle production (which may be compensated by reduced environmental impacts).

Before any measures are taken the following questions shall be answered:

1. What are the main sources of pollutants (traffic modes, industry plants, etc)?
2. To what extent are emission reductions technologically feasible at what costs?
3. Will the measures taken ensure to meet the air quality targets?

While the main emission sources are quite well known in industrialised countries, question 2. is always related to the progress in research and development and will thus never give a final answer until zero emissions are reached. Whether the measures taken are enough to reach the air quality

targets mainly depends on the defined targets. Following the recommendations of the WHO we find that still a lot of effort will be necessary to meet an environmentally sustainable level. The emissions of the transport sector exceed WHO target values clearly for CO_2, NO_x and particulate emissions e.g. (Hausberger, 2000). This suggests that reduced emission limits will escort vehicle and engine related research and development also over the next decades.

Figure 4 shows the control loop from air quality measurements to the decision of measures from the legislator with the link to the manufacturers which have to meet the legislation. Reliable tools for emission simulation are necessary to detect the main sources of the pollutant under consideration and often also to assess the effects of different potential measures. For example, exhaust gas limits need a long time span until they show the full effects on the air quality since they have to be set years before new vehicle models have to meet these limits and afterwards the distribution of the new models in the existing vehicle fleet needs years. Without a simulation of these effects future emission limits can not be planned properly.

Certainly, the effects of the measures have to be checked regularly by measurements of the air quality to validate the expected results. If the air quality does not improve in accordance with the predicted reduction of the emission levels vehicle measurements are necessary.

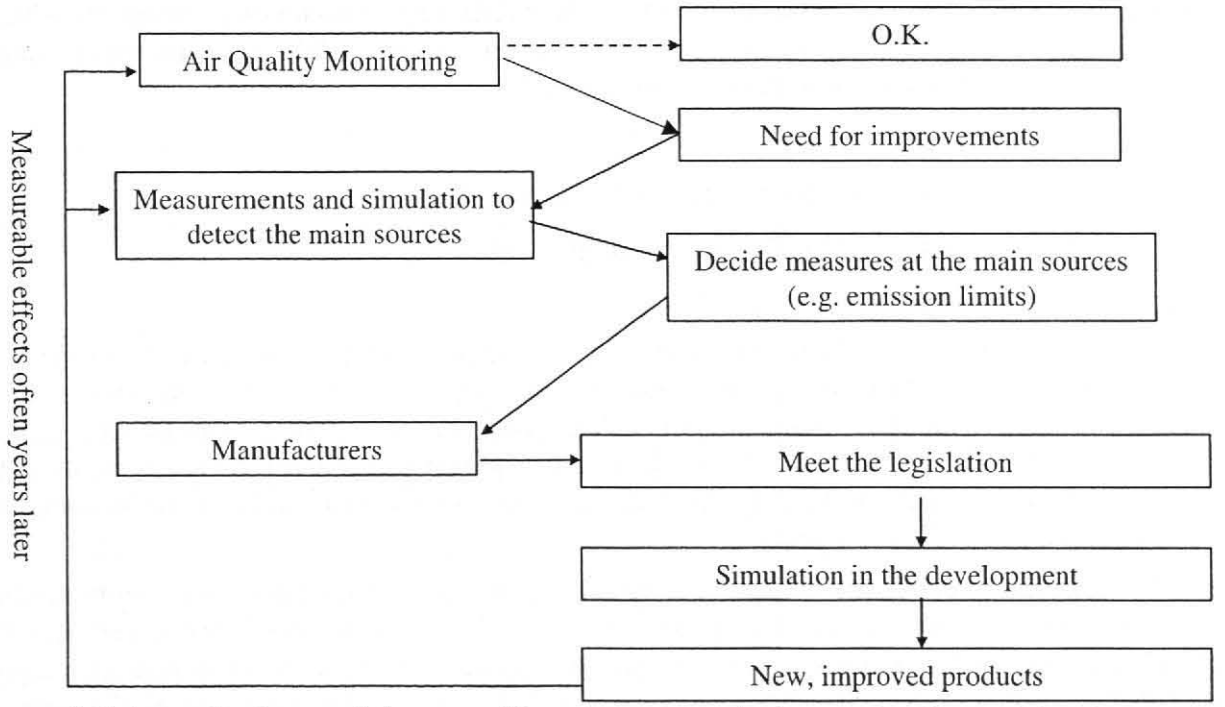

Figure 4: Schematic picture of the control loop between emission monitoring and development

The decreasing emission levels of modern vehicles increases the demands on the simulation tools used for the monitoring. The low emissions in the type approval cycles and similar real world driving conditions increase the importance of special driving situations with relatively high emissions. Short emission peaks of CO, HC and NO_x during a long driving cycle are often responsible for more than 50% of the total cycle emissions, e.g. (Stahel, 2000).

Additionally, the repeatability of the emission measurements in real world cycles gets poorer for modern passenger cars and the emission behaviour of different makes and models is often very different. This results inter alia from the increasing influence of the electronic engine control system on the exhaust gas emissions. The influence of the application work will in future increase with the growing degrees of freedom for the engine control (e.g. variable valve timing, variable turbine geometries, variable injection pressure added to the already variable injection timing etc.).

To get a realistic picture of the emission levels from vehicles on the road, the relevant effects on the emission behaviour shall correctly be taken into consideration by the models. In fact, this

needs a proper understanding of the causes for differing emission levels combined with the knowledge of real world driving behaviour and the resulting engine load patterns. Otherwise huge errors in all directions are possible.

This paper tries to explain the way from engine and vehicle measurements to the development of vehicle emission models which should fulfil the main demands described before.

2 Overview on Tools for Emission Simulation

This chapter shall give an overview on existing emission models for different applications. In the beginning methods for assessing emission inventories for the transport sector are shown. In the following some models used for the simulation of engine emissions and for the calculation of emission factors are described.

2.1 Basic approach for emission inventories

An emission inventory shall give the total emissions occurring in a defined area. Areas under consideration reach from single streets up to total countries. Manifold models for such applications exist like COPERT III (Ntziachristos, 2000), TREMOD (e.g. Lambrecht, 2001) GLOBEMI (Hausberger, 1997), HBEFA (e.g. Keller, 1998). All of these models have the same simple approach where the total emissions are calculated from:

$$E = v-km \times e$$

with E ..... total emissions in the area [e.g. g per day]

v-km ..... total vehicle mileage [e.g. km per day]

e ..... emission factor [g/km]

While this approach is very simple, the assessment of the total vehicle mileage and especially of the emission factors is rather difficult. For assessing the emission factor in an easy but expensive way a random sample of all vehicle categories (two-wheelers, cars, trucks,..) can be measured on roller test benches. The random sample should include the vehicles at least according to their age and size similar to the fleet on the road. Such an approach is very static and can not be applied to different regions or for different years.

A flexible approach clusters the vehicles according to categories with similar emission behaviour. This means that separate emission factors are set up for the different vehicle categories and that each vehicle category is subdivided into homogeneous classes. For example, passenger cars can be subdivided according to the engine type and according to the year of first registration. The years of first registrations will be clustered according to the steps of emission legislation (e.g. EURO 1, EURO 2,...).

$$E = \sum_{cat} \sum_{cl} (v-km_{cat,cl} \times e_{caty,cl})$$

with $v\text{-}km_{cat,cl}$ ..... total vehicle mileage of a vehicle class in a vehicle category [e.g. km per day and class]

$e_{cat,cl}$ ..... emission factor for a vehicle class in a vehicle category [g/km]

With such an approach different fleet compositions in different regions and for different years can be taken into consideration and such approaches also allow projections into the future if the turnover of the fleet composition is simulated properly (Hausberger, 1997). To apply such a model, the total vehicle kilometres driven have to be subdivided into the single vehicle classes. Such data usually is not available and needs extensive surveys and most often a lot of assumptions.

As already discussed in the introduction the emission behaviour of vehicles heavily depends on the actual traffic situation. Thus an average emission factor can be set up only when an average driving situation is known. For total countries such averages can only be estimated. For single driving routes vehicle speed cycles (driving cycles) can be recorded with on board instruments. Usually driving cycles are defined by such measurements; they shall represent typical traffic situations (e.g. urban centre congested up to highway free traffic flow). The average traffic situation in a greater area can then be gained as a weighted average of the single driving cycles. The models usually calculate the emissions of the total vehicle kilometres in each traffic situation (driving cycle). The total emissions are then the sum of all single cycles.

Additionally, the emission levels are very different after a cold start and in hot running conditions. Thus the engine temperature level has to be taken into consideration. Since the ambient temperature significantly changes over the seasons and from region to region and many starts happen after a rather short parking time when the engine has not yet cooled down completely, a simple division into hot and cold engine is not sensible. At least different ambient temperatures and parking times have to be taken into consideration to get a realistic result. Furthermore, the evaporative emissions have to be simulated to get a complete picture of HC emissions.

This brings the simple basic equation for assessing emissions into a rather complex form which can be described as:

$$E = F\left\langle \sum_{cy}\sum_{cat}\sum_{cl}(v - km_{cy,cat,cl} \times e_{cy,caty,cl}) + \text{Evaporation} \right\rangle$$

with $\text{v-km}_{cy,cat,cl}$ ..... total vehicle mileage in a traffic situation (driving cycle) of a vehicle class in a vehicle category [e.g. km per day and class]

$e_{cy,cat,cl}$ ..... emission factor in a driving cycle for a vehicle class in a vehicle category [g/km]

Certainly this complex structure is necessary only for basic work on vehicle emissions. The models developed are capable of calculating "average" emission factors easily for any request by simply subdividing the total emissions by the total vehicle kilometres. Thus the average user does not need all complex input data, he may use for most applications simply an average factor for cars and for HDV. But it is advisable to have at least an idea of the backgrounds and the related simplifications and uncertainties if the factors are used as basic input for studies like cost-effectiveness analyses or comparisons of different propulsion systems or road constructions.

2.1.1 Example for an emission inventory

The inventory model GLOBEMI, described in (Hausberger, 1997) and used for several studies in the mean time, is also used for the regular calculation of the emissions from the transport sector in Austria to fulfil the yearly reporting demands of the EC.

A main air quality problem in many regions of Austria are the concentrations of NO_x. In the year 2000 in Austria the air quality target value of 80 $\mu g/m^3$ (24h mean value) for NO_2 was exceeded on 36 sites. Looking at sites where air quality measurements were performed for longer time spans shows that the NO_x concentrations have remained on a stable level since 1994 (Figure 5).

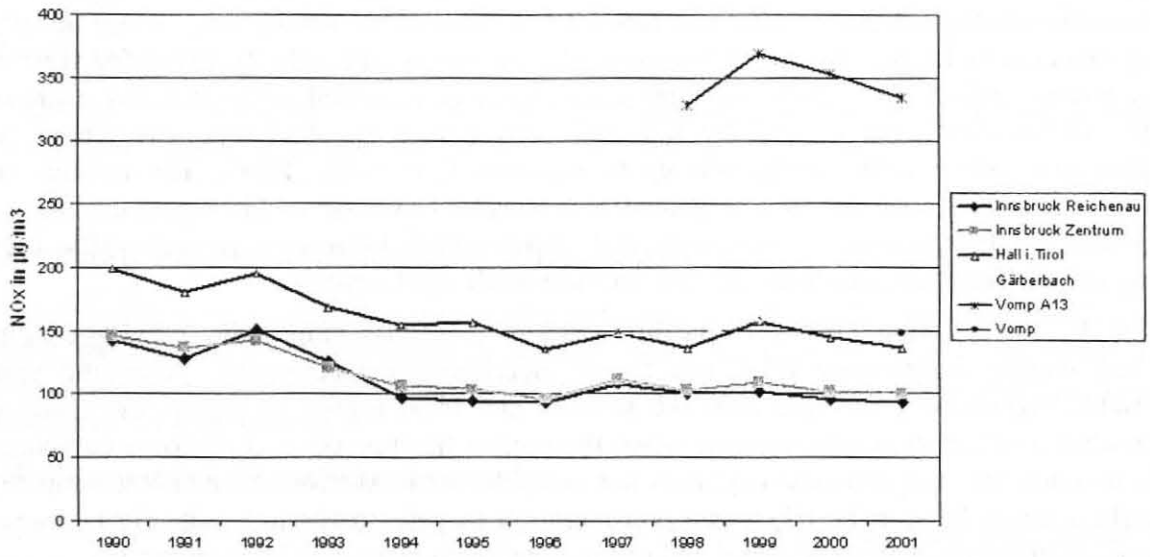

Figure 5: measured NO_x concentrations at different sites in Tirol (average 24 h mean values)

To assess the sources of emissions responsible for the NO_x concentrations at the different sites would need a detailed emission modelling coupled with the simulation of the resulting air quality. Since air quality modelling is not topic of this paper for a rough estimation the road transport sector can be assumed as the main source at most sites according to the Austrian average where the transport sector is responsible for more than 65% of the total NO_x emissions (e.g. UBA, 2002). This figure corresponds with most European countries. According to (WHO, 2000) the share of traffic on the Nitrous Oxide emissions is up to 75% in northern Europe.

While earlier emission inventories of the transport sector showed decreasing emission levels from approx. 1994 on, the most recent results are in line with the measured air quality (Figure 6). This is a result of a complete update of the input data for the model GLOBEMI (Hausberger, 2003) with the following main changes:

- Introduction of a new set of emission factors for HDV elaborated in several international projects (which are described in detail later in this report) which show a much lower decrease of NO_x emissions between 1992 and 2001 than assumed before.
- Introduction of results from a detailed study on the off road sector (Hausberger, 2000). This study included all mobile sources from the off-road sector from chain saws to tractors and construction machinery while older assessments were based on the registered machinery only. As a result the energy consumption and emissions for the off road sector approximately doubled compared to previous results. This also effected the results for the road traffic since the gasoline and Diesel sold in Austria and not used by the total off road sector is assumed to be used in road transport mainly. The new results for the vehicle kilometres driven and the ton kilometres performed from the road sector are now much better in line with the official statistics.
- Results of a new survey on traffic behaviour concerning the number and length of trips performed with cars which showed a much lower average number of starts per day and car than the data used before. This clearly has influences on the simulated cold start emissions.
- New assumptions for the average annual kilometres driven per Diesel car. The new assumptions show higher annual kilometres compared to the former data set.

The result of these updates now explains the measured air quality levels much better than before. Other sources may have significant contributions to the air quality of the sites shown in Figure 5 and the development of the traffic volume was different at each site. Additionally, NO_2 can be

transported over long distances and is involved in chemical reactions in the atmosphere. Thus a comparison between the emissions simulated for the total area of Austria and the air quality measurements has a limited accuracy. But the comparison shall give an impression of the results of an inventory model only.

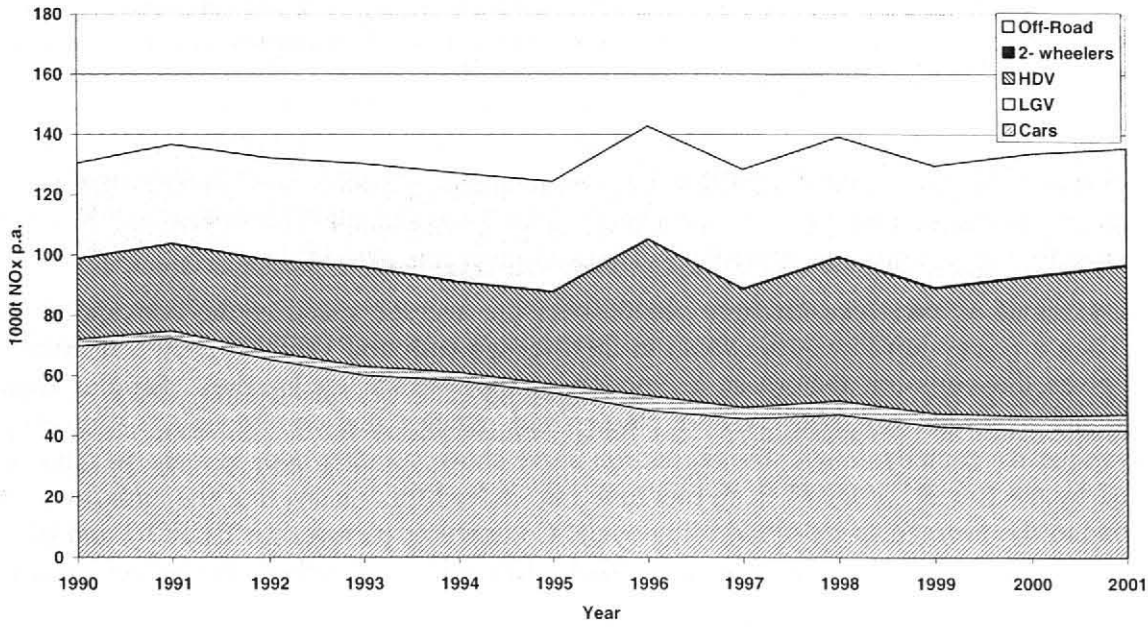

Figure 6: Simulated NO_x emissions of road traffic in Austria (Hausberger, 2003)

2.2 Models for simulating vehicle and engine emissions

Most simulation tools used for emission monitoring are global emission and inventory models. Such models are usually based on traffic statistics and measured "emission factors" where an emission factor gives the emission value e.g. in [g/km] for a defined vehicle category in a defined traffic situation. The definition of the "average" driving cycles for a traffic situation has a high influence on the resulting emission factors. Since vehicles are driven in cold and hot running conditions, uphill and downhill, empty and full loaded in situations from congestion to free flowing traffic and with drivers having very different driving styles, a huge variety of potential using patterns exist.

As a result it is very difficult to define which driving situations are "relevant" for the air quality. Certainly all driving situations in which the most vehicle kilometres are driven are relevant, e.g. highway driving with an average volume of traffic per lane. Beside that, all driving situations with high specific emissions [g/km] are relevant for the air quality if their part of the total vehicle kilometres driven is not negligible. The total of all such driving situations has a significant influence on the total emissions even if each single driving situation has a very small share on the overall vehicle kilometres driven. E.g. a total of 10 % of driving situations which have 200 % higher emission levels than the average will already give them 25 % of the total emissions.

Performing measurements on the roller test bench or on the engine test bed for all potentially relevant driving situations for a sufficient random sample of vehicles would be by far too expensive. Therefore, models capable of simulating the emissions for any driving cycles from a limited number of measurements are very valuable for air quality modelling purposes. If such models can also explain the different emission levels in different driving cycles the output can also be used for improving future type approval tests and future emission control technologies.

Manufacturers do use rather different models in research and development. Detailed emission related models e.g. are predicting emission levels from the combustion process for the engine

under development based on 0 to 3 dimensional modelling of the gas exchange, fuel injection and combustion. Such models are very valuable for assessing effects of changes in the engine design but have very long computing times and need very detailed input data. Thus they are not suited for simulating real world emission factors.

The paper concentrates on tools for assessing emission factors, where in the following an overview of existing models is given. The overview shows some typical examples and does not give a complete list of all models available.

2.2.1 COPERT

Most emission factors from COPERT III (Ntziachristos, 2000) are gained directly from measurements performed on roller test benches. Figure 7 for example shows how the function for the calculation of NO_x emissions from EURO 1 gasoline cars is gained.

The emissions of all cars measured are plotted over the average speed of the corresponding test cycles. Then a regression line is drawn from the average emission value of each test cycle. This already gives the emission factors as a function of the average cycle speed. Similar emission functions are available for other vehicle classes and exhaust gas components. Comparing the average values for each cycle with the regression curve shows a rather poor agreement. This is also expressed by the low R^2 of 0,077 from this function. Indeed this means that the emissions do not correspond to the average speed of a driving cycle. Comparable pictures for EURO 2 and EURO 3 cars have not been published yet, but most likely they will look rather similar but on a lower emission level.

The main learning of COPERT is that the emission values of single cars differ by magnitudes even if they fulfil the same emission standards. A second fact is that cars proving to be high emitters in one cycle not necessarily have to be high emitters in an other cycle. This indicates that for reliable emission factors a huge sample of cars has to be measured.

The emission factor for driving at hot running conditions on flat road can be assessed with one average value as well as with such an emission function. From Figure 7 we should rather conclude that the average emission factor is 0.5 g/km with some +/- 30 % uncertainty.

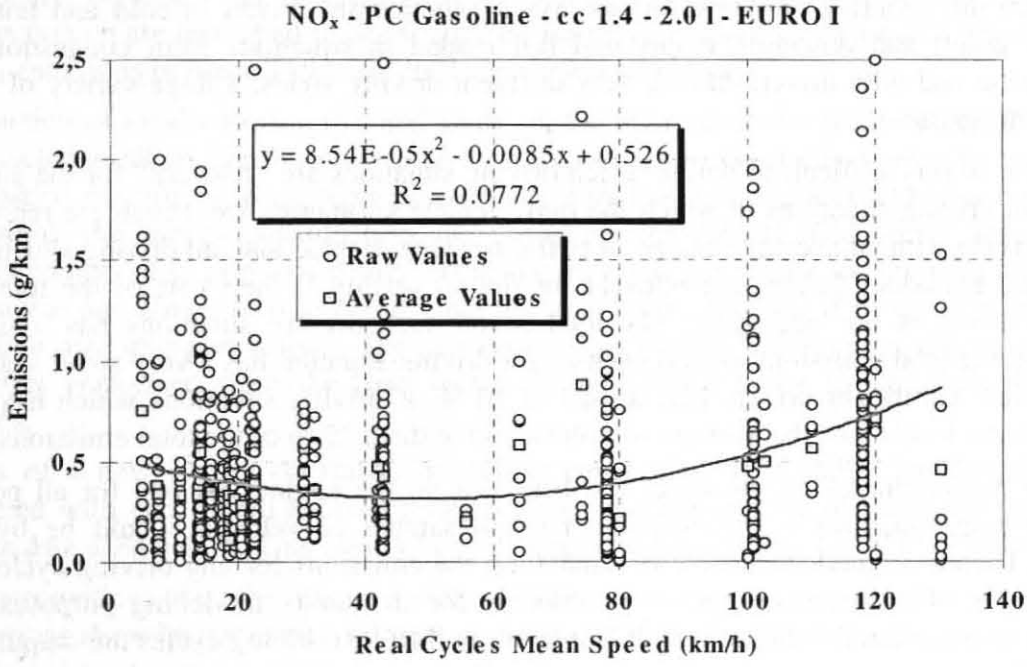

Figure 7: Function for the calculation of NO_x emissions of EURO 1 gasoline cars as function of the average cycle speed (source COPERT III)

Certainly, this method needs extensive measurement programmes as basic input. Another draw back is the very limited flexibility. For driving cycles being very different to the measured ones no emission factors can be calculated.

2.2.2 DGV, Handbook on Emission Factors

To improve the flexibility of the models and to reduce the number of cycles to be measured the model DGV (Digitalisiertes Grazer Verfahren), (Haghofer,1982), (Pischinger, 1984), was developed at our institute and has been improved in the meantime. Similar approaches are also used in the German-Swiss-Austrian Handbook on Emission Factors (e.g. Keller, 1998) for assessing emission factors for passenger cars.

This method gains emission maps based on vehicle speed and vehicle acceleration from the measurements on the roller test bench. The instantaneous emissions measured (usually registered with 1 Hz) are simply inserted in a velocity-acceleration raster (Figure 8).

To simulate a different driving cycle the emissions are taken for each second of the cycle out of the v – a raster according to the actual vehicle speed and vehicle acceleration. Such methods are called "instantaneous emission models".

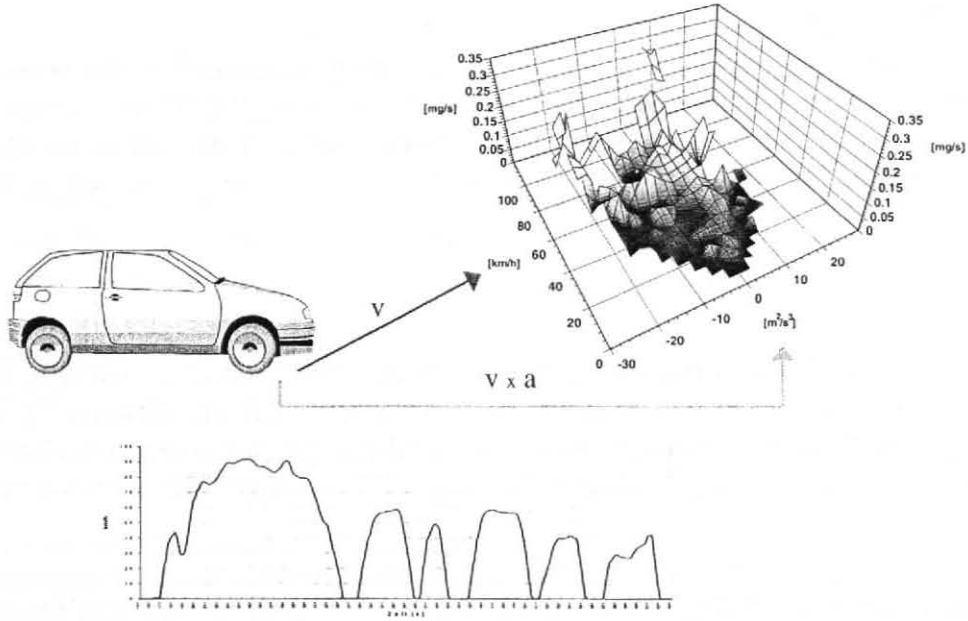

Figure 8: Schematic picture of the model DGV

This method proved to be very useful until the early 90ies. For modern passenger cars the method is getting increasingly inaccurate, e.g. (Sturm, 2000).

Figure 9 shows a result of the model DGV where the v-a raster was gained from measurements in three different driving cycles. With this v-a raster the emissions were simulated for the other measured cycles. The conclusion of the exercise is that only cycles which were measured before can be simulated with a really satisfactory accuracy.

Obviously, vehicle speed and acceleration are no parameters suited for the description of modern vehicle emissions.

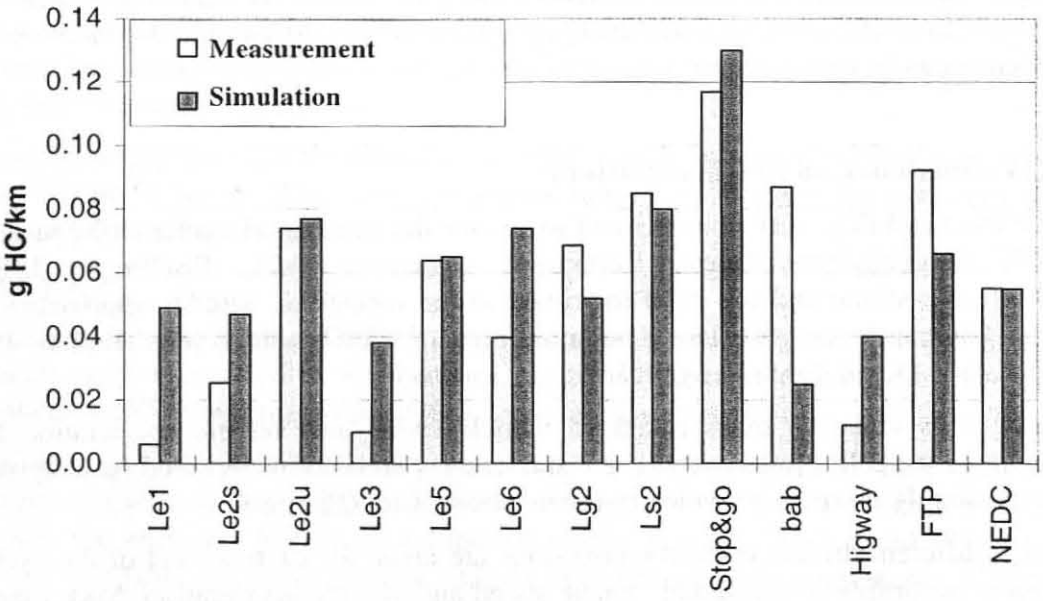

Figure 9: Comparison of measured and simulated HC emissions using the model DGV for a EURO 2 gasoline car

With this limitation such model approaches have no big advantages against simpler methods like COPERT. Attempts have been made to improve the model accuracy by adding parameters to describe the emission levels. As parameters especially values potentially describing the dynamics of a cycle were tested but no really satisfactory improvements have been achieved so far (e.g. Kohoutek, 1999).

2.2.3 PHEM

Beside their inaccuracy the main drawback of the models described before is that they can not simulate "non standard" driving cycles sufficiently. Such cycles include different gear shift behaviours, road gradients, vehicle loadings and the usage of energy intensive auxiliaries like air conditioning. All of these "non standard" situations potentially have high effects on the emission levels

Especially on HDV the influence of vehicle loading and road gradients has a very important effect. For this reason the model PHEM (Passenger car and Heavy duty vehicle Emission Model) has been developed at our institute since 1998.

With a given driving cycle and road gradient the effective engine power is calculated in 1Hz frequency from the driving resistances and losses in the transmission system. The actual engine speed is simulated by the transmission ratios and a driver´s gear shift model. The emissions are then interpolated from engine maps (Figure 10). Basically this method is capable of simulating the fuel consumption and the emissions for any driving cycle with any vehicle configuration.

Additionally, the emission simulation is much closer to the relevant parameters of the combustion and to the parameters used for the application of the engine control unit. As a result it was possible to develop functions which can take the influence of different transient conditions in driving cycles on the emission levels into consideration. These "transient correction functions" transform the emission levels from the engine map, which is usually measured under steady state conditions for HDV, on the emission levels which have to be expected under the actual transient engine load.

Basically this method was developed for HDV, where usually the engines are measured on engine test beds. In the meantime the model was also successfully applied to passenger car simulation. For passenger cars usually no measured engine emission map is available but transient tests on the

chassis dynamometer are performed. To overcome this problem a method was found to gain the engine maps directly from standard measurement programmes (chapter 5.1).

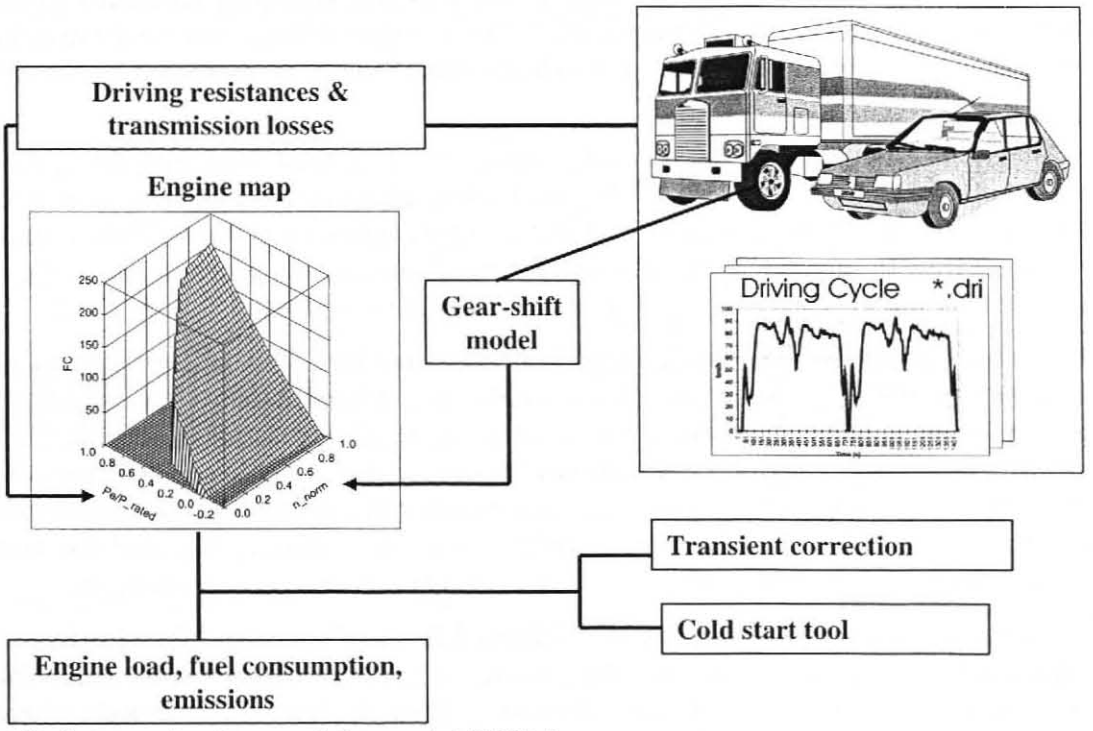

Figure 10: Schematic picture of the model PHEM

Another advantage is the flexibility to simulate emissions for alternative propulsion systems in a given vehicle by simply exchanging the engine data set.

Beside giving reliable emission factors this model approach can also give physically sound explanations for the results. This enables to draw correct conclusions for related measures to further reduce the environmental impact of the traffic. It makes the model also very useful for the development of vehicle and engine test cycles.

Such model applications have already been performed successfully in different public and industry related projects, e.g. (Hausberger, 2002-1), (Jungmeier, 2002), (Hausberger, 2002-2).

3 Measurement equipment and test cycles

All models described use emission measurements as model input and most of them use the data for model validation as well. The models are then used to reduce the number of measurements necessary and to improve the understanding of the measurement results. Thus a profound knowledge on the basic measurement equipment and related inaccuracies is necessary for model development and model application.

Measurements of fuel consumption and emissions are usually performed on roller test benches, engine test beds or on-board at the vehicle. Test beds have the advantage of exactly defined boundary conditions and thus a good repeatability. On-board measurements can be performed in real world traffic but have the disadvantage that the repeatability is rather bad and that some of the boundary conditions are difficult to record. This affects mainly the road gradient where no instruments are available which allow an easy and exact recording on the road.

For the development of the models described in this paper extensive measurement programmes on engine test beds and roller test benches were performed. The general functionality of the measurement equipment is described in the following. The chapter will close with an assessment of the accuracy of instantaneous emission measurement and methods for improvements.

3.1 Roller test bench

At a roller test bench the road load for a vehicle in the test cycle is exactly simulated. Usually the mass of the vehicle is simulated by flywheels while the rolling resistance and the air resistance are simulated by an electric brake. For HDV the vehicle mass usually is simulated by the electrical brake too.

The exhaust gas is sampled and diluted with filtered air and then lead into the CVS tunnel (Constant Volume Sampling). After the CVS tunnel a heat exchanger keeps the gas on a constant temperature (Figure 11). A blower combined with venturi tubes or a Roots blower sucks in a constant volume flow at the end of the system. Having a constant temperature before the blower results in a constant mass flow through the sampling system over the test.

From the diluted exhaust gas the probes are lead into the analysers. This is done directly in order to record the emissions instantaneously and in parallel the diluted exhaust gas is sampled into bags. The volume flows to the bags and is constant for the instantaneous measurement. The filling of the bag starts at the beginning of the test and ends after the test is finalised. Thus the content of the bag represents the average concentration over the test run. The exhaust gas analysers reflect the concentration of the exhaust gas components. With the known volume flow and the molecular weight of the components the mass emissions can be calculated from the measurement.

The particulate mass emissions are measured with the filter method. The diluted exhaust gas is lead through a defined filter which samples the particles. The difference of the weight of the filter before and after the test gives the total particulate mass from the test. This method can certainly not deliver instantaneous emission values but only an average value for the test. Methods capable of measuring particulate mass instantaneously are available (e.g. TEOM) but often give other results than the filter method.

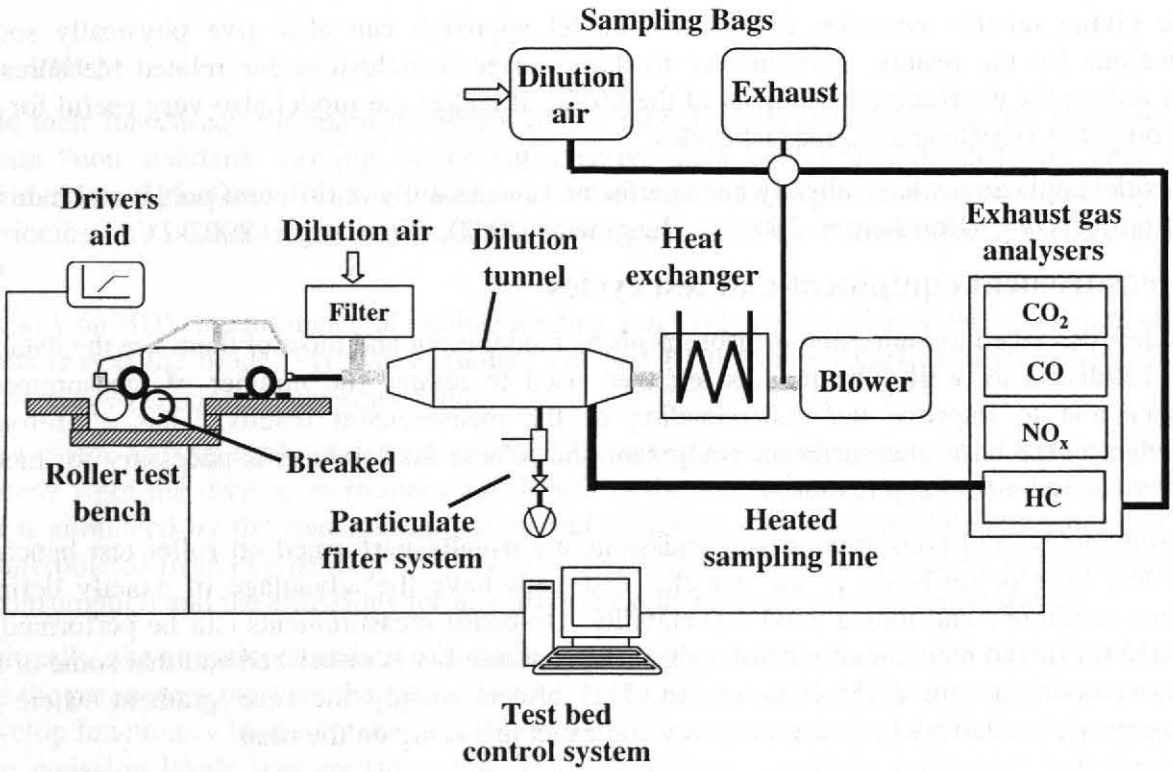

Figure 11: Schematic picture of a roller test bench

The test cycle for type approval tests is the NEDC (New European Driving Cycle). The NEDC is a synthetic cycle which shall cover the relevant ranges of real world traffic and begins with a cold start. Figure 12 gives as comparison a real world cycle according to (Andre, 2000) which was developed from extensive measurements on the road. This test cycle (CADC, Common ARTEMIS

Driving Cycle) includes different typical real world traffic situations from urban, road and motorway in line. Figure 12 clearly shows that real world driving cycles are much more dynamic than the NEDC. Beside the CADC a huge set of other real world test cycles exist.

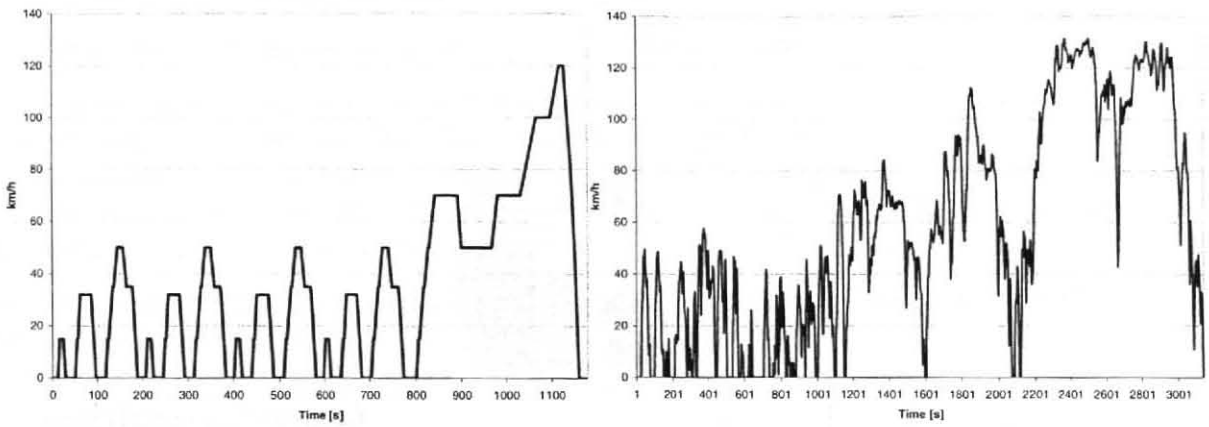

Figure 12: NEDC-Test cycle (left) and a real world test cycle (CADC)

All relevant components of the measurement set up as well as the regulations for the evaluation of the measurements and the exhaust gas limit values for passenger cars are given in the direction 70/220/EWG of the Commission which are updated regularly according to new exhaust gas legislations. The actual valid version is the update 1999/102/EG.

3.2 Engine test bed

While for passenger cars and light goods vehicles the type approval tests are performed on a roller test bed, for heavy duty vehicles as well as for tractors and several off road machinery the emission legislation prescribes tests on the engine test beds. Since similar engines are installed in manifold different vehicles and different vehicle configurations this legislation simplifies the type approval very much.

To perform exhaust gas measurements according to the actual European legislation for HDV engines (88/77EWG in the version 2001/27/EC) transient engine test beds are used. While transient tests are not absolutely necessary for Diesel engines until 2005[1], for CNG engines they are already mandatory. From 2005 ("EURO 4) on, all HDV engines will have to be tested in transient tests.

Most engine test beds use an asynchronous motor, suitable for running in four quadrants, to be able to test engines in all transient test cycles. The test bed is controlled by an engine controller which performs a synchronised controlling of the HDV-engine and the asynchronous motor of the test bed to follow the torque and engine speed curves (Figure 13).

The equipment for emission measurement is similar to the set up at the roller test bed (chapter 3.1). In addition to the CVS measurement the emissions are recorded from the undiluted exhaust gas as well. To calculate the mass emission from the undiluted measurements the intake air flow and the fuel flow of the engine have to be measured instantaneously. This gives the total exhaust gas flow from which the mass emissions of the measured concentrations of the exhaust gas components are calculated.

---

[1] Transient tests have to be performed for diesel engines when an exhaust gas after treatment system is used or when any other components suggest that the engine emission level is clearly different at steady state and transient running conditions

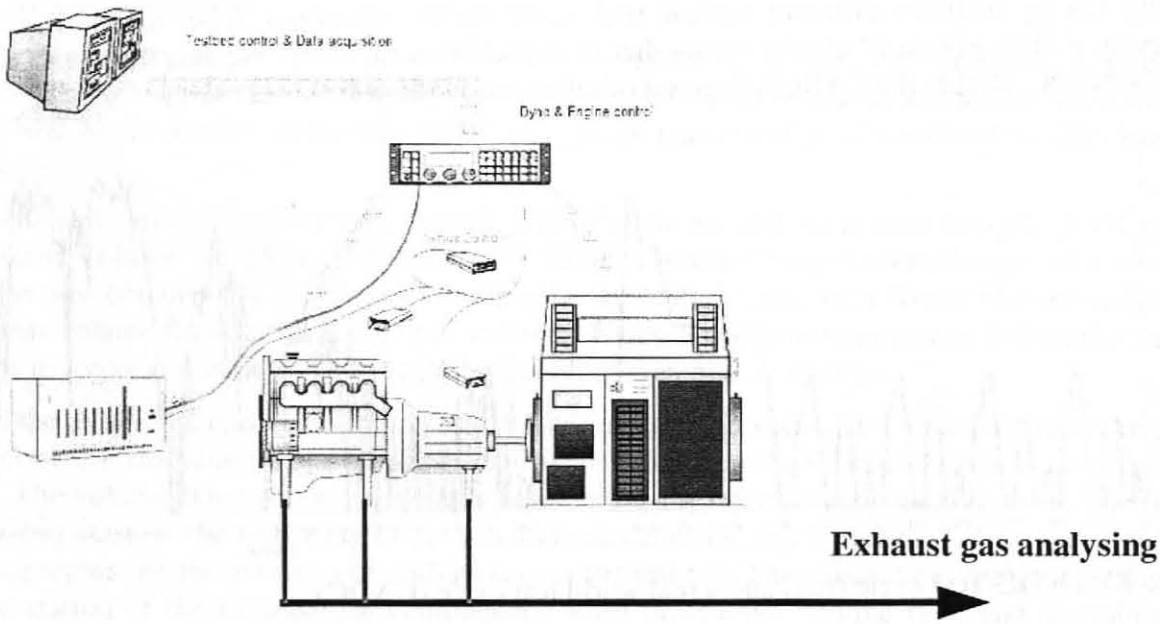

Figure 13: Schematic picture of a transient engine test bed

The actual test cycle for the type approval tests is the ESC (European Stationary Cycle). This cycle consists of 13 points (Figure 14) which are measured under steady state conditions each after a 60-second preconditioning phase. The test result is then calculated by a weighted average of the emissions from each test point as [g/kWh]. The weighting factors for the single points represent the frequency at which the areas around each point are reached in real world driving. The weighting factors are mainly valid for heavy goods vehicles in long distance traffic.

Before the ESC was introduced the R 49 was the official test cycle. The R 49 is similar to the ESC but covers only two engine speeds and idling. A main improvement of the ESC was that the NO_x emissions are limited in the range between the lowest engine speed tested (speed A) and the highest engine speed tested (speed C). Three points are selected randomly in this area and the NO_x levels at these points must not exceed the limits by more than 10%. Anyhow, the controlled area is still rather small and the test does not include transient engine loads. The ETC (European Transient Cycle) is a more comprehensive test cycle and is based on average real world driving also. A drawback of the cycle is that it only covers a rather small area of engine speeds. The engine speeds of the cycle are calculated as a function of the full load curve from the tested engine and can thus be influenced very much by the manufacturers. In the United States transient tests of HDV engines were introduced much earlier, using the US-Transient Cycle. A detailed analysis on the test cycles and the resulting emission levels of HDV is given in chapter 4.3.2.

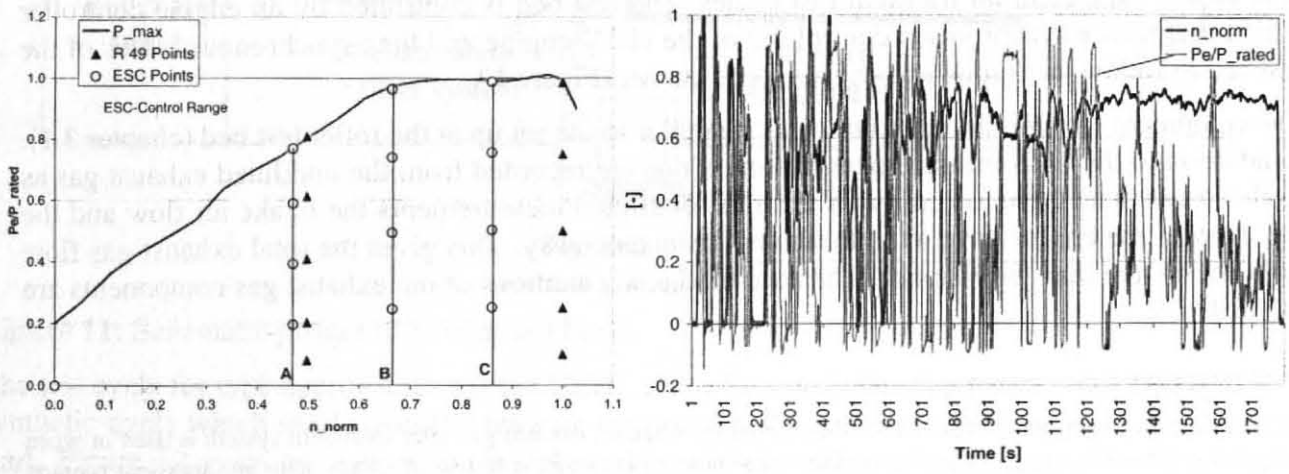

Figure 14: ESC and R 49 test cycles (left), ETC (right)

All relevant components of the measurement set up as well as the regulations for the evaluation of the measurements and the exhaust gas limit values for HDV engines are given in the direction 88/77EWG of the Commission which is updated regularly according to new exhaust gas legislations. The actual valid version is the update 2001/27/EC.

3.3 Delay times of the measurement system

When using measurements for model development and model evaluation tasks, one should be aware of the quality of the data. Beside malfunctions of the systems and potential operating mistakes there are several errors especially associated to the instantaneous emission measurement. Other potential errors resulting from variable boundary conditions during measurements are described in chapter 4.4.5 for HDV

The emissions recorded from the analysers are delayed and smoothened compared to the emission event at the engine due to

1. The transport of the exhaust gas to the analysers
2. The mixing of exhaust gas especially in the silencer and the CVS tunnel
3. The response time of the analysers

The transport time of the exhaust gas to the analyser is determined by the velocity in the exhaust system and by the velocity in the CVS tunnel and in the related connection tubes.

Especially the velocity of the undiluted exhaust gas is highly variable over time since it depends on the exhaust gas volume flow. The volume flow mainly depends on the engine speed, the temperature and pressure of the inlet air, the exhaust gas temperature and on the engine load. At gasoline engines the mass flow decreases when the throttle is closed. Since the velocity of the exhaust gas decreases with the decreasing volume flow the transport time through the exhaust system increases.

$$v = \frac{\dot{V}}{A}$$

with v..... velocity of the exhaust gas [m/s]

$\dot{V}$ ..... volume flow [m^3/s]

A..... cross sectional area in (a part of) the exhaust system [m^2]

According to (Weilenmann, 2002) the transport time for the gas in the exhaust system of cars varies between 0.07 to 6.6 seconds for a gasoline engine with 1.6 litres displacement. For a comparable Diesel engine the variation is only between 0.08 and 1.3 seconds.

In addition to the variable transport time, the exhaust gas is mixed especially in the silencer. This results in a smoothening of the emission signals over more than one second.

When the exhaust gas reaches the CVS tunnel the variation of the temperature decreases because of the constant temperature of the dilution air. Due to the different dilution ratios at different engine loads and the different exhaust gas temperatures a significant variation of the temperature still remains. Since the heat exchanger is mounted after the CVS tunnel, in the tunnel only constant mass flow but no constant volume flow exists when temperatures change. Assuming the diluted exhaust gas to follow the equations for ideal gas the velocity in the exhaust system can be calculated from

$$v = \frac{\dot{m} \times R \times T}{p \times A}$$

with $\dot{m}$ ..... mass flow [kg/s]

R..... gas constant of the exhaust gas mixture, variable due to differing dilution ratios [J/kg K]

T..... exhaust gas temperature [K]

p..... Exhaust gas pressure [N/m^2]

A..... Cross sectional area in a part of the exhaust system [m^2]

This gives variable velocities also in the CVS system. As a result the transport time varies by more than one second between full engine load and idling. The main influence of the CVS tunnel on the resulting signals of the exhaust gas analysers is a mixing of the gas. Thus the curve of the emission concentration is smoothened.

All together the varying transport times and the analysers´ response time can shift the signal of the analyser from approx. 1 and 10 seconds (depending on the engine, the exhaust system, the CVS system, the analyser used and certainly the engine load).

The calculation of the delay times can be performed for steady state conditions. But there the delay time is constant and is not a problem since the analyser signal reaches the final value after a few seconds. In transient tests the engine load and the engine speed are changing permanently over the time. As a result the exhaust system and the CVS tunnel are filled with finite gas volumes having different volume flows and different temperatures and (at least theoretically) a different speed. Figure 15 for example shows the theoretical velocities of finite gas volumes at a fixed time in a transient test. The velocity was calculated with the equation for ideal gas shown before using measured exhaust gas mass flows and temperatures for a Diesel engine. The picture includes emissions over eighteen seconds of a cycle which fill 14 meters length.

In reality the velocity will not look like shown in Figure 15 since faster gas volumes in the system will accelerate slower ones and vice versa. Thus the average velocity of a finite gas volume released at the engine is influenced by the velocities of the finite gas volumes released before and afterwards. Additionally, the different velocities of the finite gas volumes promote their mixing.

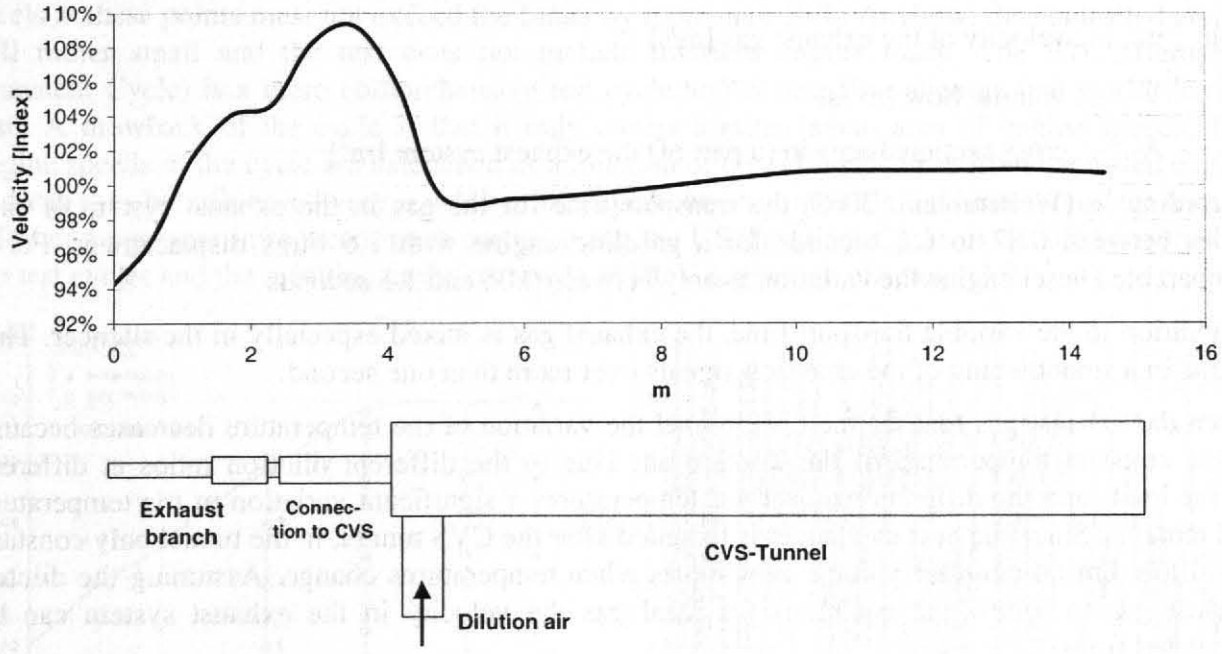

Figure 15: Example for the variation of the theoretical exhaust gas velocity over the distance in a transient test for a Diesel engine. Momentary picture in Second 18 of a test cycle

The variable transport times may be simulated by one-dimensional models. Besides the high computing effort also the exhaust gas mass flow and the exhaust gas temperature have to be

measured instantaneously. This is not the usual case on the roller test bed for cars. Thus simplified methods are necessary for daily use on the test bed.

The smoothening effects of the analysers´ signal due to the mixing in the gas flow most likely can not be reconverted completely into the original signal by any approach.

We can summarise the effects described above for CVS measurements as follows:

- Due to the response times exhaust gas concentrations are underestimated by the instantaneous measurements when they have an increasing trend and the other way round
- The time delay between the emissions at the engine and the signal of the analysers is variable by approximately +/- 3 seconds for Diesel engines, by approximately +/-5 seconds for Otto engines (depending on the test cycle, the engine, the design of the exhaust system and the design of the CVS system)

These inaccuracies are compensated over the complete test cycle, thus the integral of the instantaneous measurement is in line with the bag value. When using the instantaneous measurements for assessing shorter time periods the inaccuracies increase dramatically.

Looking at the methods used at instantaneous emission models so far, where the 1 Hz measurement signal is filled into maps, we can conclude that many values in the maps are allocated with a high error when transient test cycles are used.

As a result, improvements in the instantaneous emission modelling first of all need improved instantaneous measurement results.

Methods for Corrections

A method based on a mathematical description of the gas transport as low pass system and the inversion of the system is given in (Weilenmann, 2002). This method needs information on the volume of the exhaust system for each vehicle and a measurement of the exhaust gas flow or of λ from the exhaust gas.

A different approach is followed at our institute which shall manage a useful correction of the delay times without additional measurement demand. This approach is followed, since in several international projects measurements from different laboratories have to be used where such additional efforts shall be avoided.

For the correction all influences on the delay time are summarized into two effects:

- Response time of the analysers
- Variable transport times

Mixing effects of the exhaust gas are not taken into consideration explicitly yet.

3.3.1 Test configuration for the determination of the delay times

To measure the response times of the analysers following test configuration was used:

1. A calibration gas is connected with a valve and a pressure controller to the CVS tunnel (where usually the tail pipe of the car is connected). The valve enables a controlled and quick, complete opening and closing.
2. The emission measurement is started with closed valve until the analysers show stable concentrations for the dilution air.
3. The valve is opened and left open until the signal of the corresponding analyser is stable (this gives the target value of the concentration in the CVS)
4. The valve is closed

The measurements were performed with three different concentrations of calibration gas for each gas (CO, CO_2, Propane, NO_2) using an electromagnetic valve with 3 input connections. In Figure 16 the test configuration is shown.

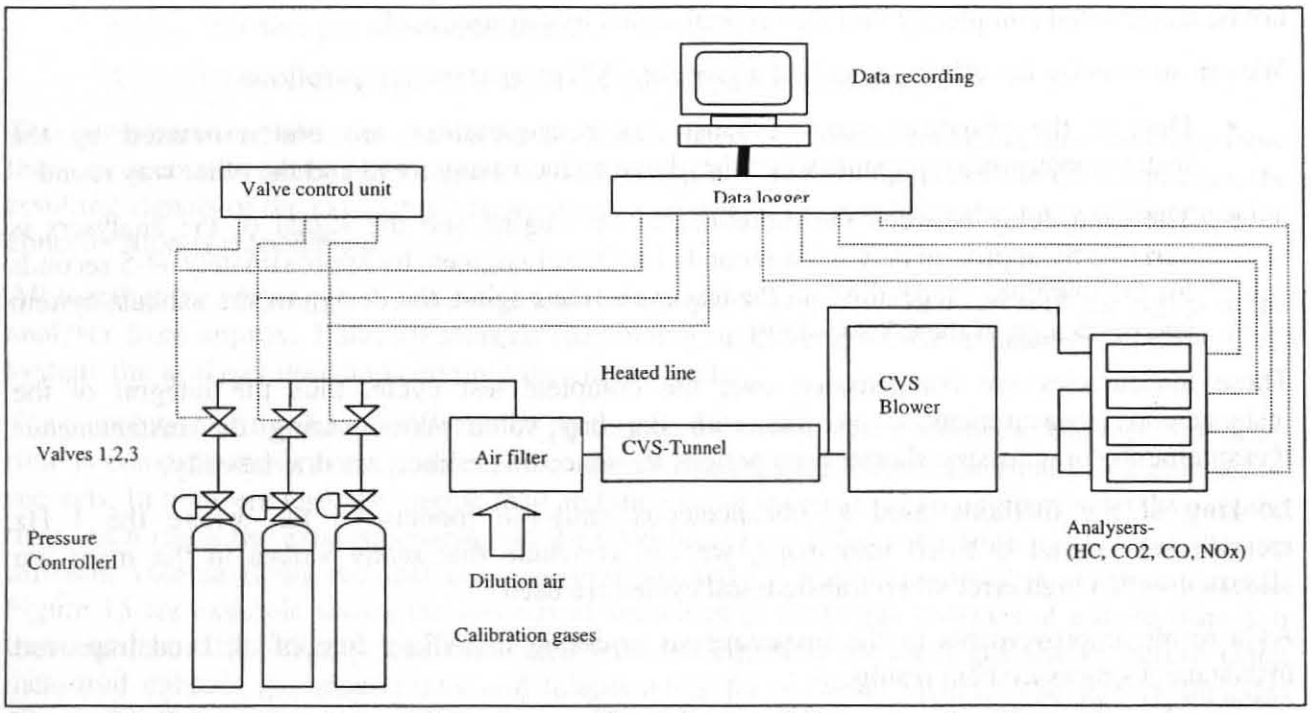

Figure 16: Schematic picture of the test configuration used for measuring the analysers response times

Figure 17 shows as example the results for NO_x. The measured concentration shows a general response time of 10 seconds until a first signal is registered. This delay time results from the transport through the CVS tunnel and the probe line to the analyser. Since the temperature in the CVS is constant in this test, also the time needed for the transport of the gas is constant.

Shifting the measured concentration by these 10 seconds shows the response time of the analyser plus mixing effects in the CVS tunnel. For this picture an old CLD analyser was used to have a better illustration of the effects. New models usually show significantly shorter response times.

The analyser used here together with the mixing effects needs approximately 5 seconds to show 90% of the actual concentration (T-90 time) and about 10 seconds to show 100% of the actual concentration. In comparison to that real world transient tests may change between high load and idling several times within 10 seconds.

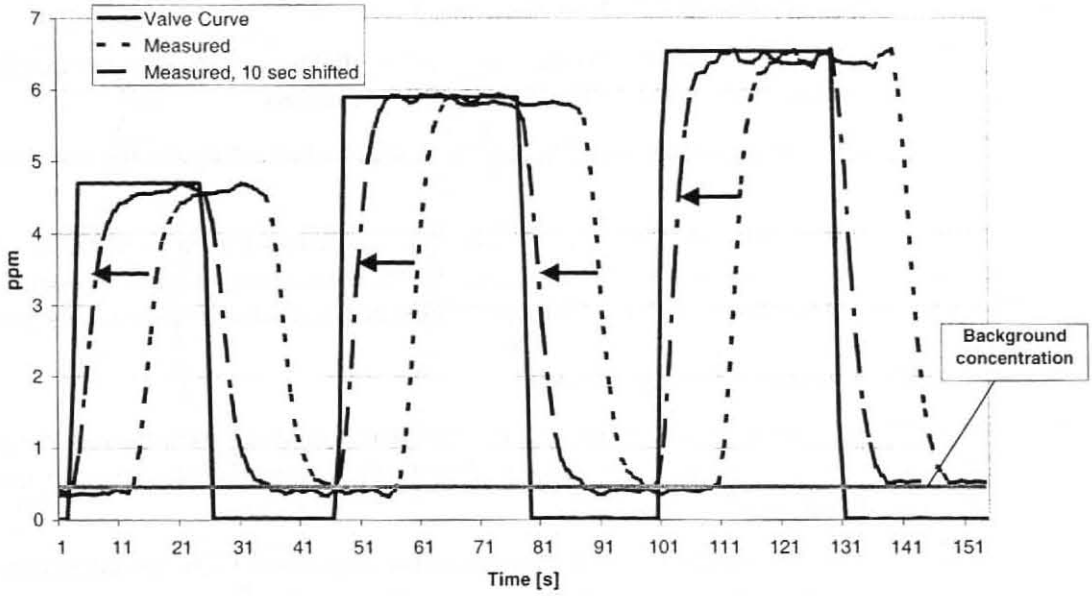

Figure 17: measured concentrations from the test configuration in Figure 16

To correct the effect of the response time and the mixing in the CVS the difference between the measured concentration (shifted by 10 seconds) and the actual concentration is calculated and approximated by a function of changes in the measured concentration. This function is then added to the measured concentrations to gain the corrected emission value (Figure 18).

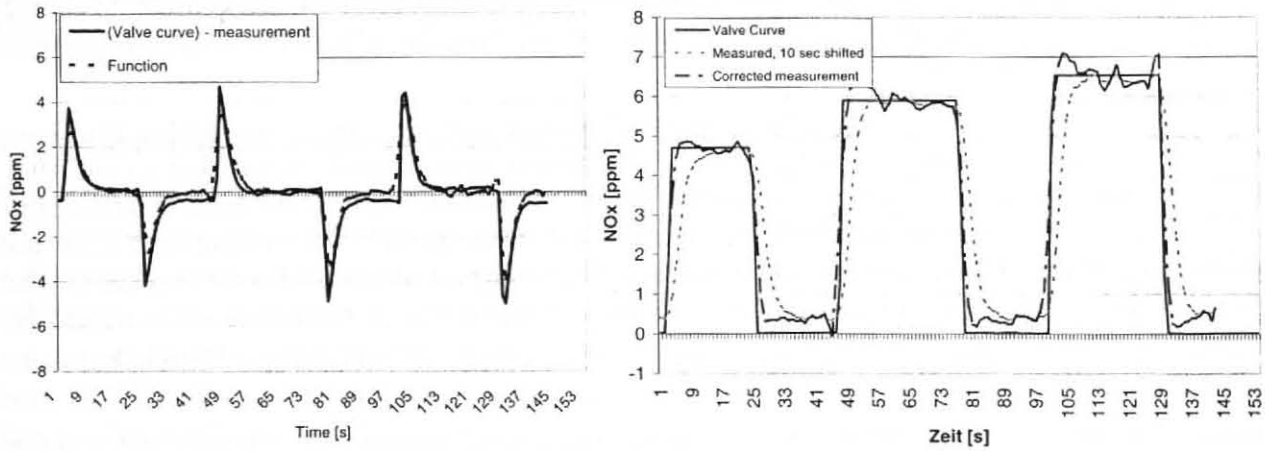

Figure 18: Difference between valve signal and analyser signal (measured and function, left picture) and measured concentration with applied correction function (right picture)

The correction function only needs the measured concentrations and is given as

Function for the correction of the response time of the analysers and the mixing in the CVS:

$$E_{corr} = E_i + \left| E_{(i+2)} - E_{(i)} + \frac{E_{(i)}}{A_1} \right| \times ARCTAN \left\{ \frac{\dfrac{E_{(i)} - E_{(i-2)}}{0.67 \times \int_{i-2}^{i} (E_i) + 0{,}0000001}}{A_2 + A_3 \times \dfrac{\left| E_{(i-1)} - E_{(i-2)} \right|}{0.5 \times \int_{i-2}^{i-1} (E_i) + 0{,}0000001}} \right\}$$

with: $E_{(i)}$..... measured concentration at second I

A_1, A_2, A_3..... calibration factors (to be adapted for different exhaust gas components, different analysers and different CVS systems)

The calibration factors can be gained easily by multiple regression analysis for the correction function.

The correction function does not take mixing effects into consideration which are a result of variable exhaust gas temperatures and exhaust gas mass flows since these parameters are constant in the test configuration. According to Figure 15 these effects are considered to be rather low.

3.3.2 Correction of the variable transport time

As described before, the attempt is made to set up the correction functions without any demand for additional measurements. For this reason an empirical method is used for shifting the measured emission concentrations in a variable way.

The basic assumption is that local maxima and minima in the measured CO_2 emission have to be at the same time step as the local maxima and minima of the effective engine power output. Looking at the instantaneous measurements this requirement can not be fulfilled by shifting the measured CO_2 emissions with a constant time delay. A result which is in line with the discussion in chapter 3.3.

To enable a variable time shifting the significant local maxima and minima of the CO_2 emission signal[2] is allocated to the maxima and minima of the engine power. This exercise gives variable demand for time shifts over the test cycle.

Then the CO_2 curve is stretched or shrinked between the allocated maxima and minima. Since the transport times have to be identical for all components of the exhaust gas, the same procedure is applied for CO, HC and NO_x.

The method is based on the findings from chapter 3.3 which says that the transport time of a finite volume depends on the exhaust gas mass flow and temperature of several seconds before and after the actual finite volume is released from the engine. If enough significant local maxima and minima exist in the test cycle, the method should deliver an acceptable time shifting for the signals between the maxima and minima. According to the transport times from the engine to the analysers approximately every 15 seconds a significant maximum or minimum value should be found . Drawback of the method is that parts of the test cycles not fulfilling this demand can not be treated correctly.

Figure 19 gives an example for the original and the corrected instantaneous measurement in the first 600 seconds of the CADC cycle for a Diesel EURO 3 car. It can be seen that the time shift varies some +/-3 seconds around the average value.

[2] The CO_2 signal corrected for the analyser response time is used

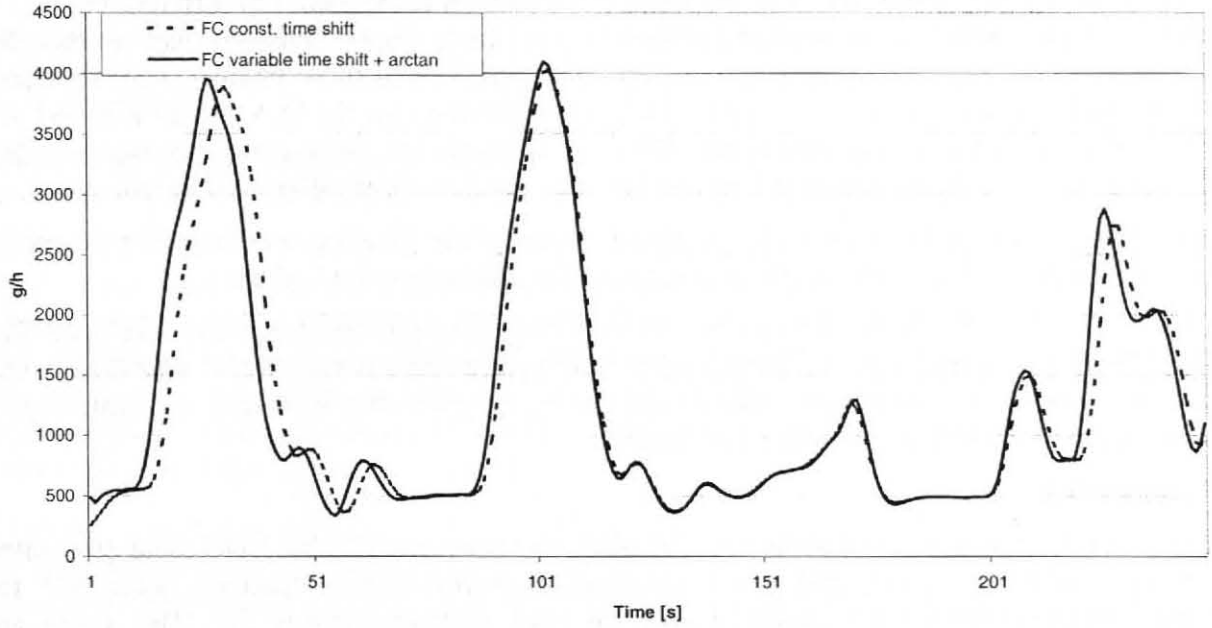

Figure 19: Measured fuel consumption (from C-balance) and fuel consumption corrected according to the analyser response time and the variable transport time

The application of the correction functions and the effects on instantaneous emission modelling are given in chapter 5.1.

Potential improvements of these functions are still necessary and are elaborated within work package 300 of the EC-5th framework programme ARTEMIS, which shall be finalised in June 2003.

4 Measurement and simulation of HDV vehicle emissions

Within a German, Austrian and Swiss cooperation (D.A.CH.) and two European projects extensive measurement programs are performed and a detailed model for the simulation of HDV emissions is developed. The European projects are ARTEMIS-Work Package 400 (within the 5th framework programme of the EU) and COST 346.

All of the projects are lead by the Institute for Internal Combustion Engine and Thermodynamic from TU-Graz. Within these projects a broad data base on new measurements and already existing data has been elaborated. All project partners agreed that the work for D.A.CH can use the data and results from the European projects and that on the other hand the results and computer programme elaborated for the D.A.CH project can be used in the European projects. End of 2002 the study for D.A.CH was finalized (Hausberger, 2002) while ARTEMIS will end mid of 2003 and COST 346 will last until 2004. In general this chapter describes the work and the results of these three projects, using the already finalized study (Hausberger, 2002).

4.1 Background

The "Handbook of Emission Factors for Road Traffic" was established in the 90ies. While emission functions for Light Duty Vehicles (LDV) have been updated with measurements regularly, the Heavy Duty Vehicle (HDV) emission values still were based on measurements of engines constructed between 1984 and 1990 (Hassel, 1995). Scope of the work was to update the emission functions for HDV with measurements of new HDV and HDV engines and to improve the general methodology for the elaboration of emission functions for HDV.

Within D.A.CH., ARTEMIS WP 400 and COST 346 data on more than 120 different engines is available. Engines which were measured at least in a complete engine emission map are included in a common data bank which until now covers 61 engines. 13 of these engines were measured according to a detailed common protocol, which was elaborated for the D.A.CH project first and was then introduced for the European projects in a revised version. These measurements include a 54 steady state point engine emission map and the test of at least three different transient cycles.

Measurements of four HDV on the chassis dynamometer of the TU-Graz were used for the model validation, for three of them the engine was measured on the engine test bed too.

For the simulation of the HDV emission factors a detailed simulation program was developed. The model PHEM (Passenger car and Heavy duty Emission model) is capable of calculating fuel consumption and emissions for any vehicles and driving cycles with a high accuracy using engine emission maps and transient correction functions.

4.2 Approach

The targeted results are emission factors for different categories of the HDV fleet (separated according to engine technology and vehicle weight classes) with different loadings of the HDV for different representative driving cycles at different road gradients (Figure 20). The results are emission factors for more than 30.000 combinations of vehicle categories, driving cycles, road gradients and vehicle loadings. These emission factors are then used as an input for the "Handbook Emission Factors" e.g. (Keller,1998), which is a databank that allows the user a simple simulation of aggregated emission factors for different traffic situations.

For the elaboration of the emission factors a methodology based on interpolations from steady state emission maps was chosen, since data on more than 100 measurements of engine maps are already available which should be used in the model. With a given driving cycle and road gradient the necessary engine power is calculated second per second from the driving resistances and losses in the transmission system. The actual engine speed is simulated by the transmission ratios and a driver's gear-shift model. To take transient influences on the emission level into consideration, the results from the steady state emission map are corrected by using transient correction functions. The method was implemented into a computer executable model with a user-friendly interface. The model is optimised for simulating fuel consumption and emissions from HDV fleets but can be used for simulations of single vehicles and passenger cars as well. Figure 20 gives a schematic picture of the model PHEM (Passenger car & Heavy duty Emission Model).

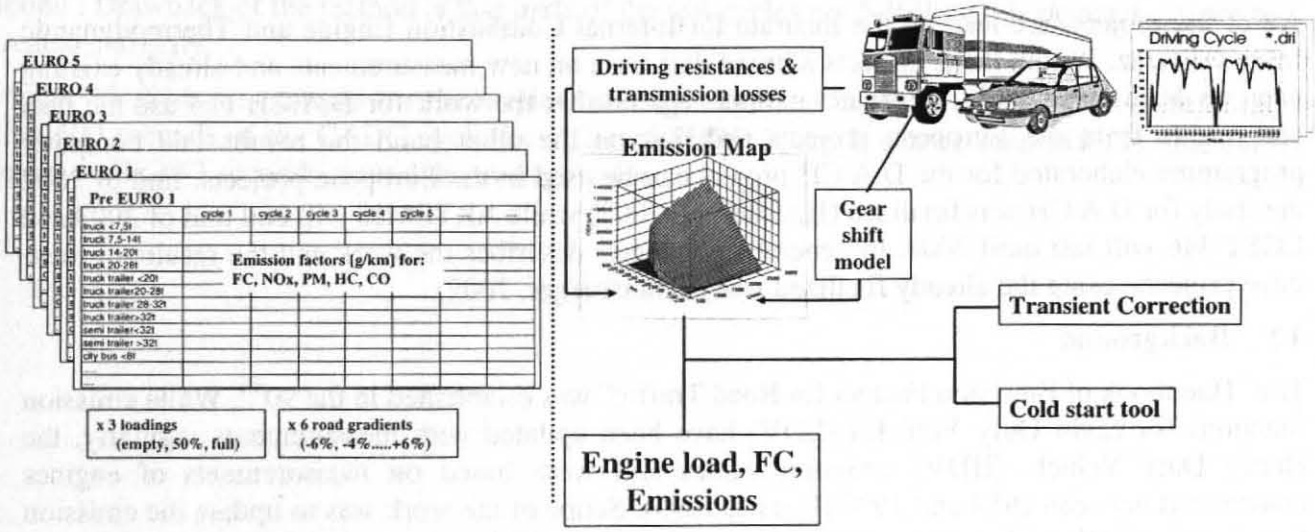

Figure 20: Emission factors to be modeled and diagram of the model PHEM from TU-Graz

Compared to direct measurement of the emission factors on the chassis dynamometer or – like done for LDV – to simulate the emissions using a vehicle speed times vehicle acceleration emission map (e.g. Hassel, 1993) this method has a disadvantage and many advantages when applied for HDV.

The main advantage of measuring emission factors directly is the higher accuracy and reliability of the factors for the tested vehicles since a model always has some simplifications and inaccuracies compared to the reality.

On the other hand, the model makes use of already existing data to a maximum possible extent. From existing measurements data on more than 60 engines is already available (steady state emission maps), which has a quality high enough to be used for the simulation of emission factors whereas only a few measurements on the chassis dynamometer are available. Additionally, different HDV configurations often use the same engines. Thus measuring one engine on the engine test bed mostly covers a lot of different HDV.

To gain useful emission factors for HDV it is essential to take the influence of the vehicle loading and the road gradient into account. The road gradient heavily influences the driving behaviour and the emission level of HDV. Since more than 50% of the maximum allowed mass is allocated to the potential payload, the actual loading of the HDV also has a considerable effect on the emission levels, especially when combined with road gradients. To measure these influences an extensive and very expensive program for each HDV would be needed, while these effects can be simulated very accurately from the engine emission map.

In addition, the driving cycles used so far for the Handbook on Emission Factors (Steven, 1995) may be updated in the project ARTEMIS. The simulation model can produce reliable results for any cycles while measured emission factors can not be changed to an other set of driving cycles later on. Another effect of the modelling is a much better understanding of the emission behaviour of modern HDV.

In total, the model based method is based on a much broader number of measured engines than a measurement campaign on the chassis dynamometer could produce with an acceptable budget. This clearly improves the reliability of the resulting fleet emission factors. The model is also capable of giving emission factors for a unlimited number of traffic situations.

4.3 Data used

The D.A.CH.-model makes use of already existing measurements to a large extent. For this purpose a coordinated data collection of all partners from ARTEMIS-WP 400 and COST 346 was launched using standardised formats for data transfer.

The measurement programme for the D.A.CH. project and accordingly for ARTEMIS-WP 400 was designed to fill open gaps and to develop a method capable of using all the data in a consistent way. Certainly the data gained from the new measurements are included into the data collection.

From the data collection campaign measurements on 122 engines are available. For approximately half of the engines only emission maps from the 13-mode test (R 49) and the new ESC are available. For the others additional off-cycle points have been measured in the steady state tests. For 15 engines transient tests and complete steady state emission maps are available. Thirteen of these engines have already been measured according to the ARTEMIS measurement programme. Most of the engines measured were derived from HDV in use for two months up to 2 years with regular service intervals.

While ARTEMIS WP 400 will go on until July 2003 and COST 346 lasts until 2004, the D.A.CH programme makes use of the data and methods available until July 2002. Table 1 to Table 4 show the engines used in the final version of the model.

Table 1: engines with construction year/certification level before EURO 1 used for the project

Engine Type	tests				Remarks	Steady state map	Rated power [kW]	rpm idle	rpm rated
	ECE R49	ESC	Off cycle points	Nr. of transient tests					
DB-OM 364 I	x		x	0	RWTÜV; 90ties German measurements	35 points	66.8	600	2800
DB-OM 441 I	x		x	0	RWTÜV; 90ties German measurements	35 points	163.36	600	2100
DB-OM 442 AI/3	x		x	0	RWTÜV; 90ties German measurements	35 points	270.43	600	1720
DB-OM 442A	x		x	0	RWTÜV; 90ties German measurements	35 points	308.98	600	2100
DB-OM 447 HAI/1	x		x	0	RWTÜV; 90ties German measurements	35 points	214.52	600	2200
DB-OM 447 HI	x		x	0	RWTÜV; 90ties German measurements	35 points	155.23	600	2200
MAN D 0826/LF02	x		x	0	RWTÜV; 90ties German measurements	35 points	168.62	500	2400
MAN D28.LF03	x		x	0	RWTÜV; 90ties German measurements	35 points	274.25	600	2000
MAN D28.LU01	x		x	0	RWTÜV; 90ties German measurements	35 points	260.28	600	2000
MAN D2866F	x		x	0	RWTÜV; 90ties German measurements	35 points	168.03	600	2200
Scania DSC1130	x		x	0	RWTÜV; 90ties German measurements	35 points	248.26	500	2000
DB-OM 314.V	x		x	0	RWTÜV; 90ties German measurements	35 points	65.34	570	2850
DB-OM 352 A.8	x		x	0	RWTÜV; 90ties German measurements	35 points	128.33	600	2850
DB-OM 352.X/1	x		x	0	RWTÜV; 90ties German measurements	35 points	97.52	570	2850
DB-OM 366LA; CH1	x		x	0	RWTÜV; 90ties German measurements	35 points	185.14	600	2600
DB-OM 401.I	x		x	0	RWTÜV; 90ties German measurements	35 points	148.89	600	2400
DB-OM 402.I	x		x	0	RWTÜV; 90ties German measurements	35 points	198.52	600	2400
DB-OM 403.I	x		x	0	RWTÜV; 90ties German measurements	35 points	223.38	600	2500
DB-OM 407 HX	x		x	0	RWTÜV; 90ties German measurements	35 points	177.4	500	2200
DB-OM 422 i/3	x		x	0	RWTÜV; 90ties German measurements	35 points	205.61	600	2300
DB-OM 422.A.II/5	x		x	0	RWTÜV; 90ties German measurements	35 points	241.65	600	2300
DB-OM 442 A	x		x	2	TU-Graz; 90ties German measurements	35 Points	269	600	2100
DB-OM 447 hII	x		x	2	TU-Graz; 90ties German measurements	35 Points	177	600	2200
DB-OM 447hII; CH 2	x		x	0	RWTÜV; 90ties German measurements	35 points	179.7	800	2200
KHD BF6L	x		x	0	RWTÜV; 90ties German measurements	35 points	114.99	650	2500
KHD F4L	x		x	0	RWTÜV; 90ties German measurements	35 points	64.29	650	2800
MAN MKF/280	x		x	0	RWTÜV; 90ties German measurements	35 points	201.7	500	2200
MAN MUH 192	x		x	0	RWTÜV; 90ties German measurements	35 points	135.89	500	2200
MAN-VW D0226	x		x	0	RWTÜV; 90ties German measurements	35 points	97.64	600	3050
Volvo TD102F	x		x	0	RWTÜV; 90ties German measurements	35 points	220.99	500	2050
VOLVO TD61F	x		x	0	RWTÜV; 90ties German measurements	35 points	145.46	600	2600
Scania DSC1112;L02;CH 4	x		x	0	RWTÜV; 90ties German measurements	35 points	253.42	600	2000

Table 2: engines with certification level EURO 1 used for the project

Engine Type	tests				Remarks	Steady state map	Rated power [kW]	rpm idle	rpm rated
	ECE R49	ESC	Off cycle points	Nr. of transient tests					
DB-OM 366LA; CH1	x		x	0	RWTÜV; 90ties German measurements	35 points	185.14	600	2600
DB OM 366 LA VII/1	x	x		0	NL in-use compliance programme	22 points	112.8	600	2600
DB OM 366 LA	x		x	2	TU-Graz; 90ties German measurements	30 points	177	600	2600
DB OM 401 LA.V/1	x		x	0	German in-use compliance programme	29 points	230	560	2100
DB OM 401 LA.IV/1	x	x		0	NL in-use compliance programme	22 points	200	600	2100
DB-OM 441 LA I/1	x		x	0	RWTÜV; 90ties German measurements	35 points	242.79	600	2100
MAN D0824 LFL05	x		x	0	German in-use compliance programme	29 points	114	785	2400
MAN D0824LF01	x	x		0	NL in-use compliance programme	22 points	114.7	650	2400
MAN D0826LF08	x	x		0	NL in-use compliance programme	22 points	164.5	600	2400
Scania DSC 1121	x	x		0	NL in-use compliance programme	22 points	235.6	525	1900
Scania DSC 1408	x	x		0	NL in-use compliance programme	22 points	304.9	450	1900
Volvo TD 73 ES	x	x		0	NL in-use compliance programme	22 points	191	600	2400

Table 3: engines with certification level EURO 2 used for the project

Engine Type	tests				Remarks	Steady state map	Rated power [kW]	rpm idle	rpm rated
	ECE R49	ESC	Off cycle points	Nr. of transient tests					
DAF XF280M	x	x	x	12	TNO; ARTEMIS tests	71 Points	280	542	2000
IVECO 120E18/FP (FIAT 8060,45,B)			x		TUG; ARTEMIS tests vehicle	38 points	130	750	2700
IVECO 120E23 (FIAT8060.45K)	x	x	x	5	EMPA; ARTEMIS tests	52 points	167	750	2700
IVECO 8060.45S	x		x	0	German in-use compliance programme	29 points	167	600	2700
MAN D0826 LF11	x	x	x	4	RWTÜV; ARTEMIS tests	52 points	162	650	2400
MAN D0826 LF17	x		x	0	German in-use compliance programme	52 points	191	600	2300
MAN D2865LF21	x		x	0	German in-use compliance programme	29 points	250	650	2000
MAN D2866 LF20/ 19.403 semi trailer	x	x	x	2	TU-Graz; ARTEMIS tests engine + vehicle	52 points	297	600	2000
MB OM 441 LA 1/10	x	x	x	3	EMPA; ARTEMIS tests	52 points	247	513	1900
MB OM 441 LA.II/1	x		x	0	German in-use compliance programme	29 points	230	550	2100
MB OM 442 LA 6/1	x	x	x	5	EMPA; ARTEMIS tests	52 points	280	560	1900
MB OM 906 LA-II/1	x		x	0	German in-use compliance programme	29 points	170	600	2300
SCANIA DSC 1201	x	x	x	3	TU-Graz; ARTEMIS tests + vehicle	52 points	294	500	1892
SCANIA DSC 1201	x	x	x	5	EMPA; ARTEMIS tests	52 points	294	590	1900
Volvo D12A380	x	x	x	5	EMPA; ARTEMIS tests	52 points	279	530	1800
Volvo D12A380EC97	x		x	0	German in-use compliance programme	29 points	279	510	1800

Table 4: engines with certification level EURO 3 used for the project

Engine Type	ECE R49	ESC	Off cycle points	Nr. of transient tests	Remarks	Steady state map	Rated power [kW]	rpm idle	rpm rated
DAF PE183C	x	x	x	25	TNO; ARTEMIS tests	44 Points	183	600	2300
MAN D0836_LF04	x	x	x	9	RWTÜV; ARTEMIS tests	40 Points	162	600	2400
Scania DC 1201 EU3	x	x	x	4	TU-Graz; ARTEMIS tests + vehicle	40 Points	305	500	1914
IVECO Cursor 10	x	x	x	5	RWTÜV; ARTEMIS tests	40 Points	316	550	2100

From measurements on the HDV chassis dynamometer data for seven HDV are available. Three of the available HDV were measured according to the D.A.CH./ARTEMIS programme, this includes nine different driving cycles and an extensive recording of relevant parameters (e.g. engine speed, temperatures and pressures of inlet air and outlet air,..) and measurements of the engine from the HDV on the engine test bed. One HDV (IVECO 120E18/FP) was instrumented with on-board measurement systems and simultaneously measured on the chassis dynamometer but the engine was not tested on the engine test bed.

Table 5: Data used from HDV chassis dynamometer tests

		Measurements available			
Vehicle Type	Certification Level	Coast down	steady state	Transient tests	Remarks
MB O 45	Pre EU 1			X	2 cycles with 3 loadings, measured 1993
MB O 303	Pre EU 1			X	2 cycles with 3 loadings, measured 1993
MB 1324	EU 1			X	2 cycles with 3 loadings, measured 1993
D2866 LF20/ MAN 19.403	EU 2	X	X	X	9 cycles + steady state
IVECO 120E18/FP	EU 2	X	X	X	9 cycles + steady state
SCANIA 400 E2	EU 2	X	X	X	9 cycles + steady state
SCANIA DC 1201	EU 3	X	X	X	9 cycles + steady state

4.3.1 Engine test bed, steady state measurements

The measurements from D.A.CH and ARTEMIS WP 400 conducted on engine test beds provided the following information:

(1) Data on steady-state engine emission maps (emissions over engine speed and engine torque)

(2) Basic data for the development of functions for the "dynamic correction" (i.e. the different emission behaviour under steady-state and transient cycles).

For (1), the main task was to devise a methodology which is capable of including the emission maps from the data collection - where most often different points have been measured - in a way, that real world engine loads can be interpolated accurately from the engine emission maps (i.e. the whole engine map has to be covered). The main projects to be included from the data collection are given in Table 6.

To develop a method capable of making use of most of the data from national projects the D.A.CH./ARTEMIS measurement programme includes most of the points measured in the main national projects.

Table 6: Description of the main national measurement programmes on HDV engines

Programme	No. of engines	Engine maps available
Netherlands in-use-compliance tests	more than 100	13-mode test, some ESC additionally
German in-use-compliance tests	20	26 different points of engine speed and engine torque
Former German HDV-programme	30	35 different points of engine speed and engine torque (all engines older than year 1993)
Smaller national programmes	more than 10	13-mode-test, ESC, others
Total:	**>160**	**> 4 different map-configurations**

The following steady-state measurements are included in the ARTEMIS programme:

- R 49 (13-mode test)
- ESC (European Steady State Cycle)
- ARTEMIS-steady state

The 13-mode test and the ESC have to be performed as given in the corresponding EC documents. This also includes the record of the full-load curve.

For the ARTEMIS steady state test interim points between the engine speeds A, B and C[3] from the ESC-test were selected to check possible increases in the emissions in this area. Additionally, points in the engine speed range below speed "A" are measured. These points are fixed independently of the full load curve. Furthermore, 2 points between speed "C" and the rated speed

[3] The engine speeds A, B and C have to be calculated as given in the EC regulation ECE R 49 and 88/77/EWG for the European Stationary Cycle (ESC):
engine speed A = nlo + 25% * (nhi-nlo)
engine speed B = nlo + 50% * (nhi-nlo)
engine speed C = nlo + 75% * (nhi-nlo)
nlo....engine speed where 50% from the rated power are reached
nhi....engine sped (above rated rpm) where the power decreases to 70% of the rated power are reached

were added. In total, 29 points are included in the ARTEMIS test, which are measured in addition to the ESC and R 49 tests. Figure 21 gives the measurement points for the ARTEMIS programme (example for a given full load curve).

Table 7 shows the calculation routine to fix the points. The normalised engine speed given is only an example for one engine. The measurement conditions are defined as in the ESC (duration of measuring each point) and the points have to be measured in a sequence according to increasing engine power.

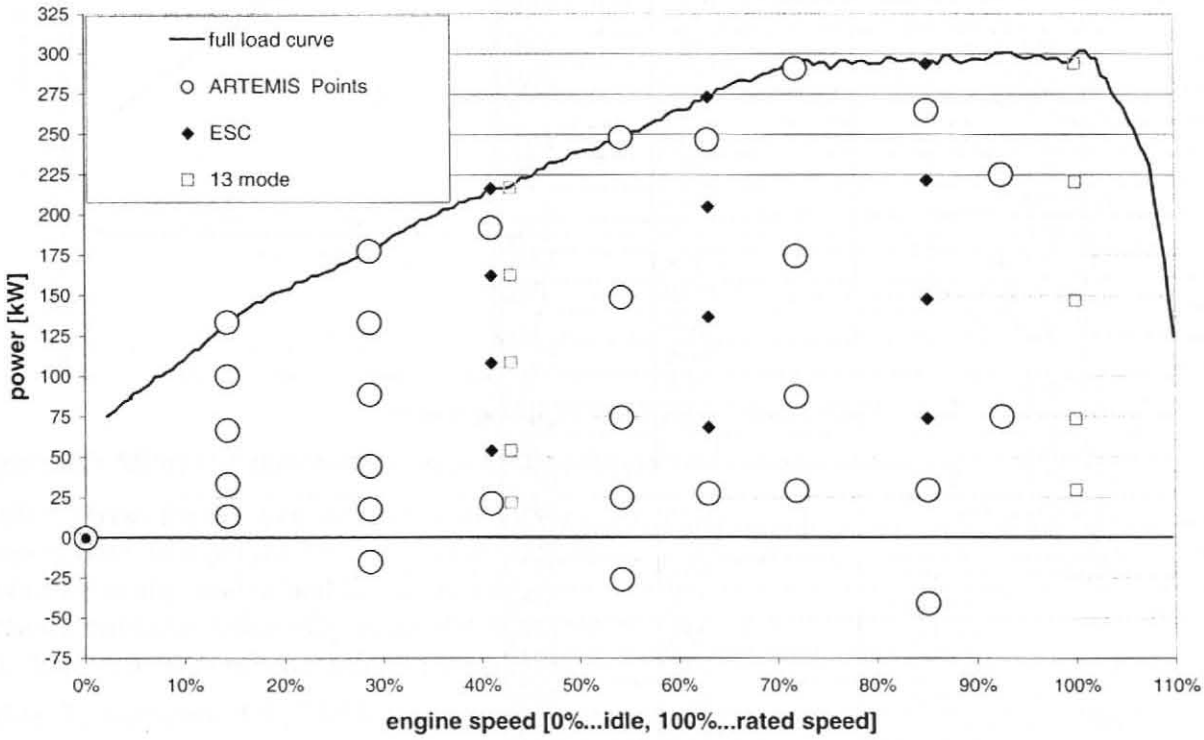

Figure 21: Steady-state points measured in the ARTEMIS programme (example)

Table 7: Test points for the ARTEMIS steady-state test

		(example) norm. speed	normalised Torque						
	n_idle	0.0%							
TUG-Interim	$0.35*n_A$	14.3%		10%	25%	50%	75%		100%
TUG-Interim	$0.7*n_A$	28.7%	-100%	10%	25%	50%	75%		100%
ESC-A	$n_{lo} + 0{,}25*(n_{hi} - n_{lo})$	41.0%		10%				90%	
ESC-B	$n_{lo} + 0{,}50*(n_{hi} - n_{lo})$	63.0%		10%				90%	
ESC-C	$n_{lo} + 0{,}75*(n_{hi} - n_{lo})$	85.1%	-100%	10%				90%	
TUG-Interim	$0.4*n_A+0.6*n_B$	54.2%	-100%	10%	30%		60%		100%
TUG-Interim	$0.6*n_B+0.4*n_C$	71.9%		10%	30%		60%		100%
TUG-Interim	$n_C+(\text{rated speed}-n_C)/2$	92.5%			25%		75%		

Explanations:

- 100% : .....motoring curve

n_norm = (n - n_idle)/(n_rated - n_idle)

Table 8: Sequence for the ARTEMIS steady-state test

Point Nr.	Comment	normalised torque	Engine speed [%] *"example"*
1	nlo + 0,75*(nhi - nlo)	-100%	72%
2	0.4*nA+0.6*nB	-100%	29%
3	0.7*nA	-100%	41%
4	0.35*nA	10%	14%
5	0.7*nA	10%	29%
6	nlo + 0,25*(nhi - nlo)	10%	41%
7	0.4*nA+0.6*nB	10%	54%
8	nlo + 0,50*(nhi - nlo)	10%	63%
9	0.6*nB+0.4*nC	10%	72%
10	nlo + 0,75*(nhi - nlo)	10%	85%
11	0.35*nA	25%	14%
12	0.7*nA	25%	29%
13	0.35*nA	50%	14%
14	0.4*nA+0.6*nB	30%	54%
15	interim C-rated speed	25%	93%
16	0.6*nB+0.4*nC	30%	72%
17	0.7*nA	50%	29%
18	0.35*nA	75%	14%
19	0.7*nA	75%	29%
20	0.35*nA	100%	14%
21	0.4*nA+0.6*nB	60%	54%
22	0.6*nB+0.4*nC	60%	72%
23	0.7*nA	100%	29%
24	nlo + 0,25*(nhi - nlo)	90%	41%
25	interim C-rated speed	75%	93%
26	nlo + 0,50*(nhi - nlo)	90%	63%
27	0.4*nA+0.6*nB	100%	54%
28	nlo + 0,75*(nhi - nlo)	90%	85%
29	0.6*nB+0.4*nC	100%	72%

Measurements for the particulate steady state map

Wherever possible, according to the schedule of each partner, a particulate emission map with all points (ESC, 13-mode test and ARTEMIS-test) is measured. Since each point has to be run for rather a long time to collect enough particulate mass (PM) on the filter, this is not possible for every engine.

Where the time schedule does not allow the measurement of particulate mass for each point in Table 7, particulates are measured at a reduced number of points (15), as defined in Table 9. The points are part of the ESC, ARTEMIS, and 13-mode tests and were selected to cover the whole map (Figure 22).

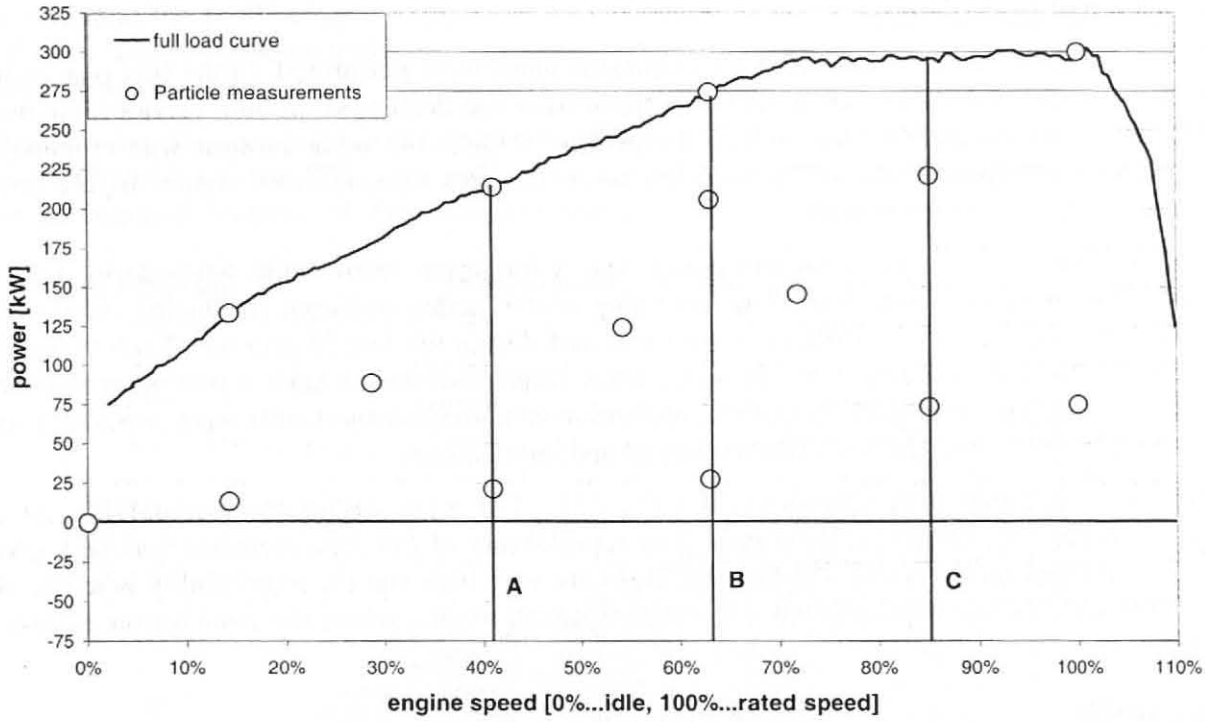

Figure 22: Minimum number of points where particulate mass emissions are measured separately

Table 9 shows the calculation routine to fix the particle points. The normalised engine speed given again is only an example for one engine. The duration of measuring each point has to be selected according to the engine and the point measured to sample a sufficient mass on the filter to gain accurate emission values for particulates. As for the total ARTEMIS test the points have to be measured in a sequence according to increasing engine power.

Table 9: Reduced ARTEMIS test for particulate emission measurements (normalised engine speeds given only as an example for one engine)

		(example) norm. speed	normalised Torque						
	n_idle	0.0%		0%					
TUG-Interim	$0.35*n_A$	14.3%		10%					100%
TUG-Interim	$0.7*n_A$	28.7%				50%			
A	$n_{lo} + 0{,}25*(n_{hi} - n_{lo})$	41.0%		10%					100%
B	$n_{lo} + 0{,}50*(n_{hi} - n_{lo})$	63.0%		10%			75%		100%
C	$n_{lo} + 0{,}75*(n_{hi} - n_{lo})$	85.1%			25%		75%		
	rated speed	100.0%			25%				100%
TUG-Interim	$0.4*n_A+0.6*n_B$	54.2%				50%			
TUG-Interim	$0.6*n_B+0.4*n_C$	71.9%				50%			
TUG-Interim	$n_C+(\text{rated speed}-n_C)/2$	92.5%							

4.3.1.1 Setting of the sequence and duration of measurement

To run the ARTEMIS emission map on the engine test bed, an order of the modes and their duration had to be defined. Therefore, the influences of these two parameters on the emissions were investigated.

Since these investigations were time correlated with the measurements planned in Switzerland, EMPA took the task to come up with the inputs needed. The results of the following measurement programme lead to the decision on the final steady state measurement programme as defined in chapter 4.3.1, see also (Hausberger, 2000).

Measurement programme

Three different versions of the ARTEMIS emission maps were performed. In the first one, engine power was increased from mode to mode, in the second one decreased. In both versions, the mode duration was set to 2 minutes like in ESC. In the third version, the mode duration was 5 minutes in order to provide sufficient sampling time for the particulates measurement. Again, engine power was increased from mode to mode.

In all versions, the change in engine power was a minimum from mode to mode in order to optimise the preconditioning time. The beginning of the modes was used for engine stabilization and the emissions (excl. particulates) were measured during the last 35 seconds. Each version of the ARTEMIS emission map was measured three times in order to have a minimum statistical impression about the repeatability of these measurements. The measurements were performed with a 12 l EURO II engine, which was turbocharged and inter cooled.

During all test modes, the emissions of CO_2, NO_X, CO were within the repeatability for all versions of the ARTEMIS emission map. The repeatability of the measurements was very good, only in some measuring points, the CO emissions are very high and the repeatability is worse. All these points are at low engine speed with relatively high torque, where the combustion process is not stable.

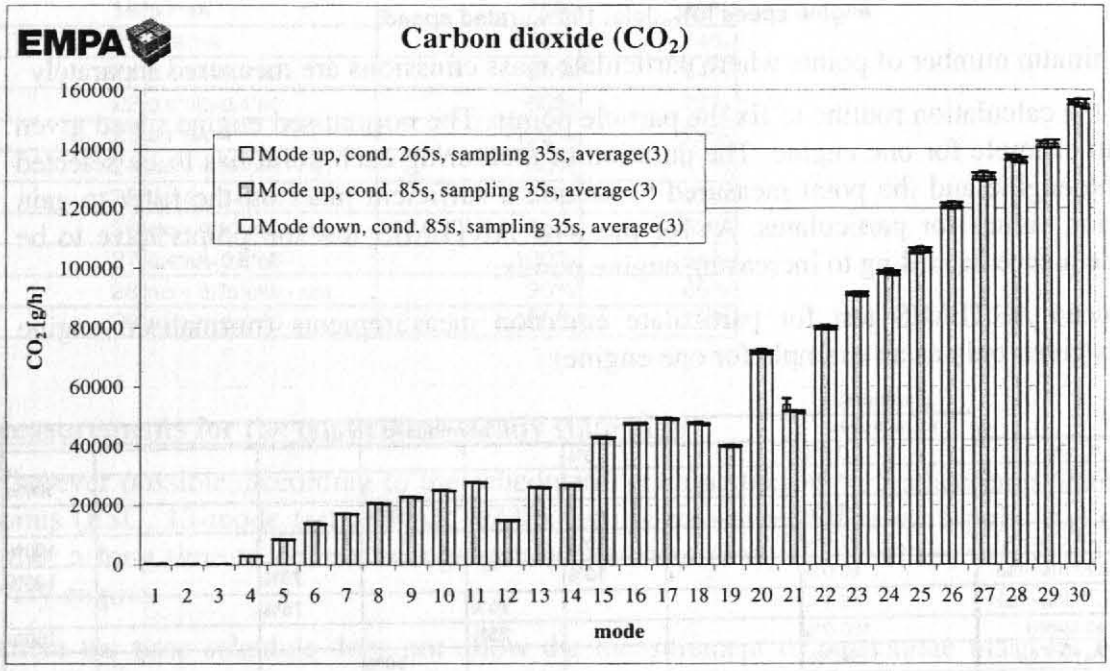

Figure 23: CO_2 emissions at three different measurement modes of the ARTEMIS steady state test

During some test modes, the hydrocarbon emissions are different in the three versions of the emission map (Figure 26). Often, the higher emissions are measured in the version with the high mode duration. Since the standard deviation of the measurements is mostly at the same order of magnitude as the differences themselves, no significant conclusion can be drawn.

Based on the results of the measurements it was decided that the ARTEMIS emission map will be performed in an upward way, i.e. with increasing engine power from mode to mode and to use a test mode duration of 2 minutes for load points where no particulate measurements were performed (procedure according to 1999/96/EG for the ESC type approval test). If measuring particulates as well (multifilter test), the test mode duration had to be set to at least 5 minutes to have enough particle loading on the filter.

The ESC and the R 49 13-mode test have been performed according to the corresponding EC regulations and the gaseous emissions have been recorded for each point separately to complete the engine emission maps.

The following figures contain the emission results obtained with the three versions of the ARTEMIS emission map. The bars represent the averages of three measurements and the lines show the standard deviation of the individual measurements.

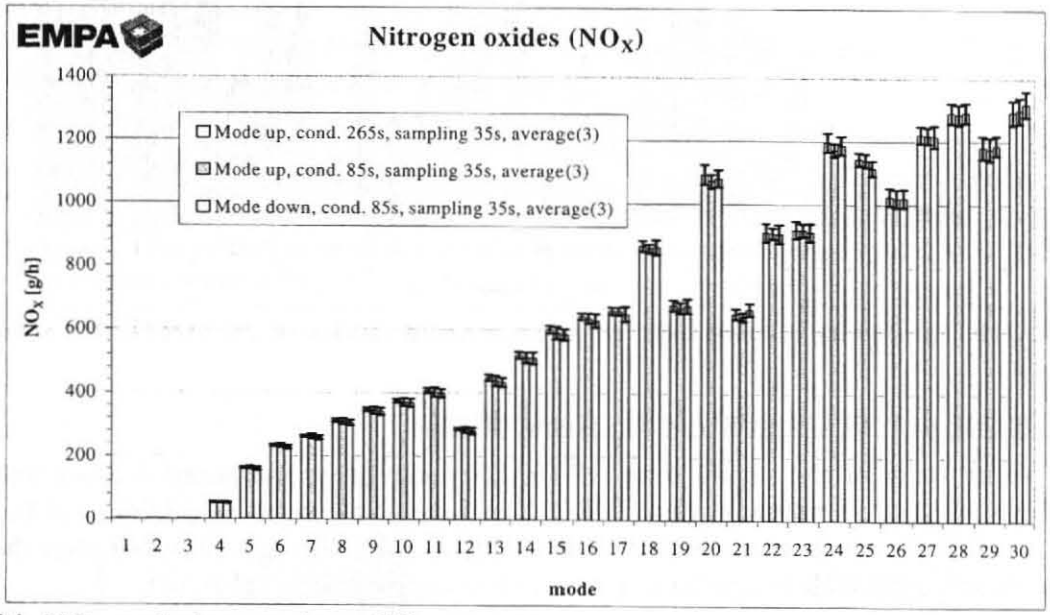

Figure 24: NO_X emissions at three different measurement modes of the ARTEMIS steady state test

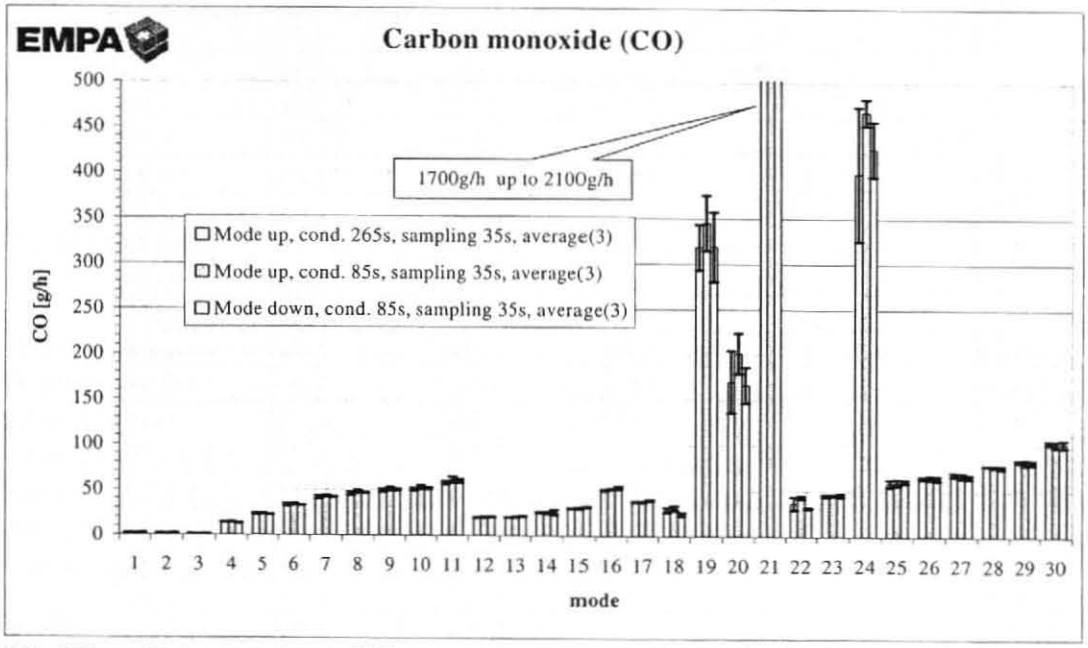

Figure 25: CO emissions at three different measurement modes of the ARTEMIS steady state test

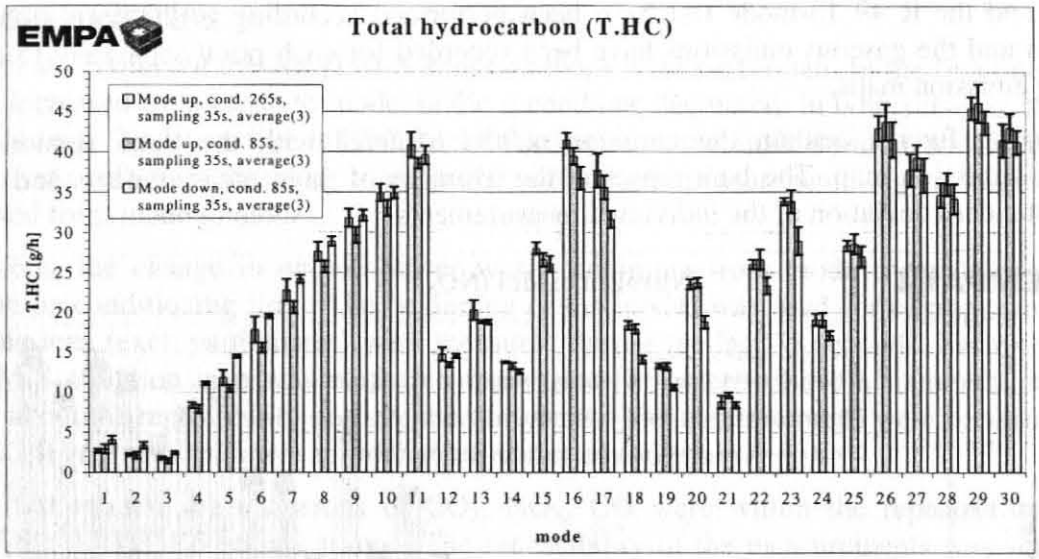

Figure 26: THC emissions at three different measurement modes of the ARTEMIS steady state test

4.3.1.2 Repeatability of the steady state measurements

At the TU-Graz some of the steady state ARTEMIS points were measured 4 times with mode durations between 2 to 15 minutes at an EURO 2 engine to assess the repeatability of the results for HDV diesel engines. As already shown in chapter 4.3.1.1 the deviation between the single measurements are small with exception of points at low engine loads (Table 10).

Table 10: Deviation of measured emissions at steady state points in 4 repetitions (EURO 2, 300 kW)

Measured point		Deviation to average measured value			
kW	U/min	NOx	HC	CO	CO_2
-0.04	600	-0.2%	1.4%	-6.9%	-1.7%
0.15	600	3.3%	3.4%	-4.8%	0.8%
-0.21	601	-4.0%	1.0%	-7.3%	-1.1%
0.10	601	0.8%	-5.8%	19.0%	2.0%
Average deviation at idling		**2.6%**	**3.4%**	**11.0%**	**1.5%**
54.02	1174	1.6%	-0.3%	1.2%	0.9%
54.09	1174	0.6%	-2.1%	-1.0%	0.5%
54.32	1174	-1.6%	3.3%	3.3%	-0.7%
54.56	1174	-0.6%	-0.8%	-3.6%	-0.7%
Average deviation at 54kW, 1174 rpm		1.2%	**2.0%**	**2.6%**	**0.7%**
108.27	1174	1.3%	1.1%	3.0%	0.3%
108.46	1174	-4.1%	0.8%	3.3%	-0.9%
108.64	1174	1.6%	-1.4%	-4.2%	0.4%
108.73	1174	1.3%	-0.4%	-2.1%	0.2%
Average deviation at 109 kW, 1174 rpm		**2.4%**	**1.0%**	**3.2%**	**0.5%**
272.71	1482	-0.1%	-4.9%	1.6%	-0.2%
273.96	1483	0.9%	0.3%	-0.5%	0.4%
274.31	1483	-0.2%	1.4%	-1.4%	0.0%
274.41	1483	-0.6%	3.2%	0.4%	-0.2%
Average deviation at 274 kW, 1483 rpm		**0.6%**	**3.0%**	**1.1%**	**0.2%**
220.46	1790	0.3%	-1.9%	-0.8%	-0.3%
222.34	1791	-0.7%	2.3%	1.3%	-0.6%
220.86	1791	-0.3%	-1.2%	0.4%	0.5%
221.29	1791	0.7%	0.8%	-1.0%	0.4%
Average deviation at 221 kW, 1791 rpm		**0.5%**	**1.6%**	**1.0%**	**0.5%**

4.3.1.3 Assessment of the steady state measurements

The assessment of the measured steady state engine maps shows that it is essential for the elaboration of real world emission factors for modern engines to use off-cycle measurements as well. Since electronic engine control systems – used from EURO 2 levels on - allow different injection timings over the engine map, optimisations in the specific fuel consumption can result in increased NO_x emissions outside of the homologation test points. Actual common rail injection systems in EURO 3 engines give additional degrees of freedom e.g. from the rail-pressure and the possibility for pre-injection and post-injection what offers also possibilities for influencing the particle emissions differently within the engine map.

Figure 27 shows two typical NO_x engine emission maps for Euro 1 engines with mechanical injection control. The emission maps are normalised for the engine speed (idling = 0%, rated speed = 100%) and the engine power (rated power = 100%). The emission values are given in $(g/h)/kW_{rated\ power}$. This format is used in the vehicle emission model (chapter 4.4.3.2). This special format makes engines with different rated power directly comparable in these graphs.

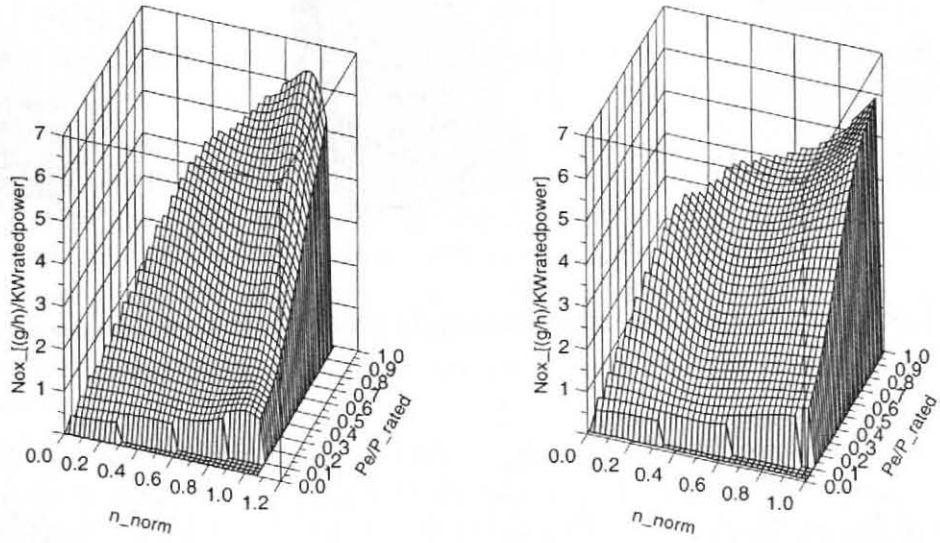

Figure 27: Typical steady-state NO_x-engine emission map for Euro 1 engines

The typical NO_x-engine emission maps from Euro 1 and "Pre-Euro 1" engines are very smooth. Figure 28 gives the NO_x emission maps for 6 different Euro 2 engines (different manufacturers). Compared to Euro 1 the NO_x levels are lower at the 13-mode test points. Off cycle the levels are rather higher than for Euro 1 engines. Obviously the injection time is later at the official test points, resulting in lower NO_x but somewhat higher fuel consumption and particle emissions. Having the demand of the customers for low specific fuel consumption of HDV in mind, for many engine models an earlier injection time is chosen at off cycle points.

The tested Euro 3 engines show a different setting according to the new ESC (European Steady State Cycle). The Euro 3 regulation also limits the NO_x emissions between the 3 engine speeds of the homologation test. Corresponding to this regulation the Euro 3 NO_x emission maps have a low level between the highest and lowest engine speed from the ESC. Outside of this range also for Euro 3 engines an optimization for the specific fuel consumption can be observed, resulting in increased NO_x emissions (Figure 29).

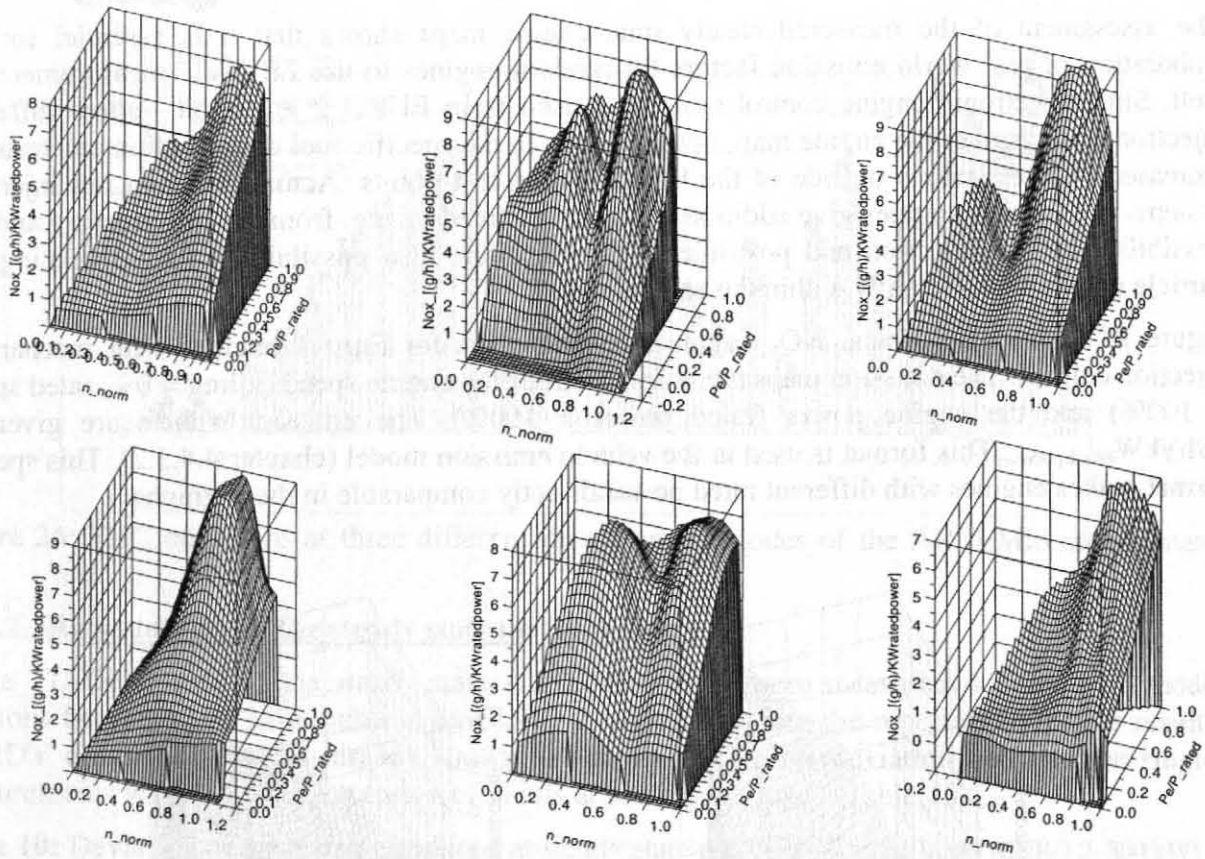

Figure 28: Steady-state NO_x-engine emission map for six different Euro 2 engines

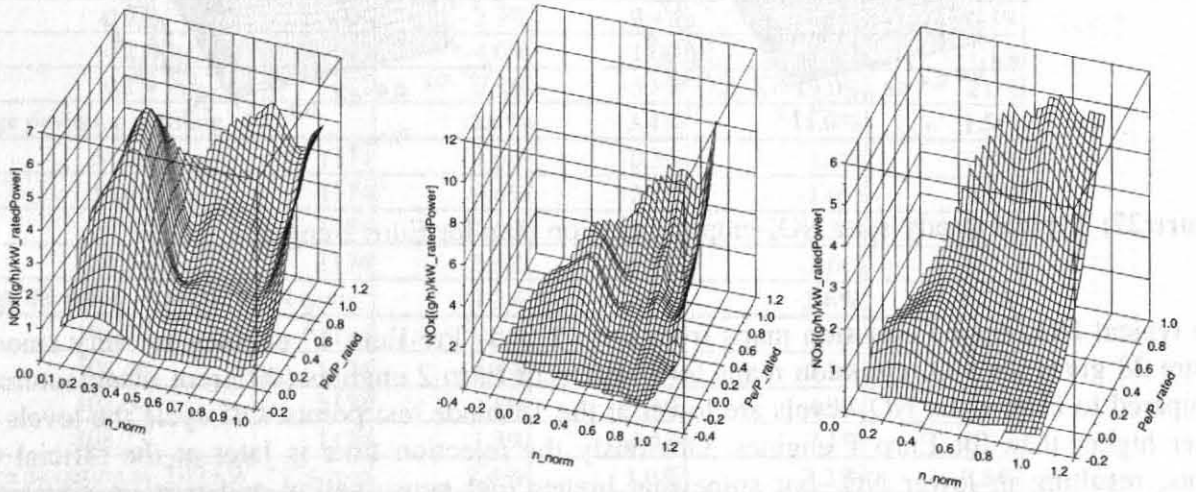

Figure 29: Steady-state NO_x-engine emission map for three Euro 3 engines

Looking at the emissions in the 13-mode test (R 49) – where for almost all engines from the data collection data is available – indicates that even in this type approval test only small reduction in the emission level has been achieved from EURO 1 to EURO 2 since EURO 2 engines on average are much closer at the limit values than the EURO 1 engines. For the EURO 3 engines the ESC test was used for the following graphs. To give an impression of the emission level over the complete engine map, the following figures show the emissions in a weighted 29-point map as well, which is drawn from the standardised engine map (see chapter 4.4.3.2). The difference to the emission values given for the ECE R49 and the ESC is that the weighted 29 Point value covers the

measured off-cycle points, too. The emission values of the single points are weighted according to an "average" engine load pattern in real world driving (see 4.4.3.2). Figure 30 shows, that the fuel consumption values correspond quite well in the ECE R49 test and the 29-point map.

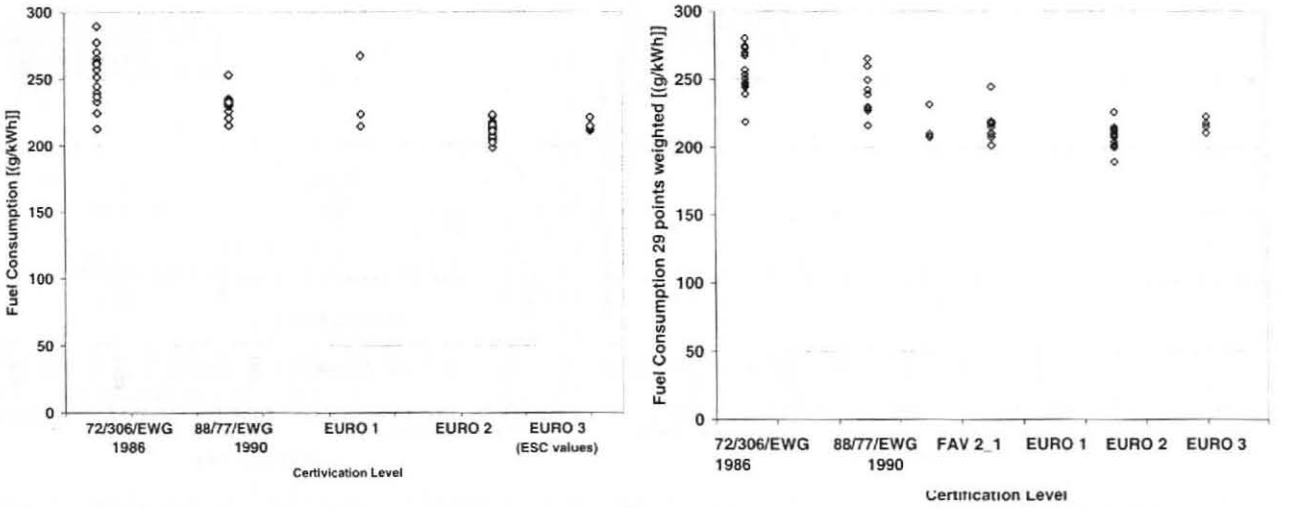

Figure 30: Fuel consumption in the type approval tests (left) and in the weighted 29-point map (right).

The average emission levels of NO_x decreased clearly from pre EURO 1 engines to EURO 1 (Figure 31). Three of the EURO 2 engines available exceed the limits in the ECE R49 test where the engine with the highest NO_x-level was not implemented into the databank for the emission factors because of obviously having malfunctions in the Engine control unit (ECU). While the NO_x-Emissions in the ECE R49 decreased from EURO 1 to EURO 2, the NO_x values in the 29-point map are on average higher for EURO 2 than for EURO 1. This indicates, that Euro 2 engines on average have higher emissions in points not covered by the R49 test. This was already visible from the engine maps given before.

The four EURO 3 engines available show lower emissions than EURO 2 engines in the type approval test (R 49 or ESC respectively), over the total engine map the NO_x values for EURO 3 are also clearly below the EURO 2 average. This results from the broader range covered by the new ESC test. The different engine control strategy at the ECE R49 points and in the other range of the engine map leads to the fact that EURO 2 and EURO 3 engines would exceed the corresponding ECE limits over the total engine map (29 point values).

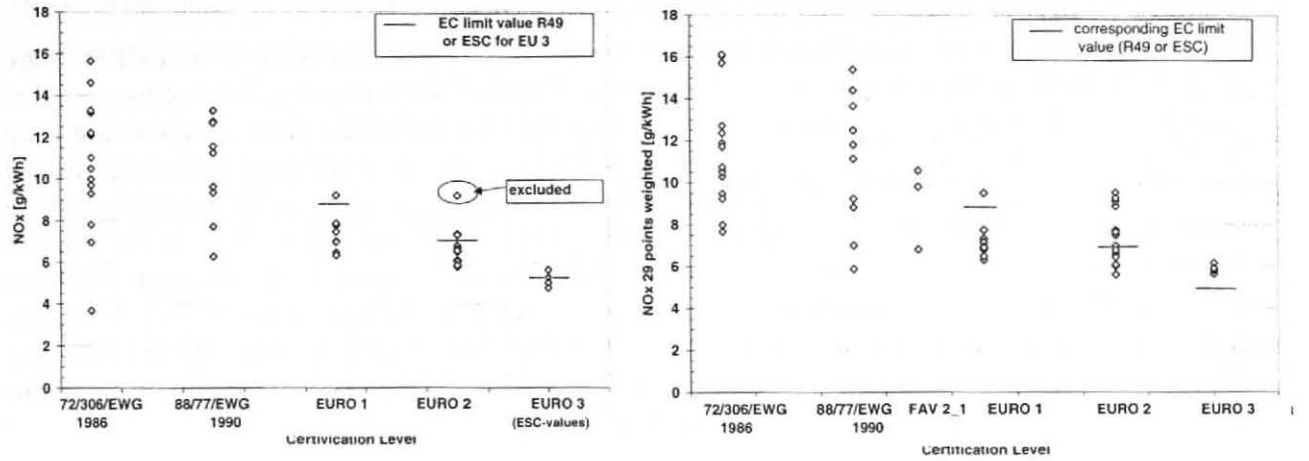

Figure 31: NO_x-emissions in the type approval tests (left) and in the weighted 29-point map (right).

Also for CO the emissions dropped from pre-EURO 1 to EURO 1 but the levels of EURO 1, 2 and EURO 3 engines look rather similar at the 29 point engine map. But CO is not a critical emission for HDV and all engines are clearly below the limits.

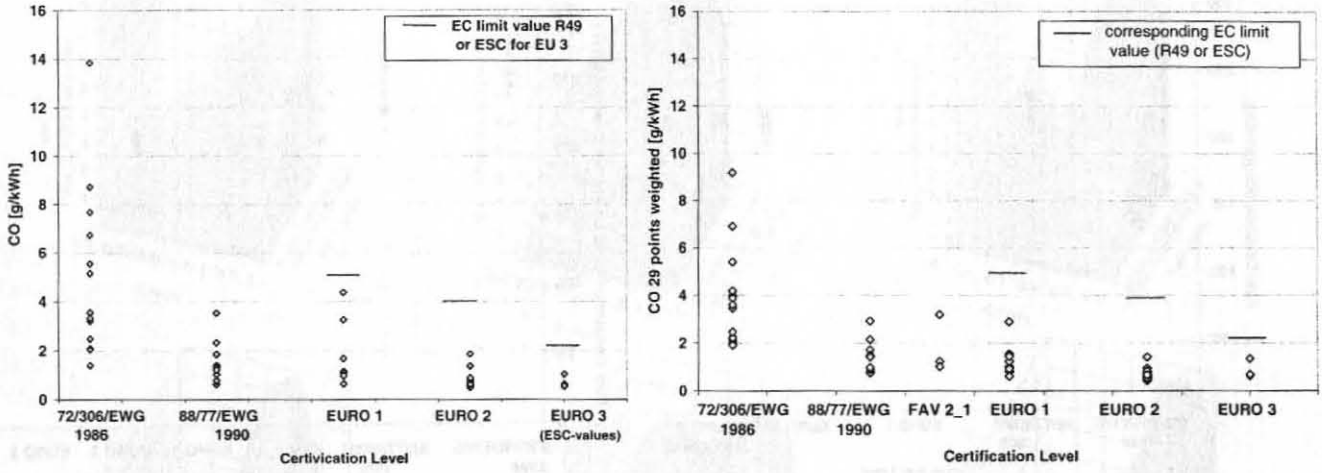

Figure 32: CO-emissions in the type approval tests (left) and in the weighted 29-point map (right).

Like for CO and NO_x the HC-emissions dropped from the construction years before 1990 to EURO 1 and only small changes occurred from EURO 1 to EURO 3.

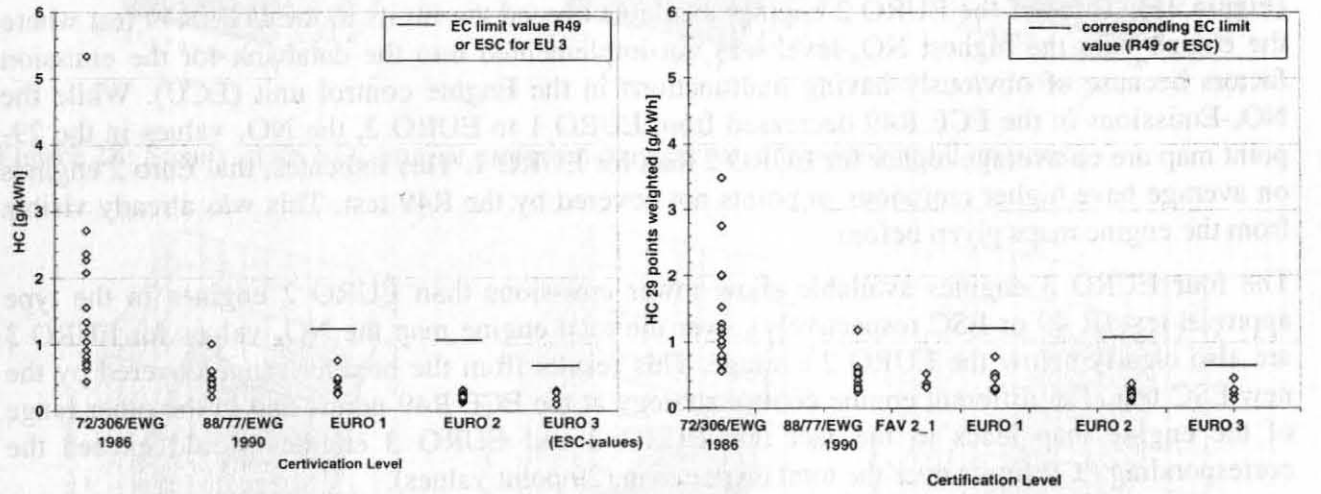

Figure 33: HC-emissions in the type approval tests (left) and in the weighted 29-point map (right).

For particle emissions no data for the R 49-13-mode tests for engines older than EURO 1 are available. Anyhow, particle engine maps are available for all of these engines, but not measured at the points according to the 13-mode test. The data on the ECE R49 tests show a significant drop from Euro 1 to Euro 2. The four EURO 3 engines have lower particulate emissions in the corresponding type approval tests than the tested Euro 2 engines. Looking at the complete engine map (29-point values) the clear decrease in the particle emissions from engines built in the 80ies to EURO 1 is visible. An even more significant drop of the particle emission levels was reached from EURO 1 to EURO 3. On the other hand, the particle emissions from the four EURO 3 engines tested are not lower than the EURO 2 values over the complete engine map, although the emission limits have been reduced by one third. Most likely this result can be addressed mainly to the more stringent NO_x limits over a broader range of the engine map.

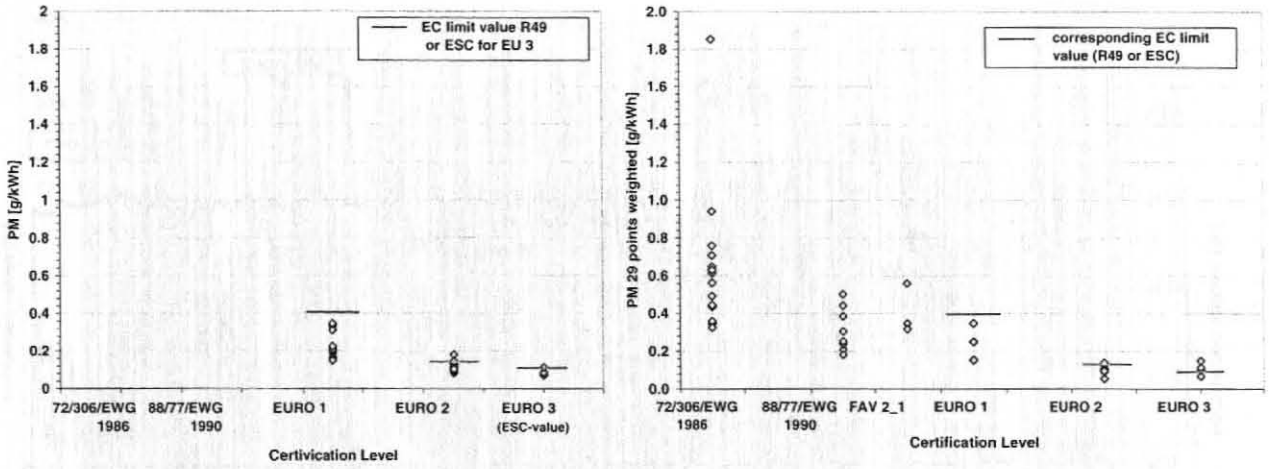

Figure 34: Particle-emissions in the type approval tests (left) and in the weighted 29-point map (right).

The analysis performed, shows clearly that the decision to take a sufficient number of off-cycle test points into the ARTEMIS steady state programme was fundamental for assessing real world emission behaviour of HDV. Emission maps obtained from the R 49 13-mode test or the ESC would only underestimate the emission level especially for NO_x significantly for many engines.

4.3.2 Engine test bed, transient measurements

The D.A.CH/ARTEMIS measurement programme consists of the following cycles:

- ETC (European Transient Cycle, Figure 35)
- ELR (European Load Response test)
- TNO-real world cycles (for 7 kW per ton total vehicle weight and 12.5 kW per ton total vehicle weight; Figure 36, Figure 37)
- DACH-Handbook-test cycle (designed to cover different transient engine load patterns for model validation rather than to reflect real world engine loads; Figure 38)

A detailed description of the test programme is given in (Hausberger, 2001).

13 engines with useful results for transient tests are available. Most of them followed exactly the ARTEMIS programme. A detailed analysis of this data for the development of transient correction functions is given in chapter 4.4.4.2.

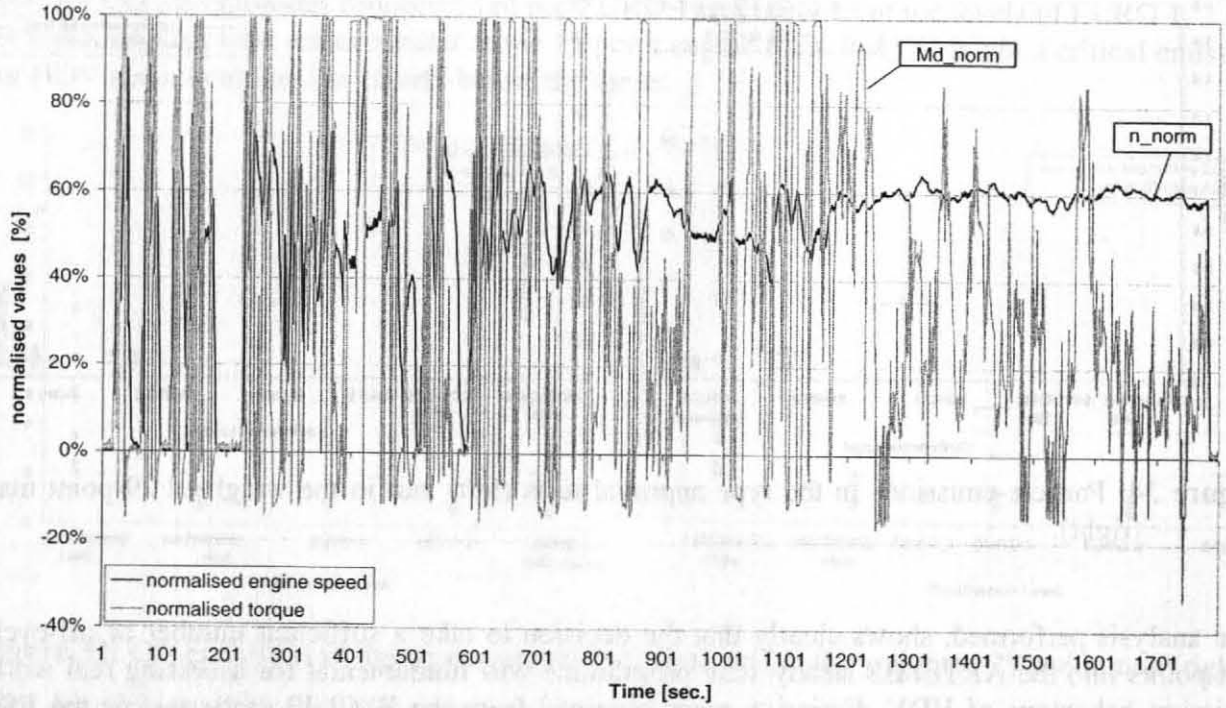

Figure 35: European Transient test Cycle (ETC)

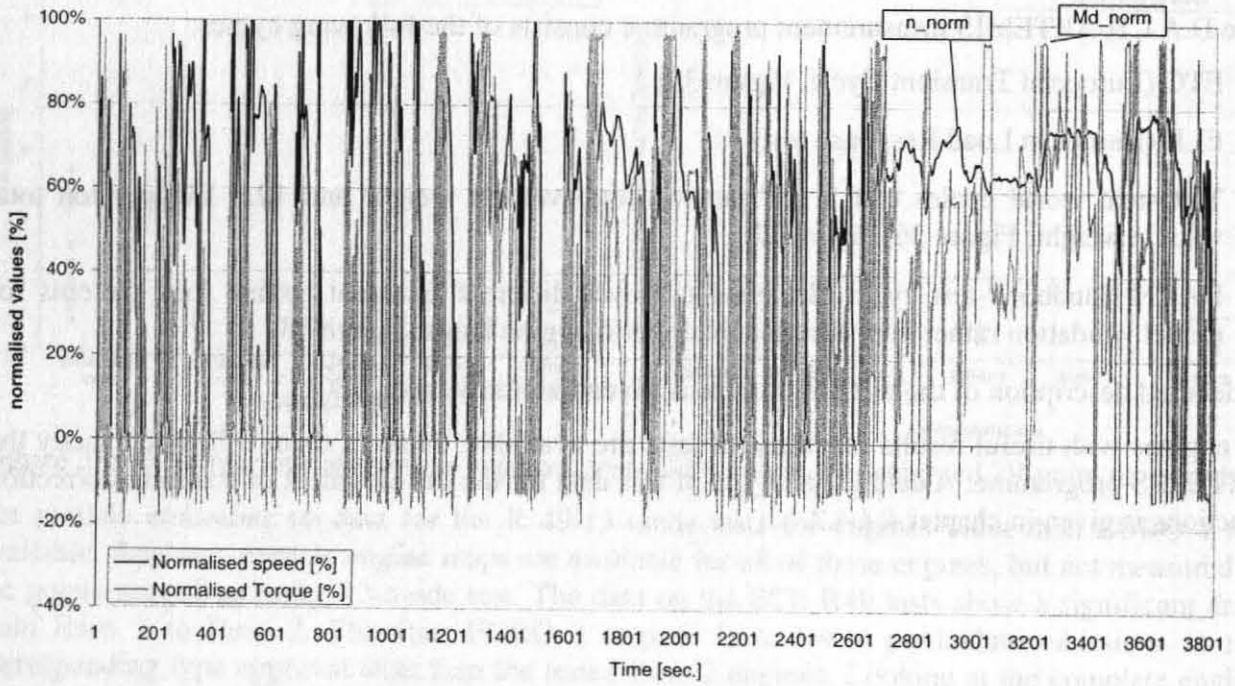

Figure 36: TNO real world test Cycle (12.5 kW/ton)

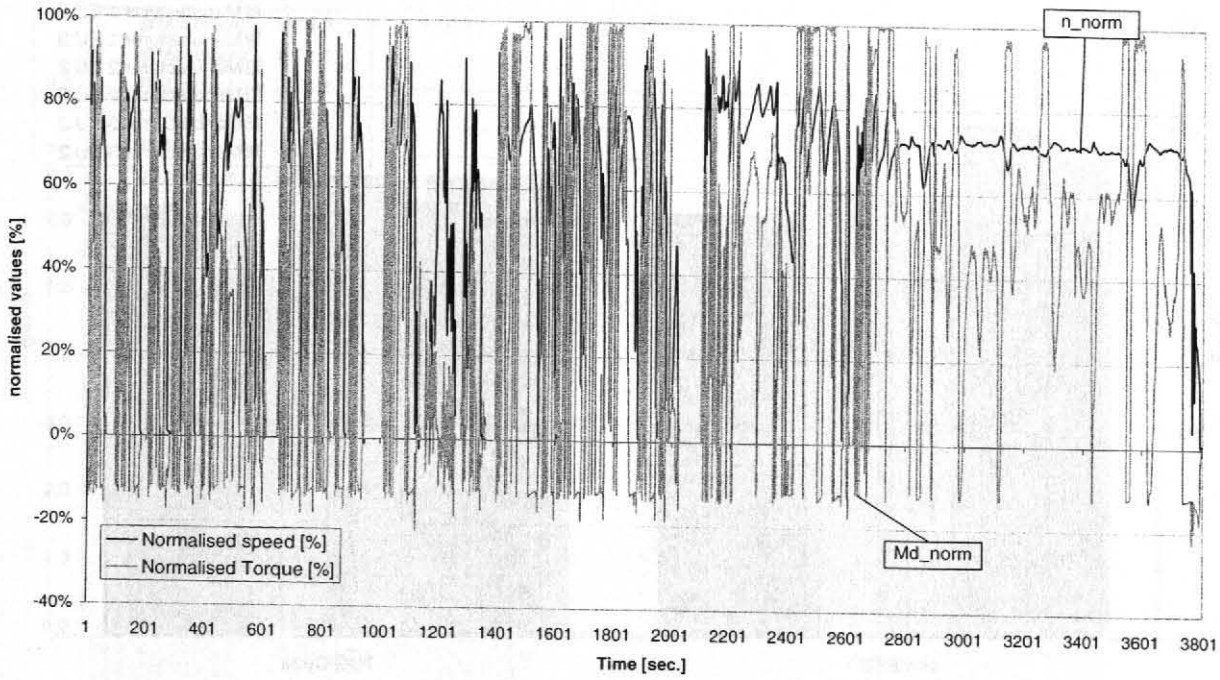

Figure 37: TNO real world test Cycle (7 kW/ton)

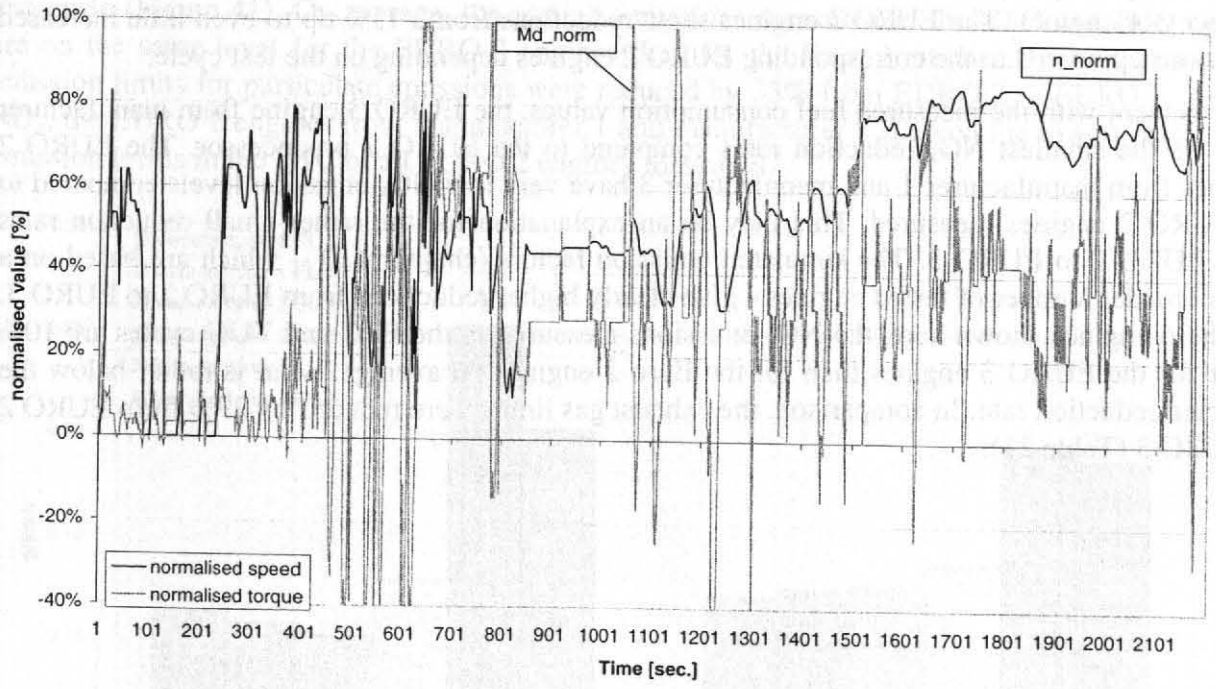

Figure 38: TUG test Cycle

4.3.2.1 Assessment of the transient engine tests

To assess the changes from EURO 2 to EURO 3 technology, for three measured EURO 3 engines also the corresponding predecessor EURO 2 engine was measured in transient tests. Figure 39 shows the measured fuel consumption [g/kWh] of the EURO 3 engines and of the EURO 2 engines. The EURO 3 engines have an about 3% higher fuel consumption compared to the EURO 2 engines. The engines of manufacturer 3 show the smallest increase from EURO 2 to EURO 3. For the EURO 3 engine of manufacturer 3 it is assumed, that the engine control strategy is different under transient load compared to steady state conditions (chapter 4.4.5.2).

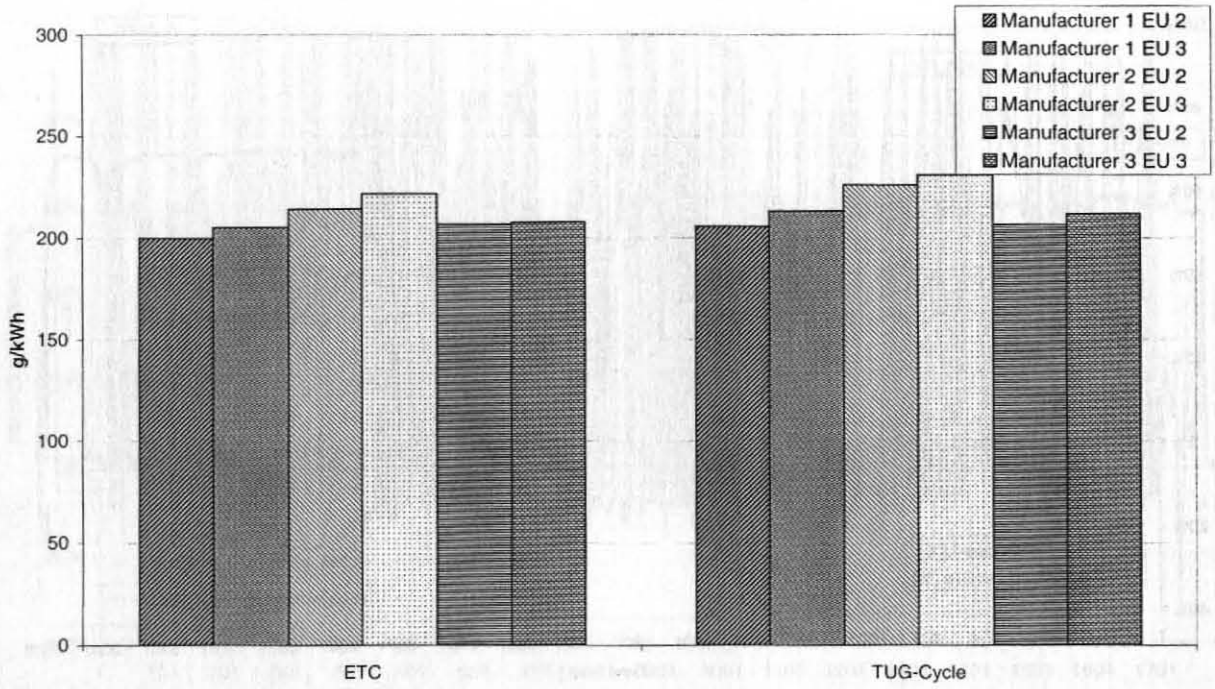

Figure 39: Measured **fuel consumption** for three EURO 3 engines and for the predecessor Euro 2 engines from different manufacturers in two different transient cycles

Figure 40 gives the measured NO_x-emissions [g/kWh] for the EURO 3 engines and the EURO 2 predecessor engines. The EURO 3 engines show reductions from –15% up to even little increased emissions compared to the corresponding EURO 2 engines depending on the test cycle.

In agreement with the measured fuel consumption values, the EURO 3 engine from manufacturer 3 shows the smallest NO_x reduction rates compared to the EURO 2 predecessor. The EURO 2 engines from manufacturer 1 and manufacturer 3 have very low NO_x emission levels compared to all EURO 2 engines measured. This may be an explanation for the rather small reduction rates from EURO 2 to EURO 3. The simulated emission factors (chapter 4.7) – which are based on a much broader number of tested engines - give clearly higher reductions from EURO 2 to EURO 3. For the 6 engines shown here, the NO_x emissions measured in the ETC and TUG cycles are 10% lower for the EURO 3 engines than for the Euro 2 engines on average, what is rather below the expected reduction rate. In comparison, the exhaust gas limits were reduced by 29% from EURO 2 to EURO 3 (Table 21).

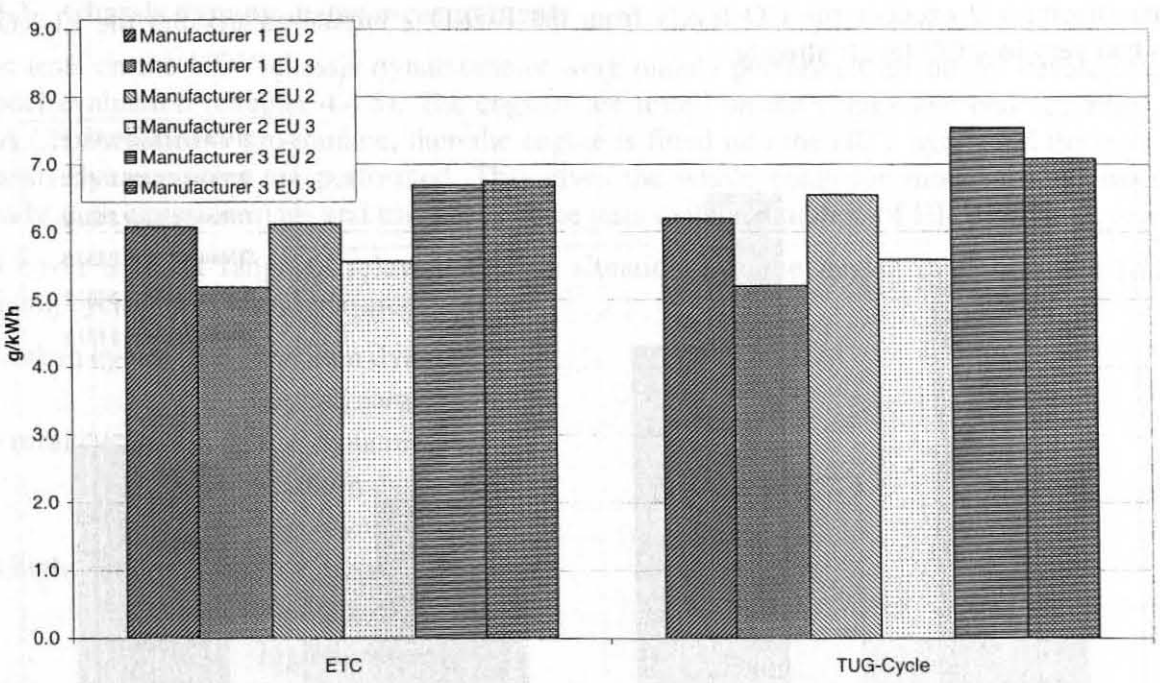

Figure 40: Measured **NO_x-emissions** for three EURO 3 engines and for the predecessor Euro 2 engines from different manufacturers in two different transient cycles

The ratio of the particle emissions from EURO 3 to EURO 2 showed a strong dependency on the test cycle (Figure 41). On average, the particle emissions measured in the ETC and TUG cycles are on the same level for the EURO 3 engines than for the Euro 2 engines. In comparison the emission limits for particulate emissions were reduced by 33% from EURO 2 to EURO 3. As for NO_x, the EURO 2 engines from manufacturer 1 and manufacturer 3 showed the lowest particulate emission levels in the ETC of all EURO 2 engines measured.

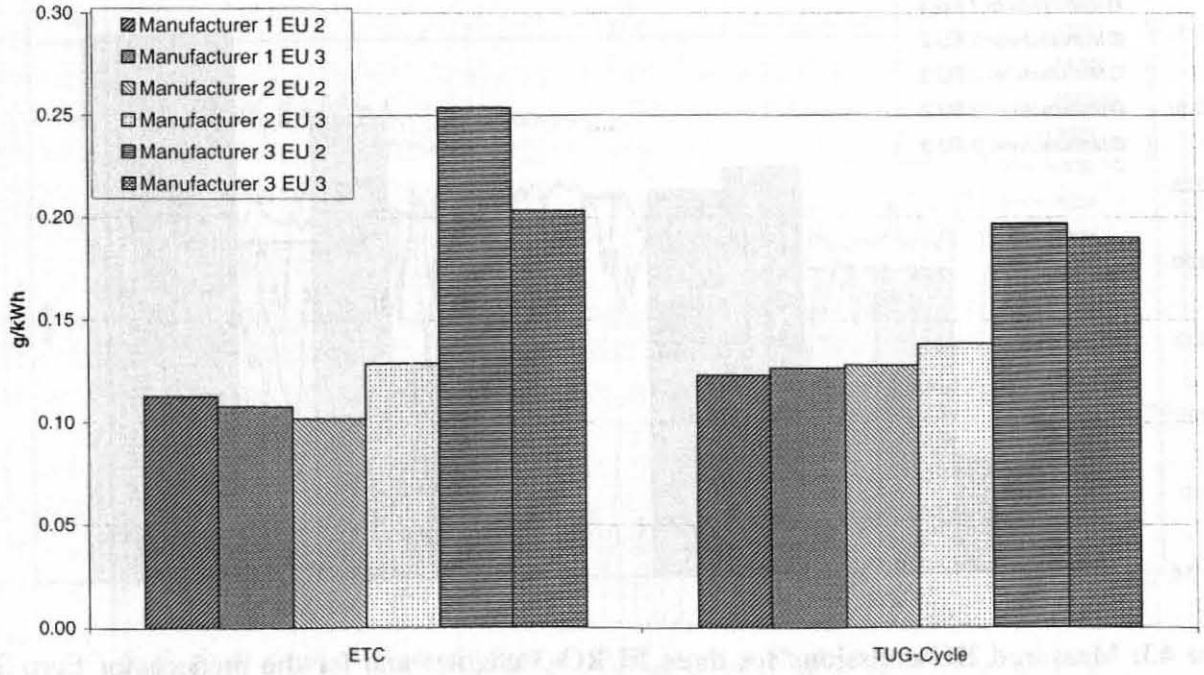

Figure 41: Measured **particle emissions** for three EURO 3 engines and for the predecessor Euro 2 engines from different manufacturers in two different transient cycles

A similar picture can be seen for CO where the EURO 3 engines have on average over the ETC and TUG cycle 37% higher emissions than the EURO 2 engines (Figure 42). The EURO 3 engine

from manufacturer 2 exceeds the CO levels from the EURO 2 engine clearly but the EURO 2 version had very low CO levels already.

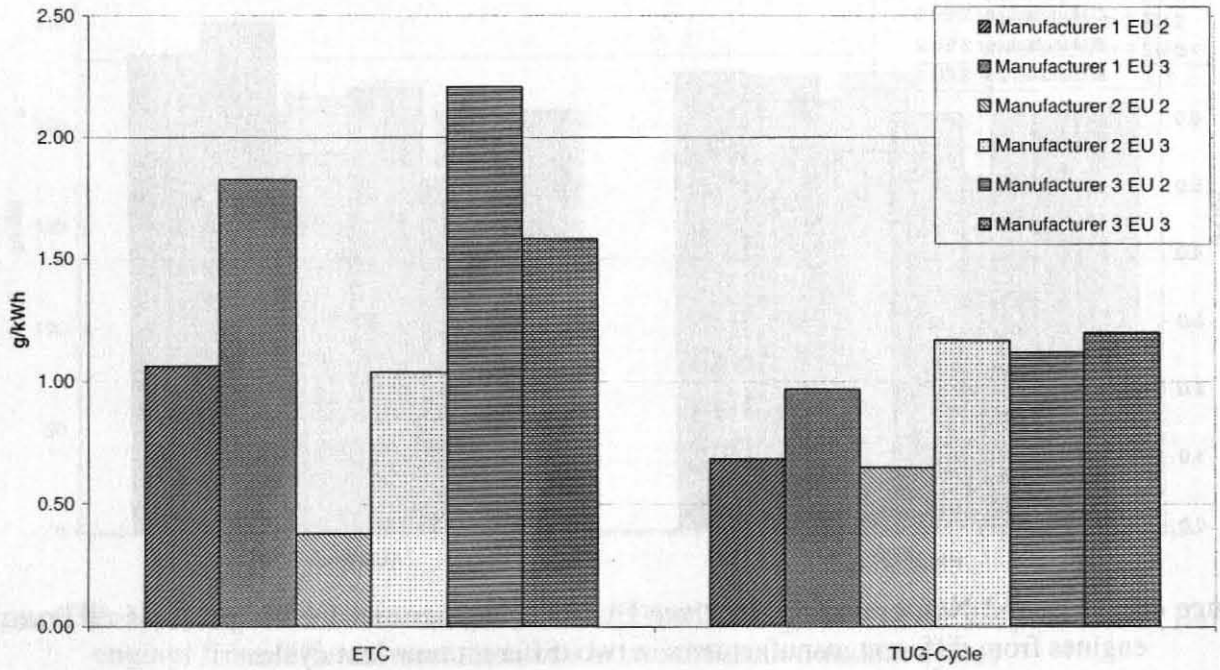

Figure 42: Measured **CO-emissions** for three EURO 3 engines and for the predecessor Euro 2 engines from different manufacturers in two different transient cycles

For hydrocarbons the evaluation gave –20% from EURO 2 to EURO 3 but again with a high dependency on the test cycle used (Figure 43).

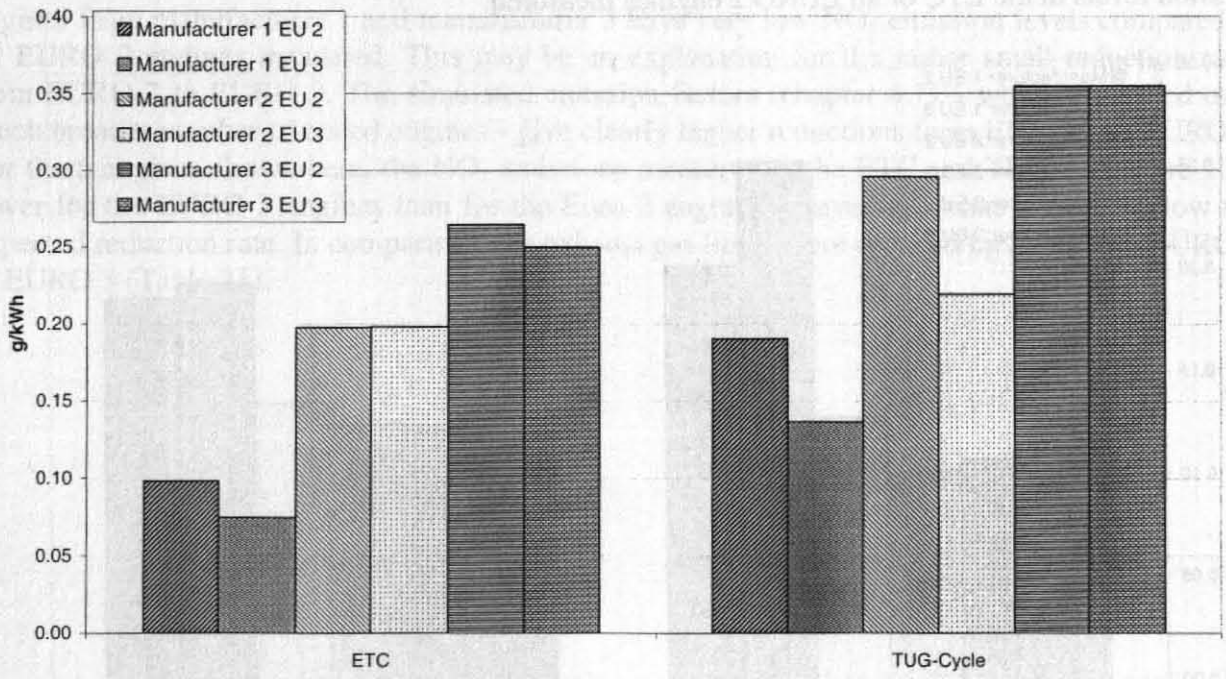

Figure 43: Measured **HC-emissions** for three EURO 3 engines and for the predecessor Euro 2 engines from different manufacturers in two different transient cycles

The transient tests showed approximately the results already expected from the assessment of the steady state engine tests. Later on in the report a detailed comparison of steady state measurements and the transient tests is given (chapter 4.4.4).

4.3.3 Chassis dynamometer measurements

The tests on the HDV-chassis dynamometer were mainly performed for model development and model evaluation (chapter 4.4.5). The engines are tested on the engine test bed according to the D.A.CH./ARTEMIS programme, then the engine is fitted into the HDV again and the tests on the chassis dynamometer are performed. This gives the whole chain for model development from steady state emission maps and transient engine tests to the simulation of HDV driving cycles.

To cover a broad range of relevant driving situations for the model validation, the following driving cycles have been measured:

2 urban cycles	medium dynamic
	high dynamic
3 rural cycles	low dynamic
	medium dynamic
	high dynamic
3 highway cycles	low dynamic
	medium dynamic
	high dynamic

The cycles are taken from the Handbook on Emission Factors (Steven, 1995) and were selected after model runs with PHEM (chapter 4.4), according to the calculated engine load, changes of the engine load (dynamics) and the vehicle speed respectively to cover low-speed to high-speed cycles and low-dynamic to high-dynamic cycles. Figure 44 shows the speed curve of these cycles which are measured with 0% road gradient simulation.

Additionally, constant speeds are measured, whereby the vehicle speed and the driving resistances are adapted to measured points on the engine test bed. This allowed an assessment of the potential inaccuracy related to different measurement systems and different boundary conditions compared to the tests on the engine test bed (chapter 4.4.5.3).

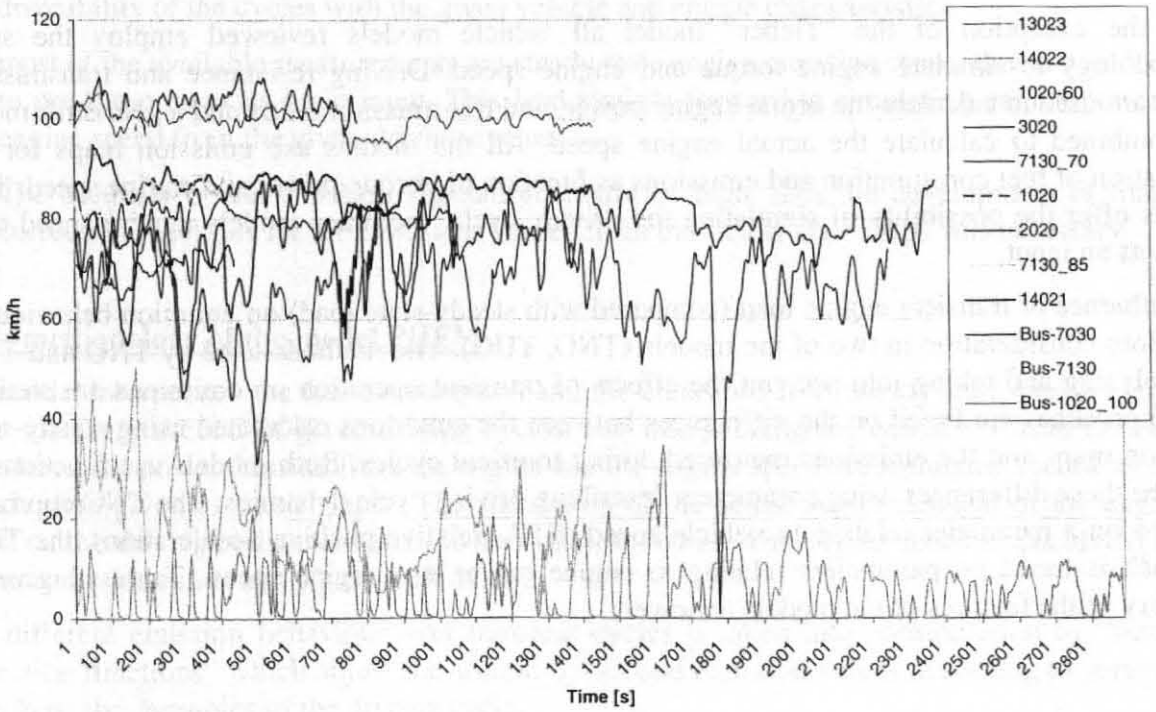

Figure 44: Driving cycles for the measurements on the chassis dynamometer.

Three HDV were tested according to the complete D.A.CH. programme. As an example Figure 45gives the measured NO_x- and PM emissions for a EURO 2 HDV for the cycles measured.

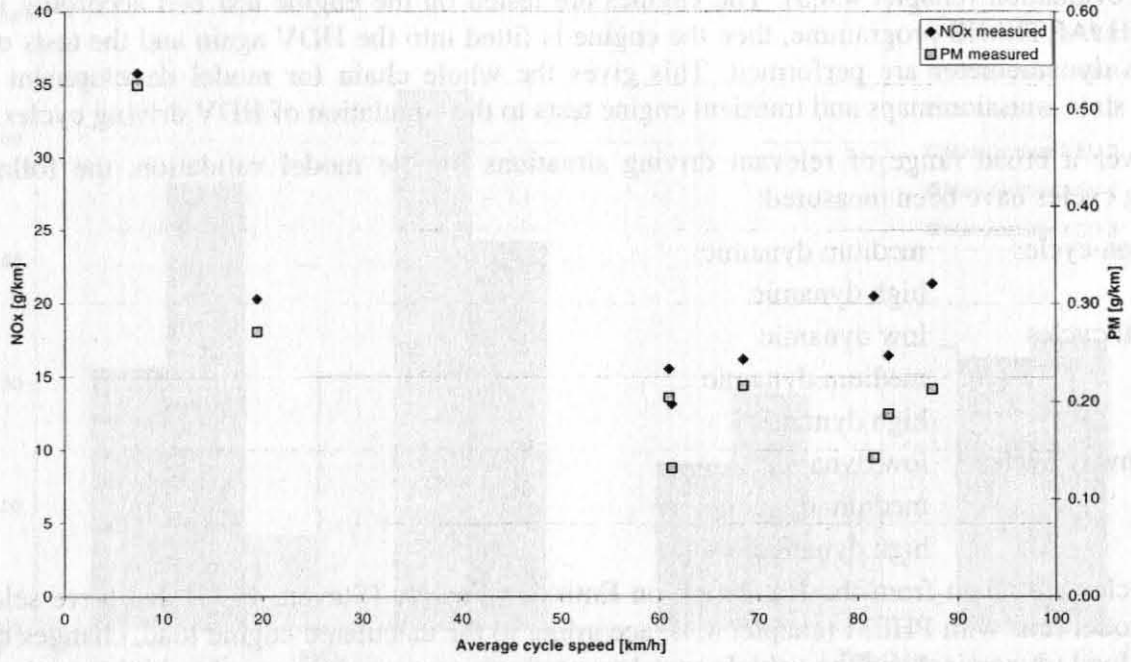

Figure 45: NO_x and PM -emissions measured for a EURO 2 HDV on the chassis dynamometer

4.4 The HDV Emission Model

The methodology chosen for the model PHEM (Passenger Car and Heavy duty Emission Model) is based on an extensive literature review and on a previous feasibility study (Hausberger, 1998). The following gives a short summary.

With the exception of the "Tieber" model all vehicle models reviewed employ the same methodology to simulate engine torque and engine speed. Driving resistance and transmission losses are used to calculate the actual engine power, and transmission ratios and a gear-shift model are combined to calculate the actual engine speed. All the models use emission maps for the calculation of fuel consumption and emissions as function of torque/power and engine speed. Two models offer the possibility of simulating the driving cycle, the other models require speed-time cycles as an input.

The influence of transient engine load (compared with steady-state load) on emission behaviour is taken into consideration in two of the models (TNO, TUG). The methods used by TNO and TUG for analysing and taking into account the effects of transient operation on emissions are similar; both approaches are based on the differences between the emissions calculated using steady-state emission maps and the emissions measured during transient cycles. Both models use functions to describe these differences using parameters describing driving cycle dynamics. The TNO approach is based on a parameter relating to vehicle speed (RPA, relative positive acceleration), the TUG approach is based on parameters relating to engine power and engine speed. Table 11 gives a summary of the features of the models reviewed.

Table 11 Main features of the models reviewed

Model	Driving cycles	torque/ power	engine speed	fuel cons.	Emis-sions	Transient correction
PHEM, TU-Graz	Speed curve as input, gears computed	Yes	Yes	Yes	Yes	Yes
Tieber, TU-Graz	Speed curve as input	Yes	No	Yes	Yes	Implicit
Vehicle Motion Simulator, Finland	Speed and gears can be computed	Yes	Yes	Yes	Yes	No
SIMULCO, INRETS	Speed and gears can be computed	Yes	Yes	Yes	Yes	No
TÜV-Rheinland	Speed curve as input	Yes	Yes	Yes	Yes	Yes
TNO van de Weijer	Speed curve as input	Yes	Yes	Yes	Yes	No
TNO-ADVANCE	Speed-curve as input	Yes	Yes	Yes	Yes	Possible
TNO HD Testcycles	Cycle and vehicle parameters as input	No	No	Yes	Yes	Implicit
VETO (VTI)	Speed and gears can be computed	Yes	Yes	Yes	Yes	No
SEEK (Danish Technological Institute)	Speed curve as input, gears computed	Yes	Yes	Yes	Yes	No

The models *PHEM*, *Vehicle Motion Simulator*, *TNO HD Testcycles*, *VETO*, and *SEEK* are included in a common procedure of model comparison and model improvement in the project COST 346.

Following boundary conditions were given for the project:

- the emission factors for the Handbook had to be calculated for given driving cycles, thus it was decided to use these cycles as model input. The model should perform only checks on the driveability of the cycles with the given vehicle and engine characteristics.
- most of the available measurements are steady state engine emission maps, thus it was decided to use these maps as basic input. This lead straight forward to simulating engine power and engine speed from the given driving cycles.
- The accuracy of the emission simulation should be high, thus the development of transient correction functions for the emissions gained from the steady state maps was necessary.

Basic methodology of the model PHEM

The model interpolates the fuel consumption and the emissions from steady state engine emission maps for every second of given driving cycles. For interpolating the emissions from the engine map the actual power demand from the engine and the engine speed are simulated according to the vehicle data given as model input. The simulation of the actual power demand of the engine is based on the driving resistances and the transmission losses. The engine speed is calculated using the transmission ratios and a gear-shift model.

The different emission behaviour over transient cycles is taken into consideration by "transient correction functions" which adjust the second-by-second emission values according to parameters describing the dynamics of the driving cycle.

The results of the model are the engine power, the engine speed, the fuel consumption, and emissions of CO, CO_2, HC, NO_x and particles every second, as well as average values for the entire driving cycle. Figure 46 gives the scheme of the model.

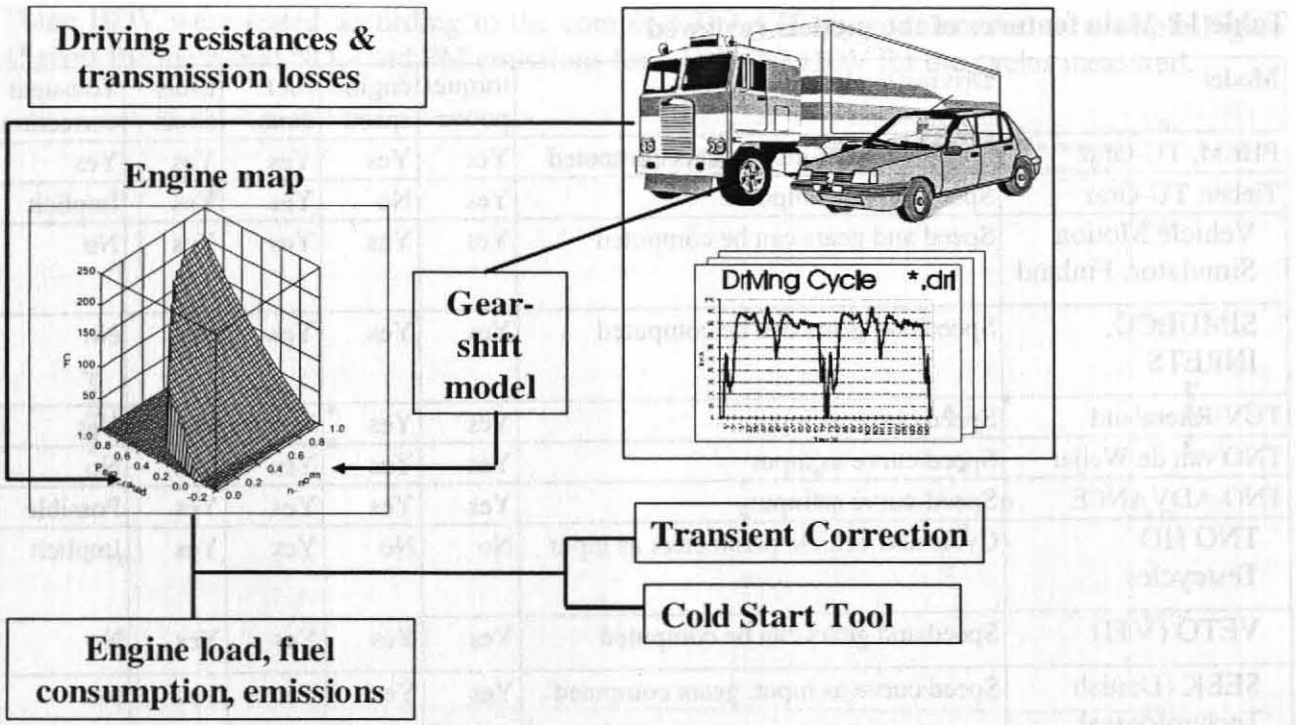

Figure 46: Diagram of the model PHEM from TU-Graz

While this method is common for most models compared (with exception of the transient correction function), the model PHEM has some special features developed straight forward to enable easy simulations of average HDV classes.

The input data is modular, i.e. different files for

- The vehicle characterisation
- The driving cycle
- The engine emission map
- The full load curve

This enables a quick simulation of manifold vehicle / driving cycle combinations.

A main problem in the elaboration of emission factors for average HDV is to have a sufficient number of engines measured for each HDV fleet segment because overall more than 60 segments of the fleet have to be covered. A "fleet segment" is defined here as the combination of a vehicle type (e.g. single truck or truck trailer) with a EURO category (e.g. EURO 3) and a size class (e.g. 34-40 tons maximum allowed payload). Since each size class has its typical values for the rated engine power, each measured engine basically can be applied to one fleet segment only.

To avoid a separation of the measured engines according to the rated engine power, the engine maps are normalized and brought into a standard format (see chapter 4.4.3.2). This enables the development of average engine maps independent of the engine size. Without this method of averaging emission maps, even the high number of measured engine maps available for the project would leave some "HDV-layers" covered by one engine only (or even without an appropriate engine at all). The method of size independent averaging guarantees that the single HDV classes are covered by a proper number of measurements of different engines.

In the input file for the driving cycle the measured engine speed or the gear position can be given as optional model input. If neither the engine speed nor the gear position is given in the input file, PHEM uses the gear-shift model to simulate the engine speed. When recalculating driving cycles measured at the chassis dynamometer differences between simulated and measured emissions

related to differences in the gear-shift strategy can be addressed exactly. This is a helpful tool in model development and model validation.

For the development of the transient correction functions and the normalisation of the engine emission maps PHEM offers an "engine only" and an "engine analyse" option. With these options engine power and engine speed cycles can be recalculated according to the measurements on the engine test bed instead of modelling the total vehicle. In the following each step of the simulation is described in detail.

4.4.1 Simulation of the engine power

For a proper simulation of the actual engine power all relevant driving resistances occurring in real world cycles have to be taken into consideration. Limit for the details to be covered is mainly the availability of data necessary for the simulation of the forces caused by single parts of a vehicle.

PHEM is developed to make mainly use of the data available from the data collection of the project. More detailed approaches have been tested too for single vehicles whether they could bring better results for the emission simulation. The experience was that more detailed data is very hard to get from manufacturers on the one hand and that on the other hand a more detailed input shows only very little influence on the simulated results. Thus the drive train system is not simulated in detail but as a unit block. This shall guarantee that all necessary model input data is covered by an adequate number of measurements.

The actual engine power is calculated according to:

$$P = P_{\text{rolling resistance}} + P_{\text{air resistance}} + P_{\text{acceleration}} + P_{\text{road gradient}} + P_{\text{transmission losses}} + P_{\text{auxiliaries}}$$

The single parts of the total power demand from the engine are calculated as follows.

4.4.1.1 Power for overcoming the rolling resistance

The power for overcoming the rolling resistance is simulated in PHEM as

$$P_R = m \times g \times (fr_0 + fr_1 \times v + fr_2 \times v^2 + fr_3 \times v^3 + fr_4 \times v^4) \times v$$

where: P_R ..... power in [W]

m ..... mass of vehicle + loading [kg]

g ..... gravitational acceleration [m/s^2]

fr_0..fr_4 ..... Rolling resistance coefficients

v ..... vehicle speed in [m/s], the vehicle speed is computed as average speed of second i and second (i+1) from the given driving cycle. The accessory acceleration is ($v_{i+1} - v_i$).

This formula for simulating the rolling resistance was chosen since the well known approach - with fr_0 and fr_1 only e.g. according to (Mitschke, 1982) – often leads to impossible air resistance values when the braking forces are calculated from the coast down tests of HDV. In this case the quadratic term of the braking forces has to be attributed only to the air resistance, what results in even negative air resistance coefficients for some tests (e.g. Figure 47). This is certainly due to some inaccurate measurements – e.g. the road gradient and the wind speed may not always have been recorded exactly. However, the dependencies of the rolling resistance are much more complex than given in the equations above[4]. But the use of a polynom of fourth order proved to be capable of simulating the measured driving resistances quite well.

[4] Main influences on the rolling resistance coefficients certainly come from the road surface and the temperature of the wheels. While the influence of the road surface could be taken into consideration no data is available yet on how the influence of the wheel temperatures could be simulated. Additionally, the loading of the HDV may have an influence on the rolling resistance coefficients (beside of a different temperature level of the wheels).

Figure 47 gives as an example the coast down measurement for a HDV. On the right the braking forces calculated from the coast down curve are given as function of the vehicle speed. As the picture shows the force due to the air resistance would be below zero (quadratic term) although the wind speed was zero during the measurements.

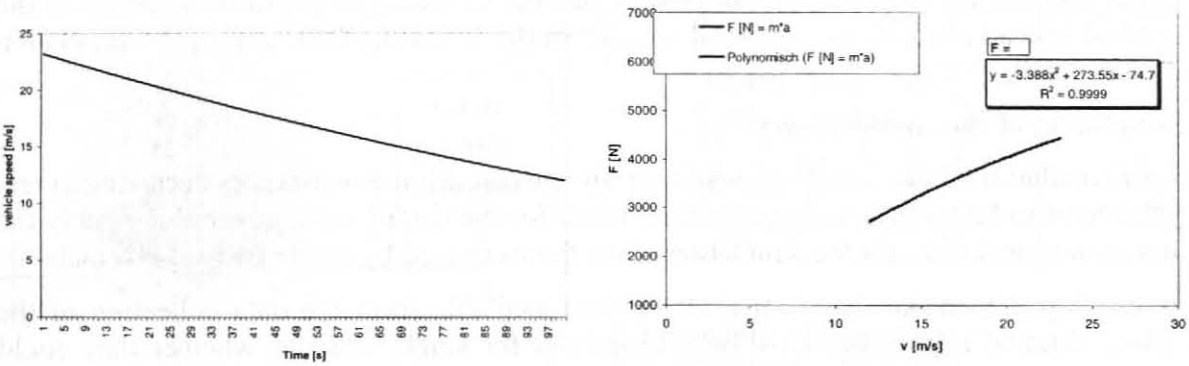

Figure 47: Measured vehicle speed at a coast down test and calculated braking forces for a semi trailer (half loaded, average of two tests in each direction).

For a correct simulation of the total braking forces from rolling resistance and air resistance together it does not matter if a negative air resistance coefficient is used as long as the sum of rolling resistance and air resistance corresponds to the formula gained from the coast down.

For elaborating data for driving resistances of average HDV it is clearly advantageous to get realistic values for the resistance coefficients from coast down measurements since additionally to the coast down tests data on those factors from manufacturers and other sources are used for setting up the data bank for describing the necessary model input values. Averaging values from a data bank to simulate emission factors is acceptable only if the data is consistent.

To overcome this problem when using the coast down data, the frontal area and the air resistance value are set according to the specifications given by the manufacturer and the forces resulting from air resistance are then subdivided from the total braking force measured in the coast down test. The remaining forces are then attributed only to the rolling resistance.

The procedure is as follows:

Braking forces from the coast down:

$$F_i = \left(m_{veh} + m_{loading} + m_{wheels}\right) \times a_i$$

where F_i..... Total braking force to the vehicle in second i of the coast down test [N]

m_{veh}..... mass of vehicle [kg]

$m_{loading}$ ..... mass of loading [kg]

m_{wheels} ..... equivalent translatory mass of the wheels for simulating the rotating acceleration forces [kg]

a_i..... deceleration in second i [m/s^2]

$$F_{roll\,i} = F_i - F_{air\,i}$$

with $$F_{air\,i} = Cw \times A_{Frontal} \times \frac{\rho}{2} \times v_i^{\,2}$$

v_i..... velocity in second i of the coast down test

The rolling resistance coefficients f_r are then calculated from the force F_{roll}:

$$f_{r_i} = \frac{F_{roll\,i}}{(m_{veh} + m_{loading}) \times g}$$

The resulting f_r curve is then approximated by an equation of the fourth order. Figure 48 summarises the results for the coast down tests available from the data collection. Obviously the rolling resistances on average do not follow a linear equation when calculated from the coast down tests.

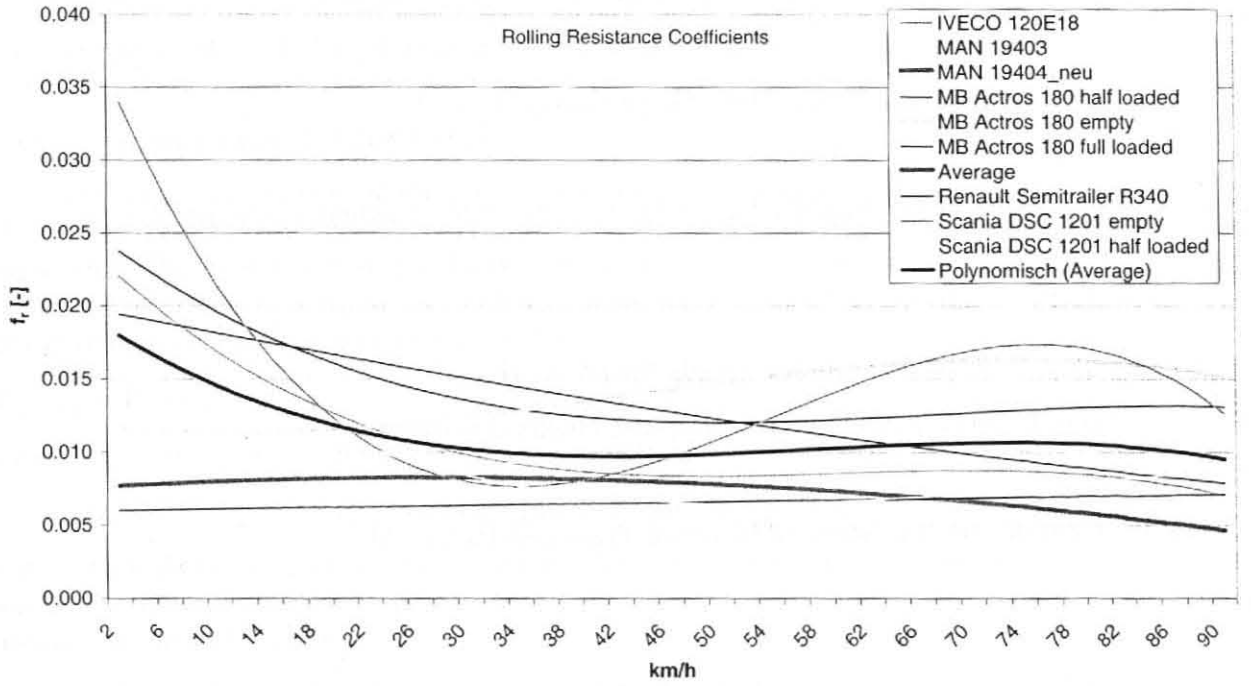

Figure 48: Calculated rolling resistance coefficients from different coast down tests

The average rolling resistance coefficients from Figure 48 are used for the simulation of the power for overcoming the rolling resistances of each average HDV segment (see chapter 4.6.1).

4.4.1.2 Power for overcoming the air resistance

The power for overcoming the air resistance is simulated as

$$P_{air} = C_d \times A_{Frontal} \times \frac{\rho}{2} \times v^3$$

with: P_{air} ..... power in [W]

C_d ..... drag coefficient [-]

$A_{Frontal}$ ..... Frontal area of the HDV in [m^2]

ρ ..... density of the air [on average 1,2 kg/m^3]

As described before, C_d and $A_{frontal}$ are taken from the specifications given by the manufacturer. If no manufacturer specifications for the C_d value were available the C_d was set according to those of a similar HDV in a data bank of the Institute.

4.4.1.3 Power for acceleration

The model offers two options for the simulation of the power demand for vehicle acceleration. The more detailed option simulates the rotating masses as three blocks: wheels, gearbox, other rotating masses:

Option 1:

For the calculation the power for the acceleration of the rotating masses is converted to the vehicle acceleration. This gives the following equation:

$$P_a = (m_{vehicle} + m_{rot} + m_{loading}) \times a \times v$$

with: m_{rot} ..... to the wheel reduced mass for rotational accelerated parts

$$..... m_{rot} = \frac{I_{wheels}}{r_{wheel}^2} + I_{mot} \times \left(\frac{i_{axle} \times i_{gear}}{r_{wheel}} \right)^2 + I_{transmission} \times \left(\frac{i_{axle}}{r_{wheel}} \right)^2$$

I ..... moment of inertia from the rotating masses [kg m^2]

v ..... vehicle speed [m/s]

The part of the wheels can be simplified assuming the wheels to be cylinders ($I = m*r^2/2$)

$$\frac{I_{wheels}}{r_{wheel}^2} = 0.5 \times m_{wheels}$$

with: m_{wheels} ..... mass of the vehicles wheels (including rims)

If the moments of inertia are not known, a simplified method is used:

Option 2:

m_{rot} from the formula above is assessed by a "rotating-mass-factor" Λ:

$$\Lambda(v) = \frac{m_{veh} + m_{rot}}{m_{veh}}$$

With this simplification the power for acceleration is:

$$P_a = (m_{veh} \times \Lambda(v) + m_{loading}) \times a \times v$$

Λ is expressed as function of the vehicle speed in this option to take the influence of the differing transmission ratios and the resulting decreasing influence of angular acceleration of the engine and the gear box block with increasing vehicle speed into consideration.

with: $\Lambda(v) = \Lambda_0 \times 0{,}833 \times [1 - 0{,}4 \times \log(v * 0{,}0667)]$ for 1m/s< v <12m/s

below 1m/s v is set equal 1, above 12m/s v is set to constant 12,0

a..... acceleration of the vehicle [m/s^2]

$m_{vehicle}$..... mass of the vehicle (ready for driving) in [kg]

$m_{loading}$ ..... mass of the payload or the passengers and luggage in [kg]

Λ_0 ..... Rotating mass factor, to be given as model input (ca. 1,05 to 1,2)

The formula for option 2 is derived from the more detailed simulation according to the model for option 1.

For the first assessment of the actual power demand always the simplified equation is used since the gear choice of the driver is modelled as a function of the actual power demand. Thus the gear and the transmission ratios are not known at the first step of iteration.

4.4.1.4 Power for overcoming road gradients

The power for overcoming road gradients is calculated as:

$$P_g = m \times g \times Gradient \times 0{,}01 \times v$$

with: P_g ..... power in [W]

Gradient ..... Road gradient in %

m ..... mass of the vehicle + loading in [kg]

The road gradient has to be given as model input value in the file containing the driving cycle on second per second basis.

4.4.1.5 Power demand of auxiliaries

A more detailed assessment of the power demand from different auxiliaries is planned within the COST 346 project. For the D.A.CH project no detailed data is available for simulating single auxiliaries. The assessment of the HDV measurements on the chassis dynamometer suggested a rather constant power demand of auxiliaries from the tested vehicles (chapter 4.4.5.3). Thus the power demand is calculated in a simplified way:

$$P_{auxiliaries} = P_0 \times P_{rated}$$

with: ..... $P_{auxiliaries}$ power in [kW]

..... P_0 power demand of the auxiliaries as ratio to the rated power [-]

For average HDV this equation is sufficient from today's point of view. For special HDV (garbage trucks, air conditioned HDV bodies, eventually for city buses) a more detailed approach may improve the model accuracy.

4.4.1.6 Power demand of the transmission system

The power losses between the engine and the wheels are simulated as a function of the actual power, the engine speed and the transmission ratio. A simplified equation according to (Tieber, 1997) – based on transmission efficiencies -is used for a first iteration since the gear choice of the driver is modelled as a function of the actual power demand. Thus the gear and the transmission ratios are not known at the first step of iteration.

The transmission efficiency is defined here as:

$$\eta_{transmisson} = \frac{P_{dr}}{Pe} = \frac{Pe - P_{transmission}}{Pe}$$

and $P_{transmission} = P_e - P_{dr}$

Simplified equation for the first assessment:

$$\eta_{transmisson} = -6 \times \left(\frac{P_{dr}}{P_{rated}}\right)^2 + 2{,}7 \times \left(\frac{P_{dr}}{P_{rated}}\right) + 0{,}57 \qquad \text{where } P_{dr}/P_{rated} < 0{,}2$$

$$\eta_{transmission} = -0{,}0561 \times \left(\frac{P_{dr}}{P_{rated}}\right)^2 + 0{,}1182 \times \left(\frac{P_{dr}}{P_{rated}}\right) + 0{,}8507 \qquad \text{where } P_{dr}/P_{rated} > 0{,}2$$

The power losses in the transmission system are:

$$P_{transmission} = \frac{P_{dr}}{\eta_{transmission}} - P_{dr}$$

with..... P_{dr} Power to overcome the driving resistances (without transmission losses)

After the first rough assessment of the power losses in the transmission system (and after the first iteration of the power necessary for the acceleration of rotating masses the next subroutine of PHEM is executed which selects the actual gear by a driver gear-shift model (chapter 4.4.2).

After the actual gear is found, the losses in the transmission system are simulated according to the following method.

(a) Manual Gear box

The losses in the transmission system are directly calculated as power loss. The use of transmission efficiencies is avoided since the transmission efficiency is near to zero in ranges of low power transmission. This would lead to a not well defined value since a low value for the engine power has to be divided by an efficiency near to zero.

Following the basic method of PHEM, the formulas used are normalised to the rated power of the engine.

Power losses in the Differential [kW]:

$$P_{Differential} = P_{rated} \times 0{,}0025 \times (-0{,}47 + 8{,}34 \times \frac{n_{wheel}}{n_{rated}} + 9{,}53 \times ABS\frac{P_{dr}}{P_{rated}}$$

with: P_{rated} rated power of the engine

n_{wheel} rotational speed of the wheels [rpm]..... $n_{wheel} = \frac{60 \times v}{D_{wheel} l \times \pi}$

P_{dr} Power demand from the engine to overcome the driving resistances (= total power demand without transmission losses)

Power losses in the gear box [kW]:

These losses are simulated for four transmission ratios. The losses for gears between these ratios are interpolated linearly. This method takes the characteristics from splitter-gear shifts – which are most common in HDV – into consideration and was gained from measured data of a gear box.

$$P_{1.gear} = P_{rated} \times 0{,}0025 \times \left(-0{,}45 + 36{,}03 \times \frac{n_{engine}}{I_{1.gear1}} + 14{,}97 \times ABS\left(P_{dr} + \frac{P_{Differential}}{P_{rated}} \right) \right)$$

$$P_{8.gear} = P_{rated} \times 0{,}0025 \times \left(-0{,}66 + 16{,}98 \times \frac{n_{engine}}{I_{8.gear}} + 5{,}33 \times ABS\left(P_{dr} + \frac{P_{Differential}}{P_{rated}} \right) \right)$$

$$P_{9.gear} = P_{rated} \times 0{,}0025 \times \left(-0{,}47 + 8{,}34 \times \frac{n_{engine}}{I_{9.gear}} + 9{,}53 \times ABS\left(P_{dr} + \frac{P_{Differential}}{P_{rated}} \right) \right)$$

$$P_{16.gear} = P_{rated} \times 0{,}0025 \times \left(-0{,}66 + 4{,}07 \times \frac{n_{engine}}{I_{16.gear}} + 0{,}000867 \times ABS\left(P_{dr} + \frac{P_{Differential}}{P_{rated}} \right) \right)$$

The total power losses in the transmission system are the sum of the losses in the differential and in the gear box. For the calibration of the absolute values a factor A_0 is introduced which can be set by the model user.

$$P_{transmission} = A_0 \times (P_{Differential} + P_{gear\,i}) \ldots\ldots\ldots\ldots [kW]$$

with: A_0 .....Factor for adjusting the losses (to be defined in the model input data, usually set to 1).

When setting the factor A_0 to 1 the transmission losses are in the range given in Figure 49 for real world driving cycles.

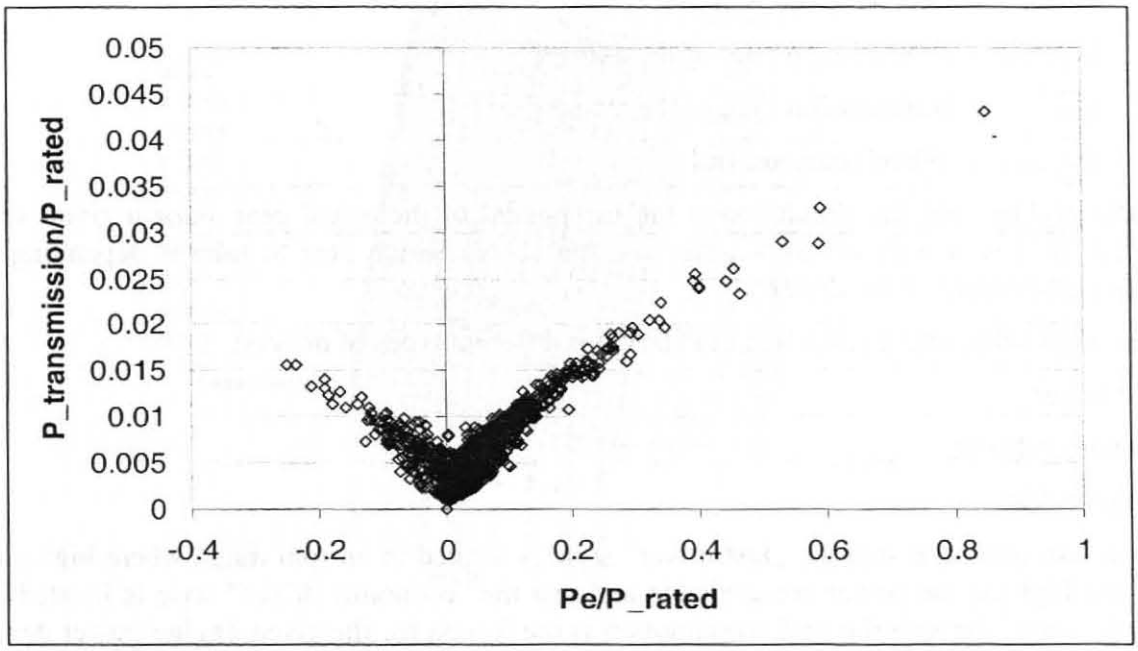

Figure 49: simulated transmission losses for a real world cycle over the actual engine power

(b) Automatic gear box:

The power losses are simulated as a function of the vehicle speed according to (Tieber, 1997). Data for the elaboration of a more detailed approach is not available yet.

$$\eta_{transmission} = 0{,}05 + 0{,}88 \times (0{,}0002 \times v \times 3{,}6)^3 - 0{,}0098 \times (v \times 3{,}6)^2 + 0{,}158 \times v \times 3{,}6 \qquad \text{at } v<5{,}56 \text{ m/s}$$

$$\eta_{transmission} = 0{,}88 \qquad \text{at } v>5{,}56 \text{ m/s}$$

The power losses in the transmission system are thus:

$$P_{transmission} = \frac{P_{dr}}{\eta_{transmission}} - P_{dr}$$

With.....P_{dr} Power to overcome the driving resistances (without transmission losses)

With the equations given in this chapter the power demand from the engine can be simulated for any vehicle / loading / driving cycle combination.

4.4.2 Simulation of the engine speed

The actual engine speed depends on the vehicle speed, the wheel diameter and the transmission ratio of the axis and the gear box.

Calculation of the engine speed

$$n = v \times 60 \times i_{axle} \times i_{gear} \times \frac{1}{D_{wheel} \times \pi}$$

with: n ..... engine speed [rpm]

v ..... vehicle speed in [m/s]

i_{axle} ..... transmission ratio of the axle [-]

i_{gear} ..... transmission ratio of the actual gear [-]

D_{wheel} ..... Wheel diameter [m]

The main problem for the simulation is the assessment of the actual gear since a given vehicle speed can be driven with different gears and the choice which gear to take is depending on a subjective assessment of the driver.

The gear shift behaviour is modelled in PHEM for different types of drivers:

a) Fast driver,

b) Economic driver,

c) Average driver.

The basic assumption is that the „fast driver" style is located in an rpm range where high engine torque and high engine power are available and that the "economic driver" style is located in an rpm range where the specific fuel consumption is the lowest for the given engine power demand. For these driving styles limits of the engine speed are defined where the gear has to be changed upwards or downwards.

The "average driver" is a mixture of style a) and style b) depending on the engine power needed within the next seconds. If the virtual "average driver" realizes that he will need a high engine power within the next seconds (e.g. for acceleration or a road gradient) he will take a gear rather according to style a), if the coming power demand is rather low he will behave like style b).

The user of the model PHEM can choose any mixtures of style a) to c).

General rules:

1) Independent of the driving style chosen the model checks for every second whether the actual needed engine power is below the given full load curve. If the full load curve is exceeded a lower gear is chosen (rules see 2). If the engine power needed is not available in any gear, the model reduces the vehicle speed for the next second (i+1). This results in a lower acceleration and thus a lower engine power demand. The vehicle speed is reduced to a level where the engine power needed is on the full load curve. In this case the model uses the reduced vehicle speed from second (i+1) and the original vehicle speed from second (i+2) to calculate the power demand for the next second. Again the vehicle speed is reduced if the power needed is not available. This method causes a smoothening of the driving cycle if the vehicle can not follow the cycle given as model input.

2) If the gear shift model has to use a lower gear as a result of 1), it is checked which is the least sensible gear. For this task the gear with the highest available power at the given vehicle speed is searched according to the transmission ratios and the full load curve. Then it is checked whether a higher gear offers at least 94% of the maximum theoretical available power. The

highest gear fulfilling this demand is then set as the lowest allowed gear. This gear shift behaviour was found from real world measurements were the rated engine speed is nearly never used from bigger HDV where the gearbox offers enough gears to stay in ranges of the engine map where the fuel efficiency is better but still nearly the rated engine power is available (Figure 50).

3) The gear is not changed more than one time within 2 seconds of driving (only to be overruled by 1).

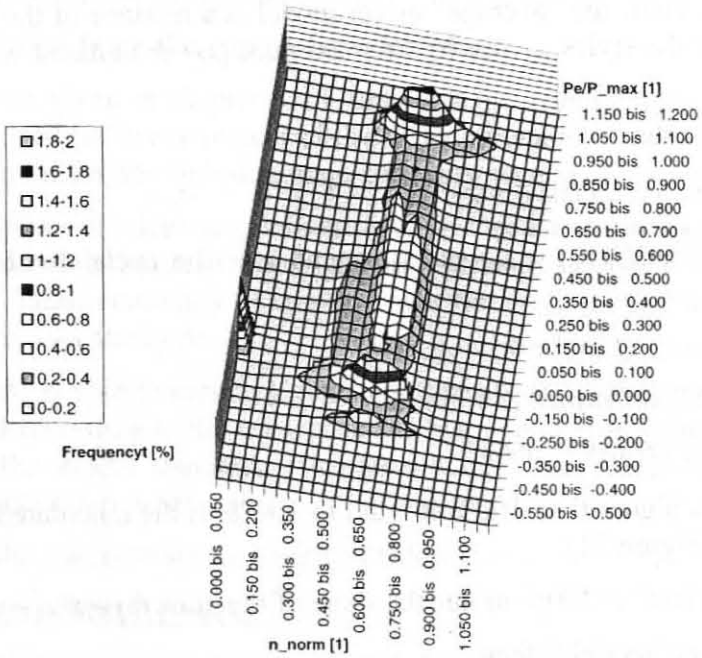

Figure 50: measured frequency of engine loads for HDV > 15t in real world driving

The simulation routines for the different driving styles are given below.

The „fast driver" model

Gear shift up:

An engine speed in the actual gear is fixed (n_{up}) where the next higher gear is selected as soon as the actual engine speed exceeds n_{up}.

Gear shift down:

An engine speed in the actual gear is fixed (n_{down}) where the next lower gear is selected as soon as the engine speed is lower than n_{down}.

The „economic driver" model

Gear shift up:

An engine speed is fixed (n_{up}) where the next higher gear is selected as soon as the engine speed in a higher gear than the actual gear is above n_{up} (shifts over two gears are possible)

Gear shift down:

An engine speed is fixed (n_{down}) where the next lower gear is selected as soon as the actual engine speed is lower than n_{down}.

The engine speeds n_{up} and n_{down} are set in a way that the virtual driver stays in the rpm range with the best fuel efficiency of the engine. Thus n_{up} and n_{down} are slightly different for the classes "pre EURO 1" up to EURO 3 For EURO 4 and EURO 5 again the same gear-shift strategy as for EURO 3 is assumed.

The "average driver" model

As expected none of these simple models gives satisfying explanations for the gear shift behaviour for longer real world cycles. When analysing the cycles the gear-shift behaviour was found to be between the styles a) and b). Thus, the "average" driver model is a mixture of the style a) and b). As criterion for the shares of the styles a) and b) the maximum power demand within the next 6 seconds is used.

Equations for the gear shifts of the "average driver"

$$P6max = \text{highest } Pe\langle \text{in second i to second } (i+5)\rangle$$

with: .....Pe(i) actual engine power at second i of the cycle divided by the rated engine power

.....i second in the driving cycle

The shares of style a) and b) are defined as follows:

$$\%"fastdriver" = 100 * (3.3333 * P6\max - 1.6667)$$

If the calculated share is higher than 100% it is set to 100%, if the calculated share is lower than 0% it is set to 0% (Figure 51).

The share of the „economic driver" is 100% minus the share of the „fast driver"

The gear for the „average driver" model is then:

Gear = $gear_{\text{fast driver}}$ x (% fast driver) + $gear_{\text{economic driver}}$ x (% economic driver)

Beside the model mix of fast driver and economic driver, the model offers also a manual mixture of fast driver and economic driver from 0% to 100% of each style. For the simulations done for the Handbook Emission Factors always the model mix was used.

The computed value for the gear is then rounded to the next integer value.

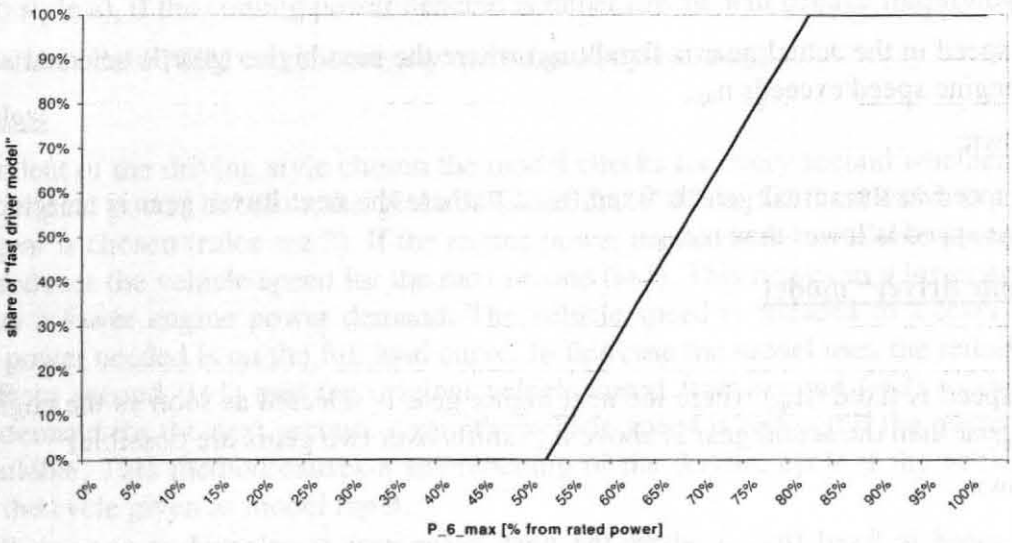

Figure 51: share of the "fast driver model" in the "average driver model" as a function of the highest engine power demand within the next 6 seconds

Certainly also this model approach can not simulate all gear changes – especially for single drivers – exactly. But the calculated engine load (rpm and kW combinations) do match the real world driving very well (chapter 4.6.2). This is the most relevant criterion when interpolating emission factors from an engine map.

As alternative for the simulation of the engine speed the model allows also to set the measured engine speed or the measured gear positions as input variables. In this case the measured values are used instead of the simulated ones. This option is helpful for validation work with measurements from the chassis dynamometer.

4.4.3 Interpolation from the engine emission map

With the equations given in chapter 4.4.1 and 4.4.2 the actual engine speed and the actual engine power are calculated for every second of the driving cycle. With this data the emission values are interpolated from the engine emission maps for every second of the cycle.

The resulting emission values are defined here as **"quasi stationary emissions"** since they are calculated from an emission map which has been measured under steady state conditions for each point. The total "quasi stationary emissions" over the driving cycle are the integral of the second per second values over the cycle.

The model PHEM is able to handle almost any formats of engine maps concerning the number of points given and according to the content of the maps (emission values, voltages, etc.) if the units are adapted to the model standards (chapter 4.4.3.2). This flexibility can be used e.g. for the simulation of temperature levels etc.

The routine for the interpolation is described below.

4.4.3.1 The interpolation routine

For the interpolation multiple options were tested on their accuracy and stability for the given task. The method according to Shepard proved to be the most stable routine for differing layouts of the engine map. With some small adaptations this method proved to be one of the most accurate interpolation routines for the given task with the additional advantage of a very simple programming.

The adapted Shepard method:

Step 1: the distances between the point to be interpolated and the given points from the engine map in the engine power / engine speed plane are calculated as R^2.

$$R^2(i) = \left(P_e - P_{map}(i)\right)^2 + \left(n - n_{map}(i)\right)^2$$

with:..... P_e actual engine power of the point to be interpolated subdivided by the rated power

..... n actual normalised engine speed of the point to be interpolated

..... $P_{map}(i)$ engine power of a point i in the engine map subdivided by the rated power

..... $n_{map}(i)$ normalised engine speed of a point i in the engine map

R^2 is used also as weighting factor for interpolating points with an engine power >0.05 from rated power.

Step 2: Selection of the points to be used for the interpolation:

Points with $R^2 < 0{,}07$ are used.

If less than 3 points from the map are within this criterion the radius is doubled until three or more points are within the given radius R^2 [5].

Step 3: Modified interpolation according to Shepard:

The emission value for the point to be interpolated is simply gained by the weighted average of the points selected in step 2. The weighting is done according to R^2 from step 1.

$$Eo_{(P_e,n)} = \frac{\sum\left(\frac{1}{R_{(i)}^{\ 2}} \times E_{map(i)}\right)}{\sum \frac{1}{R_{(i)}^{\ 2}}}$$

$Eo_{(Pe,n)}$ ..... basic interpolated value (emission, fuel consumption, etc.)

$E_{map-(i)}$ ..... value for the point i given in the engine map (points within $R^2 < 0.07$ only)

Since the basic Shepard routine is not capable of making extrapolations the basic interpolated value from the equation above is adjusted assuming a constant emission value [g/kWh] for this small adjustment.

$$E_{(P_e,n)} = Eo_{(P_e,n)} + Eo_{(P_e,n)} \times (P_e - P_{Sh}) \qquad \text{only if } P_e \text{ greater } 0.05$$

with: $E_{(Pe,n)}$ ..... interpolated value (emission, fuel consumption, etc.)

P_{Sh} ..... basic interpolated normalised engine power like for $Eo_{(Pe,n)}$

This method gives very accurate results for most parts of the engine map, especially when the standardised formats are used (chapter 4.4.3.2). Inaccuracies arise in the range of low or zero engine loads with engine speeds above idle speed. In this range the influence of the engine speed on the emission level proved to be lower than at higher loads. Thus the weighting factor for the distance in engine speed direction is decreased. Additionally, the weight of all available measured points near to zero engine power is increased.

The formula is as follows:

Equation 1: Weighting factor for interpolating points with an engine power between –0.05 and 0.05 from rated power

$$\hat{R}^2(i) = \{(P_e - P_{map}(i))^2 + (n - n_{map}(i))^2 \times 888.9 \times |P_e^3| + 0.001\} \times \{|P_e| + |P_{map}| + 0.005\} \times 9.52$$

The next modification to the Shepard routine is a lower weighting of points in the map which have a different sign of the engine power compared to the power of the point to be interpolated. This separates the map into the range with positive and negative power output of the engine since the emission behaviour between these ranges is rather different.

In combination with the modified Shepard method a standard engine map with 32 points was found to be the best compromise between accuracy and expenditures for measuring the engine emission map. The ARTEMIS steady state measurement programme is in line with these 32 points found and all standard emission maps for model input into PHEM are using these points (five virtual points below the motoring curve which are set to zero emission and three points at

[5] This is not relevant when using the standard formats for the engine maps according to chapter 4.4.3.2 since the format ensures a sufficient number of points to be located within R^2 in any case.

increased engine speed at zero engine power are added to the 32 point standard, see chapter 4.4.3.2). However, the method works in principle for all maps containing three or more points.

Figure 52 gives the results for the interpolation of 68 points measured at an EURO 2 engine from the standard 32 point engine map. Although with exception of the fuel consumption the engine map is very uneven for all components most points are interpolated with an error in the range of the measurement accuracy.

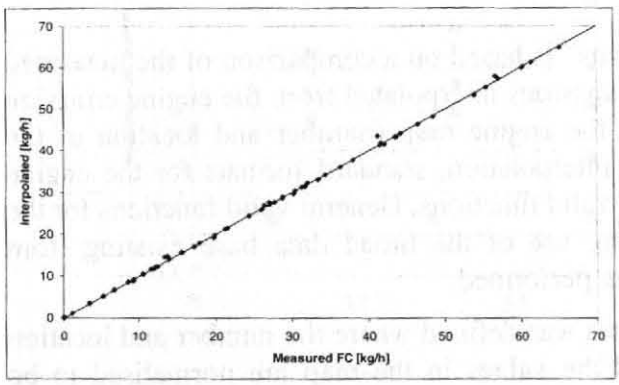

Fuel consumption

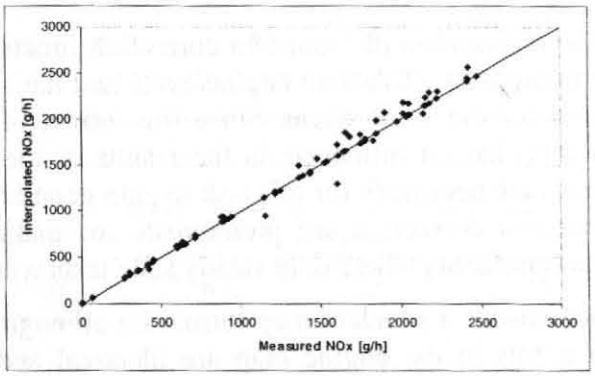

NOx

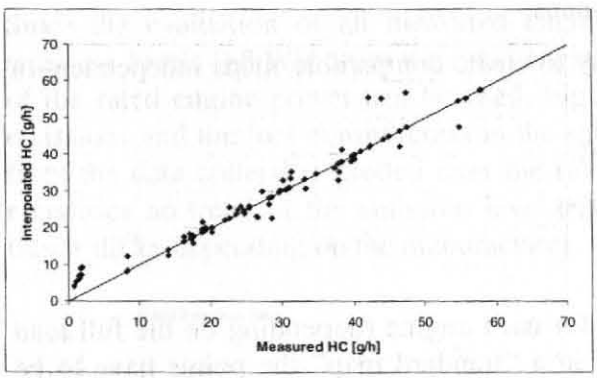

HC

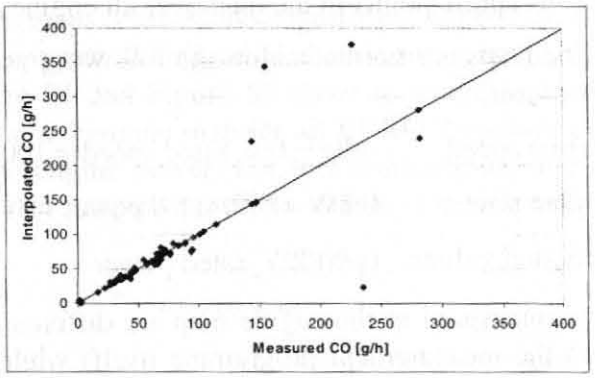

CO

Figure 52: Measured steady state emission values and results of the interpolation from the standard 32 point engine map format

4.4.3.2 Standard formats for the emission maps

As described in chapter 4.4.3.1 a standard format for the engine emission maps was elaborated as compromise between accuracy and the expenditure necessary for measuring the points on the engine test bed[6]. All formats from other projects (such as e.g. the German in-use-compliance programme) can be converted easily into the standard format.

Beside the fact that the combination of the normalised emission maps and the modified Shepard routine give reliable and well tested results for the interpolation from the engine maps the main reason for the elaboration of normalised engine maps was to provide a possibility for creating average engine maps out of the single engine maps. The advantages of average engine emission maps are:

[6] In general the accuracy of the simulation of steady state emissions increases with the number of points measured in the engine map. Since the data collection includes between 29 and 80 measured points per engine a compromise had to be found, which can handle a smaller number of measured points also.

- A main problem of the elaboration of emission factors for average HDV is to have a sufficient number of engines measured for each HDV fleet segment because in total more than 60 segments of the fleet have to be covered ("pre-EURO 1 <7 ton" up to "EURO 5 >32ton). Since each size class has its typical values for the rated engine power, each measured engine can basically be applied on only one fleet segment. A method for averaging engine maps independent of the rated engine power would increase the number of engines applicable per fleet segment approximately by a factor of 10.
- The elaboration of "transient correction functions" is based on a comparison of the measured emissions in a transient engine cycle and the emissions interpolated from the engine emission map for the same cycle. Since the format of the engine map (number and location of the points) has an influence on the results of the interpolation, standard formats for the engine maps are necessary for this task to gain general valid functions. General valid functions for the transient correction are prerequisite for making use of the broad data base existing from measurements where only steady state tests were performed.

For this reasons a standard map format for all engines was defined where the number and location of the points in the engine map are identical and the values in the map are normalised to be independent of the engine size. The average map can than be calculated simply as the average value for the single points in the map over all engine maps.

The engine maps are normalized in the following way to create comparable maps independent of the engine size:

- Engine speed: idle = 0%, rated speed = 100%
- Engine power: 0 kW = 0%, rated power = 100%
- Emission values: (g/h)/kW_rated power

The points measured in the engine map are different for each engine (depending on the full load curve and the measurement programme itself) while in a "standard map" the points have to be fixed (Figure 53). The model PHEM offers a routine to convert the measured points into the standard format by interpolation from all measured values. For this task the routine "create norm map" from PHEM can be used. This routine interpolates the 32 points from the standard map out of all points measured according to the modified Shepard routine (chapter 4.4.3.1).

The tests described in chapter 4.4.3.1 showed that the accuracy of the interpolation is not optimal in the range of very low engine loads if no measured points are given in the engine map for this range. In this region of the map also the accuracy of the measurements is rather low and furthermore shows a worse repeatability.

Since only a few engines have measured map points in this region this area was assessed from the transient tests. From the available measurements the ratio of fuel consumption and emissions at points with zero power but engine speeds above idling have been calculated. These ratios were used to add three points at zero load to all engines where no measurements in this range had been done.

Fife additional points at motoring with -25% of the rated power and different engine speeds are added in the normalised map, too. For these points fuel consumption and emissions are set to zero. This avoids unstable extrapolations in the motoring range (Figure 53).

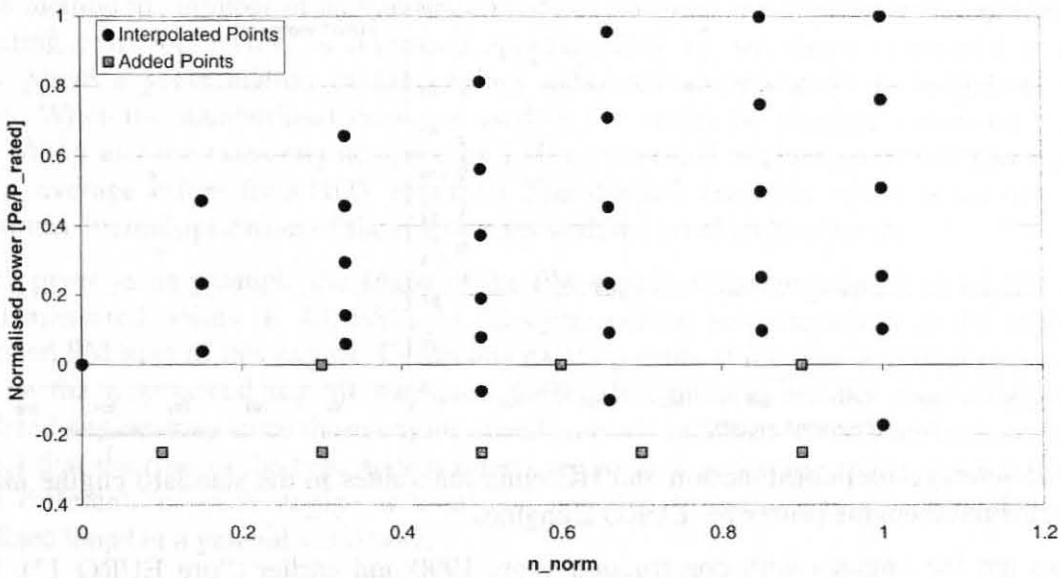

Figure 53: Location of the points in the standard engine map format of PHEM

Since the evaluation of all measured engine maps showed no significant dependency on the emission levels (g/kWh) from the rated engine power, average engine emission maps independent of the rated engine power can be used. Figure 54 and Figure 55 show as example the average emissions and the fuel consumption in the standard engine map for all EURO 2 engines available from the data collection plotted over the rated engine power. For fuel consumption and particle emissions no trend of the emission level over the engine power is visible, for NO_x and HC the trends differ depending on the manufacturer.

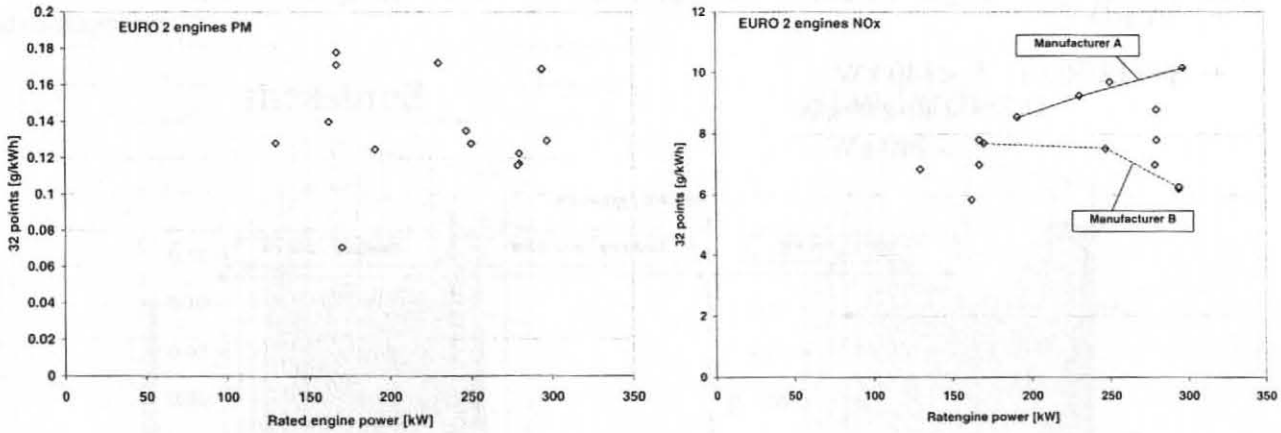

Figure 54: Average PM- and NO_x-emission values in the standard engine maps over the rated engine power for EURO 2 engines

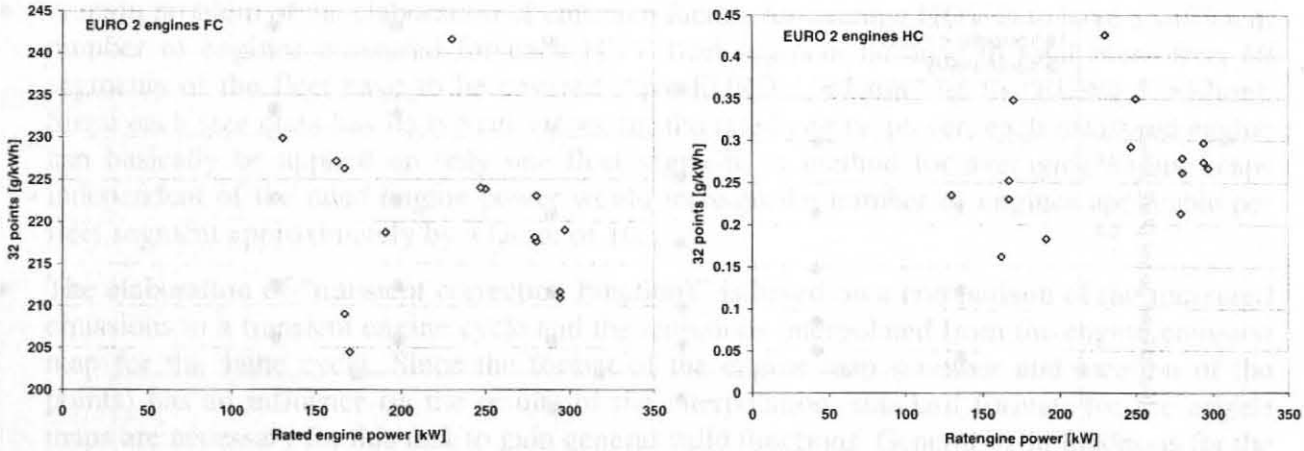

Figure 55: Average fuel consumption and HC-emission values in the standard engine maps over the rated engine power for EURO 2 engines

Exceptions are the engines with construction years 1990 and earlier ("pre EURO 1"). In these cases a clearly increasing particle level is visible with decreasing rated engine power. In absence of type approval limits smaller engines on average had cheaper and/or older technology. Especially a lot of naturally aspirated engines have rather high particle levels. For this reason three average engine emission maps were installed for "pre EURO 1" engines (**Figure 56**).

As a result of the method described above the measured engine maps are split into the following categories only:

- EURO 3
- EURO 2
- EURO 1
- pre EURO 1:
  - * <140 kW
  - * 140-240 kW
  - * > 240 kW

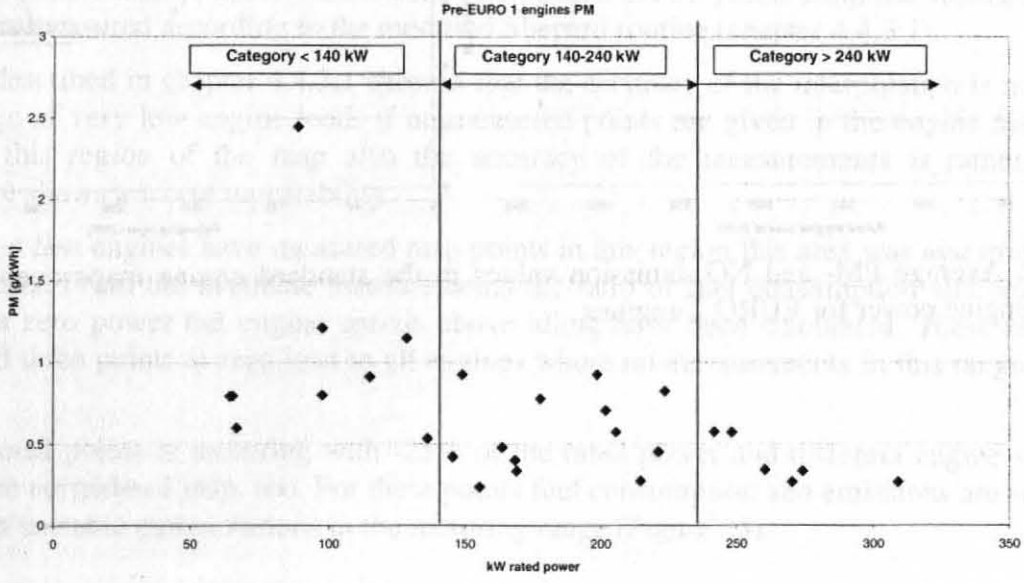

Figure 56: Average particle emissions in the standard engine maps [(g/h)/kW_rated power], "pre EURO 1" engines

With this method the number of engines measured per category and consequently the reliability of the resulting emission factors is increased approximately by ten times compared to previous methods where a segmentation of the engines measured according to the engine power was necessary. When the standardized maps are used by the model the absolute values for the engine speed at idling and the rated engine speed as well as the rated engine power are given as model input (e.g. average values for a HDV segment). The absolute emission values in the map are then gained simply by multiplication of the map values with the rated engine power.

Figure 57 gives as an example the shape of the PM-engine emission map of an EURO 2 engine using all measured points (R 49, ESC, 30 off cycle points) in comparison to the shape of the standardized PM map of this engine. Eventually existing dents at the type approval rpm which can be seen in the map containing all measured points (left picture) are not reproduced from the standardized engine map since these engine speeds are not included in the standardized map. Due to the fact that the rpm of the type approval tests are located according to the full load curve and thus are different for each engine it won't be possible to include type approval points into standardized maps in a general valid way.

Anyhow, when calculating emissions for a complete transient cycle the results usually differ not more than 3% when using all measured points compared to the usage of the standardised 40 point maps since the points of the standardized engine map are averaged values from the measured points around. Relevant differences occur if transient cycles covering only small rpm ranges which are located at or near the type approval rpm are simulated[7]. For the simulation of HDV emission factors the averaging effect of the standardized maps is rather advantageous. Using the original maps it happens for some engines that small differences in the vehicle speed result in very different emission factors.

For other purposes than calculating emission factors, such as assessing emissions in the ETC or WHDC for a specific engine, the use of the originally measured engine map can be more advantageous.

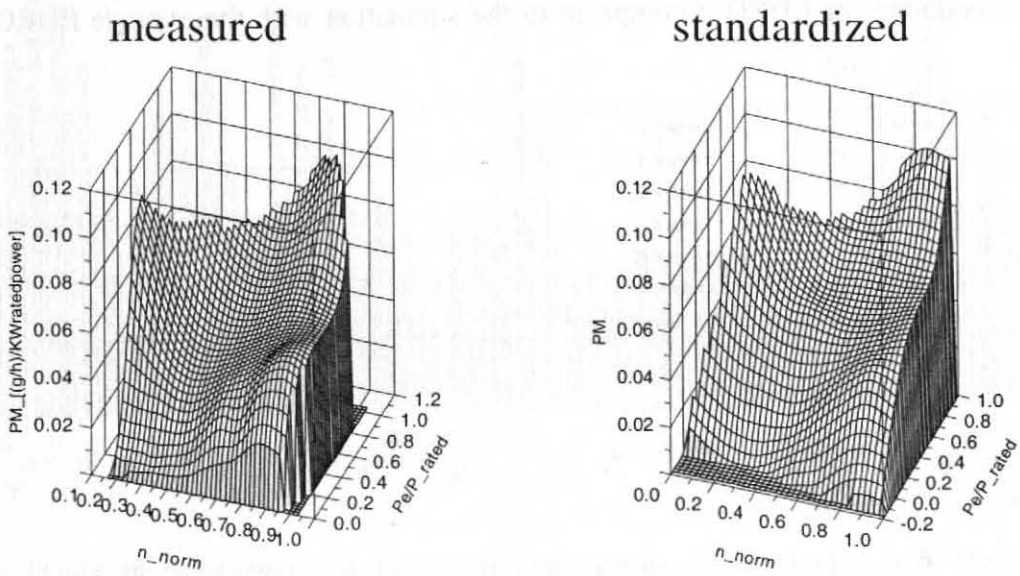

Figure 57: Comparison of the PM-engine emission map from all measured values (52 points) and the standardized emission map (32 points) for an EURO 2 engine

[7] Only relevant if the off-cycle emissions of the engine under consideration are clearly different to the emissions at the type approval points.

Comparison of using average engine maps and single engine maps

As expected the use of the average engine emission map for one technology class gives the same results of PHEM as calculating each engine separately and making the average emission factor afterwards. Figure 58 and Figure 59 give results for a model run where all available engine emission maps for EURO 2 engines were implemented into the same truck one after the other to simulate the emissions for three different real world driving cycles in comparison to the results with the average EURO 2 engine map for the same truck configuration. The results with the average EURO 2 map are identical to the average of all single simulations. This makes the method well suited to the simulation of average HDV emission factors.

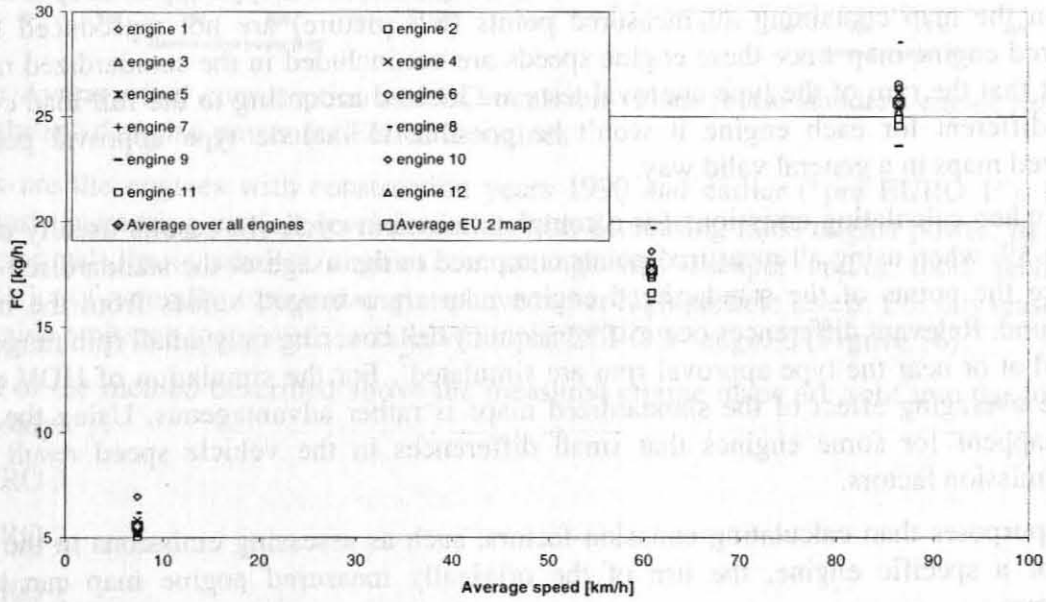

Figure 58: Simulated fuel consumption of a truck-configuration using the single engine emission maps available for EURO 2 compared to the simulation with the average EURO 2 engine map.

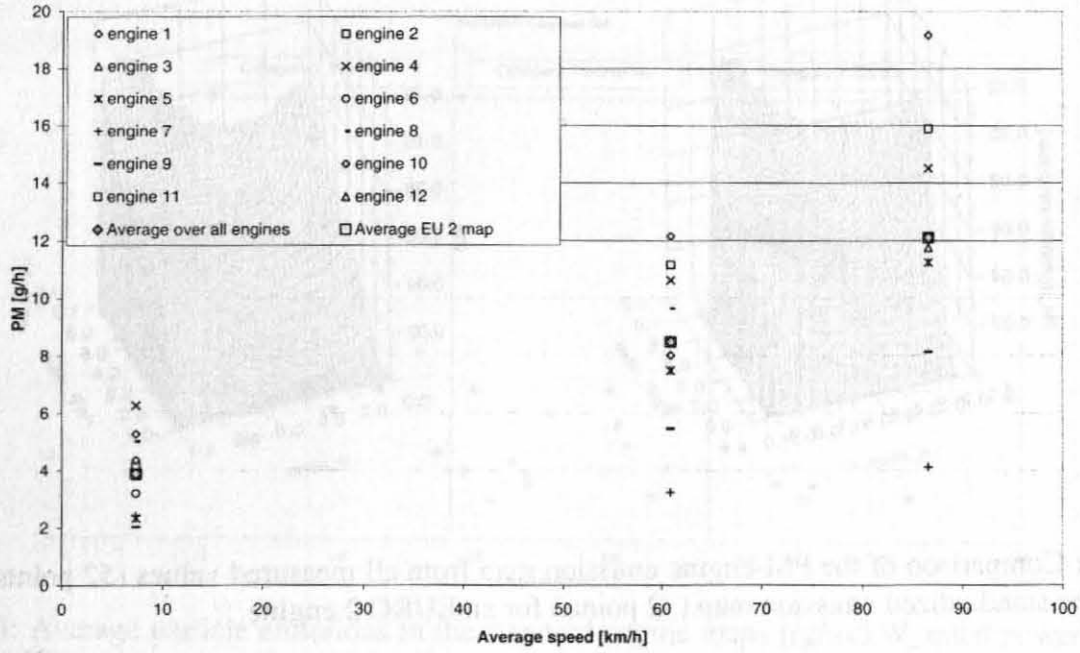

Figure 59: Simulated particulate emissions for a truck-configuration using all single engine emission maps available for EURO 2 compared to the simulation with the average EURO 2 engine map.

4.4.4 Simulation of transient cycles

Since the engine emission maps are measured under steady state conditions while the real world driving behaviour results almost always in transient engine loads, it is of high interest how accurate transient test cycles from the engine test bed can be recalculated by using the engine maps. For this analysis all 15 engines where transient tests have been performed have been taken into consideration. Thirteen of the engines are turbocharged with charge air cooling. Two "pre EURO 1" engines are included too which have been measured in 1993 already. One of these engines was turbocharged without charge air cooling the other engine was naturally aspirated.

4.4.4.1 Comparison of measured emissions and interpolation results from engine maps

When steady state engine emission maps are used to calculate emissions for transient cycles rather high differences occur between calculated and measured emissions. This is mainly valid for particle, HC and CO emissions. This difference is especially assumed to be an effect of different combustion conditions compared to the steady state measurements (e.g. inlet pressure and temperature for turbocharged engines with intercooler). Other known potential inaccuracies like the interpolation routine and the repeatability of the measurements show comparable lower effects. Figure 60 shows as an example the particle emissions measured for 15 engines (EURO 1 to EURO 3) in different transient cycles according to the D.A.CH/ARTEMIS measurement programme. It is obvious that the interpolation from the steady state engine maps underestimates the particle emissions in transient cycles by up to 50%. In general EURO 3 engines (on the right side of the graph) show less influence from transient conditions than EURO 1 and EURO 2 engines. This suggests a better application of these engines to changing conditions under transient load.

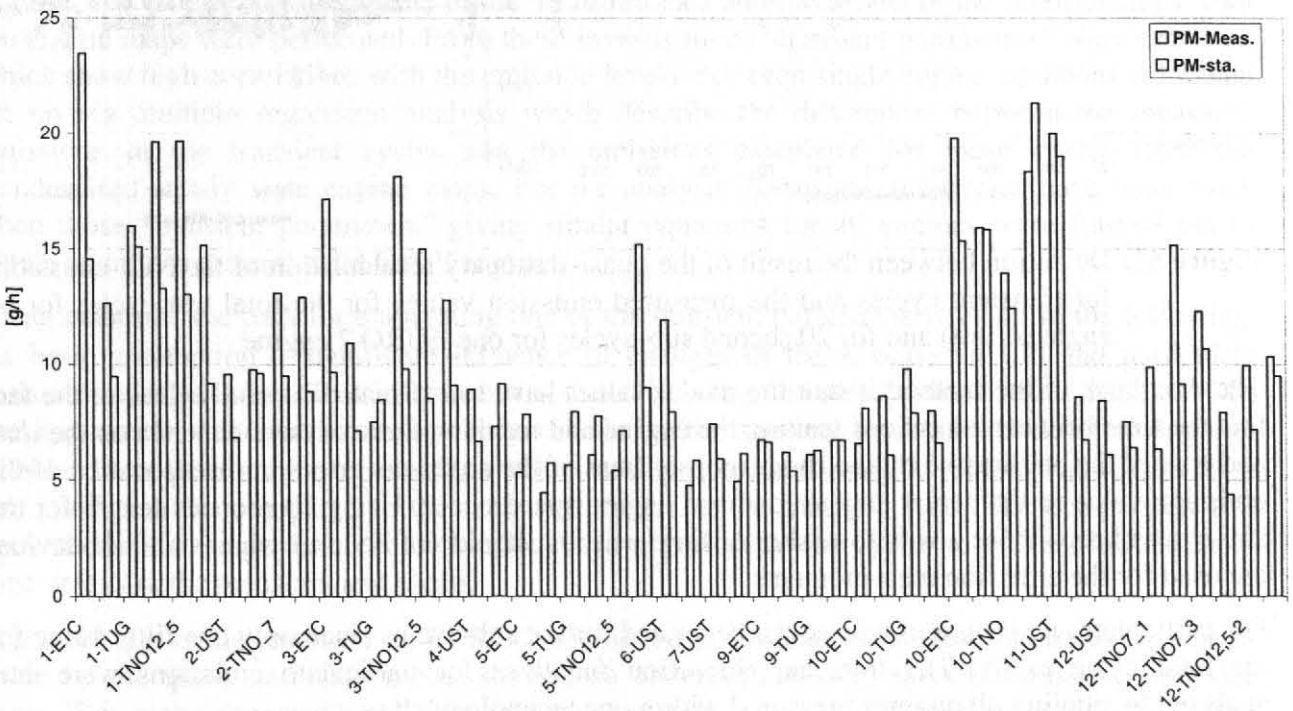

Figure 60: Deviation between the result of the quasi-stationary recalculation of the particulate emissions ("PM-sta.) and the measured emission values for the transient tests of all engines. The numbers give the engine number code (1-ETC means "engine one in the ETC")

For using statistical analysis to assess transient influences a lot of measured emission values are necessary. To increase the number of measured transient cycles the existing cycles are subdivided into "sub-cycles" with 20 seconds length by using the modal measurements. Beside increasing the number of measured values this method has also the advantage that a broader range of transient

conditions is covered. While the average for many potential transient parameters (e.g. the change of the engine power) is zero or near to zero for longer cycles like the ETC, this is not the case in the short sub-cycles.

Comparing the modal measurements[8] with the results of the interpolation out of the engine map shows, that the differences between measurement and simulation increases clearly with shorter time spans looked at. Since transient influences can increase the emission level as well as they can lower it compared to steady state conditions, the positive and negative errors in the simulation are averaged over long cycles to a great extent. Figure 61 shows as example the situation for the NO_x-emissions which are recalculated rather accurately for all engines and all test cycles if the total cycles are taken into consideration. For the 20 second sub-cycles the deviation between the interpolation and the measured emissions is up to 5 times higher, especially at low emission levels. For CO and HC the situation is even worse. Since the driving cycles to be simulated for the Handbook are rather short, reliable transient correction functions seemed to be necessary.

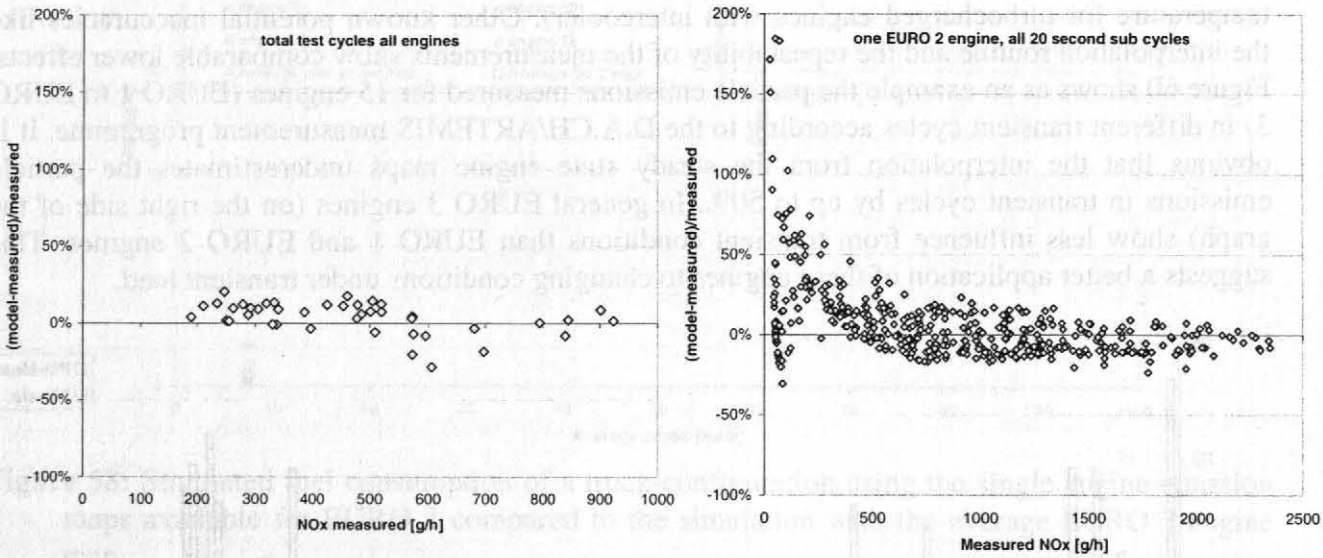

Figure 61: Deviation between the result of the quasi-stationary recalculation of the NO_x-emissions for transient cycles and the measured emission values for the total test cycles for all engines (left) and for 20 second sub-cycles for one EURO 2 engine

The drawback of the method is that the modal values have to be treated carefully. Due to the fact that the time between emissions leaving the engine and reaching the analysers depends on the load and rpm of the engine and due to the response times of the analysers errors in the allocation of the emission value to the actual engine load and engine speed occur. Using 20 seconds length for the sub-cycles keeps these errors low, shorter time periods should not be used when standard devices are used for the emission measurements.

For particulates no emission values can be gained for the sub-cycles since only one filter value for the total cycle exists. The transient correction functions for particulate emissions were thus analysed by pooling all engines measured within one technology class.

4.4.4.2 The transient correction functions

As a consequence of chapter 4.4.4.1 the results of the interpolation out of the steady state engine emission map have to be corrected according to the dynamics of the cycle to improve the accuracy of the model. Since transient engine tests are available for only 25% of all engines, the method has to be general valid for all engines, at least for all engines with the same technology.

[8] 1Hz recorded emission values

Boundary conditions for performing such an adjustment are:

- All of the 15 engines where transient tests have been performed had to be analysed to gain functions which are general valid
- The typical time resolution of the HDV simulation models is 1 second. This is also the typical resolution of driving behaviour measurements
- Engines in use must not be damaged during the measurements at the engine test beds. Therefore there was no possibility for measurements of combustion parameters (e.g. pressure in the cylinder).

These boundary conditions suggested to use statistical methods.

The statistical approach is based on the following procedure:

- transient cycles of the engine test bed are recalculated using the steady-state engine emission maps in the standardised format
- the difference between the measured emissions and the "quasi-stationary" calculation is associated with transient influences
- parameters are searched by statistical means which can explain these differences.

The basic problem at developing dynamic correction functions is finding relevant parameters expressing the dynamic aspects of a cycle which provide good correlations with the difference between measured emissions and the "quasi-stationary" emissions calculated for the transient test.

For this task extensive assessments of the measured data and the results of the interpolations from the engine maps were performed. From these investigations "transient parameters" were extracted which show high correlations with the emission levels. For each single engine equations were then set up via multiple regression analysis which describe the differences between the measured emissions in the transient cycles and the emissions calculated for these cycles from the standardised steady state engine maps. For the analysis 20-second sub-cycles have been used. Then those "transient parameters" giving similar equations for all engines were filtered out to obtain equations general valid for all engines.

As an example, the path for elaborating one of the transient parameters is given in the following. As basic assumption a significant influence of changes in the λ-value on CO and particulate emissions was assumed. This influence was tested by using the steady state engine maps for CO, fuel consumption and intake air flow for recalculating the transient test cycles of different engines. This leads to quasi stationary emission values and to quasi stationary λ-values. The results from the simulation are compared to the measured values in the transient tests. The comparison was performed for average differences over longer time periods of the cycles to prevent influences of time delays in the measurement chain.

Figure 62 shows the result for an EURO 2 engine. At all engines an overestimation of the real λ-value by the quasi stationary model showed an underestimation of the CO emissions and vice versa. This is the expected trend since an overestimation by the model does mean, that the engine has less intake air stream in the transient condition under consideration than he would have in steady state conditions at the same engine load (and the other way round).

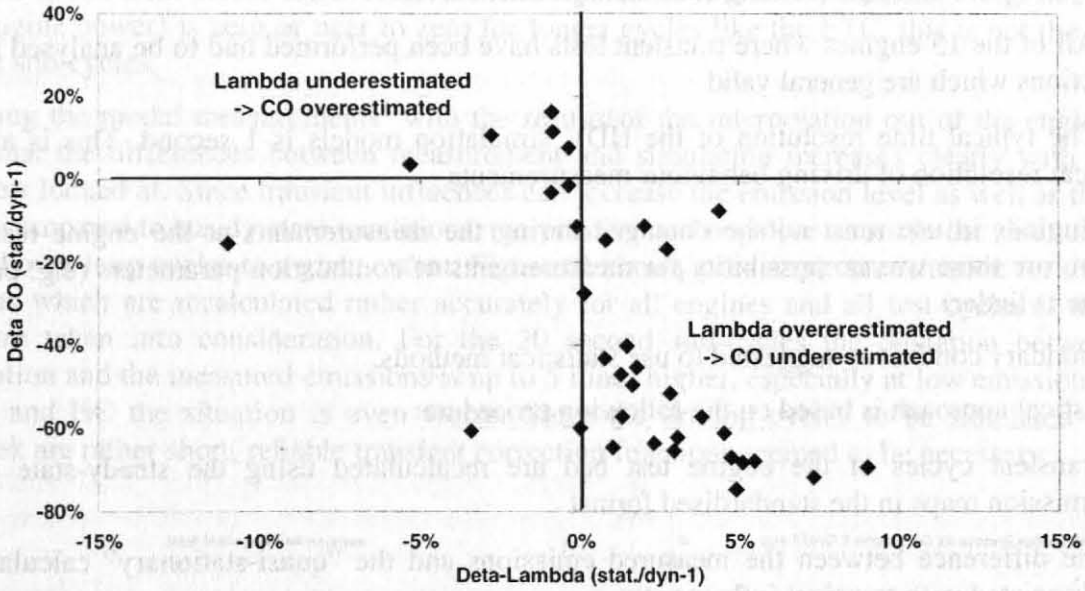

Figure 62: Influence of different λ values in steady state conditions compared to transient conditions on the CO emissions for a EURO 2 HDV engine

A physical simulation of changes in the λ value in transient tests, mainly as result from sluggishness of the turbocharger, would need detailed information on the engine as model input. Additionally this would result in an increased effort for the model development. To keep the data structure simple, parameters were searched which are able to describe the changes in the λ values by statistical means. The sluggishness of the turbocharger results from the inertia of the rotating masses and from the time the exhaust gas needs to reach the turbine and the time the intake air needs to reach the engine intake from the compressor. As a result the energy in the enthalpy stream of the exhaust gas reaches the intake air stream time delayed.

Assuming similar geometries of the turbocharger system within each EURO-class, the influence of transient load changes on the intake air flow is mainly a result of changes in the effective engine power. Thus several parameters describing this changes where tested for being able to explain the changes in the λ values and in the CO emissions compared to steady state conditions for all engines. From manifold tested potential parameters the best fitting parameter for all engines was the average amplitude of the effective engine power over 3 seconds before an actual λ or CO event (Ampl3p3s in Figure 63). Where the amplitude has the highest significance if it is counted only if a threshold of 3% from the rated engine power is exceeded in transient changes of the power.

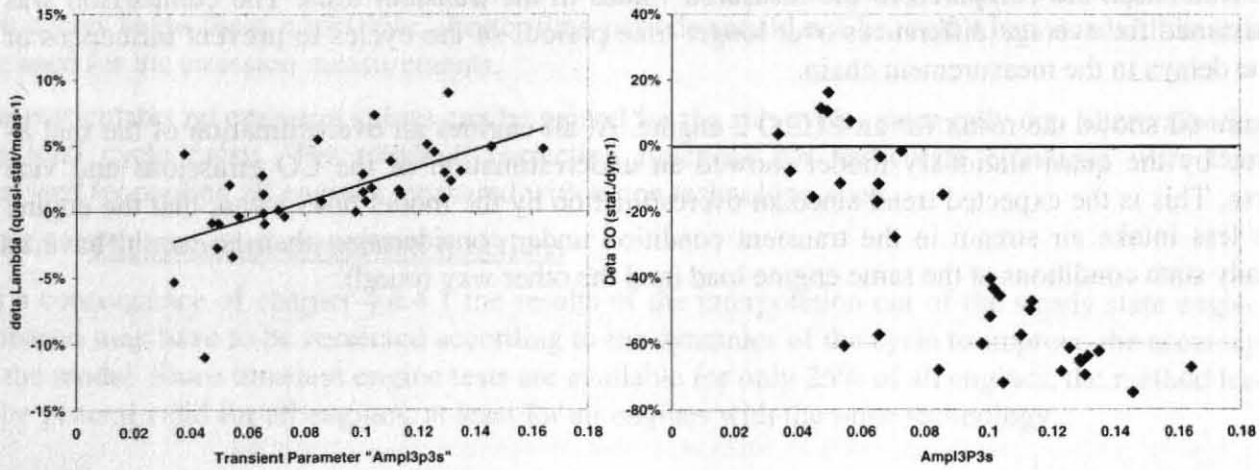

Figure 63: Correlation between the change of the λ values, the CO emissions and the transient parameter Ampl3p3s for a EURO 2 HDV engine

As a result, we may assume that the parameter Ampl3p3s explains transient influences on the λ value and on CO and particulate emissions on average for all turbocharged engines quite well.

Similarly in total six parameters were filtered out which show high correlation to changes in the emission level when steady state and transient tests are compared. The analysis showed that using the difference between quasi-stationary model results and the measured emissions proved to result in much better functions than the ratio of stationary model results to the measured emissions. This leads to the following methodology for transient corrections.

$$E_{trans} = E_{QS} + P_{Rated} \times F_{trans}$$

with E_{trans}..... emission value under transient condition [g/h]

E_{QS} ..... emission value interpolated from the steady-state emission map [g/h]

P_{rated}..... rated engine power [kW] (again the emission values are normalized)

F_{trans}..... dynamic correction function [(g/h)/kW_rated power]

$$F_{trans} = A \times T_1 + B \times T_2 + C \times T_3$$

with A,B,C .....factors (different according to the exhaust gas component but constant for one engine technology)

T_1, T_2, T_3 .... transient parameters (calculated by the model PHEM from the engine speed and engine power course).

More than 3 parameters are not included into the functions to have stable and general valid results although for single engines equations using more parameters give much better results. To make the function suitable for calculating average HDV with different engine sizes it is – as the emission maps - normalised with a division by the rated engine power.

The transient parameters used are the following:

LW3P3s.....number of load changes from the engine power in the cycle over three seconds before an emission event. Load changes are counted only if their absolute value is higher than 0.03*(Pe/P_rated)

Ampl3P3s .....average amplitude of LW3P3s

P40sABS.....difference of the normalised engine power at the emission event and the average normalised engine power over 40 seconds before the emission event

Dyn_Pneg3s.....average negative engine power over three seconds before an emission event; set to zero if the negative engine power was not reached transiently.

Dyn_Ppos3s.....average positive engine power over three seconds before an emission event; set to zero if the positive engine power was not reached transiently.

ABS_dn2s.....absolute change of the normalised engine speed within 2 seconds before the emission event in second i ($0.5* (n_{\_norm}(i)-n_{\_norm}(i-2))$)

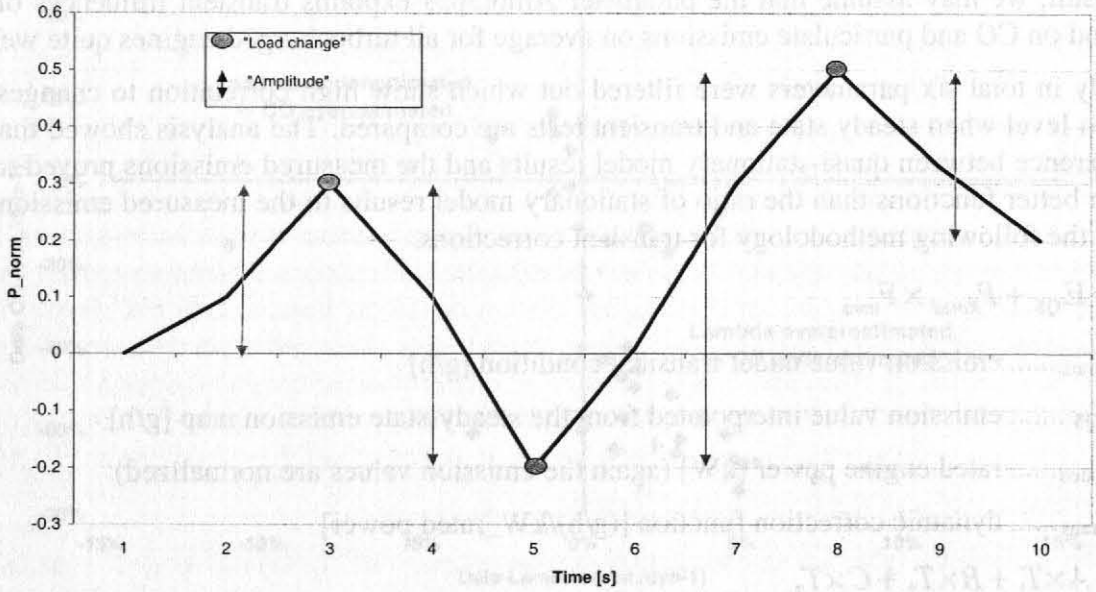

Figure 64: Schematic picture of the transient parameters load change (LW3P3s) and Amplitude (Ampl3P3s) in a test cycle

The transient correction functions are implemented in the model PHEM and can be switched on or off. The user simply has to select the emission level ("pre EURO 1" to "EURO 5").

Table 12 shows the factors and the transient parameters for the correction of NO_x. According to these values, the correction function for the NO_x emissions of EURO 2 engines is given as example.

Equation 2: transient correction function for EURO 2 engines

$$F_{trans-NOx} = -1.06 \times Ampl3P3s - 0.534 \times P40sABS + 5.57 \times Dyn\_Pneg3s \quad [(g/h)/kW_{rated\ power}]$$

Table 12: Transient factors for the NOx correction

	Ampl3P3s	P40sABS	ABS_dn2s
EURO 0	0.180	-0.290	-1.800
EURO 1	0.151	-0.303	-1.994
EURO 2	0.151	-0.303	-1.994
EURO 3	1.051	-0.289	-1.488
EURO 4	as EURO 3		
EURO 5	as EURO 3		

HC and CO are corrected in an analogous way. The corresponding transient factors are shown in Table 13.

Table 13: Transient factors for the CO and HC correction

	CO			**HC**		
	Ampl3P3s	P40sABS	LW3P3s	Ampl3P3s	LW3P3s	Dyn_Pneg3s
EURO 0	3.982	0.375	-0.104	-0.0723	0.002154	-0.121
EURO 1	3.982	0.375	-0.104	-0.0723	0.002154	-0.121
EURO 2	3.982	0.375	-0.104	-0.0723	0.002154	-0.121
EURO 3	3.190	0.238	-0.0908	-0.0413	-0.0228	-0.0283
EURO 4	As EURO 3			As EURO 3		
EURO 5	As EURO 3			As EURO 3		

Because of the limited number of measured particulate emissions (no sub-cycles possible) it was not possible to elaborate separate functions for the "pre EURO 1" engines, especially for the three engine-power-sub-categories in this class (chapter 4.4.3.2). The few available transient tests for those engines showed a similar general tendency as the EURO 1 and EURO 2 engines. Thus the same functions are applied (Table 14). Euro 3 engines generally show less increase of the particle emission level under transient cycles compared to steady state tests. This results from a better engine application using inter alia the features provided by modern fuel injection systems and optimised turbo charge systems using variable turbine geometries. The low particle emission limits from EURO 4 on will not allow significant increases under transient conditions compared to steady state operation if the ETC has to be passed. Thus the transient correction functions for EURO 4 and EURO 5 engines were set to zero (chapter 4.5).

Table 14: Transient factors for the particulate emission correction

	Ampl3P3s	LW3P3s	Dyn_Pneg3s
EURO 0	0.525	-0.0153	0.442
EURO 1	0.525	-0.0153	0.442
EURO 2	0.525	-0.0153	0.442
EURO 3	0.141	-0.0099	-0.584
EURO 4	0	0	0
EURO 5	0	0	0

With this set of equations the accuracy of the simulation is improved for all engines in nearly all cycles.

Since the fuel consumption can already be simulated very accurately without any correction function, no such function is applied. Particle emissions are clearly underestimated when simply interpolated from the steady state engine maps. The transient correction function brings the simulation to the measured level (Figure 65).

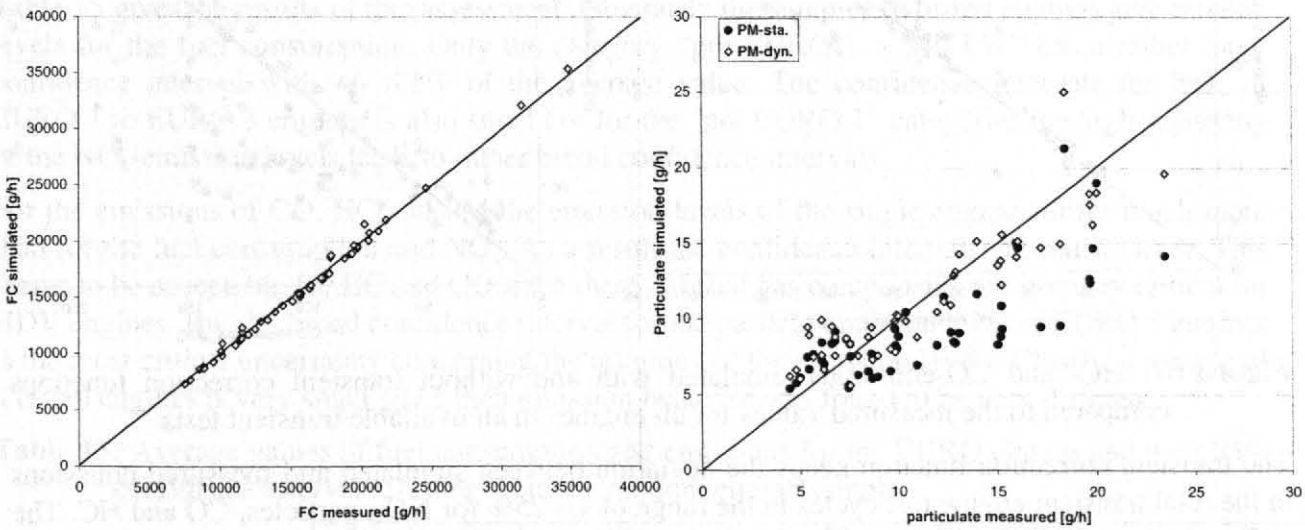

Figure 65: Fuel consumption and particle emissions simulated with and without transient correction functions compared to the measured values for all engines in all available transient tests

For NO_x emissions the transient influences are small over the cycles shown, thus the transient correction function gives only slight improvements. For the 20-second sub cycles the improvements are higher. Figure 66 compares the measured with the simulated NO_x emissions for

the total transient cycles (left picture) and for the 20-second sub-cycles for all transient cycles measured at on engine as example.

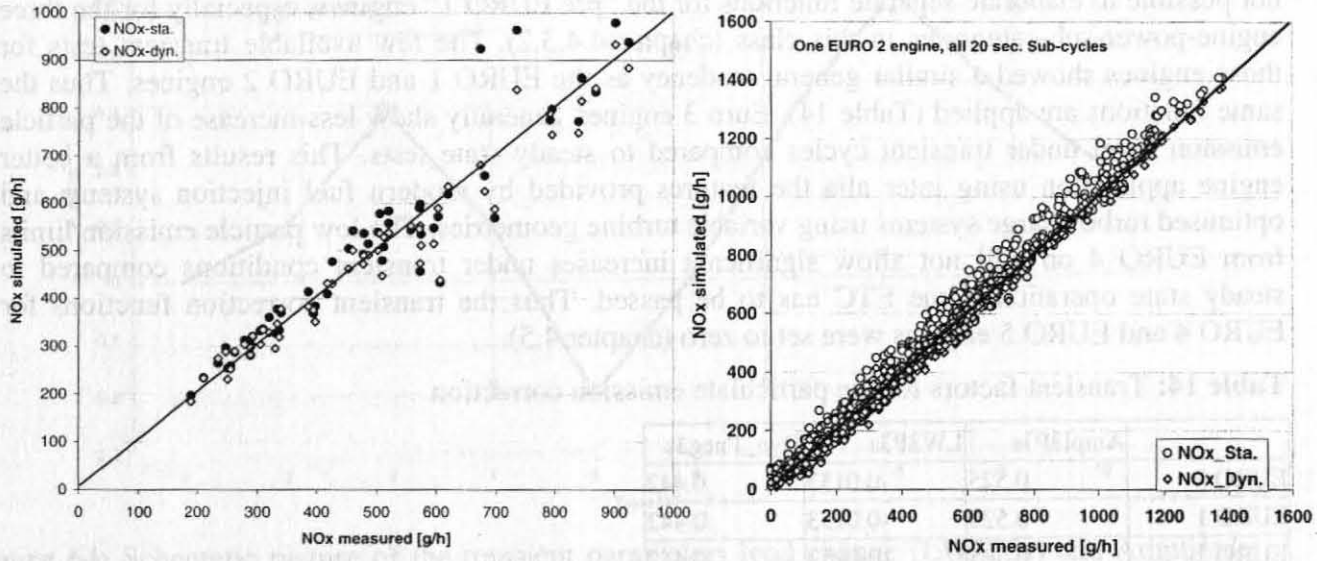

Figure 66: NO_x-emissions simulated with and without transient correction functions compared to the measured values for all engines in all available transient tests (left) and for one EURO 2 engine in all 20-second sub-cycles (right)

For CO similar improvements can bee seen as for particulates while the accuracy for HC emissions is also without transient correction functions astonishing good (Figure 67).

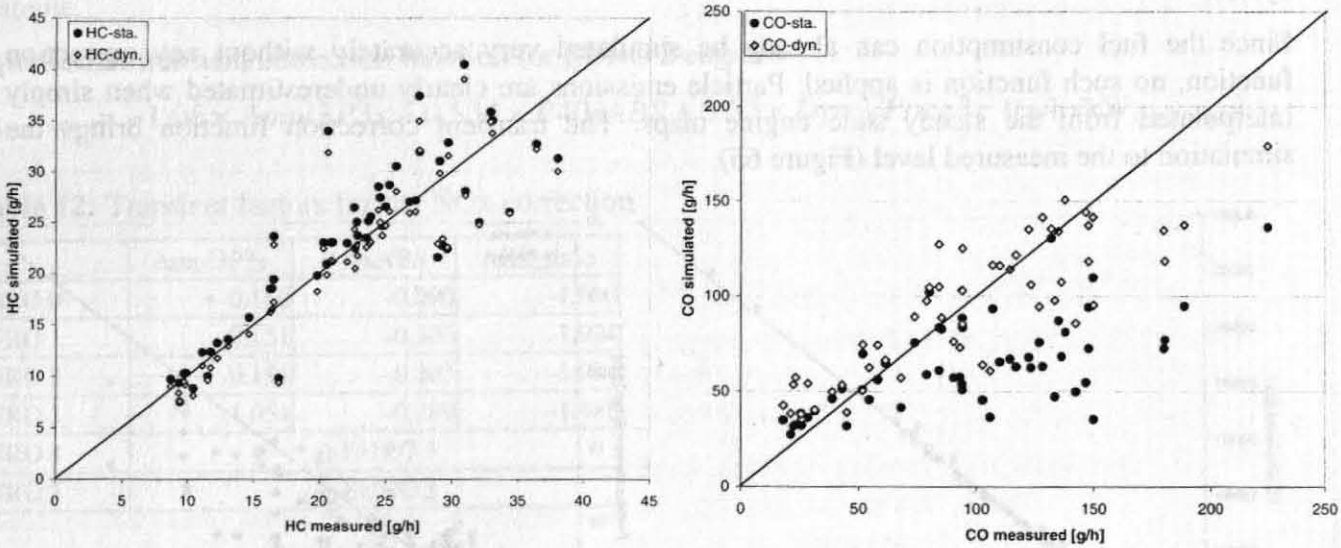

Figure 67: HC- and CO-emissions simulated with and without transient correction functions compared to the measured values for all engines in all available transient tests

The transient correction function keeps the deviation between simulated and measured emissions in the total transient engine test cycles in the range of +/- 25% for NO_x, particles, CO and HC. The percent error generally decreases by increasing emission values. For the fuel consumption no transient correction is applied because the error is already below +/-5%.

Since the same function can successfully be applied to all engines within a technology class, obviously a general valid method was found which can be used for the average engine emission maps in the normalised formats ("pre EURO 1" to "EURO 3" engine maps).

A closer look to the accuracy of the emission simulation is given in chapter 4.4.5.

4.4.5 HDV Emission Model Accuracy

In this chapter the method described in the chapters before is analysed to assess the accuracy of the model and the resulting emission factors. The accuracies analysed are those related to

(1) The engine sample (relevant for the average engine maps and the average transient correction function)

(2) The accuracy of simulating emissions for given engine speed and engine power cycles (recalculation of transient engine tests)

(3) the accuracy of simulating emissions for given vehicle speed cycles (recalculation of chassis dynamometer tests of HDV).

Whereas (1) takes into consideration that the engine sample included into the model data base has to be seen as a random sample of all engines on the road, (2) shows the accuracy reached when the cycles for the engine power and the engine speed are given as model input of the measurements of transient engine tests. This is theoretically the maximum accuracy the model can reach for the simulation of a single HDV since for (3) the engine power and the engine speed cycles have to be simulated from the vehicle speed cycle.

4.4.5.1 Influence of the engine sample

Since the emission levels of the different engines within the categories "pre EURO 1" to EURO 3 show a scattering, the accuracy of predicting the average emission level within an engine category depends on the number of engines tested. Although the data base is the largest available within Europe, the sample size is small compared to the number of engines on the road. Thus uncertainties arise from the limited number of engines tested.

To assess this uncertainty for each EURO category the average emission value, the standard deviation of the emission values and the 95% confidence interval, was calculated assuming that the engines in the data base are a random sample. The emission values used here for each engine are the averages of the 32 point standard engine map, since these values are the only emission levels available for all engines (chapter 4.3.1.3 and 4.4.3.2).

Table 15 gives the results of this assessment. Obviously the samples of tested engines give reliable levels for the fuel consumption. Only the category "pre EURO 1 > 240 kW" has a rather large confidence interval with +/- 8.1% of the average value. The confidence intervals for NO_x of EURO 1 to EURO 3 engines is also small but for the "pre EURO 1" categories the high scattering of the NO_x-emission levels leads to rather broad confidence intervals.

For the emissions of CO, HC and PM the emission levels of the single engines differ much more than for the fuel consumption and NO_x. As a result the confidence intervals are much larger. This seems to be acceptable for HC and CO since these exhaust gas components are not very critical for HDV engines. But the broad confidence interval for the particle emission level of EURO 3 engines is the most critical uncertainty concerning the accuracy of the emission levels. Clearly, a sample of 4 tested engines is very small since their emission behavior was found to be very different.

Table 15: Average values of fuel consumption and emissions for the EURO classes and their 95% confidence interval resulting from the random engine sample

		Fuel consumption		NOx		CO		HC		PM	
	Nr. of engines	average [g/kWh]	95% confidence +/-	average [g/kWh]	95% confidence +/-	average [g/kWh]	95% confidence +/-	average [g/kWh]	95% confidence +/-	average [g/kWh]	95% confidence +/-
pre EURO 1 <140 kW	8	280.8	4.6%	10.6	22%	4.77	19%	2.27	27%	0.851	19%
pre EURO 1 140-240 kW	13	266.3	4.3%	12.9	11%	3.21	27%	1.01	22%	0.563	23%
pre EURO 1 >240 kW	6	255.9	8.1%	11.9	24%	1.75	21%	0.50	35%	0.392	29%
EURO 1	11	228.2	3.5%	7.5	6%	1.41	17%	0.51	23%	0.289	15%
EURO 2	15	220.3	2.1%	7.8	9%	1.04	16%	0.27	13%	0.138	11%
EURO 3	4	227.7	2.7%	6.7	10%	1.23	38%	0.33	50%	0.139	37%

As a result of this analysis it has to be recommended to add measurements of EURO 3 engines in the near future to gain a more reliable data base for their emission factors. The data available now do not allow to make a statement whether EURO 3 engines on the road have on average higher or lower particle emission levels over the engine map than EURO 2 engines (Figure 68).

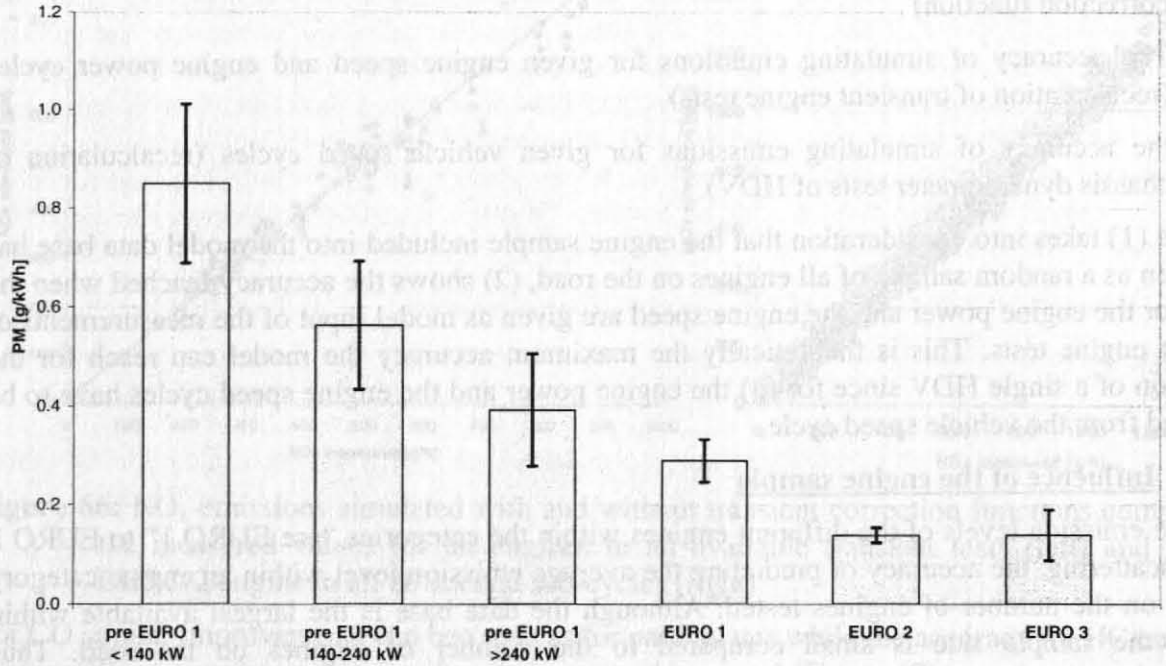

Figure 68: Average emission value in the standardised 32 point engine map and 95% confidence interval of these value for the engine categories.

4.4.5.2 Accuracy of simulating transient engine tests

Since the emission factors are not derived from measuring the corresponding cycles directly but from simulation tools, this certainly adds inaccuracies in the results. To assess the potential magnitude of errors, the results of the simulation of transient engine tests are compared to the measured values in the following.

When elaborating the transient correction factors it proved rather soon that no functions can be derived explaining the differences between the simulation of the steady state engine maps and the measured emissions in transient cycles absolutely satisfying for all engines. The reason is that the engines are constructed and adjusted to transient loads very different depending on the make and the model. Different adjustments in the engine application (especially the fuel injection timing,) are visible rather clearly by the quality of the simulated fuel consumption and NO_x emission values. Other parameters, such as the construction of the turbo charger and also the application of the fuel injection pressure and – if available – also multiple fuel injection are visible mainly in the quality of the simulation for particle emissions and CO. From the measured engines none had an exhaust gas re-circulation. This may add another major source of differences in the transient behaviour of different models in future.

Some of the engine specific results are shown below.

Figure 69 gives the accuracy reached in the single test cycles for fuel consumption and NO_x. For the fuel consumption the highest deviation from the measured value is 7%. On average the model reaches the measured value with +/- 2.2% accuracy (average absolute deviation, Table 16). For NO_x one EURO 3 engine is underestimated in all cycles up to –27%. All other engines are simulated within +/- 15% difference to the measured values.

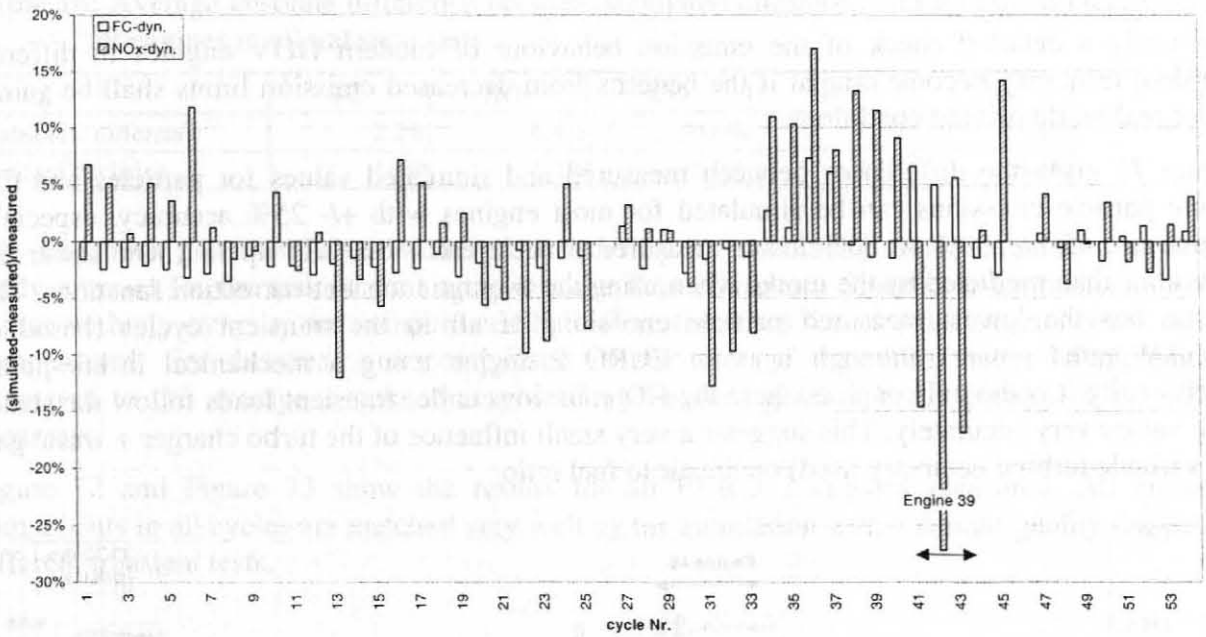

Figure 69: relative difference between simulated emissions and measured emissions for all transient tests for all engines.

Looking at the simulation of NO_x emissions and fuel consumption for EURO 3 engines in some more detail shows that the NO_x-emissions are simulated very accurately for three of the four EURO 3 engines. The engine (no. 39) where the NO_x emissions are clearly underestimated by the model also shows significantly lower fuel consumption values compared to the simulation. Therefore it may be assumed that this engine changes the engine control mechanism under transient load compared to the steady state tests.

The results for engine no. 39 are shown separately in Figure 70. While the fuel consumption is overestimated by approximately 6% the NO_x emissions are underestimated by more than 20% when the transient cycles are interpolated from the steady state engine map. This corresponds quite well with what can be expected from shifting the fuel injection timing to some degrees earlier.

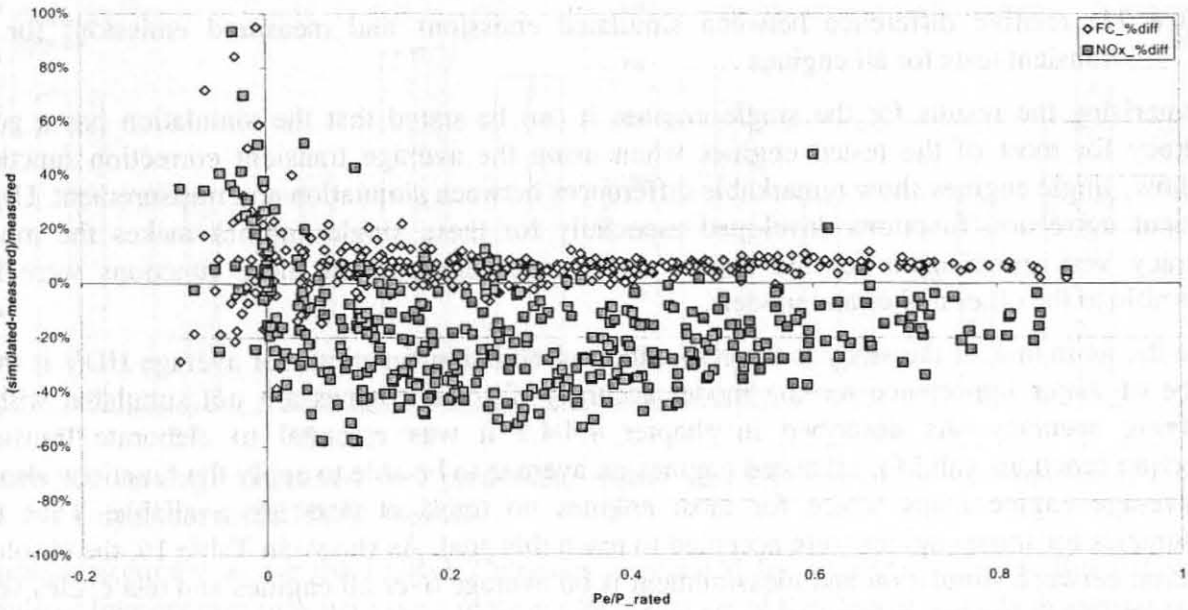

Figure 70: Difference between measured fuel consumption and NO_x emissions to the simulated values in the 20-second sub cycles of all transient tests for engine 39.

Obviously a detailed check of the emission behaviour of modern HDV engines in different transient tests may become crucial if the benefits from decreased emission limits shall be gained under real world driving conditions.

Figure 71 gives the differences between measured and simulated values for particles and CO. While particle emissions can be simulated for most engines with +/- 25% accuracy, especially engine no. 45 has 30% to 80% lower measured particle emissions and up to 150% lower CO emissions than predicted by the model when using the average transient correction functions. This engine has the lowest measured particle emissions of all in the transient cycles (based on (g/h)/kW_rated power) although it is an EURO 2 engine using a mechanical in-line-pump. Additionally it is the only engine where the CO emissions under transient loads follow the steady state values very accurately. This suggests a very small influence of the turbo charger + waste gate (no variable turbine geometry used) on the air to fuel ratio.

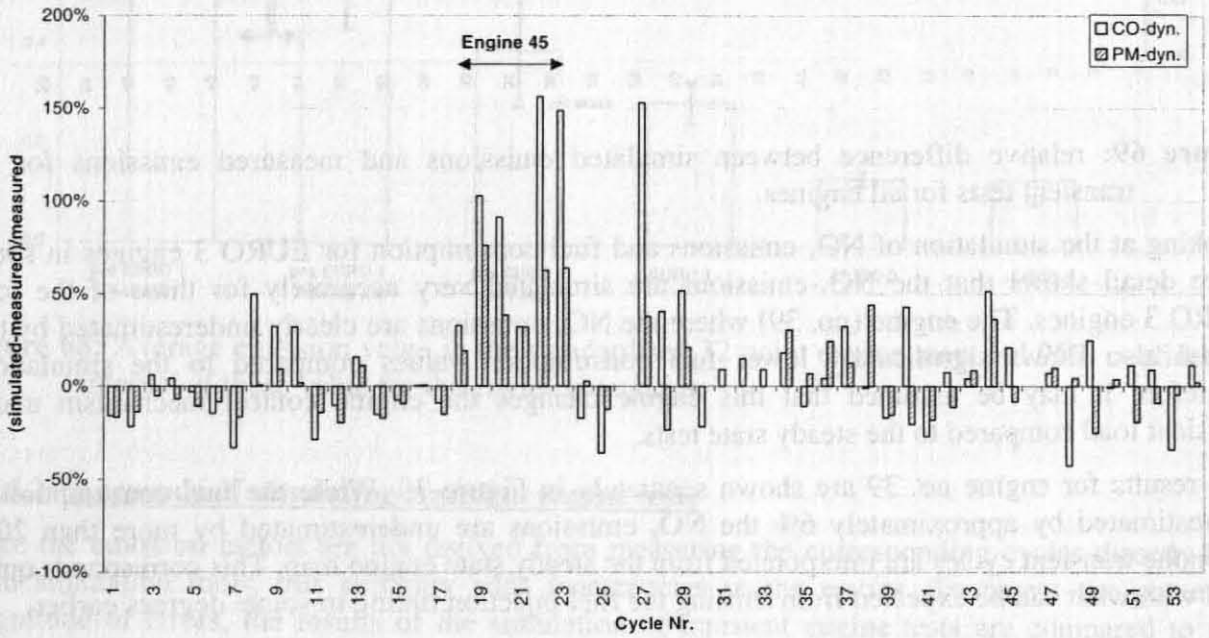

Figure 71: relative difference between simulated emissions and measured emissions for all transient tests for all engines

Summarising the results for the single engines it can be stated that the simulation has a good accuracy for most of the tested engines when using the average transient correction function. Anyhow, single engines show remarkable differences between simulation and measurement. Using transient correction functions developed especially for these single engines makes the model accuracy very good again for the engine under consideration, but these functions were not applicable to the other makes and models.

Since the main task of the study is the elaboration of emission functions for average HDV it shall not be of major importance for the model accuracy if some engines are not simulated with a satisfying accuracy. As described in chapter 4.4.4.2 it was essential to elaborate transient correction functions valid for all tested engines on average to be able to apply the functions also to the average engine maps where for most engines no transient tests are available. Thus the inaccuracies for some engines were accepted to reach this goal. As shown in Table 16, the absolute deviation between simulation and measurement is on average over all engines and test cycles very low. Only CO emissions are predicted with rather low quality with an average deviation of 30%.

Table 16: Average absolute difference between simulated emissions and measured emissions for all engines in all transient tests

	FC	NOx	CO	HC	PM
% absolute difference	2.2%	6.4%	30.6%	7.1%	18.1%
Standard deviation	1.5%	5.4%	36.0%	8.3%	16.4%

The deviations given in Table 16 show the accuracy for simulating single engines, what is not really relevant for the task of simulating average fleet emissions. Since over estimations for one engine within a category are compensated by underestimations for an other engine, errors can be compensated. For this reason a comparison of the average measured values of all engines compared to the average simulated results of all engines gives a better picture of the model accuracy.

Figure 72 and Figure 73 show the results for all EURO 2 engines measured. All emission components in all cycles are matched very well by the simulation with a similar quality for all five different transient tests.

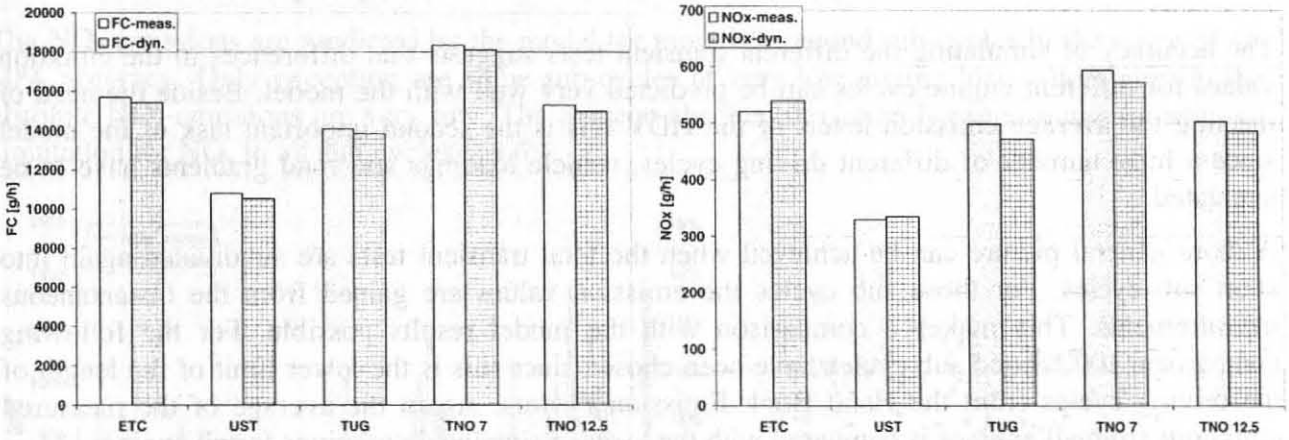

Figure 72: Average measured fuel consumption and NO_x emissions vs. simulation results (-dyn.) for all EURO 2 engines.

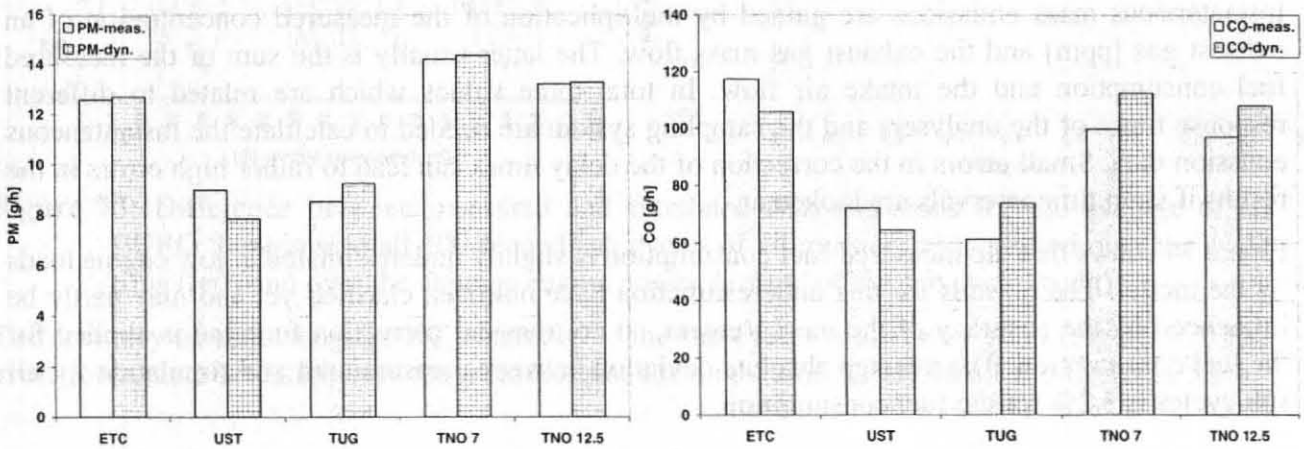

Figure 73: Average measured fuel particulate matter and CO emissions vs. simulation results (-dyn.) for all EURO 2 engines.

A similar accuracy as for the EURO 2 engines is reached for EURO 3 models. But the small sample of four engines may not give a representative picture of the fleet as already discussed in the previous chapter.

Table 17 summarises the model accuracy for the simulation of the average EURO 2 and EURO 3 emission behaviour in the transient test cycles. The results show that the errors are below 3% for the fuel consumption, below 6% for NO_x and below 12.5% for HC and PM. Since these deviations are in the order of magnitude of the repeatability of measurements the model accuracy reached is very good. Only for CO higher deviations to the measured values occur but CO is a rather uncritical exhaust component for HDV.

Table 17: percent difference between the average of the measured fuel consumption and emissions to the average simulation results for all EURO 2 and all EURO 3 engines

	EURO 2 engines					Euro 3 engines				
Test cycle	FC	NOx	CO	HC	PM	FC	NOx	CO	HC	PM
ETC	-1.6%	3.7%	-9.8%	-1.6%	0.9%	2.6%	0.0%	-6.1%	10.2%	5.4%
UST	-2.5%	1.5%	-10.7%	0.1%	-12.5%	-0.3%	4.3%	-28.9%	-4.6%	-2.3%
TUG	-1.8%	-5.3%	20.7%	-2.6%	8.5%	2.8%	-5.6%	20.5%	5.3%	-10.6%
TNO 7	-1.3%	-3.6%	12.7%	5.1%	1.1%	0.4%	-1.0%	6.1%	-5.0%	-9.8%
TNO 12.5	-2.1%	-3.2%	11.4%	0.9%	0.4%	2.8%	-2.8%	2.9%	-4.5%	4.1%

The accuracy of simulating the different transient tests suggests that differences in the emission values for different engine cycles can be predicted very well with the model. Beside the need of meeting the average emission levels of the HDV this is the second important task of the model since a huge number of different driving cycles, vehicle loadings and road gradients have to be simulated.

A more general picture can be achieved when the total transient tests are subdivided again into short sub cycles. For those sub cycles the emission values are gained from the instantaneous measurements. This makes a comparison with the model results possible. For the following comparison 100 second sub cycles have been chosen since this is the lower limit of the length of the driving cycles from the Hand Book Emission Factors. Again the average of the measured emissions from all engines is compared with the average simulated emissions for all engines.

Taking instantaneous measurements for gaining the emission factors for rather short cycles also increases the inaccuracy in the measured values. This results mainly from the fact that the instantaneous mass emissions are gained by multiplication of the measured concentration of an exhaust gas [ppm] and the exhaust gas mass flow. The latter usually is the sum of the measured fuel consumption and the intake air flow. In total three values which are related to different response times of the analysers and the sampling system are needed to calculate the instantaneous emission data. Small errors in the correction of the delay times can lead to rather high errors in the results if short time intervals are looked at.

Figure 74 shows that the measured fuel consumption is slightly underestimated at low engine loads by the model. The reasons for this underestimation have not been clarified yet and may partly be influenced by the accuracy of the measurement, so no transient correction function is applied for the fuel consumption. The average absolute deviation between measurement and simulation for all sub-cycles is 3.2% for the fuel consumption.

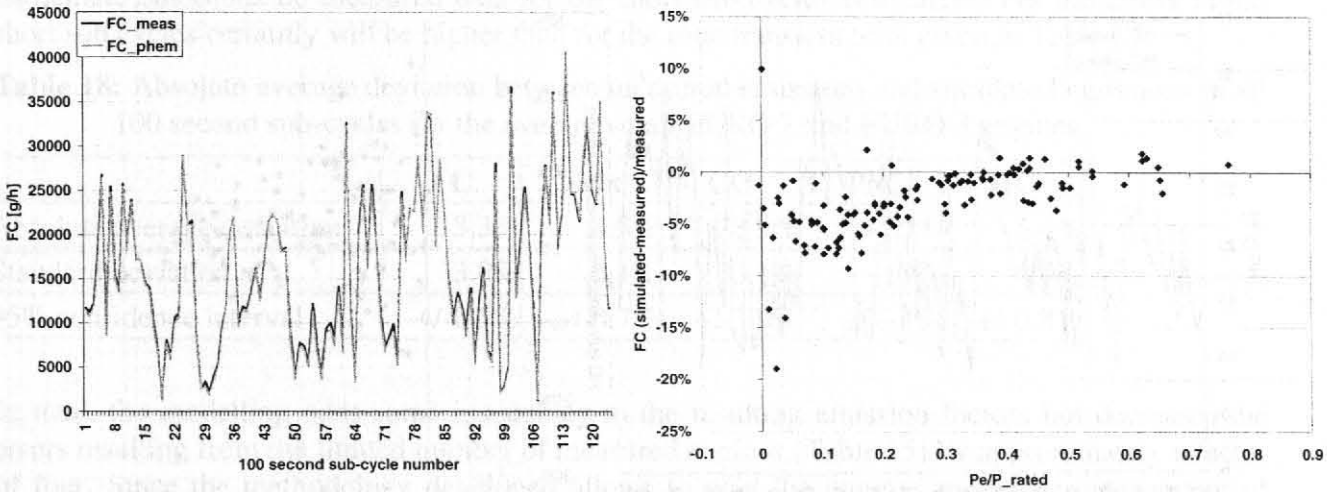

Figure 74: Difference between measured and simulated FC for the average of all EURO 2 engines in all 100 second sub cycles of all transient tests plotted over the cycle time (left) and over the average engine power demand of the sub cycle (right)

The NO_x emissions are predicted by the model for most 100 second sub-cycles in the range of +/- 10% accuracy. Only exception are some sub-cycles at very low engine load where already the absolute NO_x-emissions are very low. The average absolute deviation between measurement and simulation for NO_x in all sub-cycles is 4.6%.

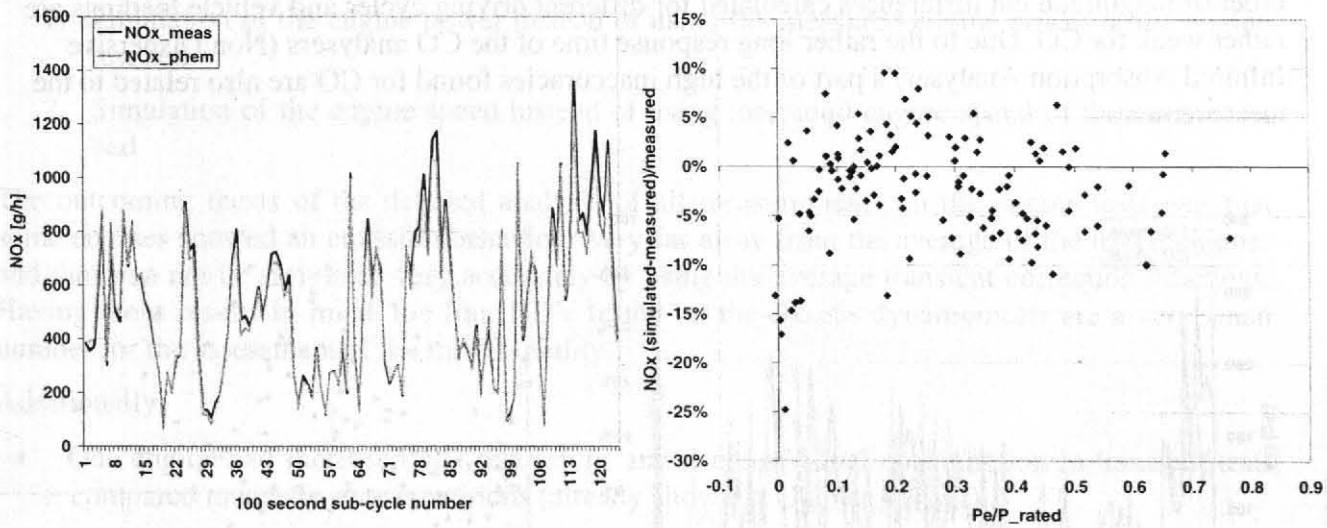

Figure 75: Difference between measured and simulated NO_x-emissions for the average of all EURO 2 engines in all 100 second sub cycles of all transient tests plotted over the cycle time (left) and over the average engine power demand of the sub cycle (right)

The accuracy of simulating the HC-emissions of the sub-cycles is also very good (Figure 76). The average absolute deviation between measurement and simulation for HC in all sub-cycles is 5.5%.

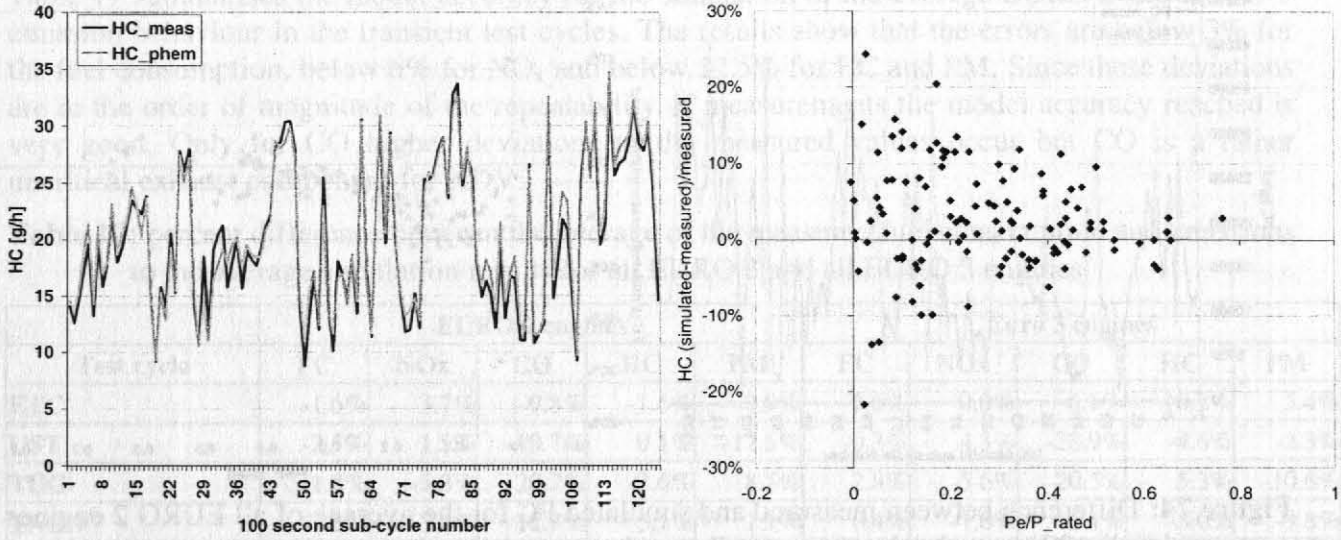

Figure 76: Difference between measured and simulated HC-emissions for the average of all EURO 2 engines in all 100 second sub cycles of all transient tests plotted over the cycle time (left) and over the average engine power demand of the sub cycle (right)

The CO emissions are simulated quite inaccurately with errors up to 100%. Although the transient correction function reduces the errors by more than 50% the model does not give reliable results for CO emissions in short cycles. Thus the resulting emission factors for CO of HDV give the right order of magnitude but differences calculated for different driving cycles and vehicle loadings are rather weak for CO. Due to the rather long response time of the CO analysers (Non Dispersive Infrared Absorption Analyser) a part of the high inaccuracies found for CO are also related to the measurement.

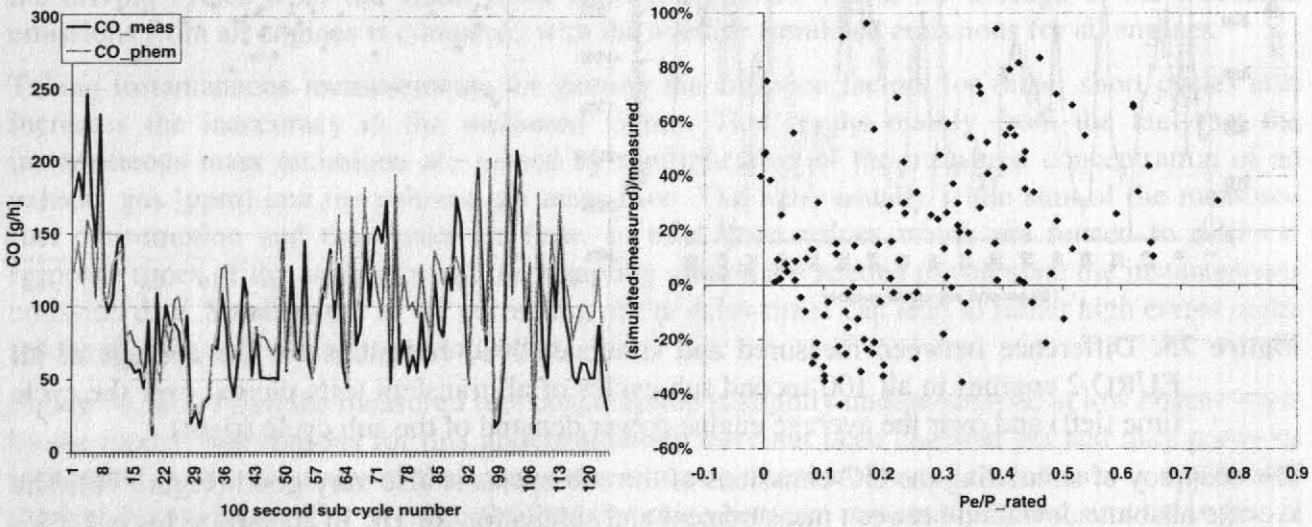

Figure 77: Difference between measured and simulated CO-emissions for the average of all EURO 2 engines in all 100 second sub cycles of all transient tests plotted over the cycle time (left) and over the average engine power demand of the sub cycle (right)

The results for the EURO 3 engines are very similar to those for EURO 2 engines shown above and not are not printed here.

Table 18 summarises the probable errors related to the simulation of the emission factors for average HDV categories. These estimated errors are the average absolute deviations between measurement and simulation of all 100 second sub cycles for the average of all engines. For

particulate emissions no measured data for the short sub cycles is available but the errors in the short sub cycles certainly will be higher than for the total transient tests given in Table 17.

Table 18: Absolute average deviation between measured emissions and simulated emissions in all 100 second sub-cycles for the average of all EURO 2 and EURO 3 engines

	FC	NOx	CO	PM	HC
Absolute average deviation	3.3%	4.5%	28.9%	~20%	5.4%
Standard deviation	3.0%	4.1%	23.1%	~15%	4.9%
95% confidence interval	+/-0.5%	+/-0.7%	+/-3.9%	+/-~3%	+/-0.8%

In total, the modelling adds some inaccuracy to the resulting emission factors but decreases the errors resulting from the limited number of measured engines (Table 15) by approximately a factor of four. Since the methodology developed allows to pool the engines measured independent of their rated power. This increases the number of measured engines per HDV category on average by a factor of nine.

4.4.5.3 Accuracy of simulating HDV driving cycles

Beside providing data necessary for model development and model improvement the measurements of HDV on the chassis dynamometer should also indicate the accuracy of the model when simulating total HDV in different driving cycles. Compared to the simulation of transient engine tests following potential sources of errors are added with the simulation of a total HDV:

1. Simulation of the engine power instead of using the measured engine power of the engine test bed
2. Simulation of the engine speed instead of using measured engine speed of the engine test bed

The outcoming thesis of the detailed analysis of all measurements on the engine tests was that some engines showed an emission behaviour very far away from the average of the tested engines and thus can not be simulated very accurately by using the average transient correction functions. Having these results in mind, the four HDV tested on the chassis dynamometer are a very small number for the assessment of the model quality.

Additionally

- One engine had increased NO_x emissions and decreased fuel consumption in transient tests compared to steady state conditions (already shown in chapter 4.4.5.2).
- For one HDV the engine map had to be measured on the chassis dynamometer since the owner did not allow to remove the engine.

Beside the complex modelling of total HDV also the measurements on the HDV chassis dynamometer are not trivial.

Compared to the real world driving on the street following influences have to be considered when measuring emissions on the chassis dynamometer:

1. Potential different engine behaviour when running in the HDV instead of running on the engine test bed (on the engine test bed several boundary conditions, like cooling and exhaust gas back pressure, are simulated by the test bed)
2. Potential different slip compared to driving on the street
3. Potential instable rolling resistances resulting from the high heat of the tyres at longer periods of high engine loads

With the knowledge of these effects HDV measurements can be performed more accurately on the chassis dynamometer.

Influences of temperature and pressure of the intake air

Different conditions of the intake air to the engine and the exhaust gas backpressure on the engine test bed, the chassis dynamometer and on the road may result in significantly different emission behaviour. These values are controlled on the engine test bed by the setting of the test stand according to the values given by the manufacturers, on the chassis dynamometer mainly by the fan for simulating the air stream and thus may be different compared to real driving on the road.

To check whether the temperature and the pressure of the intake air to the engine are on the same level on the road and at the time when the engine is tested on the engine test bed or on the chassis dynamometer one HDV was equipped with several sensors during the chassis dynamometer tests and during real world driving.

To compare the temperature and pressure levels between engine test bed, chassis dynamometer and road, the temperatures and pressures measured in the steady state points on the engine test bed were taken as input values for the engine map in the model PHEM. With this temperature and pressure map the driving cycles on the road and on the chassis dynamometer were simulated.

The pressure values showed comparable levels on the road and on the test beds while the intake air temperatures after the charge air cooling were in the city cycle on average higher on the chassis dynamometer than on the engine test bed (+13°C in the city cycle and +7°C in the highway cycle). The values measured on the road were between the chassis dynamometer measurements and the engine test bed measurements (Figure 78).

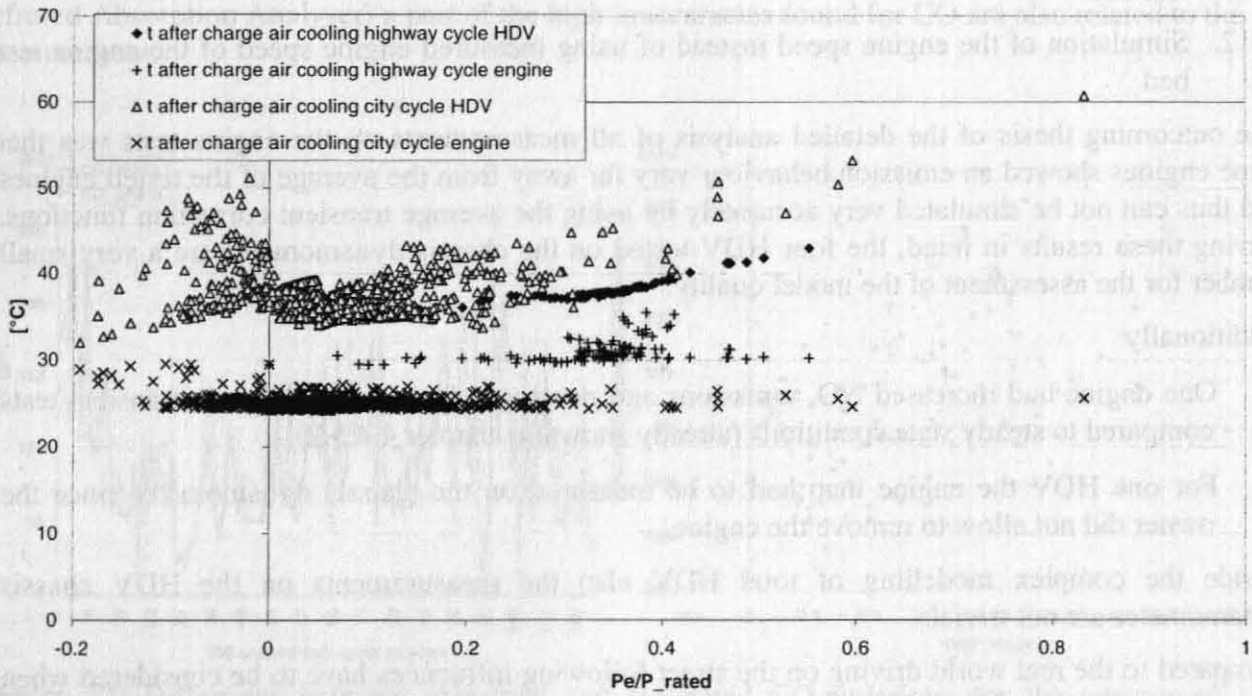

Figure 78: intake air temperatures in a slow city cycle and a fast highway cycle (HDV=measured on chassis dynamometer; engine = interpolated from engine test bed measurement)

This result indicates that the cooling on the chassis dynamometer has been somewhat less efficient than on the road. But this effect also strongly depends on the actual ambient temperature which is constant 25°C on the chassis dynamometer but certainly is very variable on the road. The

temperature levels from the engine tests rather give an optimum value for ambient temperatures in the range of 15°C to 20°C.

To clarify the potential influences on the emission levels a slow urban cycle and a fast highway cycle were tested on the chassis dynamometer with different settings of the fan for simulating the air stream and thus a changed cooling of the charge air.

The findings are that the speed of the air stream had little influence for this HDV when varied in a sensible range. The particle emissions at high speeds showed a clear increase when the fan speed was reduced to 25% of the original wind speed (Figure 79).

The measured trend that NO_x emissions increase with higher speed of the cooling air (= more cooling) while particulate emissions decrease with more cooling is rather controversial to the expected effect. A possible explanation is a temperature dependent engine control strategy e.g. to protect the engine from overheating[9].

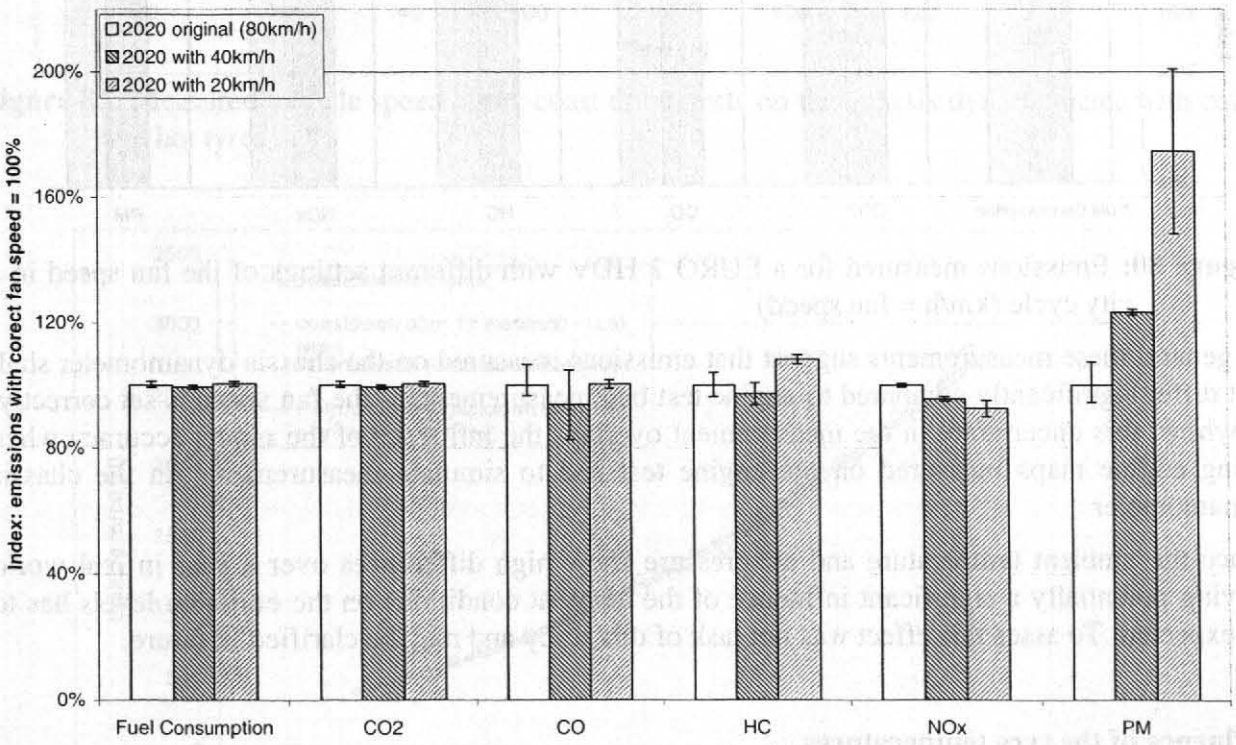

Figure 79: Emissions measured for a EURO 2 HDV with different settings of the fan speed in a highway cycle (km/h = fan speed)

[9] Also at the measurements of cold starts for all four HDV clearly increased NOx emissions have been measured compared to the same cycles started with a hot engine. This is most likely due to a different engine control strategy for cold engine conditions compared to hot engine conditions.

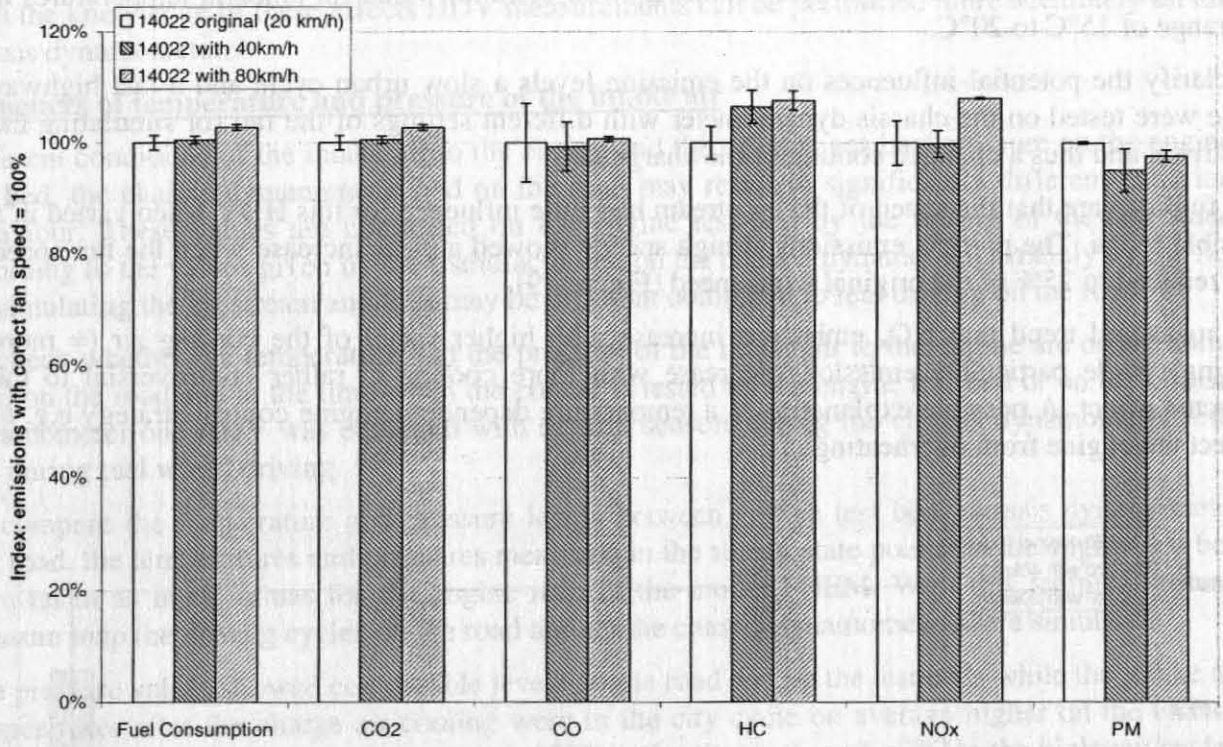

Figure 80: Emissions measured for a EURO 2 HDV with different settings of the fan speed in a city cycle (km/h = fan speed)

In general these measurements suggest that emissions measured on the chassis dynamometer shall not differ significantly compared to engine test bed measurements if the fan speed is set correctly. Anyhow, this uncertainty in the measurement overlaps the influence of the model accuracy when using engine maps measured on the engine test bed to simulate measurements on the chassis dynamometer.

Since the ambient temperature and air pressure show high differences over a year in real world driving potentially a significant influence of the ambient conditions on the emission levels has to be expected. To asses this effect was not task of this study and may be clarified in future.

Influence of the tyre temperatures

Especially at highway cycles the tires have a high thermal stress on the chassis dynamometer. In tests of long cycles at high speed and high loads the tyres can even catch fire. To check the influence of changing tyre temperatures on the driving resistances at the chassis dynamometer coast down tests with different preconditioning of the vehicle were performed. One coast down test was run immediately after driving a highway cycle (hot tyres), another coast down was performed after one hour standstill (cold tyres but still with the power train at operating temperature) (Figure 81). The setting and preconditioning of the test bed was identical for all tests, thus differences in the speed curve of the coast down can be allocated to the temperature levels of tires and bearings of the HDV. For each of this coast down tests the resistance forces were calculated (polynomic approximation, Figure 82). Although this test reflects a worst case of performing measurements at the chassis dynamometer, the driving resistances do not differ by more than 2% for hot tyres compared to cool tyres.

Since before each emission measurement the HDV is preconditioned by driving on the test bed in a similar way, the influence of changing temperature levels of the tires obviously can be neglected.

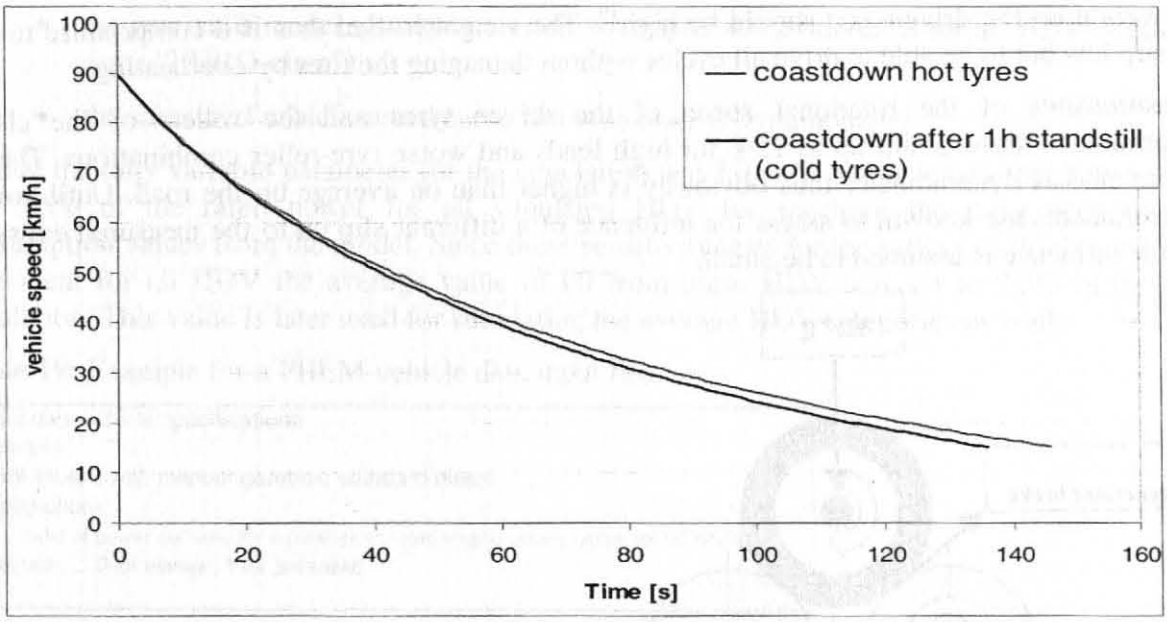

Figure 81: Measured vehicle speed at the coast down tests on the chassis dynamometer with cold and hot tyres

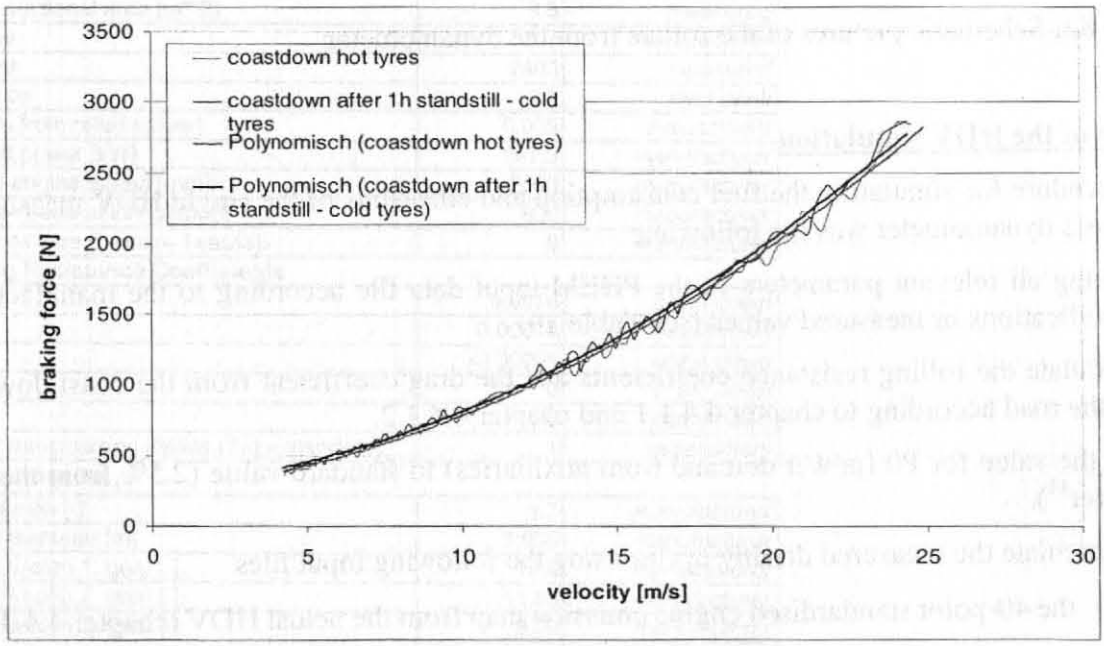

Figure 82: Calculated resistance forces as a function of the vehicle speed for cold and hot tires

Slip on the chassis dynamometer

The tyres are rested between two rollers on the test bed whereas one of them is connected with the generator, the other is rolling free (Figure 83). As mentioned before, this causes a higher thermal stress to the tires compared to driving on a street. The thermal stress increases with a higher weight on the driven axle, thus this weight shall be kept low. On the other hand the forces which can be transmitted from the tyres to the rollers decrease with lower weight on the axle. To avoid high slip

the weight on the driven axis should be high[10]. The weight loaded thus is a compromise to keep the slip low but to be able to drive all cycles without damaging the tires by overheating.

Measurements of the rotational speed of the driven tyres and the rollers of the chassis dynamometer show a slip up to 15% for high loads and worse tyre-roller combinations. The slip on the chassis dynamometer thus obviously is higher than on average on the road. Until now no measurements are known, to assess the influence of a different slip on to the measured emissions but the influence is assumed to be small.

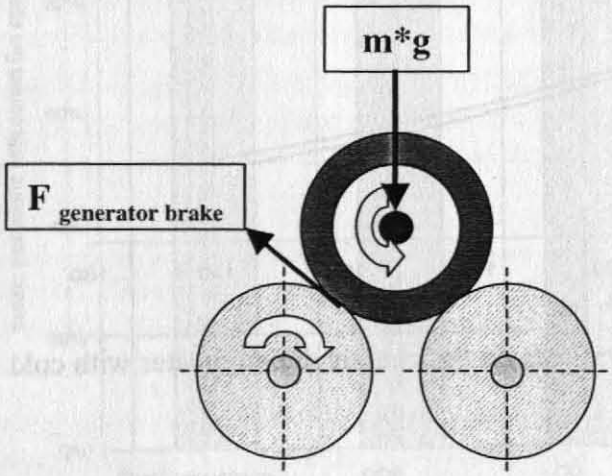

Figure 83: Schematic pictures of the rollers from the dynamometer

Results of the HDV simulation

The procedure for simulating the fuel consumption and emissions of the single HDV measured on the chassis dynamometer was the following:

1) Setting all relevant parameters in the PHEM input data file according to the manufacturers' specifications or measured values (see Table 19)
2) Calculate the rolling resistance coefficients and the drag coefficient from the coast down test on the road according to chapter 4.4.1.1 and chapter 4.4.1.2.
3) Set the value for P0 (power demand from auxiliaries) to standard value (2.5% from the rated power[11]).
4) Recalculate the measured driving cycles using the following input files
   - the 40-point standardised engine emission map from the actual HDV (chapter 4.4.3.2)
   - the full load curve from the actual HDV
   - the average transient correction function for the relevant EURO-category (chapter 4.4.4.2)

[10] The influence of the vehicle weight on the driving resistances is simulated by the generator via the control unit of the test bed (rolling resistance forces and acceleration forces) in a way, that the same resistances than measured on the street are reached in the coast down test on the chassis dynamometer. Thus the driving resistances are generally independent of the weight loaded on the vehicle on the chassis dynamometer as long as no significant slip occurs and the temperatures of the tyres keep within an acceptable level compared to the coast down test on the chassis dynamometer.

[11] Since neither in literature nor from manufacturers any detailed data on the power demand from auxiliaries was available the value for P0 had to be found by comparing the simulated fuel consumption with the measured one.

- the gear-shift model settings according to chapter 4.4.2 (identical for all HDV within the same "EURO-class")
- the measured vehicle speed curve from the chassis dynamometer

In total the only variable parameter for the simulation was P0, which was tested first between 2% and 3.5% of the rated power for all simulated HDV for reaching the most accurate fuel consumption values from the model. Since these sensitivity tests for the setting of P0 showed close agreement for all HDV the average value of P0 from these HDV was set to 2.5% in the final simulation. This value is later used for simulating the average HDV categories as well.

Table 19: Example for a PHEM vehicle data input file

c Input data vehicle specifications
c Remarks:
c **MAN 19.403** with manual gearbox; standard diesel
c Explanations:
c P0.....ratio of power demand for auxiliaries to rated engine power (value for 50 km/h)
c Gear box:..... 0 for manual; 1 for automatic
c

c

c Driving resistances:		*source*
c vehicle mass [kg]:	15000	*weighted out*
c Loading [kg]	15500	*weighted out*
c --Cw-value [-]	0.5	*data bank*
c cross sectional area [m**2]	9.5	*measured*
c IEngine	1.7	*manufacturer*
c IWheels	2400	*measured*
c IGearbox	0.3	*data bank*
c --P0 [% from rated power]:	0.035	*assessment*
c --Rated power [kW]	297.3	*manufacturer*
c --rated engine speed [rpm]:	2000	*manufacturer*
c Engine speed at idling [rpm]:	600	*manufacturer*
c Gear box type (0=man; 1=auto):	0	*manufacturer*
c Rolling Resistance Coefficients		
c Fr0:	0.0076	*coast down*
c Fr1:	0.00018	*coast down*
c Fr2	-0.00001	*coast down*
c Fr3:	0	*coast down*
c Fr 4	0	*coast down*
c Factor transmission losses (1.0 = standard)	1	*assessment*
c Transmission:		
c Achsle ratio [-]:	3.7	*manufacturer*
c Wheel diameter [m]	1.035	*manufacturer*
c Transmission 1. gear [-]:	13.8	*manufacturer*
c Transmission 2. gear [-]:	11.55	*manufacturer*
c Transmission 3. gear [-]:	9.59	*manufacturer*
c Transmission 4. gear [-]:	8.02	*manufacturer*
c Transmission 5. gear [-]:	6.81	*manufacturer*
c Transmission 6. gear [-]:	5.7	*manufacturer*
c Transmission 7. gear [-]:	4.58	*manufacturer*
c Transmission 8. gear [-]:	3.84	*manufacturer*
c Transmission 9. gear [-]:	3.01	*manufacturer*
c Transmission 10. gear [-]:	2.52	*manufacturer*
c Transmission 11. gear [-]:	2.09	*manufacturer*
c Transmission 12. gear [-]:	1.75	*manufacturer*
c Transmission 13. gear [-]:	1.49	*manufacturer*
c Transmission 14. gear [-]:	1.24	*manufacturer*
c Transmission 15. gear [-]:	1	*manufacturer*
c Transmission 16. gear [-]:	0.84	*manufacturer*

The results for the single HDV are shown below. The fuel consumption values are simulated quite accurately, the highest deviation was +13% (vehicle 4) but as mentioned before the engine of this HDV obviously used a more economical engine control strategy under transient cycles than at the steady state tests. For vehicle 4 NO_x-emissions are underestimated by up to 30% (Figure 86). This is also in line with the findings from the engine tests.

The fuel consumption simulated for the other HDV are within -10% to +14% agreement to the measured values. In general, the deviations between measurement and simulation are approximately double the deviations reached for the simulation of the engine tests.

The NO_x-emissions are simulated within +/-25% agreement to the measured values. In comparison the engine tests were simulated within +/- 15% for NO_x.

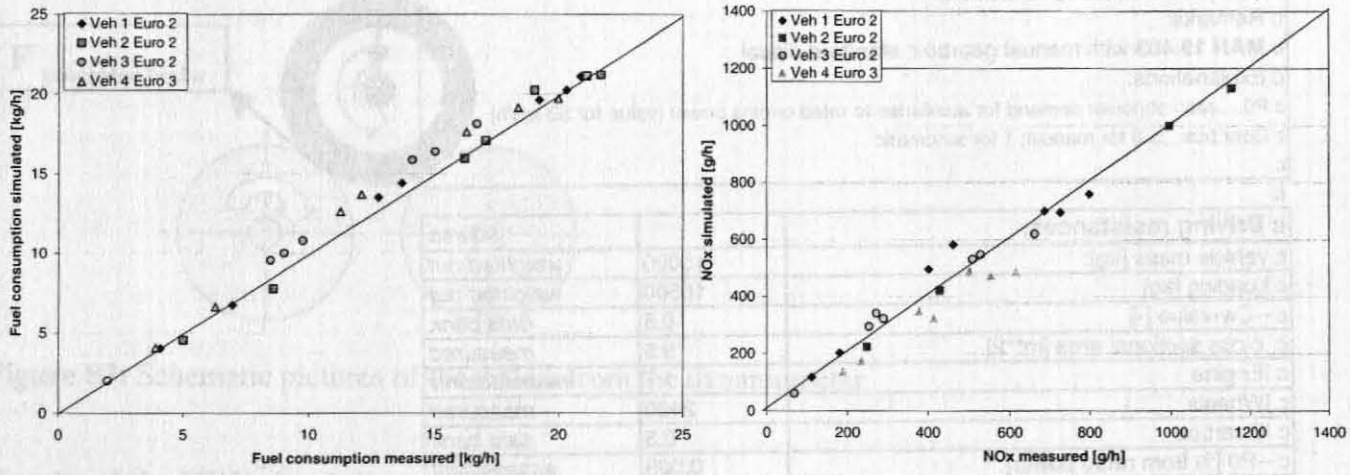

Figure 84: Comparison of fuel consumption and NO_x-emissions measured on the chassis dynamometer versus the simulated values

The deviations for simulating the HC- and CO emissions of the HDV are in the same order of magnitude than found for the simulation of engine tests. The deviation for HC is between –30% and +50%. Again the simulation of the CO-emissions of single HDV is very inaccurate (-40% to +100% deviations). The accuracy of the simulation of the particulate emissions of single HDV is on the level of HC (Figure 88).

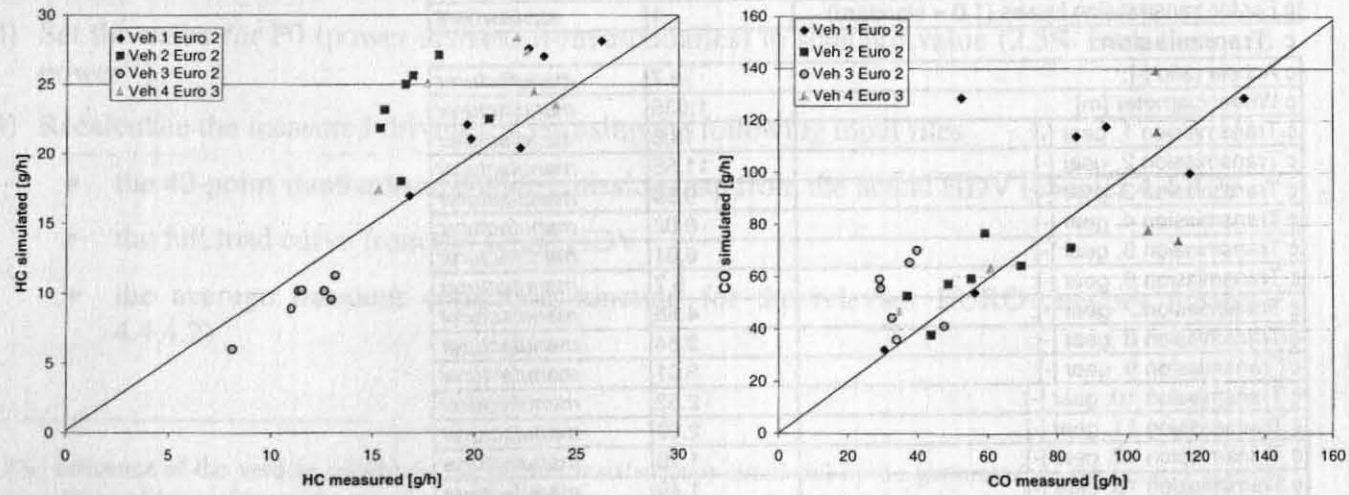

Figure 85: Comparison of HC- and CO-emissions measured on the chassis dynamometer versus the simulated values

In general the results are very well in line with all findings of the simulation runs of the engine test cycles. The accuracy for the simulation of the total HDV is somewhat lower than for the

simulation of just the engine. But this was clearly expected due to the fact that the engine power demand and the engine speed have to be simulated for the calculation of HDV driving cycles.

As already mentioned before, the main task of the "average transient correction function" is to correct the emissions of the "average" HDV in an optimum way since the output of the study are emission factors for "average" HDV in different categories.

Thus – as for the assessment of the engine simulation – the comparison between measurement and simulation shall be based on the average of the measured HDV within the different categories. As only three EURO 2 HDV and one EURO 3 HDV were measured, the results of all four vehicles are averaged for the following comparison to get a (more or less) representative sample.

Although only four HDV are in the sample, the average emissions of these vehicles are simulated very accurately. The error for the fuel consumption is below 7% for all cycles (Figure 86). For NO_x an accuracy of –6% to +18%% is reached. The underestimation of the highly transient cycles at low speed are also related to the NO_x-emission behaviour of the EURO 3 HDV where a different engine control strategy may be used for transient and steady state loads.

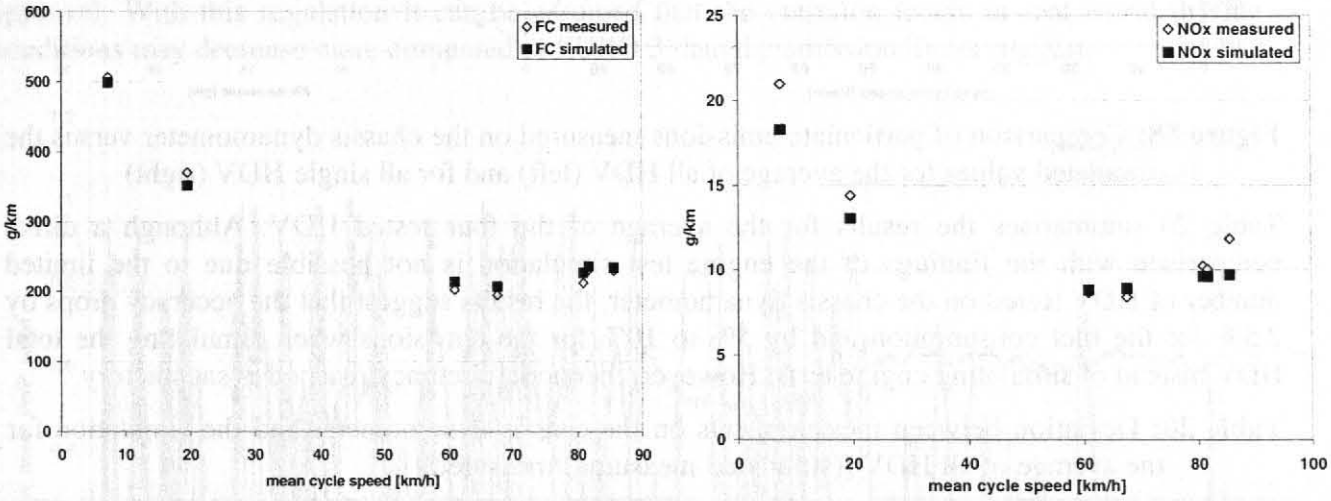

Figure 86: Comparison of the fuel consumption and the NO_x-emissions measured on the chassis dynamometer versus the simulated values for the average of all measured HDV

Also HC and CO are simulated very accurately for the average of the tested vehicles, where for the HC-emissions the error is below 22%, for CO the error is below 40%. The high relative deviations occur at the cycles with very low specific emissions only (Figure 87).

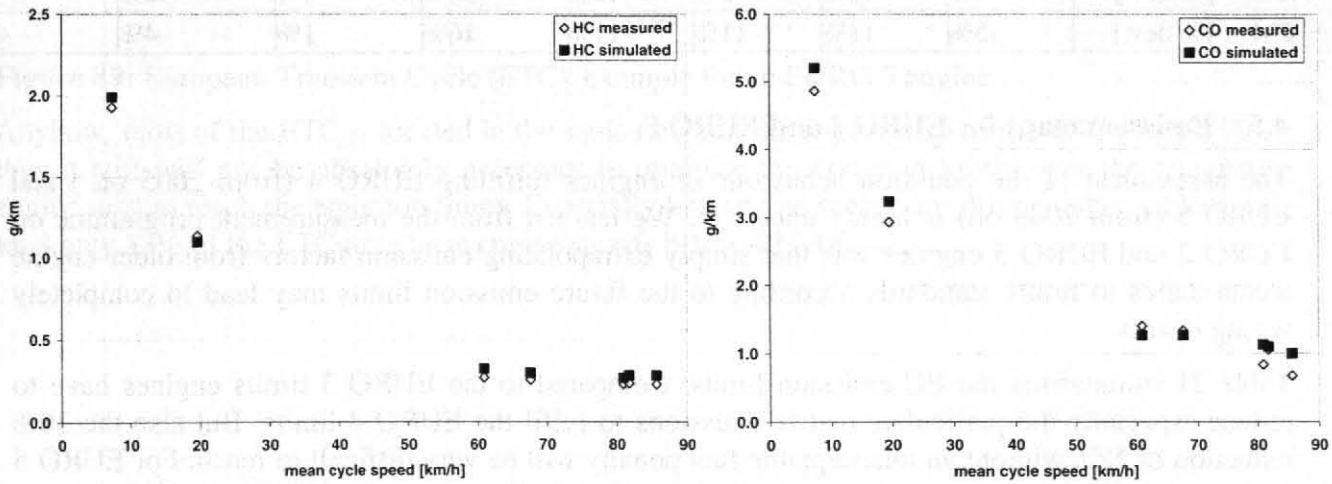

Figure 87: Comparison of the HC- and the CO-emissions measured on the chassis dynamometer versus the simulated values for the average of all measured HDV

For particulate emissions the deviations between the measurement and the simulation of the single vehicles are between +/-50%, which is worse than those on the engine test bed. For the average of the vehicles the differences between measurement and simulation are between +/-15% (Figure 88). This accuracy for the PM emissions of the "average" HDV is similar to the results found on the engine test bed.

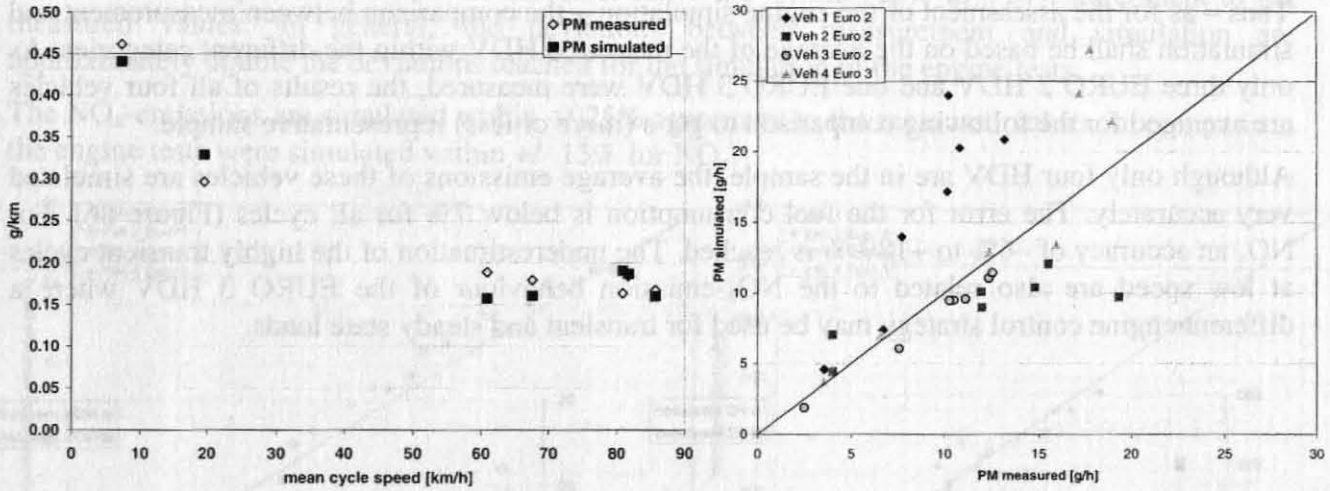

Figure 88: Comparison of particulate emissions measured on the chassis dynamometer versus the simulated values for the average of all HDV (left) and for all single HDV (right)

Table 20 summarises the results for the average of the four tested HDV. Although a direct comparison with the findings of the engine test simulation is not possible due to the limited number of HDV tested on the chassis dynamometer, the results suggest that the accuracy drops by 2.5% for the fuel consumption and by 5% to 10% for the emissions when simulating the total HDV instead of simulating engine tests. However, the model accuracy reached is satisfactory.

Table 20: Deviation between measurements on the chassis dynamometer and the simulation for the average of all HDV [(simulated-measured)/measured]

	13023	14022	7130_70	3020	2020	7130_85	1020	Average
velocity [km/h]	7.3	20	68	71	81	82	86	58
Fuel [% dev.]	-2%	-5%	6%	6%	7%	2%	2%	1%
NOx [% dev.]	-13%	-9%	6%	2%	-6%	-4%	-18%	-8%
HC [% dev.]	3%	-3%	17%	20%	17%	21%	24%	6%
CO [% dev.]	7%	10%	-5%	-10%	35%	4%	48%	8%
PM [% dev.]	-5%	11%	-11%	-17%	16%	1%	-4%	-1%

4.5 Emission maps for EURO 4 and EURO 5

The assessment of the emission behaviour of engines fulfilling EURO 4 (from 2005 on) and EURO 5 (from 2008 on) is highly uncertain. We learned from the measurement programme on EURO 2 and EURO 3 engines was that simply extrapolating emission factors from older engine technologies to future standards according to the future emission limits may lead to completely wrong results.

Table 21 summarises the EC emission limits. Compared to the EURO 3 limits engines have to reduce especially the particulate matter emissions to fulfil the EURO 4 limits. But also the 30% reduction of NO_x without an unacceptable fuel penalty will be very difficult to reach. For EURO 5 limits NO_x emissions have to be reduced by another 43% compared to EURO 4. This is very unlikely to be possible at acceptable engine efficiencies for conventional combustion technologies without exhaust gas after treatment.

Table 21: Emission limits for HDV in the EU

			CO	HC	NO_x	Particle
Introduction	Name	Test cycle	[g/kWh]			
1993	EURO 1	ECE R 49	4.90	1.23	9.00	0.40
1995	EURO 2	ECE R 49	4.00	1.10	7.00	0.15
2000	EURO 3	ESC (+ETC)	2.10	0.66	5.00	0.10
2005	EURO 4	ESC + ETC	1.50	0.46	**3.50**	**0.02**
2008	EURO 5	ESC + ETC	1.50	0.46	**2.00**	**0.02**

Compared to EURO 3 diesel engines EURO 4 and EURO 5 engines have to fulfil the emission limits also in a transient engine test (ETC, European Transient Cycle, Figure 89). Thus optimisations on the single test points of the ESC will not help to reach the emission levels at type approval. With this regulation it can be assumed that the emission levels in real world driving conditions may decrease more compared to EURO 3 than the emission limits suggest.

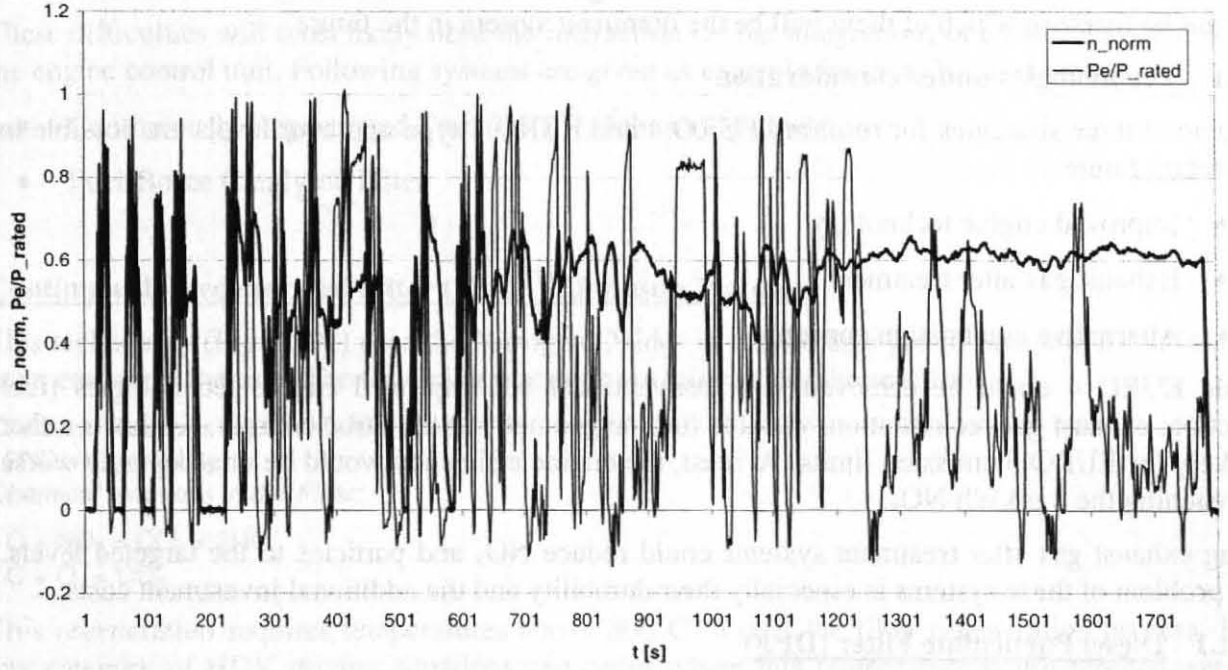

Figure 89: European Transient Cycle (ETC), example for an EURO 3 engine

Anyhow, most of the ETC is located in the same range of the engine map as the ESC (Figure 90), thus it still will not be absolutely necessary to optimise the emission levels over the complete engine map to reach the emission limits. Especially low engine speeds are driven rather seldom. In total only 13% of the ETC time have engine speeds below 40% (n_{norm}).

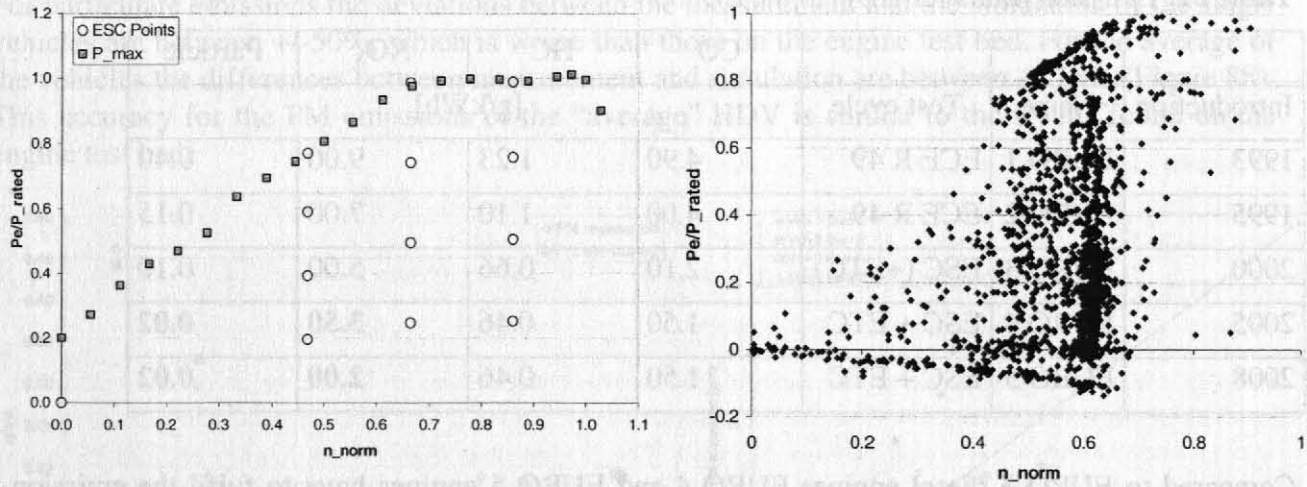

Figure 90: European Stationary Cycle (ESC) and European Transient Cycle (ETC) in the engine map, example for an EURO 3 engine

The main question for the assessment of the emission maps for EURO 4 and EURO 5 engines is whether technologies will be used that may have a different efficiency over the engine map. Potential technologies for EURO 4 and EURO 5 engines are discussed below but at the moment it can not be foreseen which of them will be the dominant system in the future.

4.5.1 Technologies under consideration

In general three strategies for reaching EURO 4 and EURO 5 type approval levels are possible in the nearer future:

- Improved engine technology
- Exhaust gas after treatment
- Alternative combustion concepts

While EURO 4 could be achieved with conventional but improved engine technologies (fuel injection, exhaust gas recirculation, variable turbine geometry at the turbo charger,...) this is rather unlikely for EURO 5 emission limits. At least, the engine efficiency would be unacceptably worse for reaching the 2 g/kWh NO_x.

Using exhaust gas after treatment systems could reduce NO_x and particles to the targeted levels. The problem of these systems is especially their durability and the additional investment costs.

4.5.1.1 Diesel Particulate Filter (DPF)

Today different after treatment systems to reduce particulate matter (PM) emissions are under development for HDV application. For all systems the main technological task is a controlled regeneration of the filter where the particle load has to be burned below temperatures critical for damaging the filter material. Without or with delayed regeneration the filter becomes blocked, which rapidly increases the exhaust gas back pressure. To start the filter regeneration process today temperatures above 300°C are necessary which do not occur under all loads for today's HDV engines (e.g. Figure 91). Already an overloading by only 3-4 grams per litre filter volume causes a rise in regeneration temperature in the order of 300-400°C. Such temperatures can damage the filter.

Beside the burning of the particles the accumulation of remaining ashes from lubricating oil additives is problematic. These ashes will melt at high temperatures (>1100°C) during regeneration and can react with the filter substrate and clog the filter permanently (glazing effect). Therefore, the loading rate and temperature of the filter have to be monitored accurately to prevent overheating and damage to the filter.

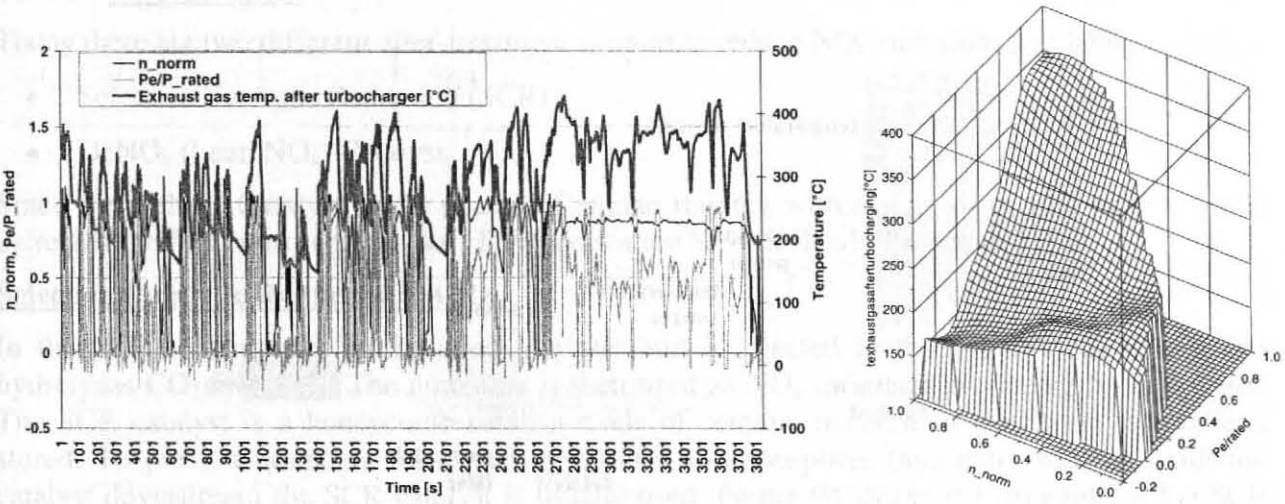

Figure 91: Measured exhaust gas temperatures at an EURO 3 engine in a real world test cycle (TNO 7.5 kW/ton cycle) and resulting engine exhaust gas temperature map.

These difficulties will most likely need the interaction (or the integration) of a control system with the engine control unit. Following systems are given as example for today's development:

- Continuously Regenerated Trap (CRT™, Johnson Matthey)
- Fuel-Borne Catalysed Filter

Continuously Regenerated Filter (CRT™, Johnson Matthey)

This technology (Figure 92) uses the Nitrogen Oxides in the exhaust gas to maintain a continuous regeneration of the trap. The following reactions are relevant for the reaction:

Chemical reactions in the NO_2-Catalyst:

$2NO + O_2 = 2NO_2$

Chemical reactions in the Filter:

$C + NO_2 = CO_2 + 2NO$

$C + O_2 = CO_2$

This regeneration requires temperatures above 300°C to start the filter regeneration process. For any category of HDV driving situations can occur where this temperature is not reached over a longer period. This leads to an accumulation of particles in the filter which are then burned at high temperatures once the needed temperature is reached again. Such situations can damage the filter. Thus, additional systems for active regeneration may be needed which may be electrical or fuel burner heaters potentially supported by a fuel additive. These regeneration aids can be used at other particle filters also (e.g. fuel burner regenerated trap).

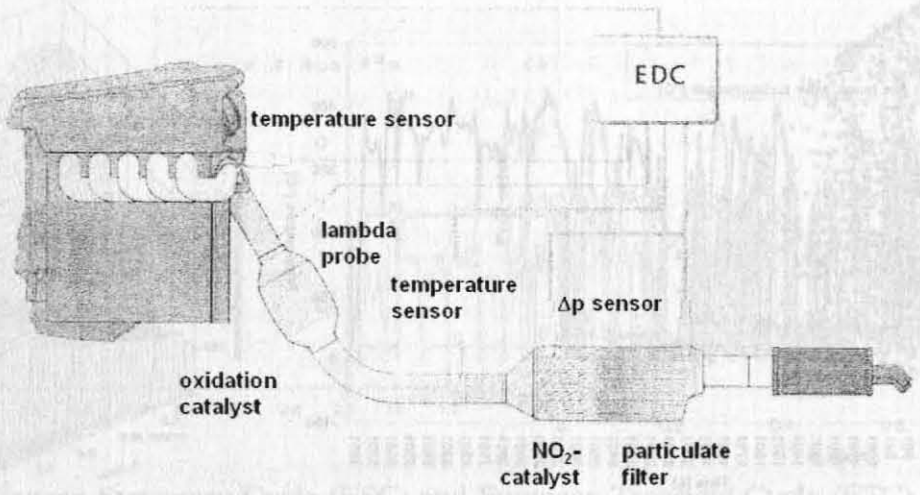

Figure 92: Schematic picture of a continuously Regenerated Filter

Fuel-Borne Catalysed Filter

In this system (Figure 93) an additive is used to reduce the soot ignition temperature and is introduced into the fuel system after refuelling in proportion to the fuel on-board the vehicle. Additives currently used are cerium, iron and strontium. A comparable system has been introduced in the passenger car market already in series production (PSA, ©FAP). Main disadvantage is the need of an additional tank on board.

Faults that are specific to this system are most likely to occur in the additive supply system, e.g. too little dosing could lead to delayed regeneration and overheating during the regeneration process like for the CRT system.

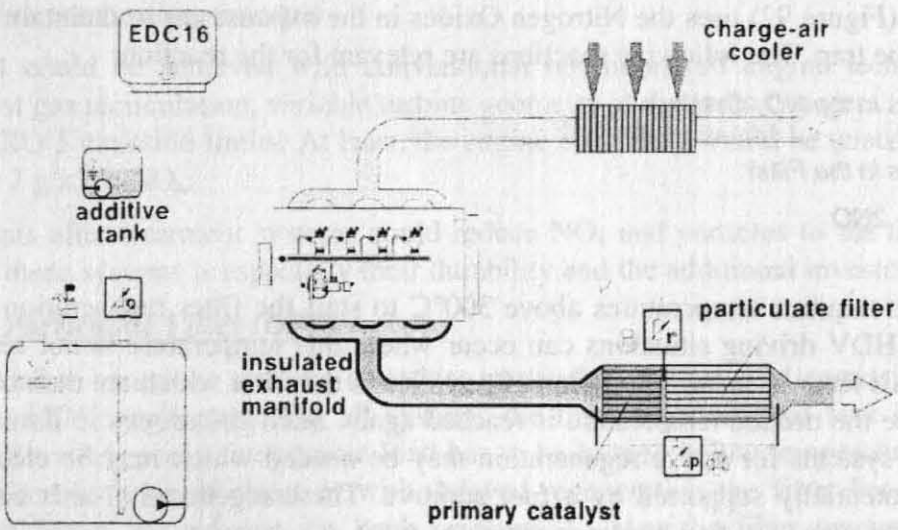

Figure 93: Fuel-Borne Catalysed Filter (Source: Bosch)

Beside the technological tasks to be solved particulate traps cause additional investment costs and result in a slight penalty in fuel efficiency. Thus, research on improving engine technologies to reach the particle limit values without filters in future is under progress.

4.5.1.2 NO_x Catalysts

Today there are two different after-treatment systems to reduce NO_x emissions available.

- Selective Catalytic Reduction (SCR)
- $DeNO_x$ (Lean NO_x) Catalyst

Since the $DeNO_x$ Catalyst needs phases of engine running with a rich air to fuel ratio – which increases the fuel consumption - for HDV application SCR is clearly favoured.

Selective Catalytic Reduction (SCR)

In the SCR system urea is dissolved in water and is injected in the exhaust gas stream and hydrolyses CO_2 and NH_3. The ammonia is then used as NO_x reductant producing N_2 and water. The SCR catalyst is a honeycomb catalyst made of ceramic material in which the ammonia is stored. To prevent ammonia from passing through to atmosphere (ammonia slip) an oxidation catalyst downstream the SCR catalyst is usually used. Figure 94 shows the principle of the SCR Catalyst.

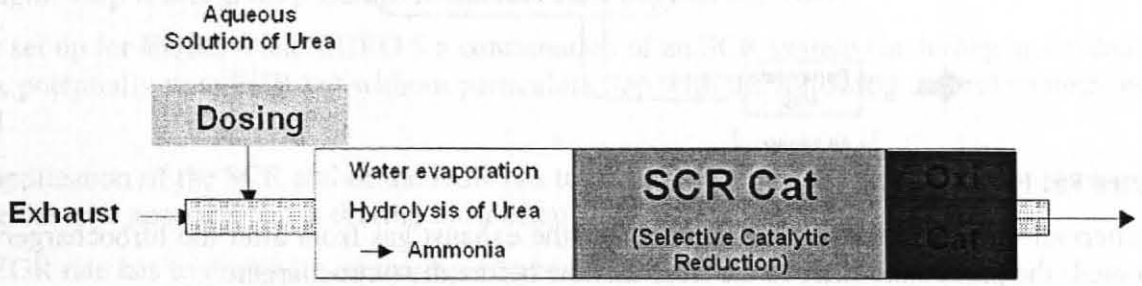

Figure 94: Principle of the SCR Catalyst (Source: PUREM)

At proper exhaust gas temperatures the SCR is capable of reducing the NO_x emissions by more than 65%. Drawbacks from today's systems are that the SCR catalyst does not work at temperatures below approximately 150°C. Thus the urea injection starts at a defined exhaust temperature and engine speed and is controlled by a temperature sensor. Engines running a considerable time at idle speed, e.g. in city busses, may have problems reaching the required temperature, especially in winter. Additionally after cold starts the system will not be active until the operating temperature is reached.

A main concern is an empty urea tank. Since there are no vehicle performance penalties when the reactant tank is empty, such a situation will not be recognised by the driver without a control system. Monitoring of the reactant level in the tank therefore is crucial for compliance but can be managed by adequate control systems.

4.5.1.3 Exhaust Gas Recirculation (EGR)

EGR is used to reduce NO_x emissions by recirculating a proportion of the exhaust gas back into the combustion cylinder. This reduces the oxygen available in the cylinder for combustion and creates lower peak temperatures that inhibit the formation of NO_x.

There are different principles of exhaust gas recirculation.

- External High Pressure EGR
- External Low Pressure EGR
- Internal EGR

All of these options may be used at EURO 4 and/or EURO 5 HDV engines.

In a high pressure EGR the exhaust gas is diverted back into the intake manifold from the exhaust manifold under pressure from the combustion cylinder. For cooling the exhaust gas a EGR cooler is used. (Figure 95). A problem of this system is the potential pollution of the valves by the exhaust gas.

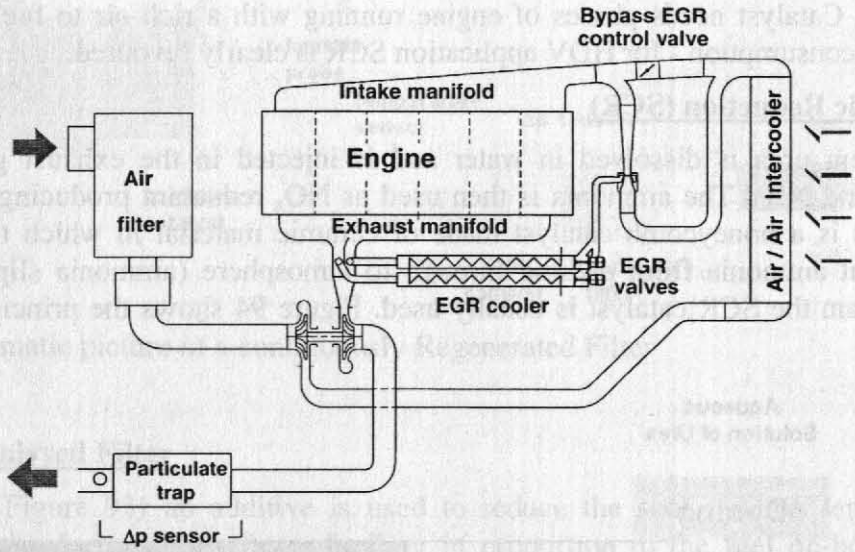

Figure 95: High pressure EGR (Source: AVL)

As alternative the low pressure EGR re-routes the exhaust gas from after the turbocharger and (if mounted) the particulate filter to the fresh airflow before the turbocharger.

Beside external EGR also an overlapping opening of the exhaust and the intake valve can be used to bring in a mixture of fresh air and exhaust gas in the cylinder (Figure 96). Different systems for a variable valve control are on the market today.

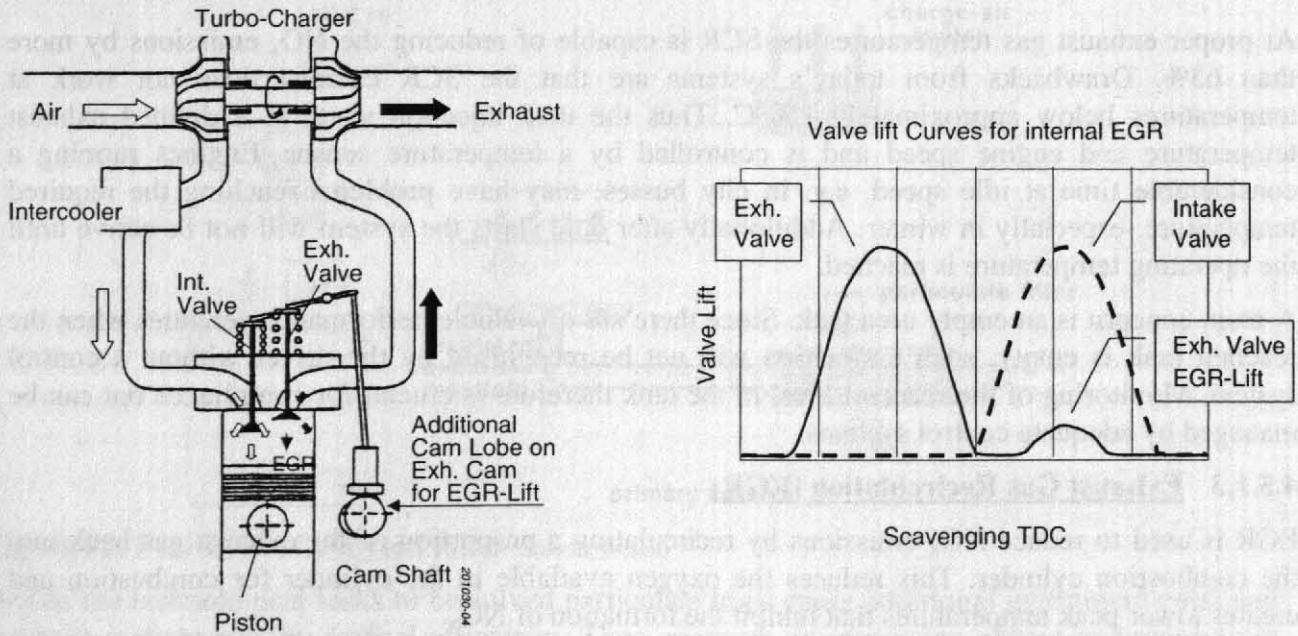

Figure 96: Internal EGR (Source: Hino Motors Limited)

4.5.2 Estimation of EURO 4 and EURO 5 emission maps

An experience of the assessment of the measurements on EURO 2 and EURO 3 engines was that a high fuel efficiency is a main target for HDV engines and a crucial point for the competitiveness of a HDV on the market. It certainly has to be assumed that also for EURO 4 and EURO 5 the manufacturers have to find solutions with a high fuel efficiency at low investment and running costs.

Following boundary conditions for EURO 4 and EURO 5 engines are assumed:

- The technological solution for reaching future emission limits is not clear today
- For different typical operational conditions of different HDV there may even be different combinations of the before mentioned technological options
- Emission reduction strategies have to be followed to an extent necessary to reach the type approval levels in the ETC and in the ESC test cycles
- Emission reduction strategies will most likely not be followed where not urgently necessary in the engine map if this gives penalties in the fuel consumption and costs

As basic set up for EURO 4 and EURO 5 a combination of an SCR system (including an oxidation catalyst), potentially with EGR but without particulate trap with the following control strategy was assumed:

- The application of the SCR and of the EGR has to be optimised in the ranges of the engine map where the type approval test is driving most often
- The EGR rate has to drop with increasing engine loads
- Ranges reached rather seldom in the ETC will have somewhat less efficiency from the EGR + SCR
- In ranges not driven in the ETC or ESC no urea dosing will happen to reduce the number of refilling the urea tank and the EGR may run with lower EGR rates
- The reduction of particle emissions will be realised by the oxidation catalyst, an optimised fuel injection and combustion in combination with multiple fuel injection
- The efficiency of the oxidation catalyst drops at high engine loads due to sulphate formation even with less than 10 ppm Sulphur content in the fuel. At lower engine loads, especially with high engine speeds the efficiency drops also due to the low temperature levels.
- Multiple fuel injection will be used only in the ranges of the engine map where the type approval test runs frequently to avoid penalties in the fuel efficiency
- HC and CO emission levels are reduced only if necessary for reaching the type approval limits. The afore mentioned measures for particulate and NO_x emission reduction certainly will also affect the HC and CO emissions, but the overall effect can not be quantified with any reliability.

With these assumptions the emission levels of each of the available EURO 3 engine maps (in the standardised format) were reduced until emissions at least 5% below the type approval limits for EURO 4 and EURO 5 were reached. For this task the ETC and the ESC were simulated for each of the virtual EURO 4 and EURO 5 engines with the model PHEM.

The exercise was made at the single engines to take the different shapes of the full load curves into consideration. For EURO 4 and EURO 5 no change in the full load curves have been assumed compared to EURO 3. This would have changed the engine speeds of the ETC and the ESC respectively.

The resulting necessary reductions of NO_x and particulate emissions to reach EURO 4 and EURO 5 are impressing. Particulate emissions will have to be reduced by approximately 70% to 90% compared to EURO 3 in the engine map (depending on the basic EURO 3 engine). The reduction rates applied for the NOx emissions over the engine map to reach EURO 5 are in the range of 40% to nearly 80%.

Figure 97 gives as example the reduction rates applied to an EURO 3 engine to reach EURO 5 emission levels. These reductions will certainly still need a lot of efforts and the technologies necessary will make the system much more complex. From the environmental point of view a main question for the future is the durability of the technologies used. While today's HDV diesel engines show a rather constant emission level over their life time this may change with the introduction of much more complex systems.

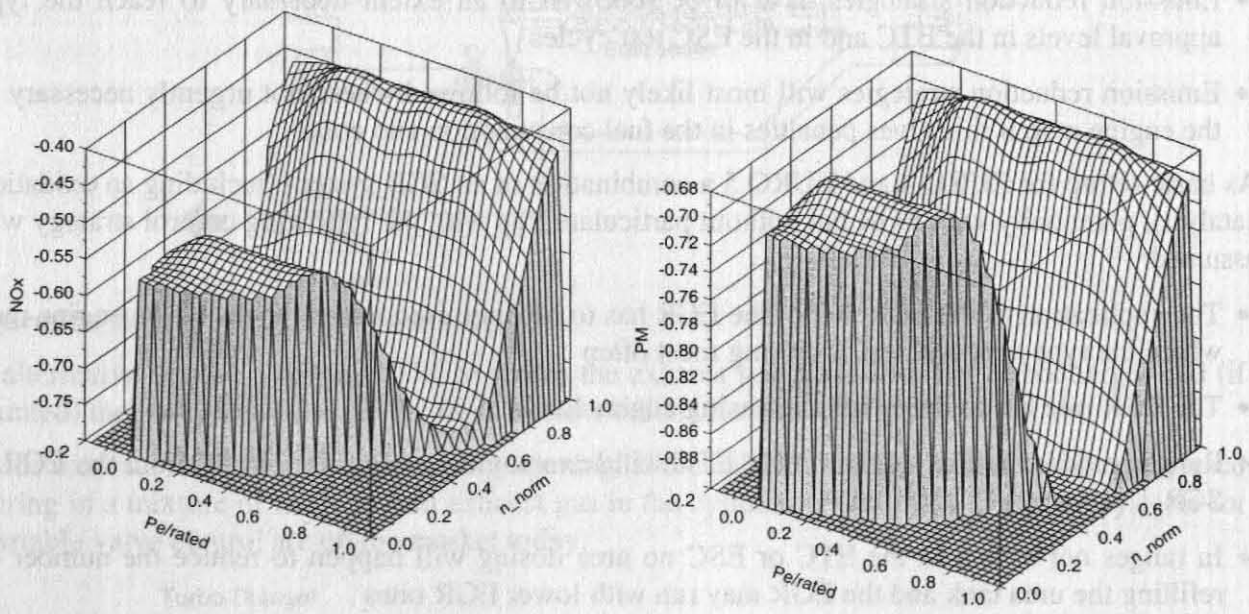

Figure 97: Reduction rates for an EURO 3 engine to reach EURO 5 emission levels for NOx (left) and particulates (right). *Reduction rate = (EURO 5/EURO 3) -1*

The resulting engine emission maps for EURO 4 and EURO 5 are shown in the next chapter.

4.5.3 Average Emission Maps for Pre EURO to EURO 5

This chapter documents the engine emission maps used for the EURO categories. The graphs of the maps were drawn up with the software UNIPLOT using the standardised engine emission map formats as input[12].

[12] Very uneven values in a map cause problems for interpolation routines, also for those of commercial graphical software programs. As a result the pictures shown include some artifacts from the software used and are not necessarily representing exactly the values of the standardized engine emission maps.

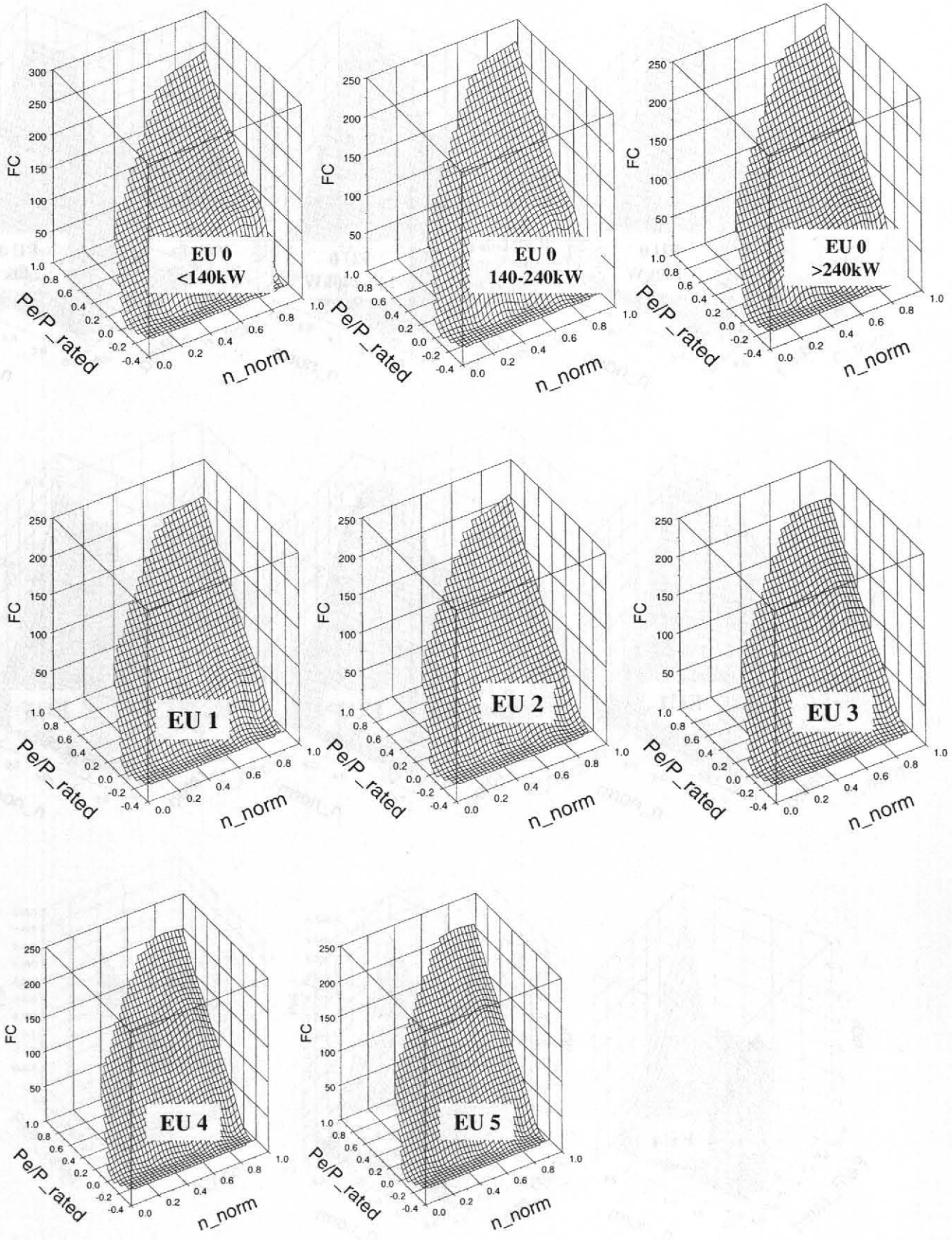

Figure 98: Fuel consumption maps for the average technology classes (standardised map formats, values in (g/h)/kW $_{\text{Rated Power}}$

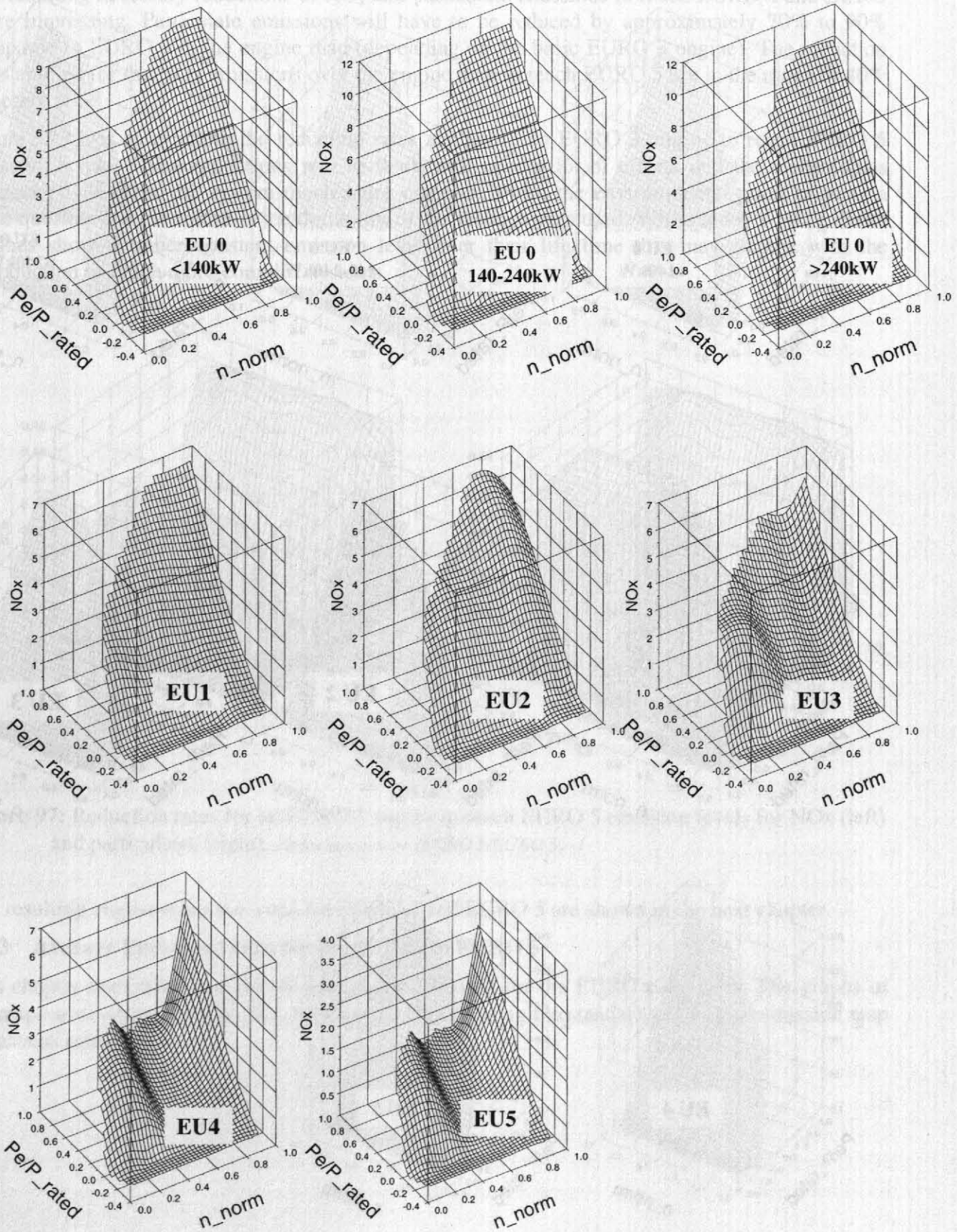

Figure 99: NO_x-emission maps for the average technology classes (standardised map formats, values in (g/h)/kW $_{\text{Rated Power}}$

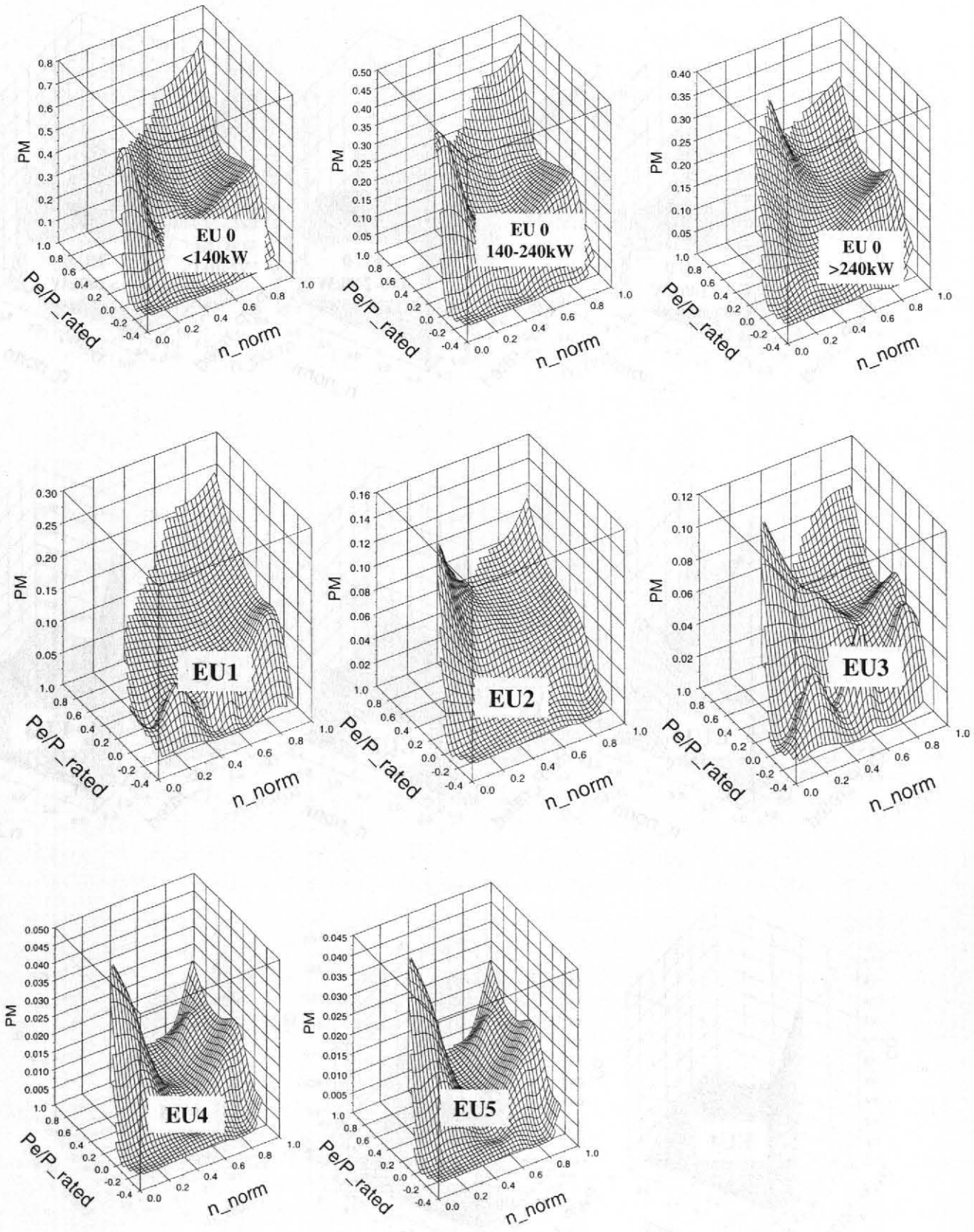

Figure 100: Particulate matter-emission maps for the average technology classes (standardised map formats, values in (g/h)/kW $_{\text{Rated Power}}$

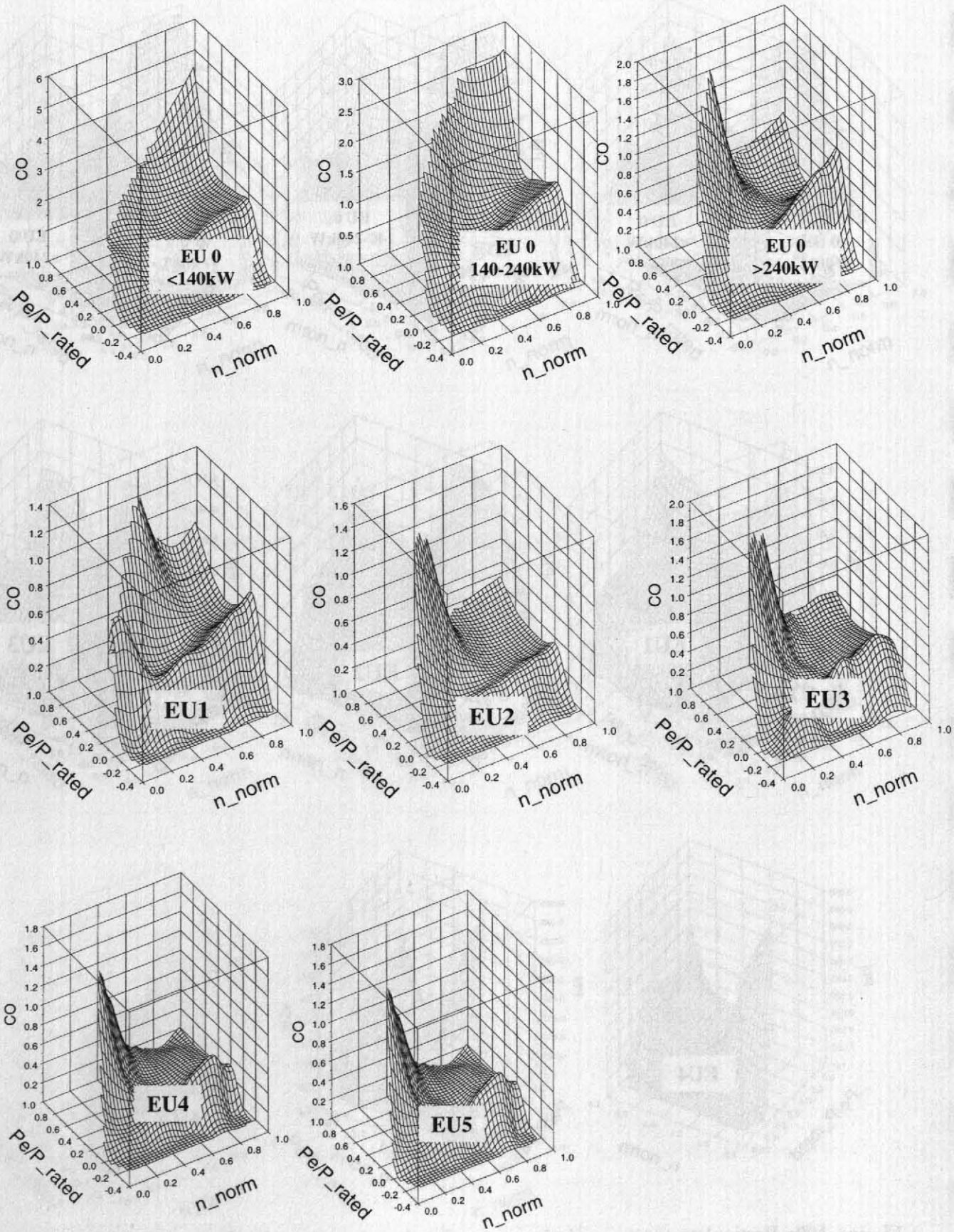

Figure 101: CO-emission maps for the average technology classes (standardised map formats, values in (g/h)/kW $_{\text{Rated Power}}$

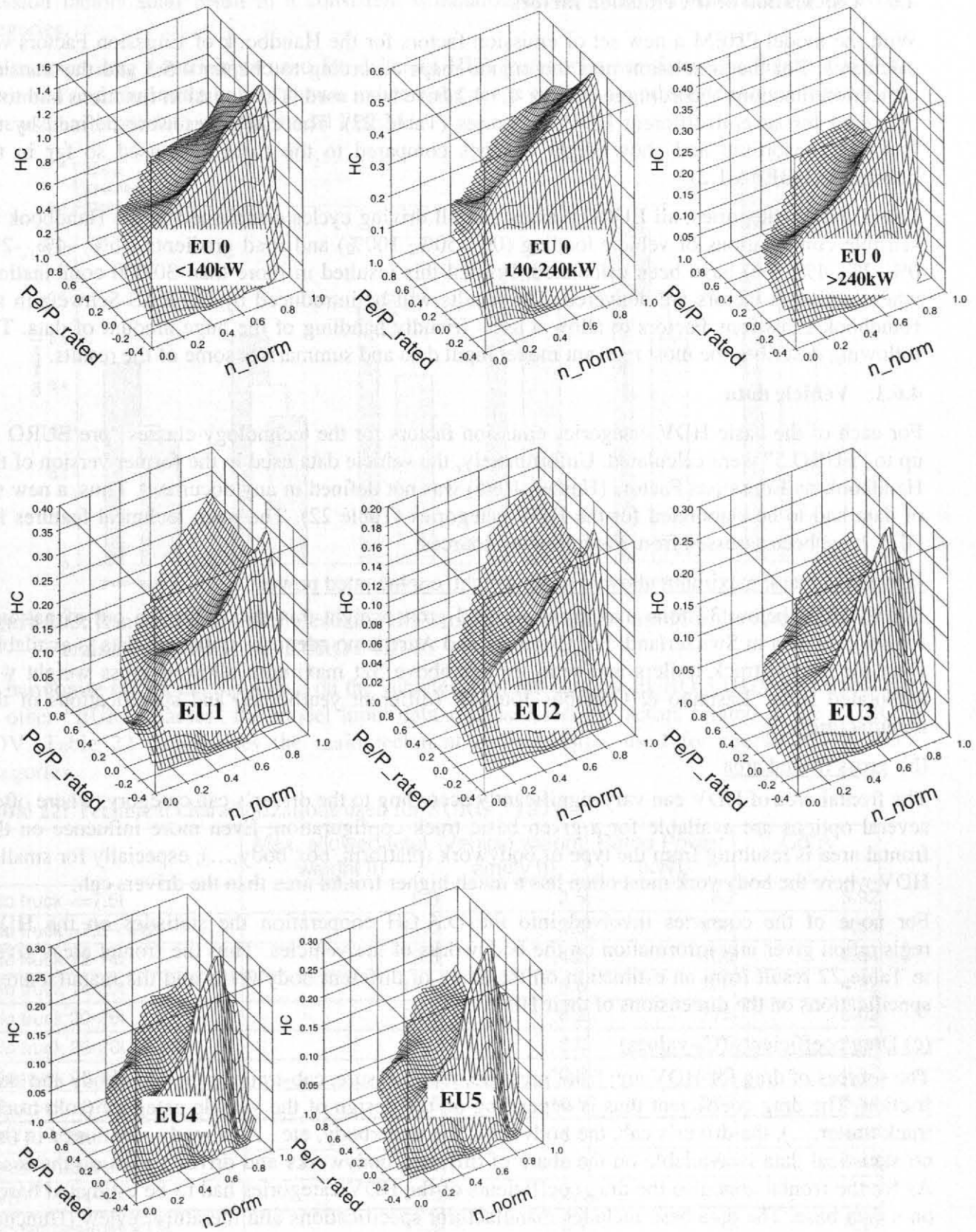

Figure 102: HC-emission maps for the average technology classes (standardised map formats, values in (g/h)/kW $_{\text{Rated Power}}$

4.6 Calculation of the emission factors

With the model PHEM a new set of emission factors for the Handbook of Emission Factors was calculated. For the simulation runs the engine maps according to chapter 4.5.3 and the transient correction functions according to chapter 4.4.4.2 have been used. The emission functions had to be delivered for several different HDV categories (Table 22). The categories were defined by the D.A.CH consortium and show slight changes compared to the categories used so far in the handbook (HBEFA 1.2).

For all HDV categories, all EURO classes and all driving cycles established in the Handbook all sensible combinations of vehicle loading (0%, 50%, 100%) and road gradients (-6%, -4%, -2%, 0%, 2%, 4%, 6%) have been calculated. In total this resulted in more than 30.000 combinations where emission factors are delivered. The results will be introduced by INFRAS-Schweiz in the Handbook Emissions Factors to allow a user- friendly handling of the huge amount of data. The following describes the most relevant model input data and summarises some of the results.

4.6.1 Vehicle data

For each of the basic HDV categories emission factors for the technology classes "pre EURO 1" up to "EURO 5" were calculated. Unfortunately, the vehicle data used in the former version of the Handbook on Emissions Factors (Hassel, 1995) was not defined in any document. Thus, a new set of data had to be elaborated for the HDV categories (Table 22). The main technical features for HDV have been assessed from the following sources:

(a) vehicle mass, maximum allowed gross weight, engine rated power

For all HDV below 32 tons maximum allowed gross weight this data is drawn out of national registration data in Switzerland. For Germany and Austria no adequate statistical data is available. Data for trucks, truck trailers and semi trailers above 32t maximum allowed gross weight was elaborated from "Lastauto & Omnibus Journal" (different yearbooks) and specifications of the manufacturers.

(b) gross frontal area

The frontal area of HDV can vary significantly according to the driver's cab category, where often several options are available for a given basic truck configuration. Even more influence on the frontal area is resulting from the type of bodywork (platform, box body,...), especially for smaller HDV where the bodywork most often has a much higher frontal area than the drivers cab.

For none of the countries involved into the D.A.CH cooperation the statistics on the HDV registration gives any information on the bodyworks of the vehicles. Thus the frontal areas given in Table 22 result from an estimation on the share of different bodyworks and the manufacturers specifications on the dimensions of their HDV.

(c) Drag coefficients (C_d-values)

The sources of drag for HDV are: front pressure, rear pressure, cab-trailer gap, underbody and skin friction. The drag coefficient thus is depending on the design of the vehicle category (solo truck, truck trailer,...), the driver's cab, the bodywork, the underbody, etc.. As already mentioned in (b), no statistical data is available on the share of different bodyworks and driver's cabs on the road. As for the frontal area also the drag coefficients of the HDV categories had to be estimated based on a data base. The data base includes manufacturer specifications and literature review (Huncho, 1998), (Nakamura, 2002), (Saltzman, 1999).

As already explained in chapter 4.4.1.1 the total of the driving resistances is basically estimated from the coast down tests available. To split the forces calculated from the coast down tests into rolling resistance and air resistance, the drag coefficients were set according to the data base. Using the same data bank to set the drag coefficients for the simulation of the average HDV

emission factors shall result in a consistent simulation of the driving resistances for all HDV categories.

The average drag coefficients used for different HDV categories are shown in Figure 103. The maximum and minimum values shown indicate the range of data found while the average values were used as input data into the model PHEM.

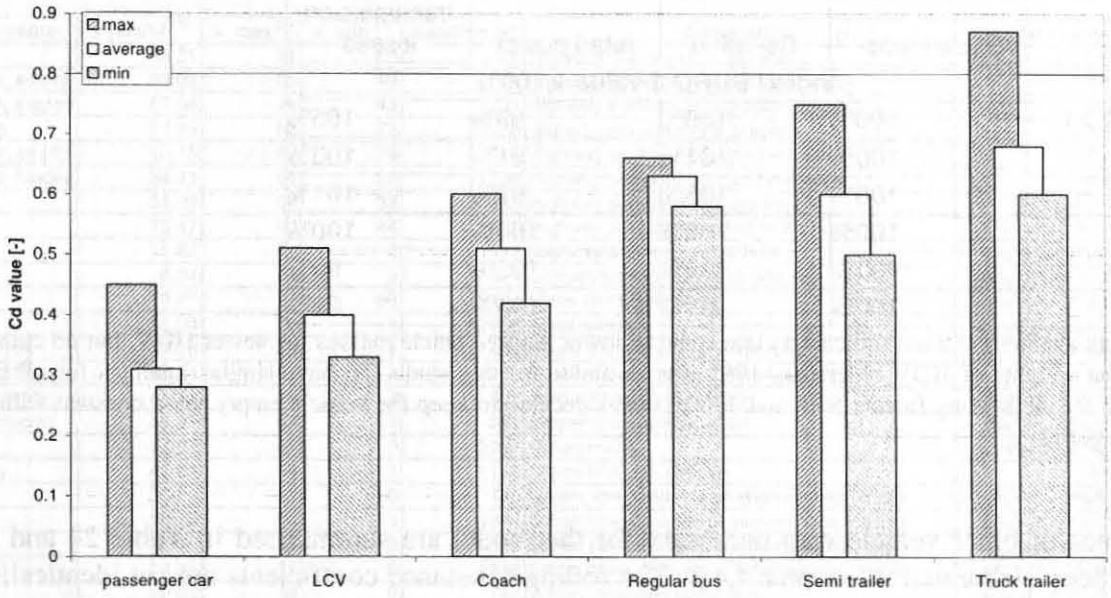

Figure 103: Range of drag coefficients for HDV and average values used for the assessment of the emission factors (basis EURO 3 HDV)

To harmonise the model input data on the vehicles, first the data for EURO 3 HDV was fixed. For all other "EURO-classes" the model input data was assessed by factors related to the EURO 3 HDV. Table 22 summarises the main technical characteristics used for the EURO 3 HDV categories.

Table 22: Technical characterizations used for EURO 3 HDV

	Max. allowed total weight [t]	Vehicle weight empty [t]	Rated Power [kW]	Cd*A
Solo truck <=7.5t	5.8	2.5	85	3.92
Solo truck >7,5-<=12t	11.0	3.8	140	4.55
Solo truck 12-14t	13.5	4.2	160	4.64
Solo truck 14-20t	17.2	5.8	230	4.92
Solo truck 20-26t	25.5	8.2	275	5.02
Solo truck 26-28t	27.0	8.6	275	5.04
Solo truck 28-32t	32.0	10.0	290	5.47
Solo truck >32t	35.5	10.8	305	5.54
TT/ST(1) <28t	18.0	5.6	210	4.90
TT/ST(1) 28-34t	32.0	10.0	260	5.44
TT/ST(1) >34-40t	39.8	12.8	305	5.70
Regular bus-midi <15t	11.5	6.7	165	4.17
Regular bus standard 15-18t	17.8	10.4	210	5.26
Articulated bus >18t	27.0	15.0	230	5.18
Coach standard <18t	18.0	10.8	250	4.82
Coach 3-axle >18t	24.0	14.0	300	4.89

(1) truck trailers and semi trailers

The ratios for technical characteristics of the other EURO-classes (Table 23) to EURO 3 HDV are estimations from data given in "Lastauto & Omnibus" in different yearbooks and the data bank of the Institute where technical characteristics of HDV are collected from specifications of the manufacturers and from literature.

Table 23: Ratios used for technical characteristics compared to EURO 3 HDV

	vehicle mass (1)	Cd-value	rated power	transmission losses
	Index: EURO 3 value = 100%			
Pre EURO 1	100%	108%	89%	105%
EURO 1	100%	104%	91%	103%
EURO 2	100%	103%	97%	101%
EURO 3	**100%**	**100%**	**100%**	**100%**
EURO 4	100%	99%	102%	99%
EURO 5	100%	98%	104%	99%

(1) the data available did not indicate a clear trend to lower empty vehicle masses for newer HDV, but no consistent data on the weights of HDV older than 1995 was available for this study. To have similar loadings for all EURO categories for the loading factors 50% and 100%, it was decided to keep the vehicle empty mass constant within the HDV categories.

The values of other vehicle data necessary for the model are summarised in Table 24 and have already been elaborated in chapter 4.4.1. The rolling resistance coefficients are set identically for all EURO classes. Although the tires have been improved over the years, tyres are changed rather frequently so that EURO 0 and EURO 3 HDV are used today with the same tyre-road combination and shall therefore have identical rolling resistances.

Table 24: Power demand for auxiliaries and rolling resistance coefficients used

P_0 [% from rated power]	2%
Rolling Resistance Coefficients	
Fr_0 [-]	0.019
Fr_1 [s/m]	-0.002
Fr_2 [s^2/m^2]	0.000136
Fr_3 [s^3/m^3]	-0.0000029

The parameters relevant for the transmission (wheel diameter, axle-ratio, gear ratios) have been set according to manufacturer specifications for typical HDV in each HDV category and are not listed in detail here.

4.6.2 Driving Cycles

The vehicle categories described above were simulated in various traffic situations. Where a traffic situation is defined here as combination of a driving cycle, a vehicle loading and a road gradient.

As basic driving cycles the cycles of the former version of the Handbook on Emission Factors were used (Steven, 1995). The driving cycles given there do, by far, not cover all traffic situations. Basically for 0% road gradient all cycles are defined. For combinations of road gradients and vehicle loading only a few cycles are available (Table 25).

In the former version of the Handbook the emission factors for those driving cycles were interpolated from the emission factors derived from the existing cycles. For the update of the HDV emission factors it was agreed to fill these gaps with simulation runs by the model PHEM.

Table 25: Driving cycles simulated (nomenclature for cycle names: number + extensions. Extensions: xs...valid for x% uphill, xg...valid for x% downhill, empty...valid for empty HDV, loaded...valid for loaded HDV, no extensions: used for all gradients and loadings as model input)

Cycle name	v [km/h] (1)	v_max (1)	v_min (1)	duration [s]	Description	Simulated with gradients of
1020	86.21	91	80	1328	Highway standard 0% gradient	-2%/0%/2%
1110_4s_empty	69.02	85	49	981	Highway standard 4% gradient empty	4%
1130_4s_loaded	57.34	74	43	1231	Highway standard 4% gradient loaded	4%
1020_4g	77.59	82	72	1328	Highway standard -4% gradient	-4%
1210_6s_empty	46.15	69	26	415	Highway standard 6% gradient, empty	6%
1230_6s_loaded	36.41	64	22	1204	Highway standard 6% gradient loaded	6%
1420	51.09	64	38	443	Highway standard -6% gradient	-4%/-6%
14021	73.47	90	44	1053	Highway partialy bounded traffic flow	-6%/-4%/-2%/0%/2%/4%/6%
14022	18.82	51	0	1442	Highway bounded traffic flow	-6%/-4%/-2%/0%/2%/4%/6%
13023	6.34	35	0	2824	Congestion highway and urban	-6%/-4%/-2%/0%/2%/4%/6%
2020	79.27	87	66	2294	Motor road, multi-lane	-6%/-4%/-2%/0%/2%/4%/6%
3020	66.08	86	1	2050	Road, others	-6%/-4%/-2%/0%/2%
3110_empty	59.26	86	1	1031	Road, 4% und 6% gradient, empty	4%/6%
3130_loaded	48.51	81	1	1250	Road, 4% und 6% gradient loaded	4%/6%
12010_empty	41.17	79	3	805	Serpentines uphill, empty	-6%/-4%/-2%/0%/2%/4%/6%
12030_loaded	34.85	67	11	361	Serpentines uphill loaded	-6%/-4%/-2%/0%/2%/4%/6%
4020	47.03	67	0	2012	Urban HVS	-4%/-2%/0%/2%/4%/6%
4020_6g	41.01	59	1	1103	Urban HVS 6% Gefälle	-6%
5010	31.27	62	0	745	Urban, long distance of intersections empty	-6%/-4%/-2%/0%/2%/4%/6%
5030	18.73	58	0	1344	Urban long distance of intersections loaded	-6%/-4%/-2%/0%/2%/4%/6%
6010	20.13	58	0	2028	Urban short distance of intersections, empty	-6%/-4%/-2%/0%/2%/4%/6%
6030	14.38	52	0	2618	Urban short distance of intersections, loaded	-6%/-4%/-2%/0%/2%/4%/6%
13022	10.52	39	0	767	Urban, bounded traffic flow	-6%/-4%/-2%/0%/2%/4%/6%
7030	102.99	110	97	766	Coach, highway loaded	-6%/-4%/-2%/0%/2%/4%/6%
8030	98.29	109	91	1413	Coach road loaded	-6%/-4%/-2%/0%/2%/4%/6%
9040	15.62	47	0	1197	Regular bus urban, high station density	-6%/-4%/-2%/0%/2%/4%/6%
10040	21.46	64	0	2725	Regular bus urban low station density	-6%/-4%/-2%/0%/2%/4%/6%
11040	39.25	76	0	2184	Regular bus town to town	-4%/-2%/0%/2%/4%
11240_6s	27.66	46	0	635	Regular bus town to town, 6% gradient	6%
11440_6g	30.97	62	0	503	Regular bus town to town, -6% gradient	-6%

(1)...model input values. Model output cycles may have lower values if the vehicle loading and the road gradient do not allow the velocities of the input cycle with the given engine power performance

Since the vehicle loading and the road gradient do have a significant influence on the driving style and the possible velocity of HDV, the absence of appropriate driving cycles is rather problematic.

As described in chapter 4.4.2, the model PHEM has a subroutine which permanently checks whether the actual engine power demand is above the full load curve. In this cases first of all a gear with higher engine speed is searched. If the actual power demand is still not available, PHEM reduces the velocity of the actual part of the driving cycle until the power demand can be delivered by the engine. A main difficulty of the project was to construct this routine in a way that realistic engine speeds and engine loads are simulated even with very inappropriate input driving cycles.. Since the resulting engine loads show very similar patterns to those measured on the road, the resulting emission factors shall be reliable estimations.

Anyhow, driving cycles on roads with gradients of more than 2% will vary in real traffic significantly over the location and over the time if some density of HDV traffic is on the road. This simply results from the fact that full loaded HDV have a rather low maximum speed on such roads, while HDV with less load can drive much faster, but often have to slow down because of slower HDV in front of them. Today no set of driving cycles for different interactions between HDV with different loadings is available.

In the following some examples of simulated traffic situations are explained. Since for 22 driving cycles the velocity had to be modelled for the different combinations of road gradient and vehicle ladings, it is not possible to show graphs of all resulting cycles. The results are 176 more or less

different cycles within one HDV-category according to the vehicle load and the road gradient. Additional differences result from different HDV categories and the different EURO-classes since the power to weight ratios is different.

Figure 104 and Figure 105 show the basic version of the highway cycle 1020 simulated with the smallest truck configuration (solo truck < 7.5t) and the largest one (semi trailer and truck trailer 34-40t). All vehicle configurations are able to follow the cycle rather easy. The engine speed range of the small trucks are higher than for the large ones. This is a result of the gear boxes used. While small trucks most often use a gear box with fife gears with a velocity of 85 km/h corresponding to approx. 65% normalised engine speed, large semi trailers do have up to 16 gears where 85 km/h can be driven with normalised engine speeds below 60%; this results in a better fuel economy.

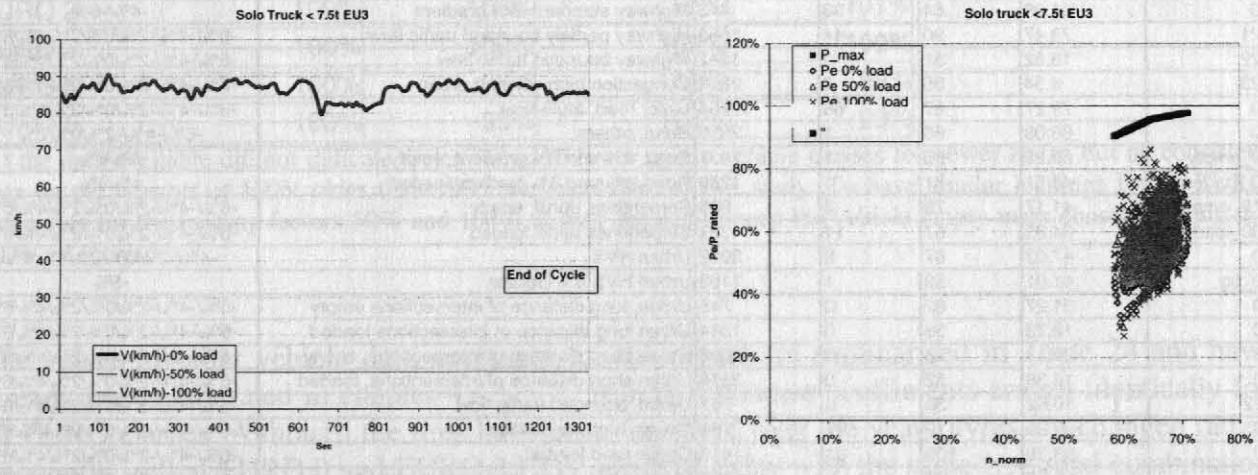

Figure 104: Cycle 1020 (Highway standard, 0% gradient) simulated with a solo truck < 7.5t, EURO 3 (cycle= left, engine load = right)

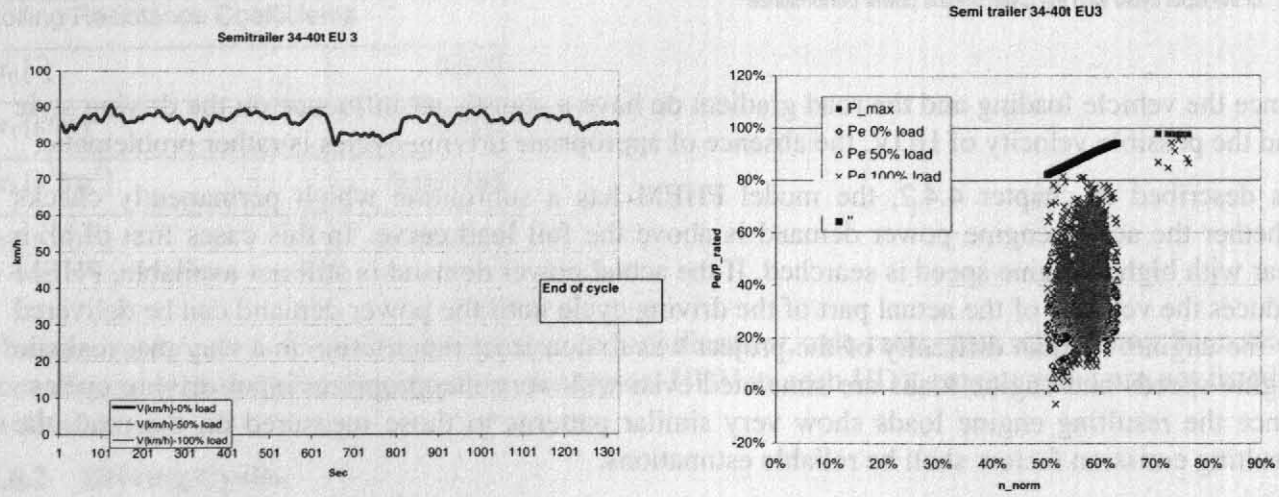

Figure 105: Cycle 1020 (Highway standard, 0% gradient) simulated with a semi trailer 34-40t, EURO 3 (cycle= left, engine load = right)

A road gradient of 2% already leads to the fact that full loaded HDV can not follow the given driving cycle (Figure 106). For small HDV this results in a reduced velocity and a significant share of time driven near full load.

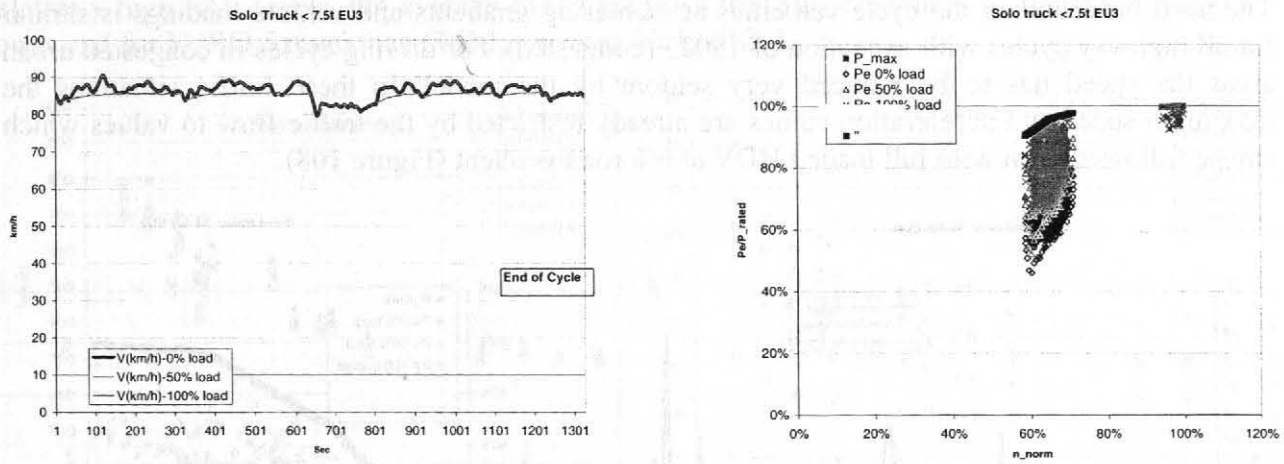

Figure 106: Cycle 1020 (Highway standard, 2% gradient) simulated with a solo truck < 7.5t, EURO 3 (cycle= left, engine load = right)

The cycle 1020 is not used for simulating any higher road gradients. Higher gradients on highway are covered by special cycles. Figure 107 shows as example the cycle 1130_4s_loaded which is representing highway driving with 4% road gradient for 50% and 100% loaded HDV. Obviously the cycle can be followed most of the time from a 50% loaded HDV but not at all with a full loaded truck. With 100% loading the available engine power simply do not allow such high speeds and accelerations.. Since this cycle results of measurements in real world traffic it has to be assumed that the measurements were performed with a HDV loaded slightly below 50%. The rather unsteady driving cycle can be explained by the results for the full loaded truck. The maximum speed of the full loaded semi trailer is approximately the minimum speed of the original 1130 cycle. Thus empty and less loaded HDV had to break frequently in this cycle because of slower full loaded HDV in front of them until they took the chance for passing the slower truck. In general this seems to be realistic, but only if the HDV traffic intensity is high enough and passing other trucks is possible (or allowed) at all under consideration on the highway.

The engine speed levels are met by the simulation very well compared to measured data. Heavy trucks usually do not drive at rated engine speed at all, but drive at gears one or two above the gear which meets the rated engine speed even if the available engine power is by some percent lower at this gear. This is simulated with the sophisticated gear shift model in a realistic way, even if the input cycle is changed by PHEM completely.

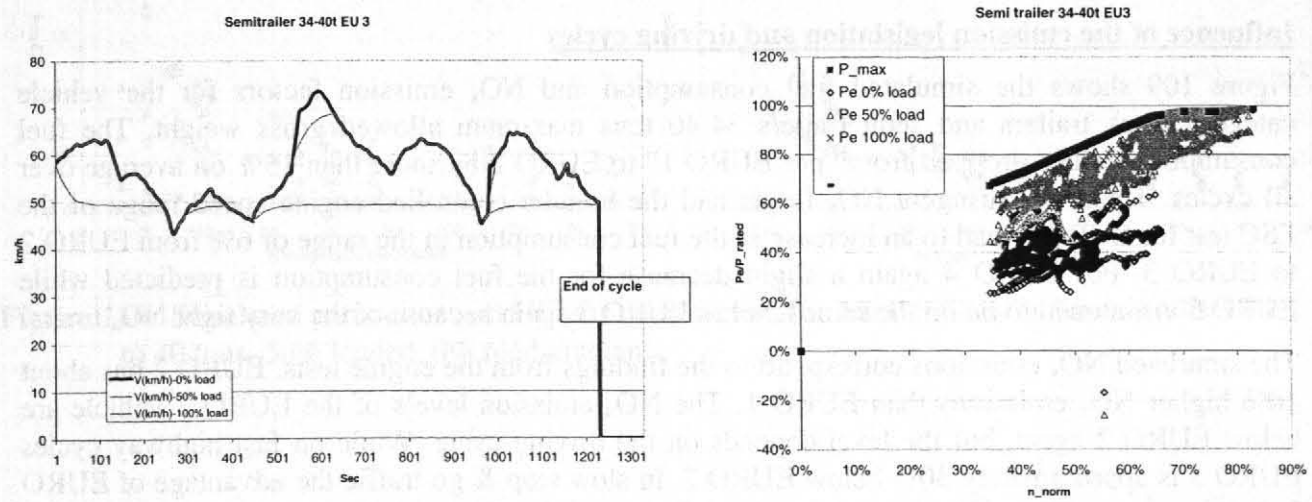

Figure 107: Cycle 1130_4s_loaded (Highway standard, 4% gradient) simulated with a semi trailer 34-40t, EURO 3 (cycle= left, engine load = right)

The need for reducing the cycle velocities at increasing gradients and vehicle loadings is similar for all highway cycles with exception of 13023 (congested). For driving cycles in congested urban areas the speed has to be reduced very seldom by the model. In these traffic situations the maximum speed and acceleration values are already restricted by the traffic flow to values which can be followed even with full loaded HDV at 6% road gradient (Figure 108).

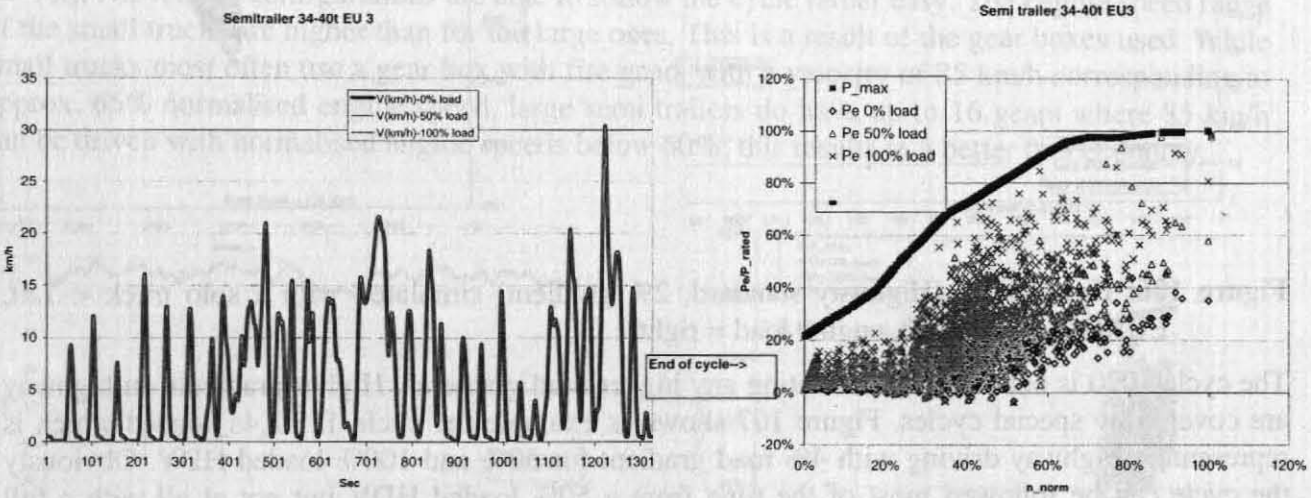

Figure 108: Cycle 13023 (Congested, 6% gradient) simulated with a semi trailer 34-40t, EURO 3 (cycle= left, engine load = right)

The simulated average cycle speed was delivered to INFRAS for each combination of traffic situation and HDV-category together with the emission factors. The data set includes also the share of times where the cycle speed was reduced by the model. The data shall be available in the Handbook of Emission Factors if some users will need these information.

4.7 Emission factors calculated

As mentioned before, 30.000 combinations of vehicle categories, EURO-classes, driving cycles, road gradients and vehicle loadings have been simulated by the model PHEM. To list all results is not possible in this report. The results will be available in the data base of the Handbook on Emission Factors.

In the following principle results are summarised for single vehicle categories.

Influence of the emission legislation and driving cycles

Figure 109 shows the simulated fuel consumption and NO_x emission factors for the vehicle category truck trailers and semi trailers 34-40 tons maximum allowed gross weight. The fuel consumption values dropped from "pre EURO 1" to EURO 2 by more than 15% on average over all cycles. The more stringent NO_x limits and the broader controlled engine speed range of the ESC test for EURO 3 lead to an increase in the fuel consumption in the range of 6% from EURO 2 to EURO 3. For EURO 4 again a slight decrease for the fuel consumption is predicted while EURO 5 is assumed to be on the same level as EURO 3 again because of the very tight NO_x limits.

The simulated NO_x emissions correspond to the findings from the engine tests. EURO 2 has about 10% higher NO_x emissions than EURO 1. The NO_x emission levels of the EURO 3 vehicle are below EURO 2 again, but the level depends on the driving cycle. While on fast highway cycles EURO 3 is approximately 30% below EURO 2, in slow stop & go traffic the advantage of EURO 3 drops to some 5%. This results from the different engine loads of the cycle. In the stop & go cycle a high share of low engine speeds occur where the ESC has no test points. As discussed in chapter 4.3.1.3 the engines are optimised for low fuel consumption in these ranges, resulting in

relatively high NO_x levels. On average over the cycles the NO_x emissions of EURO 4 are 30% lower and for EURO 5 more than 60% lower than for EURO 3.

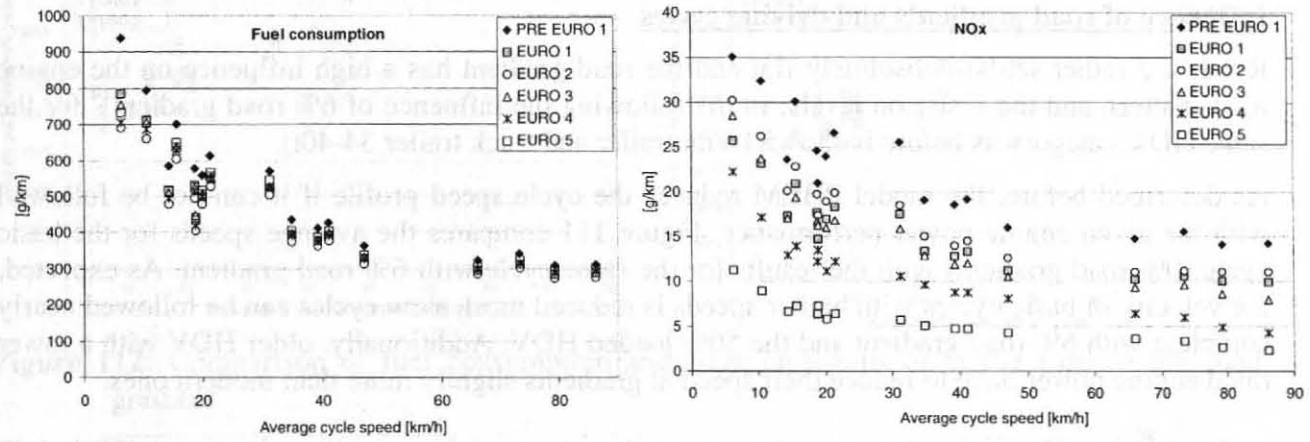

Figure 109: Simulated fuel consumption and NO_x-emission factors for truck trailers and semi trailers 34 to 40 tons, 50% loaded, 0% road gradient

Figure 110 shows the results for particulate matter and HC for the same HDV category. Particulate emissions dropped by nearly 70% from "pre EURO 1" to EURO 2 vehicles. This reduction is even higher for smaller HDV since the larger engines introduced cleaner technologies within the "pre EURO 1" category first (chapter 4.4.3.2). For the EURO 3 vehicles approximately 30% higher particulate emissions are simulated than for EURO 2, but with different levels for the cycles under consideration. Again the emissions in slow cycles are relatively high for EURO 3 while in the highway cycles the particle levels from EURO 3 and EURO 2 are the same. Anyhow, it has to be pointed out that the sample of measured EURO 3 engines is rather small (chapter 4.4.5.1). Compared to EURO 3 more than 80% reduction is predicted for EURO 4 and EURO 5 vehicles.

For HC emissions reductions were found until EURO 2. From that EURO class on the HC emissions kept on the same level. Higher reductions were achieved for CO, but both, CO and HC are no critical exhaust gas components of HDV.

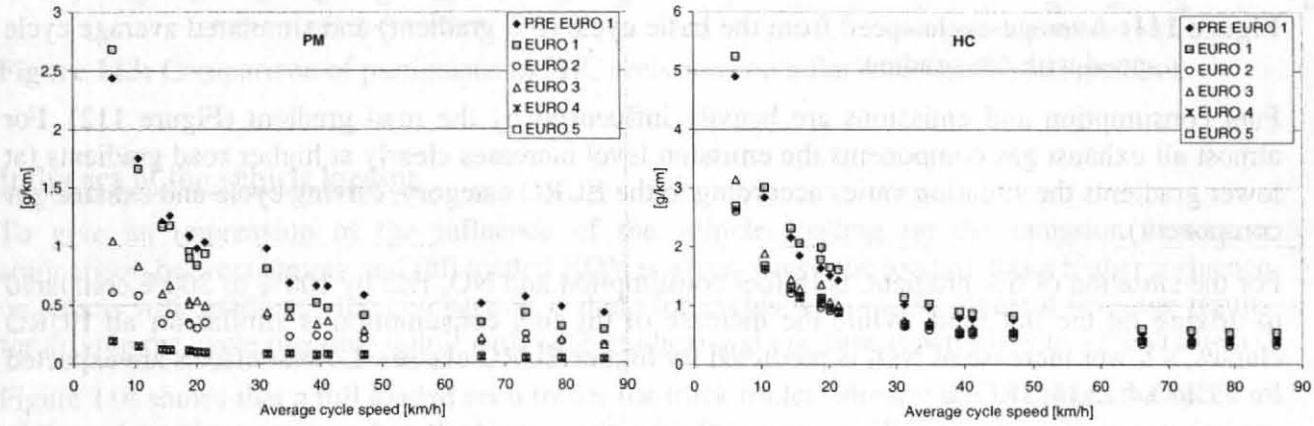

Figure 110: Simulated particulate and HC-emission factors for truck trailers and semi trailers 34 to 40 tons, 50% loaded, 0% road gradient

Obviously the more stringent emission levels for EURO 2 and EURO 3 did not result in appropriate reductions of the emissions in real world driving[13].

Influence of road gradients and driving cycles

Roads are rather seldom absolutely flat and the road gradient has a high influence on the engine loads pattern and the emission levels; in the following the influence of 6% road gradient[14] for the same HDV category as before is shown (semi trailer and truck trailer 34-40t).

As described before, the model PHEM reduces the cycle speed profile if it can not be followed with the given engine power performance. Figure 111 compares the average speeds for the basic cycle (0% road gradient) with the results for the same cycle with 6% road gradient. As expected, the velocity of basic cycles with higher speeds is reduced most, slow cycles can be followed nearly complete with 6% road gradient and the 50% loaded HDV. Additionally, older HDV with a lower rated engine power have to reduce their speed at gradients slightly more than modern ones.

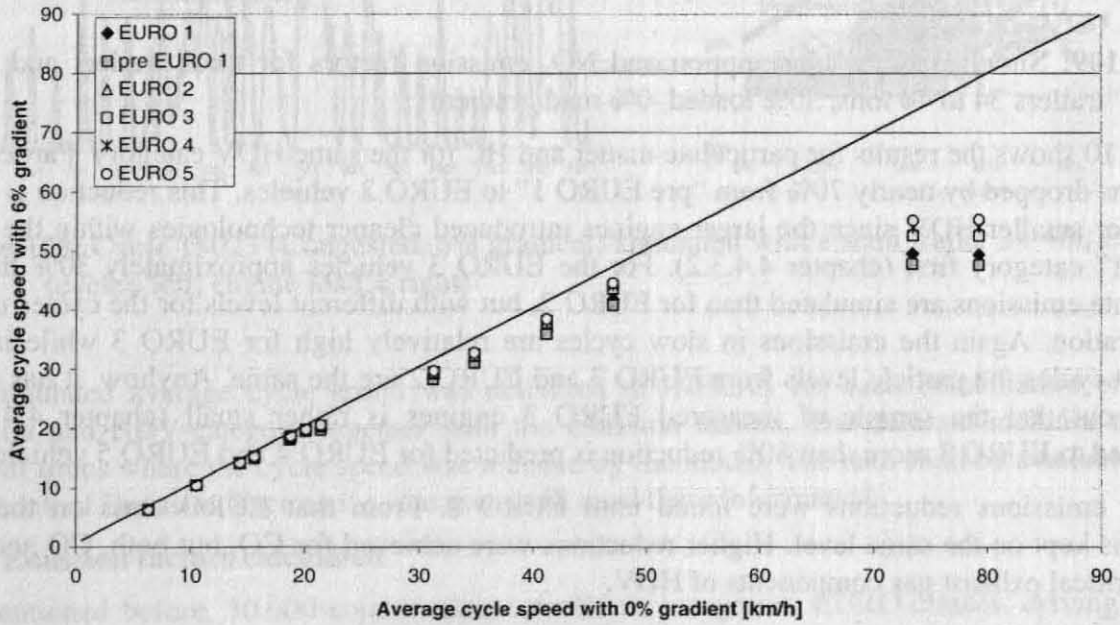

Figure 111: Average cycle speed from the basic cycle (0% gradient) and simulated average cycle speed with 6% gradient

Fuel consumption and emissions are heavily influenced by the road gradient (Figure 112). For almost all exhaust gas components the emission level increases clearly at higher road gradients (at lower gradients the situation varies according to the EURO category, driving cycle and exhaust gas component).

For the situation of 6% gradient, both fuel consumption and NO_x rise by 100% to 300% compared to driving on the flat road. While the increase of the fuel consumption is similar for all EURO classes, a lower increase of NO_x is predicted for higher EURO classes. Lowest effects are expected for EURO 4 and EURO 5.

---

[13] The above shown results shall only be seen as an example, since the results are often different for other combinations of vehicle categories, vehicle loading and road gradients.

[14] The results are not linear over changing road gradients, thus an interpolation of the influence of other road gradients is very inaccurate for some cases. Together with the influence of the vehicle loading (which has higher effects at higher gradients), the use of simplified "gradient factors" and "loading factors", as used in some other models can not be recommended.

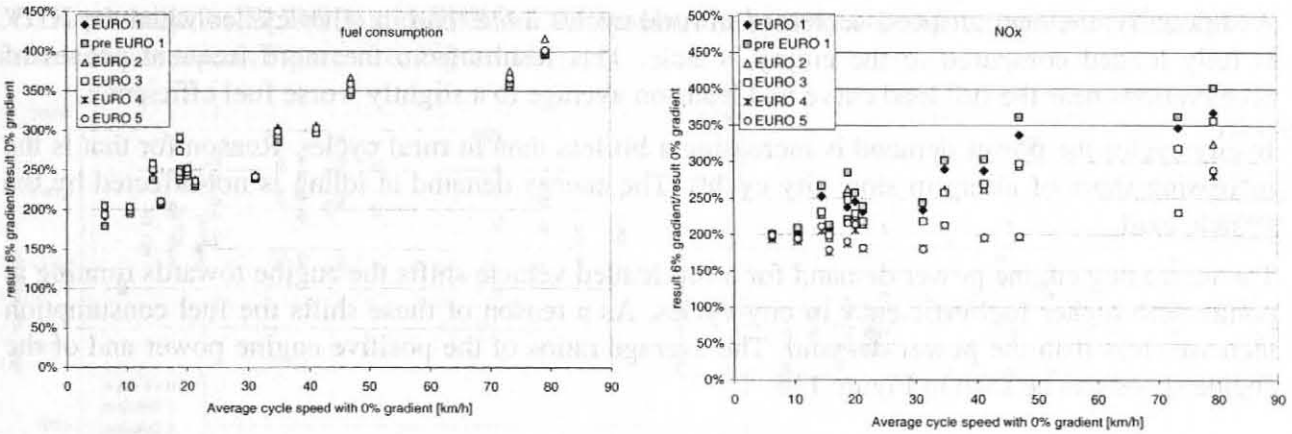

Figure 112: Comparison of fuel consumption and NOx emissions on a flat road to 6% road gradient

High differences in the influence of the road gradient occur for particulate and CO-emissions. For EURO 3 the increases at high road gradients are predicted to be much smaller than for "pre EURO 1" to EURO 2 vehicles. The influence of gradients for EURO 4 and EURO 5 is predicted to be even lower (Figure 113). In comparison, the influence of gradients on HC emissions is predicted to develop similar for all EURO classes.

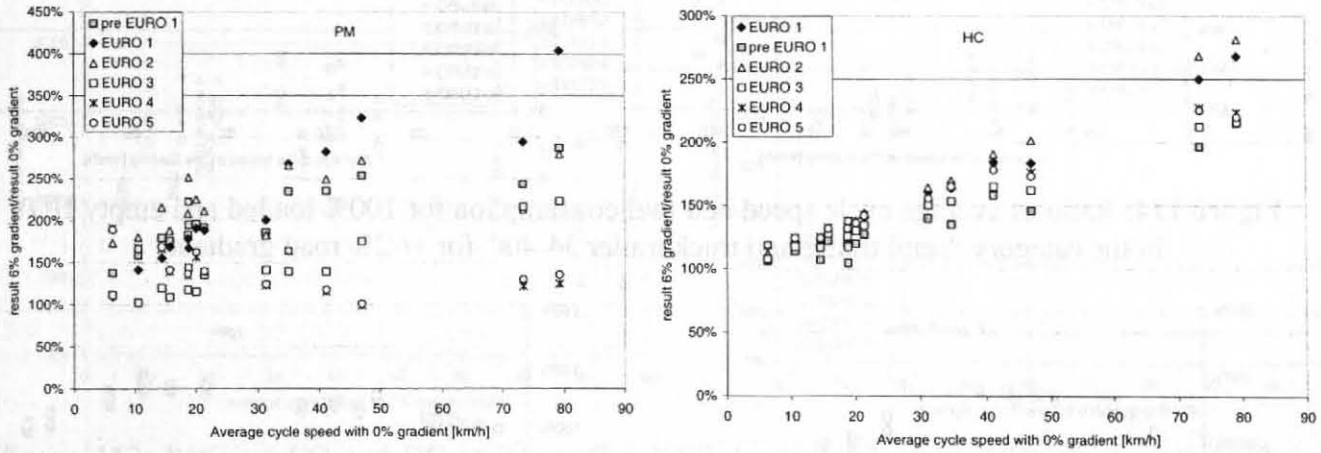

Figure 113: Comparison of particulate and HC emissions on a flat road to 6% road gradient

Influence of the vehicle loading

To give an impression of the influence of the vehicle loading on the emission factors, a comparison between empty and full loaded HDV is given. Since the loading has a higher influence on streets with gradients, the comparison is done for cycles with +/-2% gradient (average results for driving the cycle one time uphill with +2% gradient and one time downhill with –2% gradient).

Figure 114 shows that a full loaded semi trailer (or truck trailer) already has to reduce the speed at +2% road gradient compared to the basic cycle with 0% gradient. The empty vehicle can follow the basic cycles nearly every second.

The fuel consumption values are between 125% and 225% higher for the full loaded vehicle compared to the empty one. The increase in the fuel consumption is highest at "road" cycles and lower in urban and fast highway cycles. The reasons for this effect are manifold. Since the rural cycles do have a much higher dynamic than the fast highway cycles, more energy is lost for braking than on highways. These losses are higher with a loaded vehicle. Furthermore, the vehicle load does not influence the air resistance, which is the dominant driving resistance at high speeds. Thus the increase of the power demand due to a higher vehicle load is lower at highway cycles.

Additionally, the engine speed decreases in rural cycles more than in other cycles when the HDV is fully loaded compared to the empty vehicle. This results from the more frequent phases of accelerations near the full load curve and leads on average to a slightly worse fuel efficiency.

In city cycles the power demand is increasing a bit less than in rural cycles. Reason for that is the increasing share of idling in slow city cycles. The energy demand at idling is not affected by the vehicle load.

The increasing engine power demand for a full loaded vehicle shifts the engine towards running at points with higher fuel efficiency in city cycles. As a reason of these shifts the fuel consumption increases less than the power demand. The average ratios of the positive engine power and of the engine speed can be seen in Figure 115.

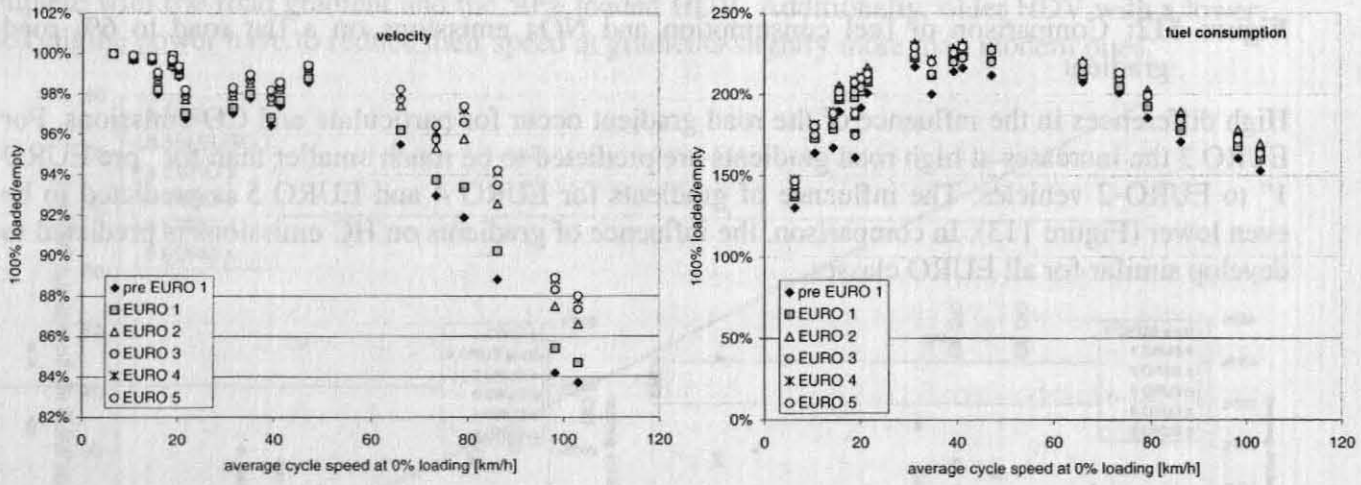

Figure 114: Ratio of average cycle speed and fuel consumption for 100% loaded and empty HDV in the category "semi trailer and truck trailer 34-40t" for +/-2% road gradient

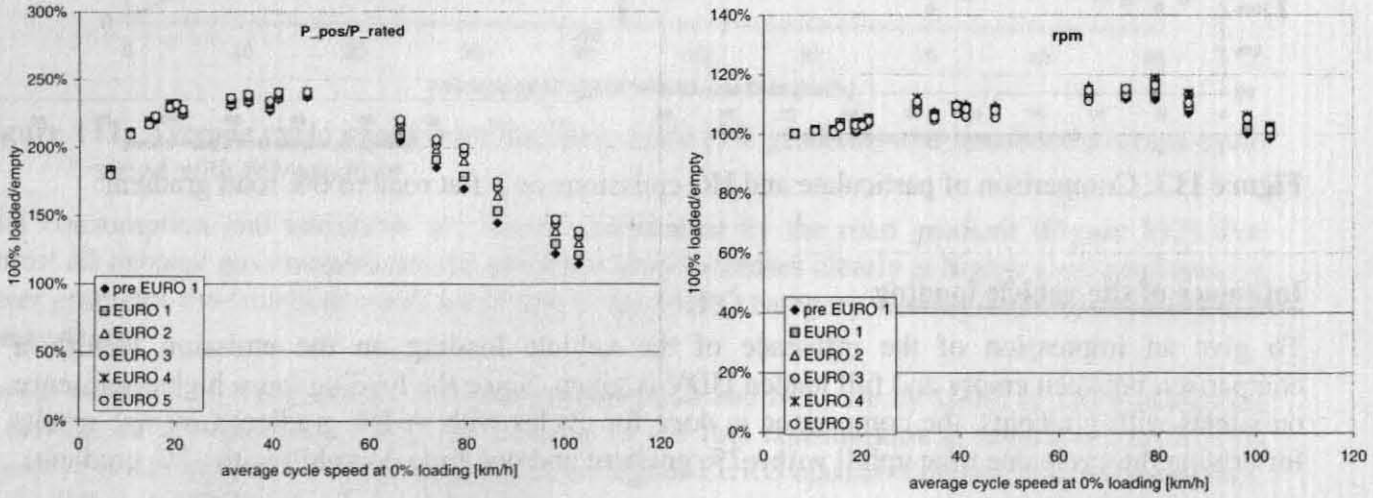

Figure 115: Ratio of average positive engine power needed and average engine speeds for 100% loaded and empty HDV in the category "semi trailer and truck trailer 34-40t" for +/-2% road gradient

While the influence of the EURO category is small when looking at the influence of vehicle loadings on the fuel consumption, this is not the case for the emission factors. Depending on the size of the engine emission map, NO_x emissions increase by 150% to nearly 250% with 100% load compared to 0% load at this traffic situations. In general the increase is smaller for newer engine technologies. The differences between the EURO categories are highest for particulate matter and

CO. Especially for EURO 1 and EURO 2 the results are heavily depending on the driving cycle under consideration (Figure 116, Figure 117).

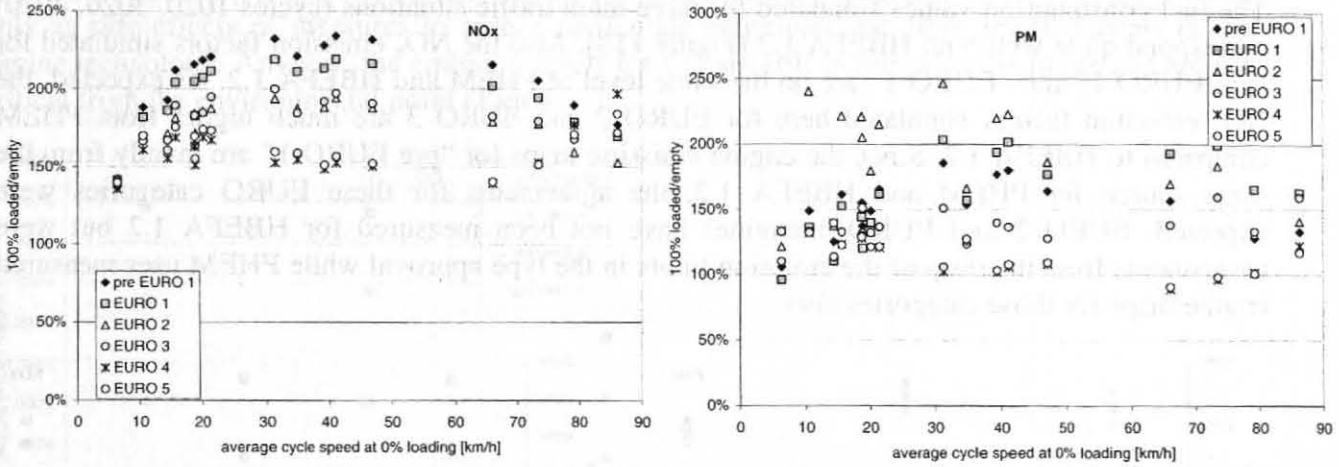

Figure 116: Ratio of NOx and PM emissions for 100% loaded and empty HDV in the category "semi trailer and truck trailer 34-40t" for +/-2% road gradient

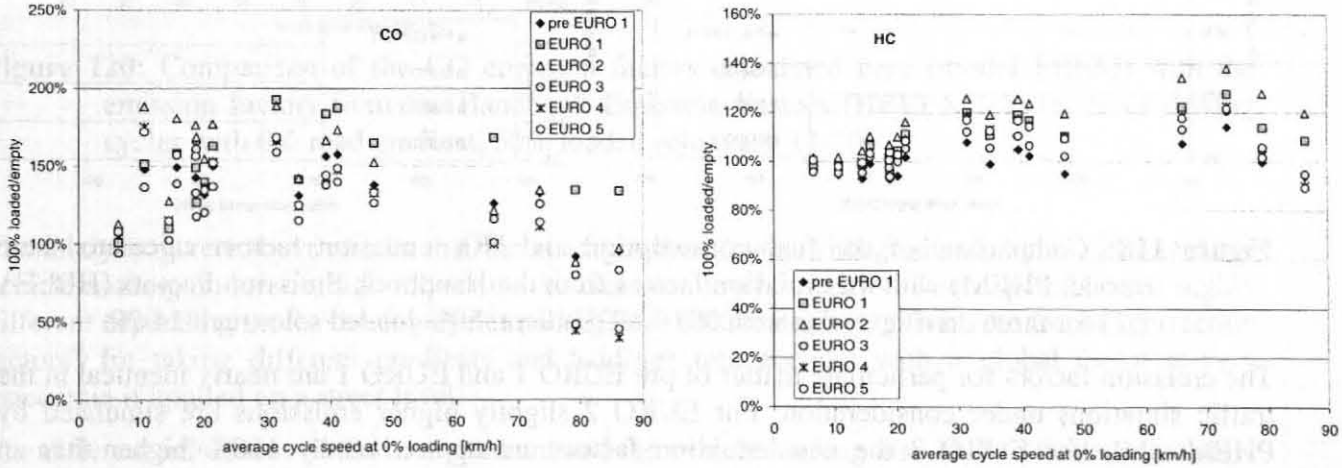

Figure 117: Ratio of CO and HC emissions for 100% loaded and empty HDV in the category "semi trailer and truck trailer 34-40t" for +/-2% road gradient

Comparison with the former version of the HDV emission factors (Hassel, 1995)

As already written in chapter 4.6, no information on the vehicle specifications used for the HDV emission factors in (Hassel, 1995) are available. Additionally, the results above show that the relative ratio of the emission factors between the different EURO categories very much depend on the loading, the cycle and the road gradient. The results of the Handbook on Emission Factors (HBEFA 1.2) suggest that constant factors have been used between the EURO categories. Thus, a comparison of the results of the new model PHEM and (Hassel, 1995) is only indicative. A more complete comparison between the new emission factors and the former ones shall be made when the updated Handbook on Emission Factors is available. The Handbook will allow an easy comparison of average fleet emission factors

For a rough comparison the HDV category "solo truck 14-20t" is used. In the new model this category has 17.2 tons maximum allowed gross weight (Table 22), with an empty vehicle weight of 5.8 tons. 50% loading correspond to 5.7 tons. The simulations in (Hassel, 1995) may have been done for any maximum allowed gross weight between 14 tons and 20 tons, and "half loaded" is also not defined since the vehicle empty weight is unknown. Anyhow, for the HDV category "solo

truck 14-20t" the simulated fuel consumption corresponds quite well, so we assume that the vehicle characteristics are similar.

The fuel consumption values simulated for three main traffic situations (cycles 1020, 3020, 4020) correspond quite well with HBEFA 1.2 (Figure 118). Also the NO_x emission factors simulated for "pre EURO 1" and "EURO 1" are on the same level of PHEM and HBEFA 1.2. As expected, the NO_x emission factors simulated here for EURO 2 and EURO 3 are much higher from PHEM compared to HBEFA 1.2. Since the engine emission maps for "pre EURO 1" are mainly from the same source for PHEM and HBEFA 1.2, the agreements for these EURO categories were expected. EURO 2 and EURO 3 engines have not been measured for HBEFA 1.2 but were assessments from the drop of the emission limits in the type approval while PHEM uses measured engine maps for those categories also.

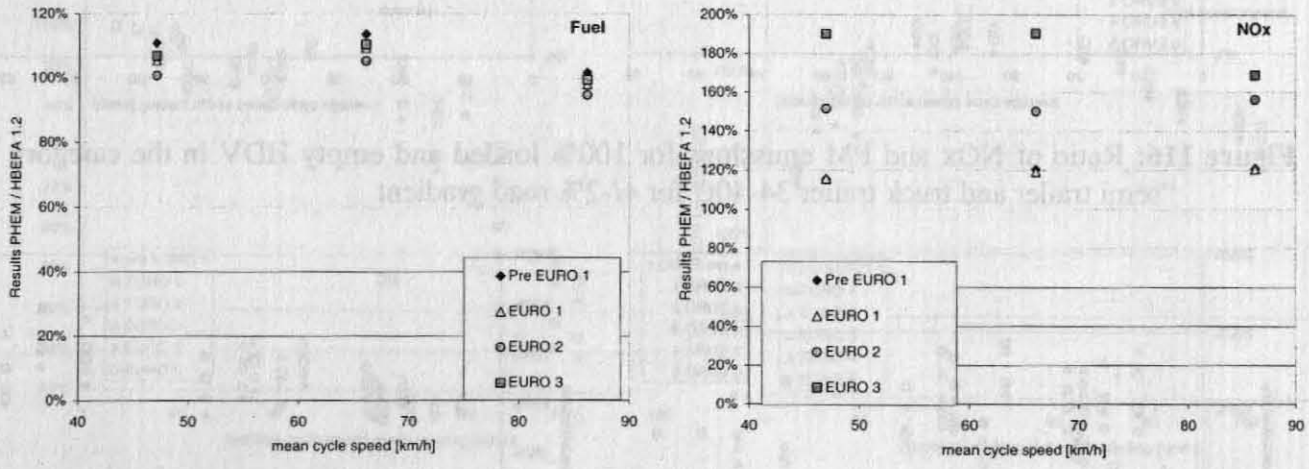

Figure 118: Comparison of the fuel consumption and NO_x emission factors calculated here (model PHEM) with the emission factors from the Handbook Emission Factors (HBEFA 1.2) for three driving cycles with 0% road gradient, 50% loaded solo truck 14-20t

The emission factors for particulate matter of pre EURO 1 and EURO 1 are nearly identical in the traffic situations under consideration. For EURO 2 slightly higher emissions are simulated by PHEM while for EURO 3 the new emission factors are approximately 100% higher than in HBEFA 1.2. For HC the new emission factors are in general on a lower level. Only EURO 3 emission factors are similar from PHEM and HBEFA 1.2.

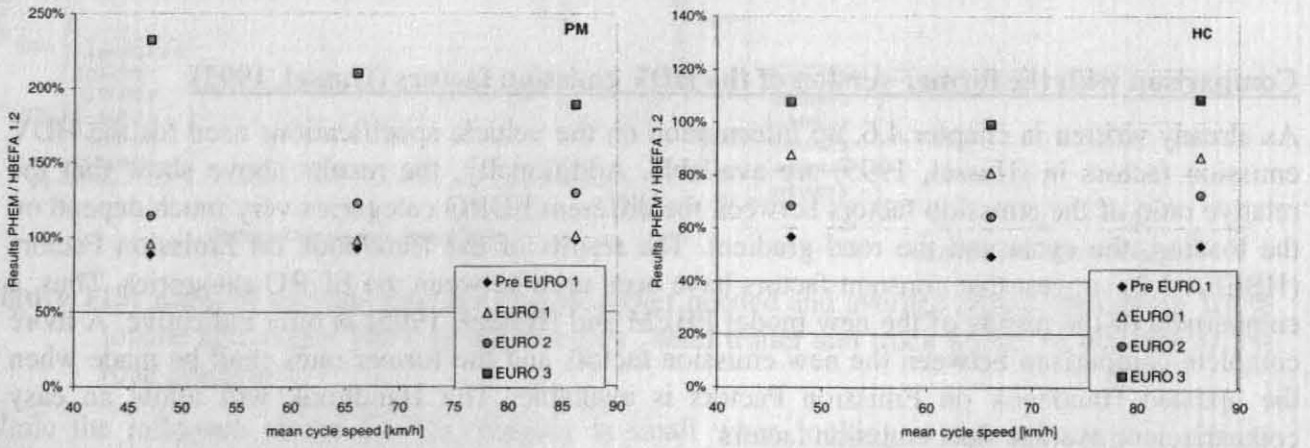

Figure 119: Comparison of the particulate and HC emission factors calculated here (model PHEM) with the emission factors from the Handbook Emission Factors (HBEFA 1.2) for three driving cycles with 0% road gradient, 50% loaded solo truck 14-20t

For CO the emission factors are very similar again for the "pre EURO 1" category. For newer HDV PHEM gives much higher CO emissions. Most likely the emission factors from HBEFA 1.2

were reduced according to the type approval values for EURO 1 to EURO 3. In reality the CO emission levels of HDV have already been far below the limit values for EURO 1 and there was no need for reducing CO systematically for EURO 2 and EURO 3 engines. Thus, CO was reduced only as side effects of measures to reduce particulate emissions and other improvements in the engine technology. Anyhow, the emission levels for CO are still in line with the limits and are not critical from the environmental point of view.

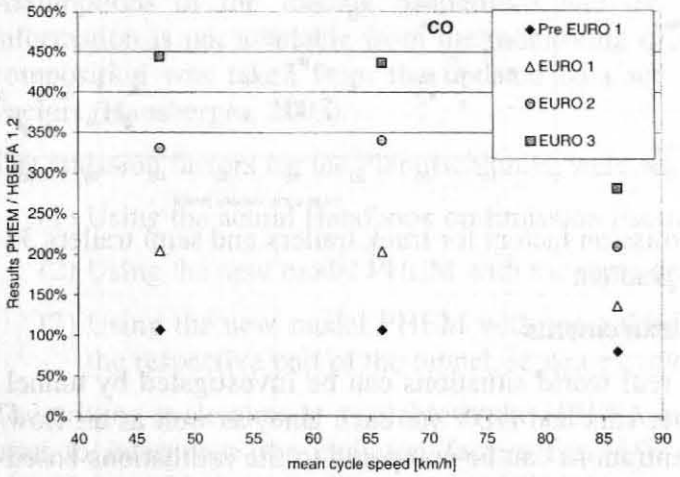

Figure 120: Comparison of the CO emission factors calculated here (model PHEM) with the emission factors from the Handbook Emission Factors (HBEFA 1.2) for three driving cycles with 0% road gradient, 50% loaded solo truck 14-20t

The analysis given above shows that the road gradient (even with gradients below 2%) and the vehicle loading do have a high impact on the emission levels of HDV. The impact is often highly different depending on the driving cycles and HDV-EURO-categories. Thus, the use of "correction factors" for taking different gradients and loadings into account with a global factor is very inaccurate if applied on a street level.

The different influences of the road gradient and the vehicle loading also lead to the fact that there are no general valid "improvement factors" for the emission levels of pre EURO 1 to EURO 5. Figure 121 shows the emission factors for a full loaded HDV category on +/-2% road gradients. Compared to the emission factors from Figure 109 and Figure 110 where the same HDV category was simulated with 50% load on flat road the ratios of emissions between the EURO classes show similar effects but are clearly different.

The main reason for such results are the rather uneven engine emission maps of modern HDV when different strategies were followed in the application for EURO 1, EURO 2 and EURO 3. Thus changes in the engine load and engine speed patterns have different effects on the different Euro-classes.

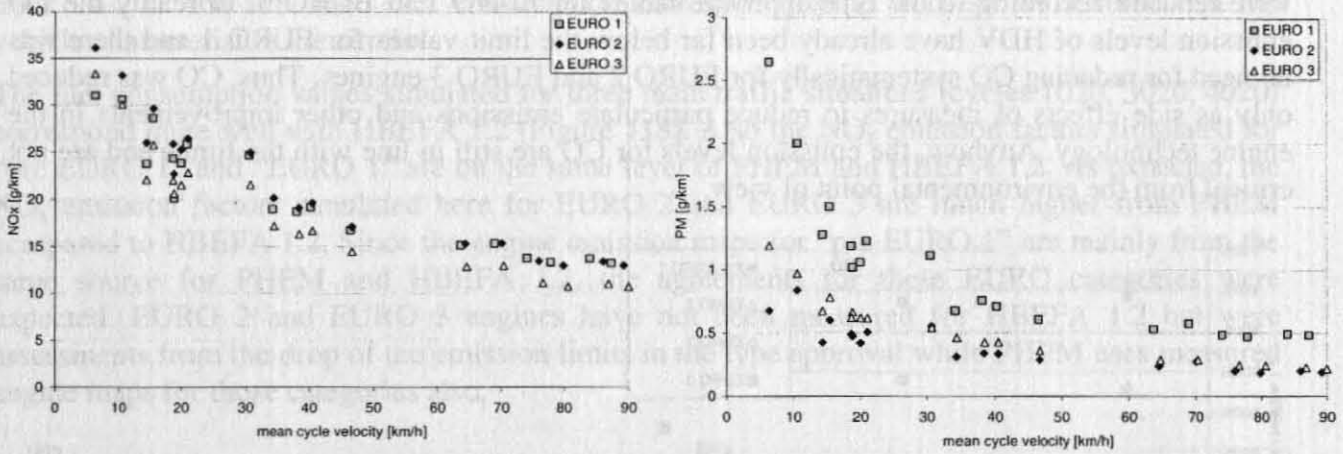

Figure 121: Simulated NOx- and particulate emission factors for truck trailers and semi trailers 34 to 40 tons, 100% loaded, +/-2% road gradient

4.8 Model Validation by Road Tunnel Measurements

The validity of emission factors or models in real world situations can be investigated by tunnel measurements. Traffic flow (split into passenger cars and HDV for each lane) as well as air flow are recorded and the measured pollution concentrations can be compared to the estimations based on emission factors.

Such measurements were performed in the Plabutschtunnel in November 2001, which serves as a by-pass for the City of Graz, Austria. Further tunnel measurements are done in the project ARTEMIS but are not available for the validation of the emission factors yet.

The Plabutschtunnel is a 10-km-long one-bore tunnel with two lanes (operated in counter flow), carrying the A9 Highway (Pyhrnautobahn). It is divided into 5 ventilation sections and operated as a transverse ventilation system. The sampling site was located some 4 km inside the tunnel in the middle of ventilation section 3 where a homogeneous mixture of air and pollutants could be assumed. A container equipped with standard air quality monitoring device (AQM) was installed in a pull off bay within the considered ventilation section. The road gradient in this section is +/- 1 % (Figure 122).

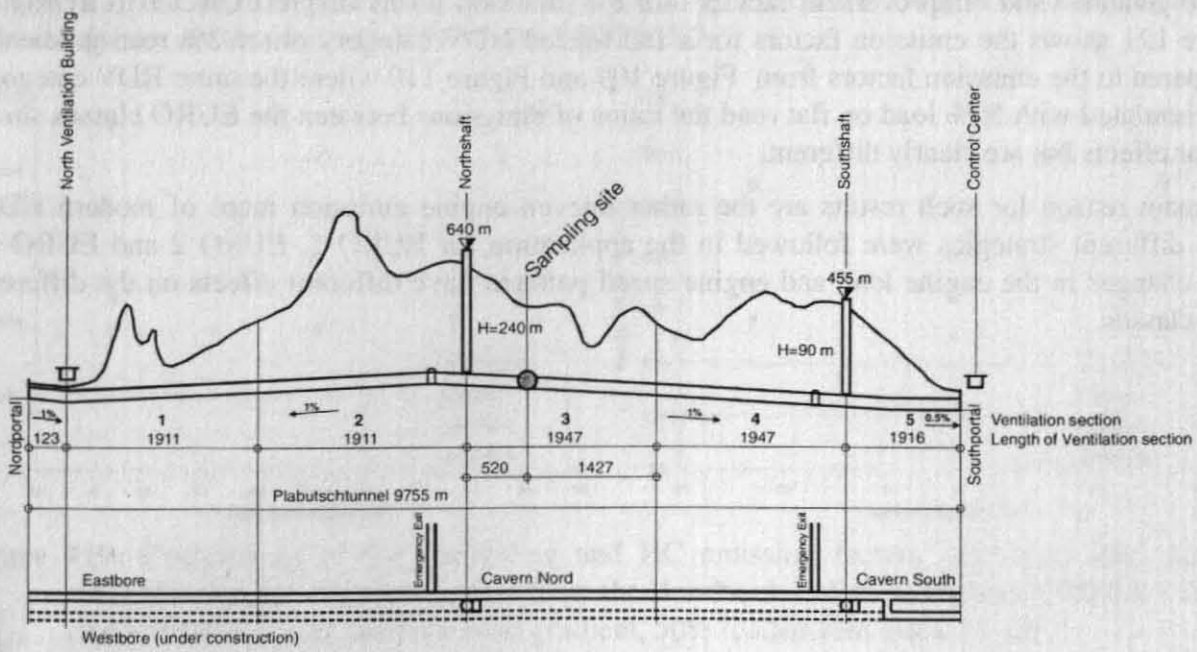

Figure 122: Plabutschtunnel - General profile and ventilation system

The measured data was analysed from a statistical aspect (non-linear regression) from which the estimation for the fleet emission factors of the passenger cars and heavy duty vehicles were won. This was valid for both driving directions (i.e. in this case +/- 1% road gradient) where the separate emission factors for uphill and downhill were gained from the different volume of traffic over the time in the two directions.

The emissions in the checked ventilation section were also recalculated with the model PHEM. Assumptions of the loading proportions and the fleet distribution are necessary since this information is not available from the monitoring of the traffic flow. This data on the HDV fleet composition was taken from the updated data set for Austria for the Handbook on Emission Factors (Hausberger, 2003).

The emission factors for the Plabutschtunnel were simulated in three different ways:

(1) Using the actual Handbook on Emission Factors 1.2

(2) Using the new model PHEM with the same driving cycle as in (1)

(3) Using the new model PHEM with the a driving cycle recorded in the Plabutschtunnel (in the respective part of the tunnel, separate cycle for +1% and –1% road gradient)

The driving cycle already available in the HBEFA each with –2%, 0% and 2% road gradient was used to interpolate the emission factors for +1% and –1% road gradient. This process is in accordance with the use of the updated HBEFA.

The emission factors gained from these calculations were corrected with regard to the ambient conditions in the tunnel which are promoting the development of NO_x (lack of humidity, higher temperature). The correction was done with the help of the correction function according to the EC regulations. The results are shown in Figure 123 and Table 26.

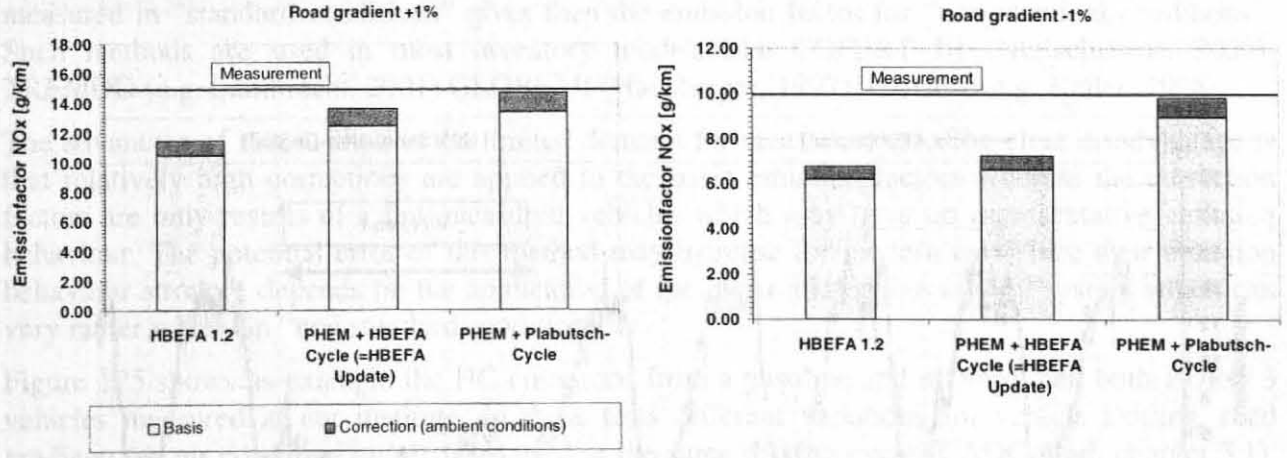

Figure 123: Comparison of emission factors gained by tunnel measurements and by calculation with HBEFA 1.2 and the new model PHEM

As expected the HBEFA 1.2 shows a clear under-estimation of the NO_x emission level. Using the model PHEM actually shows higher NO_x values for the same driving cycle as used in HBEFA 1.2 but the level of the actual emissions is not reached. Since the driving cycles in the HBEFA give the road gradient only in 2% steps, the emission factor for +/- 1% gradient had to be gained by means of linear interpolation from emission factors of other road gradients. The influence of gradient, loading and driving cycle on the emission level of heavy duty vehicles is remarkably high and often non linear. A correct assessment of these non-linear interrelations can only be achieved by detailed simulation of the combination of all relevant parameters. In a third step the model PHEM was used with a driving cycle measured in the Plabutschtunnel and the actual road gradients ("PHEM+Plabutsch-Cycle"). The results of this simulation are now in line with the

emission factors gained from the road tunnel measurements. This exercise shows the importance of the driving cycle for the simulation results.

Table 26: Emission factors gained by tunnel measurements and by calculation

Emission-Factors NOx [g/km]		Measurement Nov 2001 (95% confidence interval in fine-print letters)	Simulation		
			HBEFA 1.2	PHEM + HBEFA Cycle (=HBEFA Update)	PHEM + Plabutsch Cycle
Road Gradient +1%	Basis		10.48	12.46	13.39
	Correction (ambient conditions)		1.01	1.20	1.29
	Result	15.79 **14.90** 14.01	**11.50**	**13.66**	**14.69**
Road Gradient -1%	Basis		6.19	6.61	8.95
	Correction (ambient conditions)		0.60	0.64	0.86
	Result	10.95 **9.98** 9.00	**6.78**	**7.25**	**9.81**

Furthermore, the time-dependent process of the pollutant concentration in the respective ventilation part was recalculated with the help of the simulated emission factors[15], the registered traffic flow and the ventilation rate. The results were then compared with the measurement data (Figure 124). These show a clear and remarkably high conformance, especially on weekdays. On the weekends (in this case 11th and 12th November) the mechanical ventilation is strongly reduced and the air renewal rate can hardly be estimated due to elusive flow effects. (p. e. vehicle trust). Hence, the pollutant concentration cannot accurately be recalculated.

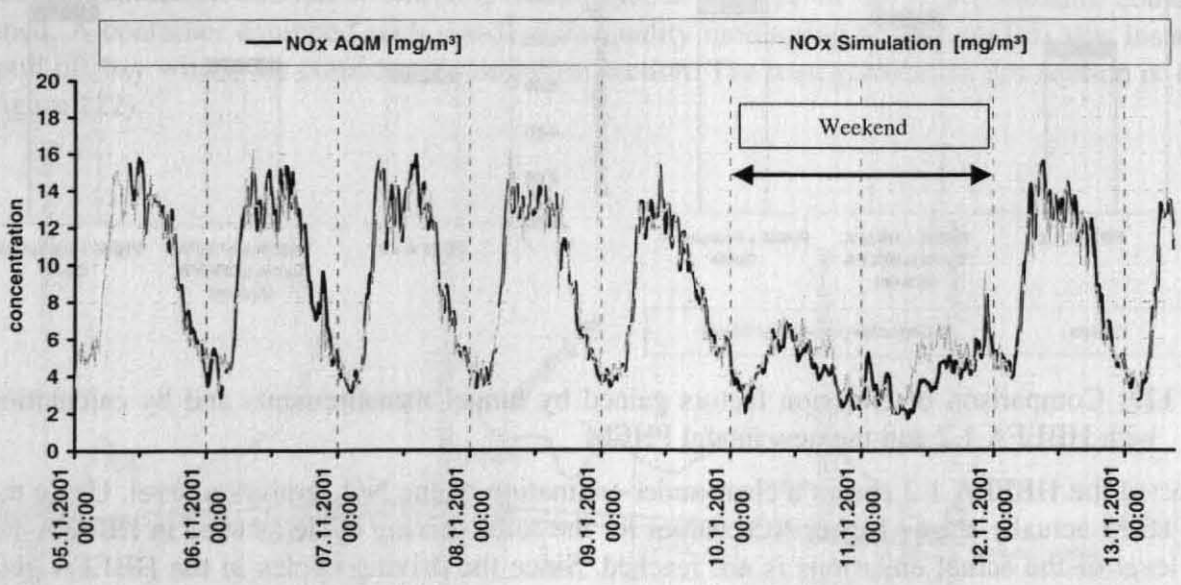

Figure 124: Comparison between measured and simulated NO_x concentrations for a period of 8 days

[15] The emission factors for passenger cars were taken from the HBEFA 1.2 (HBEFA obviously gives a reliable estimation of the actual emission level of passenger cars). As emission factors of heavy duty vehicles the values gained from simulation "PHEM+Plabutsch-Cycle", corrected due to ambient conditions, were used.

5 Simulation of passenger car emissions

In the 5th EU-Framework programme ARTEMIS (Assessment of Reliable Transport Emission Models and Inventories) work package 300 is dealing with passenger car emissions. Main tasks are the investigation of influences from varying boundary conditions on the measurement results and the elaboration of a new set of emission factors for cars and light goods vehicles.

The investigations of influences from fuel quality, ambient temperature and humidity and the setting of the fan for simulating the air stream on the test bed are still ongoing. The following assessment of emission factors from the measurements and from instantaneous emission modelling thus are preliminary. At the final stage of the project it is planned to bring the simulation for passenger cars on the quality level already achieved for HDV (chapter 4).

As already described in chapter 2.2.2, the accuracy of established instantaneous emission models is rather poor when used for simulating emissions of modern cars. Additionally, the established models are not flexible for the calculation of "non standard conditions[16], like different vehicle loadings, road gradients, the use of auxiliaries and for including cold start effects on the emission level.

Thus no advantage can be seen in such models compared to emission factors directly based on measurement results. However, the influences of "non standard conditions" on the emission level are high and it is beyond each budget to measure a sufficient number of cars in all relevant combinations of such "non standard conditions". To overcome this problem, usually only a small sample of cars is tested in extra tests, in which e.g. the road gradient is varied. The changes in the measured emissions compared to the standard conditions are then defined as correction factors. Applying the correction factors to the emission factors gained from the large vehicle sample measured in "standard conditions" gives then the emission factor for "non standard conditions". Such methods are used in most inventory models like COPERT III (Ntziachristos, 2000), TREMOD (e.g. Lambrecht, 2001) GLOBEMI (Hausberger, 1997), HBEFA (e.g. Keller, 1998).

The advantage of this method is the limited demand for measurements. The clear disadvantage is that relatively high corrections are applied to the basic emission factors whereas the correction factors are only results of a few measured vehicles which may have no representative emission behaviour. The potential error of this method may increase for modern cars since their emission behaviour strongly depends on the application of the electronic engine control system which can vary rather widely in "non standard conditions".

Figure 125 shows as example the HC emissions from a gasoline and a Diesel car, both EURO 3 vehicles measured at our institute. In these tests different variations for vehicle loading, road gradient and air condition on/off were used at the same driving cycle (CADC road, chapter 3.1). The emission levels vary by more than +/- 100% compared to the "standard condition", which is empty (90 kg load), no air conditioning and flat road.

[16] Where „standard conditions" are defined here as zero percent road gradient, hot running conditions, no auxiliaries running and vehicle loading according to the type approval requests

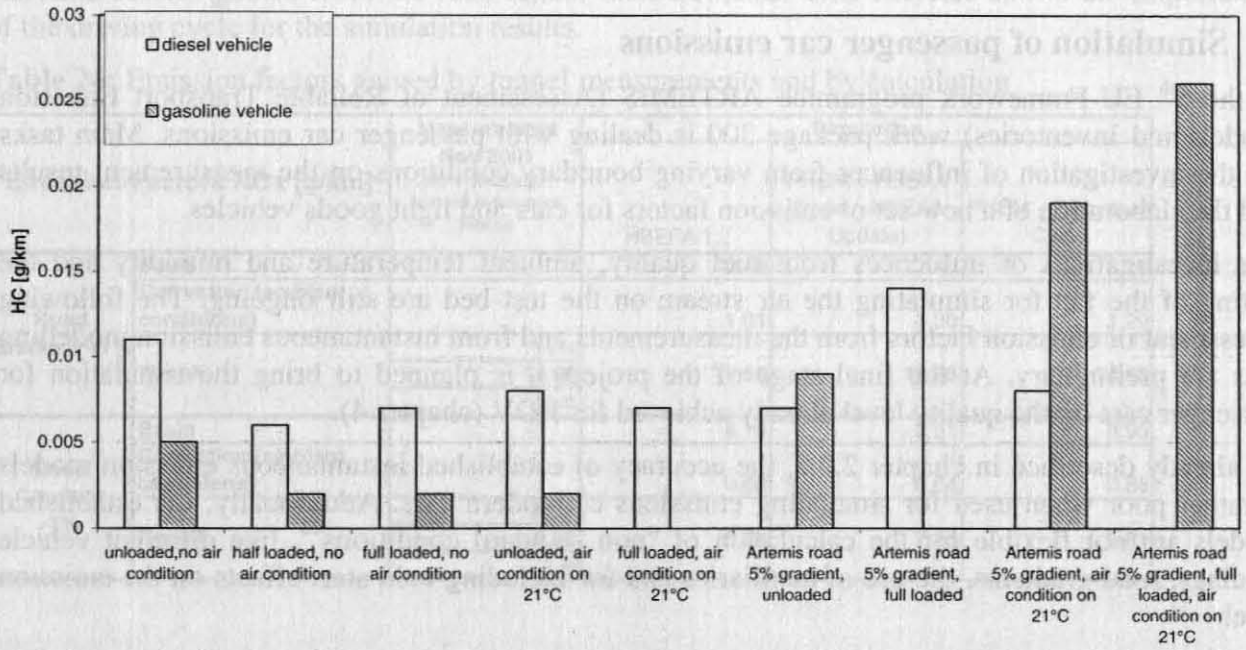

Figure 125: Measured HC emissions in the CADC-road cycle with different settings for vehicle loading, road gradient and air condition on/off

Similar results are found for NO_x and CO while the influence of "non regular conditions" on the particulate emissions was even higher. For CO_2 and the fuel consumption the scattering is much lower.

In the ARTEMIS project four cars are measured in total in a matrix of variable road gradients and variable vehicle loadings while more than 100 cars are measured in the CADC and in the NEDC under standard conditions. A similar situation exists for cold starts and auxiliaries, where the corresponding tests are performed at other laboratories.

Combining all single "correction factors" - if a vehicle e.g. drives uphill after a cold start with full loading - is a rather risky task. Since increased emissions often result from a worse efficiency of the catalyst (resulting from cold start or poor λ regulation), adding the single correction factors may lead to high overestimations of the emission levels. On the other hand the real emission level can be stable if e.g. only the vehicle loading is increased, but in combination with road gradients the influence of a different vehicle loading can be high.

These drawbacks of correction factors make the use of a detailed vehicle emission model very attractive. Basic demands for a detailed vehicle emission model for passenger cars in the project ARTEMIS are:

- All necessary input data has to be gained from the basic measurement programme performed with all cars (NEDC, CADC test cycles)
- The model has to reach an acceptable accuracy, at least it has to be more reliable than the use of correction factors for non standard driving conditions
- The model must be able to simulate all relevant combinations of non standard driving conditions.

5.1 Hot running conditions

For the task of simulating passenger car emissions in hot running conditions the model developed for HDV (chapter 4) was extended for the application at passenger cars. The model development is

still going on, thus in the following chapters only the solution of some main problems and some results are illustrated.

5.1.1 Preparation of engine emission maps

The main problem of applying the model PHEM to the simulation of passenger cars was a suitable method in order to gain engine emission maps from the measurements on the chassis dynamometer. Steady state engine maps can be measured on the roller test bed with sufficient accuracy, but such measurements are not in the basic programme of ARTEMIS which is performed by the majority of the tested cars. As a result the method already used for established instantaneous models had to be applied to gain engine emission maps from transient vehicle tests.

To prepare a more reliable basis the instantaneous emissions measured are corrected for the delay times of the analysers and the variable transport time in the measurement system according to chapter 3.3.

From the driving resistances and the transmission losses the engine power is simulated second per second according to the equations given in chapter 4.4.1. The actual engine speed is calculated from the transmission ratios, the wheel diameter and the gear shift rules of the actual test cycle according to chapter 4.4.2.

Then the resulting instantaneous data on the engine power, the engine speed and the exhaust gas emissions is used as engine map for the model and the emission values for the engine map to be created from the measured driving cycle are interpolated using the modified Shepard method (chapter 4.4.3.1). This method is preferred to simply rastering the measured values into a grid of the engine map since the interpolation method does not leave cells free and is in line with the calculation applied for simulating the vehicle emissions from a given driving cycle. Figure 126 gives a schematic picture of the allocation of emission values to the effective engine power and the actual engine speed.

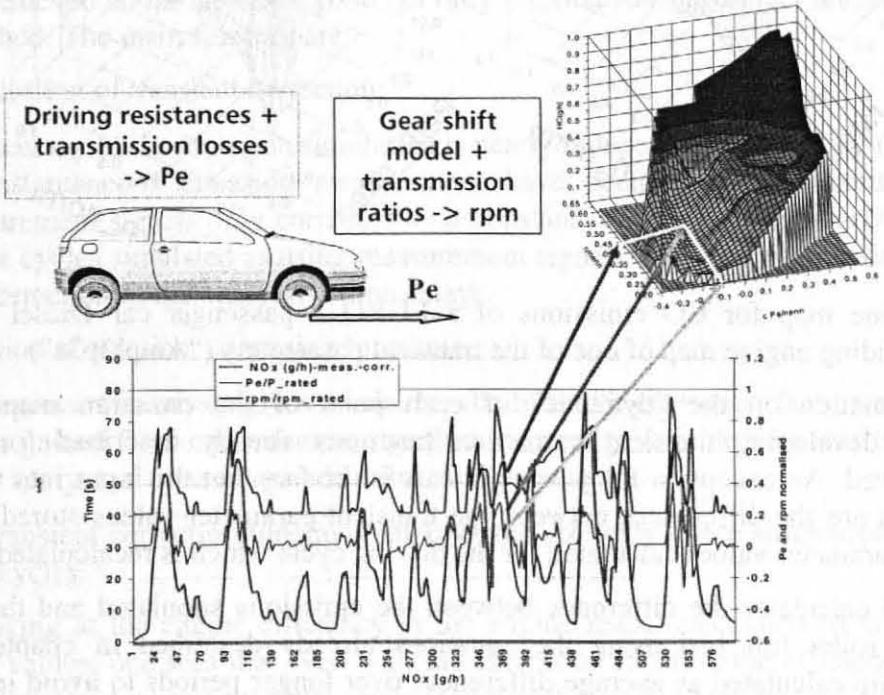

Figure 126: Schematic picture of gaining engine emission maps from measurements on the roller test bed

5.1.2 Transient correction functions

Compared to the application to HDV, where engine maps from steady state measurements are available, the engine emission maps for passenger cars already include influences of transient conditions.

To be able to apply transient correction functions similar to the HDV application, the information on the transient effects included in each point of the engine map has to be stored. For this task the set of potential transient parameters is calculated from the course of the test cycles used for the preparation of the engine map. Then the transient parameters are interpolated into the points of the engine map as was done for the emission values.

Figure 127 for example shows the CO emission map calculated for the engine of an EURO 3 Diesel passenger car and the engine map for the transient parameter "Ampl3p3s", which gives the average amplitude of the engine power course over three seconds before an actual emission event (chapter 4.4.4.2). Typically the average of the transient parameters interpolated into the engine map is different at each point of the map.

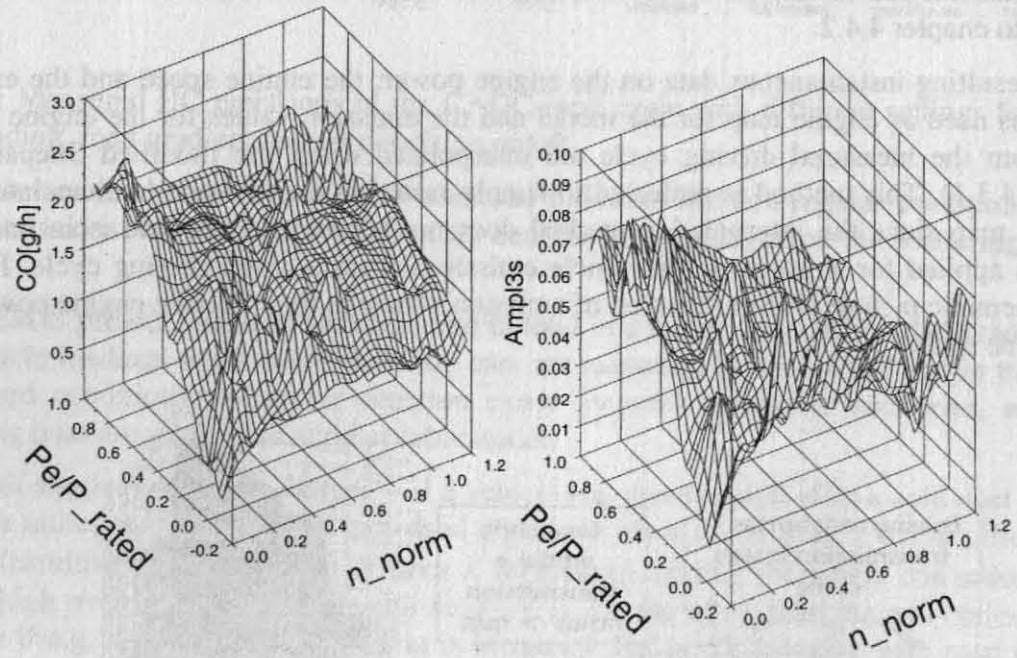

Figure 127: Engine map for CO emissions of a EURO 3 passenger car Diesel engine and corresponding engine map of one of the transient parameters ("Ampl3p3s")

Having the information on the "dynamic" of each point of the emission map stored the methodology for developing transient correction functions already described for HDV can basically be followed. An exception for passenger cars is the fact that the input into the multiple regression analysis are the differences between the transient parameter values stored in the map and the transient parameter values calculated for the driving cycle which is recalculated[17].

The model PHEM calculates the difference between the emissions simulated and the emissions measured on the roller test bed using the equations already described in chapter 4.4. The differences are again calculated as average differences over longer periods to avoid influences of time delays in the measurement chain. The time periods to be used can be given as model input

[17] For HDV simply the absolute value of the transient parameters calculated for the driving cycle were used since the engine maps for HDV are measured under steady state conditions and thus the values of the transient parameters in the engine map are zero.

and shall be at least 20 seconds. Figure 128 gives a graphical impression of the input data for the statistical analysis.

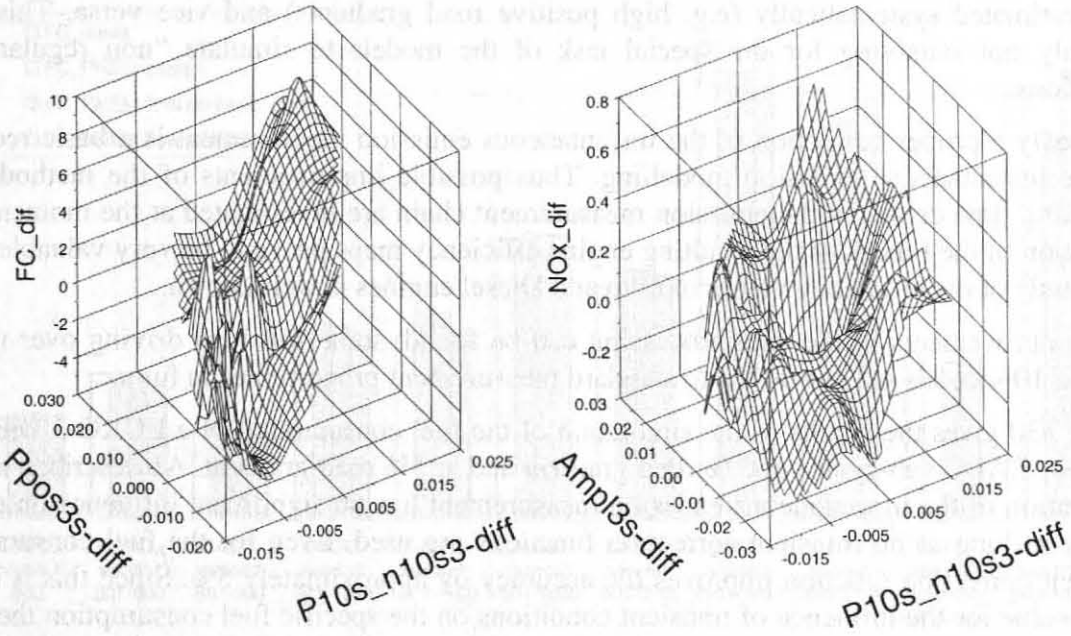

Figure 128: Schematic picture of the basic input data into the multiple regression analysis (difference between simulated and measured emissions versus the difference between the transient parameters in the engine map and in the driving cycle)

5.1.3 Accuracy of the emission simulation for passenger cars

The results achieved so far are quite good but only the first four passenger cars were investigated with this method. The main findings are:

Without application of transient correction:

- the accuracy of the emission simulation is nearly independent of the way the time delays of the instantaneous emission measurement have been taken into consideration. Using measurement signals only corrected by a constant time shift gives nearly the same results for the cycles simulated as using measurement signals corrected with variable time shifting and correction of the analysers´ time delays.

With application of transient correction functions

- The regression analysis gives results for the transient correction factors only if the engine map is gained from measurement signals corrected by variable time shifting and correction of the analysers´ time delays according to chapter 3.3.2.
- The transient correction functions improve the accuracy of the simulation significantly for most cycles.

Anyhow, looking at the engine efficiency in the engine maps, calculated from the specific fuel consumption values, one sees that even with the correction function the efficiency at high engine loads is overestimated whereas the efficiency is underestimated at low loads. This is a result of the still not perfect correction of the instantaneous emission measurement for transient cycles. Since time spans with high loads are most often very short in the standard test cycles and only occur in very transient phases of acceleration, the delay times of the analysers and the mixing in the exhaust system and the CVS have the highest influences on the results there. For short periods of driving in overrun conditions the situation changes; in this case the emissions are overestimated.

For the simulation of driving cycles where high engine loads and overrun are distributed similar to the standard test cycles from which the engine emission maps are gained the error has no influence on the accuracy of the result. But cycles where high engine loads dominate the emissions are underestimated systematically (e.g. high positive road gradients) and vice versa. This result is certainly not satisfying for the special task of the models to simulate "non regular" driving conditions.

Obviously a proper correction of the instantaneous emission measurement is a basic requirement for the instantaneous emission modelling. Thus possible improvements of the methodology for correcting time delays in the emission measurement chain are investigated at the moment. For the validation of the functions the resulting engine efficiency maps prove to be very valuable since the magnitude of the efficiency values of Otto and Diesel engines is well known.

If no improvements in the data processing can be found, some full load driving over more than approx. 10 seconds may be added to standard measurement programmes in future.

Figure 130 gives the results of the simulation of the fuel consumption of a EURO 3 Diesel car in different CADC sub-cycles at 0 % road gradient and at 5% road gradient. As described above, the preparation of the instantaneous emission measurement has no significant influence on the model quality as long as no transient correction functions are used. Even for the fuel consumption the transient correction function improves the accuracy by approximately 5%. Since this is rather the upper value for the influence of transient conditions on the specific fuel consumption the transient correction function obviously corrects parts of the remaining delay times in the instantaneous emission data as well.

This assumption results from the fact that the model accuracy is improved by the transient correction functions especially at high engine loads when the time delay of the emission measurement has the highest influence. Figure 129 summarises the average engine loads and engine speeds of the cycles simulated here.

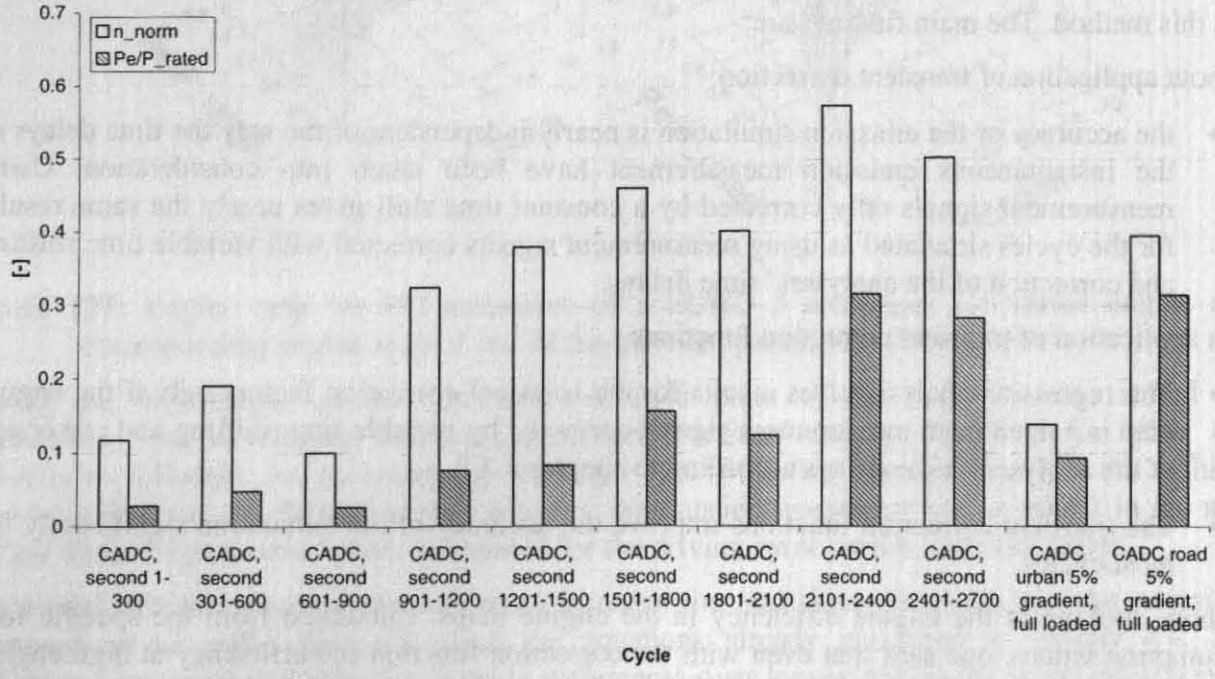

Figure 129: Average normalised engine speed and average normalised engine power demand for sub-cycles of the CADC at different road gradients and vehicle loadings

The simulation of emissions and fuel consumption reaches a high accuracy despite of the problems at high engine loads up to 5% road gradient and full loaded vehicles if the engine emission maps

are gained from the standard measurement programme (0 % road gradient, 90 kg loading). The higher the road gradient the higher is the inaccuracy.

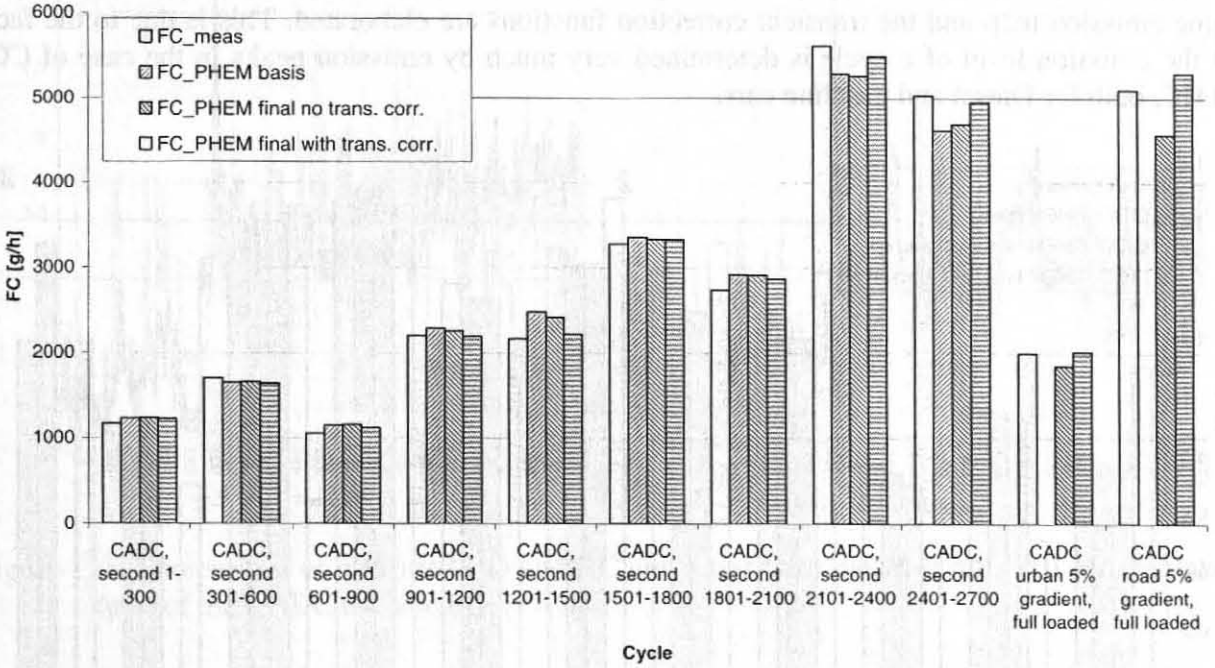

Figure 130: Comparison of measured fuel consumption with model results using different methods for the preparation of the instantaneous emission measurement (basis: constant time shift of the instantaneous data, final: variable time shift of the instantaneous data + correction of analysers´ respond time)

For NO_x emissions the accuracy is similar to the one for the fuel consumption (Figure 131). Also the trends for the improvements of the transient correction function are comparable.

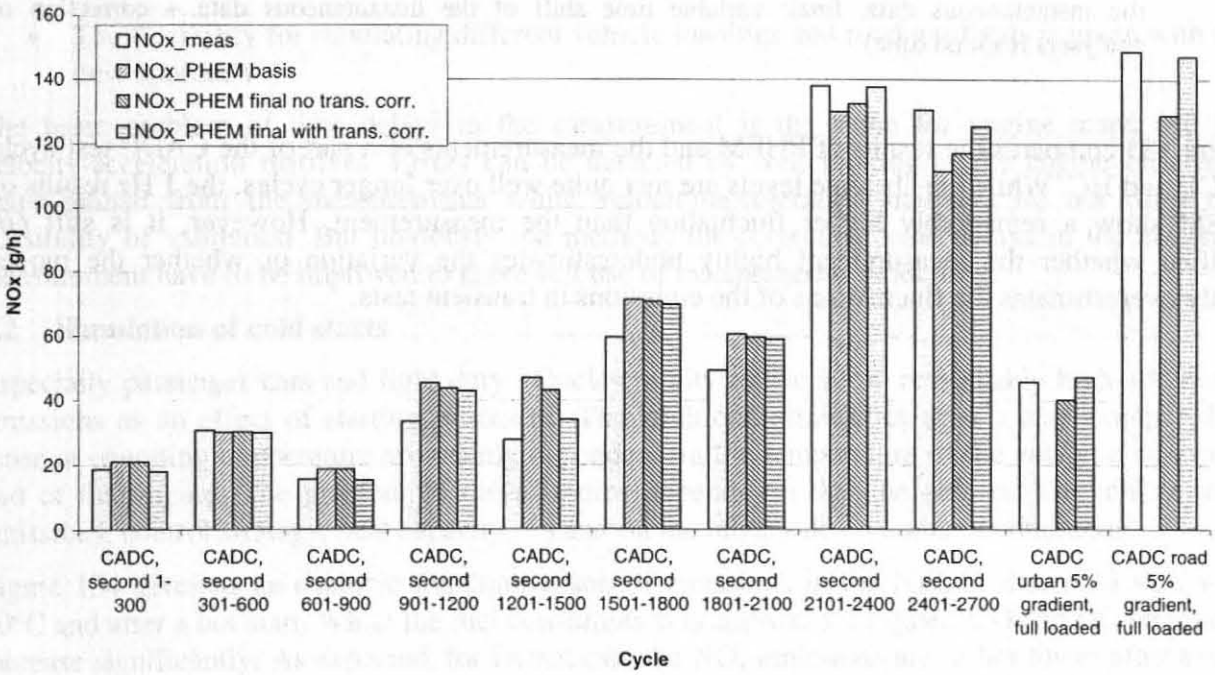

Figure 131: Comparison of measured NO_x emissions with model results using different methods for the preparation of the instantaneous emission measurement (basis: constant time shift of the instantaneous data, final: variable time shift of the instantaneous data + correction of analysers respond time)

As expected, the accuracy for simulating CO and HC emissions is lower than for NO_x emissions but still reaches a good level for most cycles. A correct time shifting of the instantaneous measurements is much more relevant for HC and CO than for the fuel consumption when the engine emission map and the transient correction functions are elaborated. This is due to the fact that the emission level of a cycle is determined very much by emission peaks in the case of CO and HC, both for Diesel and gasoline cars.

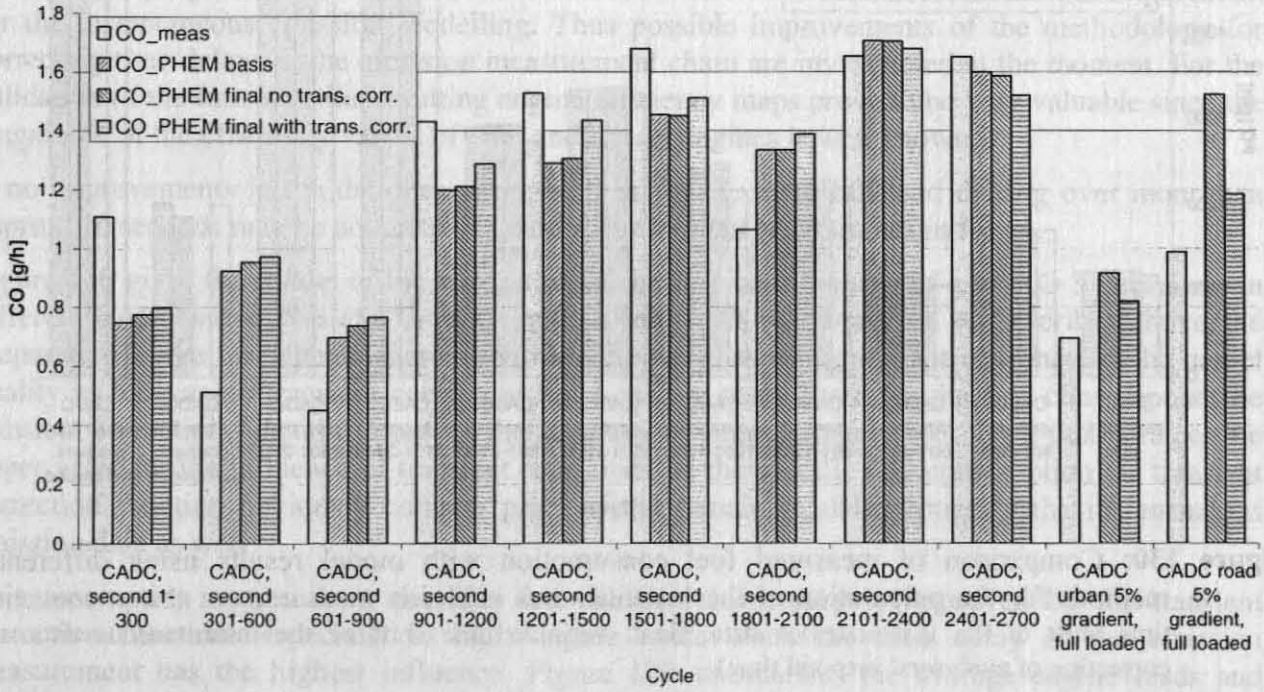

Figure 132: Comparison of measured CO emissions with model results using different methods for the preparation of the instantaneous emission measurement (basis: constant time shift of the instantaneous data, final: variable time shift of the instantaneous data + correction of analysers respond time)

Figure 133 compares the results of PHEM and the measurements of a part of the CADC test cycle for CO and HC. While the absolute levels are met quite well over longer cycles, the 1 Hz results of PHEM show a remarkably higher fluctuation than the measurement. However, it is still not clarified whether the measurement highly underestimates the variation or whether the model highly overestimates the fluctuations of the emissions in transient tests.

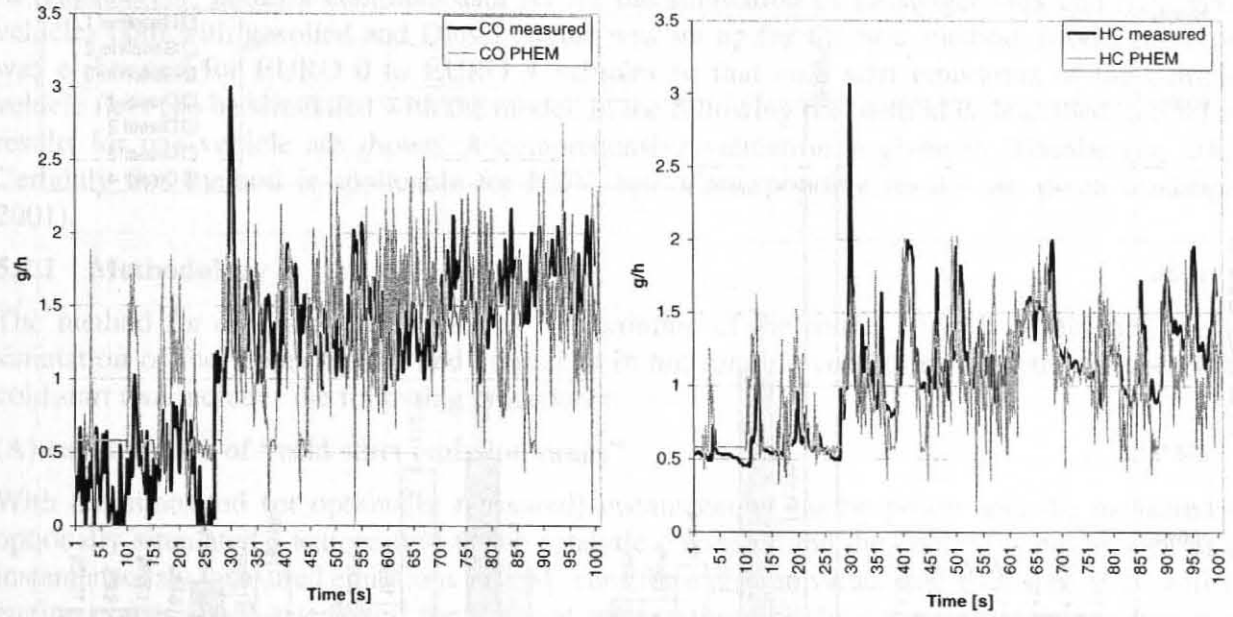

Figure 133: Comparison of measured CO and HC emissions with model results in 1 Hz resolution (part of the CADC test cycle)

In general, the new approach followed here shows many advantages against the established instantaneous models which are based on a velocity-acceleration matrix:

- Transient correction functions can be established which increase the accuracy
- A limited set of basic measurements fills an engine map approximately fife times better than a velocity-acceleration matrix since the contribution of each gear is the same in the engine map whereas different gears cover different velocities
- The flexibility for simulating different vehicle loadings and road gradients is given with the new approach

The basic problem of time delays in the measurement is the same for engine maps and for velocity-acceleration matrixes. Errors can be detected by well looking at the engine efficiency maps gained from the measurements while velocity-acceleration matrixes do not offer this possibility of validation. But obviously the methods for correcting time delays in the emission measurement have to be improved to make full use of instantaneous modelling.

5.2 Simulation of cold starts

Especially passenger cars and light duty vehicles in city traffic show remarkably high additional emissions as an effect of starting processes. The additional emissions after a start compared to those at operating temperature are mainly dependent on the temperature of the catalytic converter and of the engine. The gradient of these figures depends on the one side on the vehicle (raw emissions, control strategy, heat capacity, ...) and on the other side on ambient conditions.

Figure 134 gives as an example the comparison of emissions in the NEDC after cold start with 20°C and after a hot start. While the fuel consumption is approx. 8% higher, CO and HC emissions increase significantly. As expected, for Diesel cars the NO_x emissions are rather lower after a cold start. It has to be pointed out that the high, relative increase in the emission levels after cold starts results very much from the very low emission levels at hot running conditions.

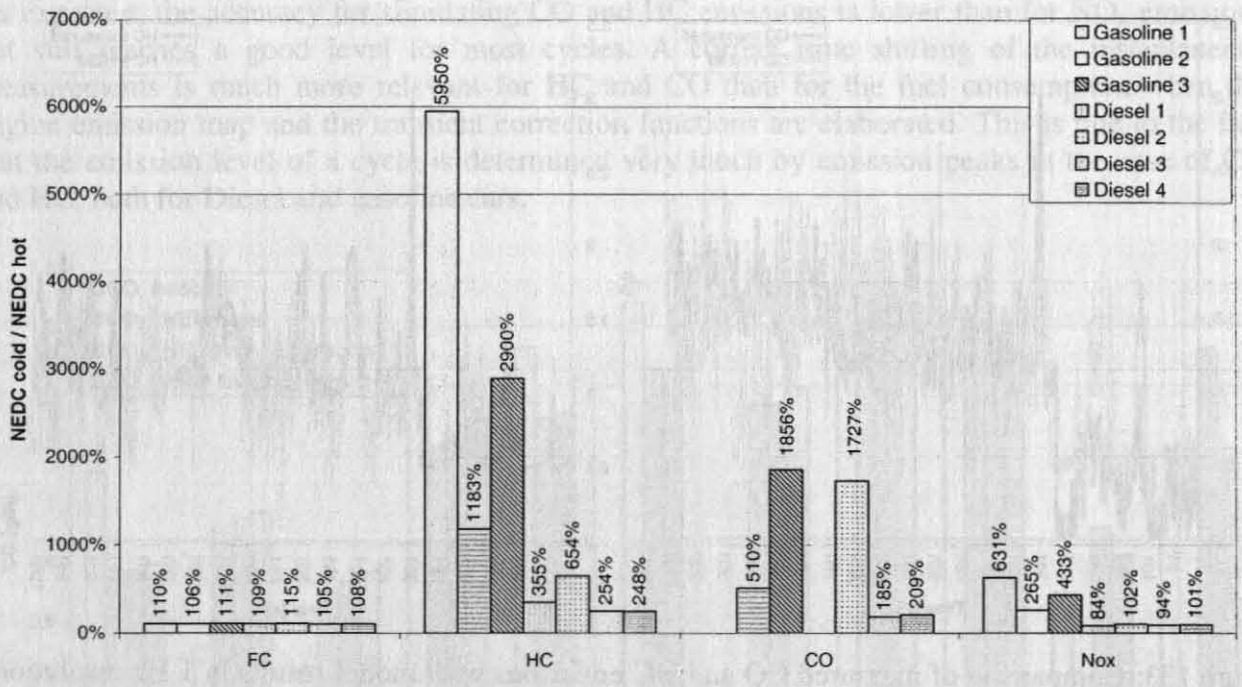

Figure 134: Measured ratios between fuel consumption and emissions after a cold start at 20°C compared to a hot start in the NEDC

From the ambient conditions the following values are most important:

- ambient temperature before the start
- switching-off time before the start
- driving cycle followed after the start and length of the journey

Depending on these figures, the ratio between emissions in cold and hot running conditions may differ significantly from the measurements in the NEDC. Thus the use of simple empirical "cold start factors", which give either average ratios from cold start to hot start emissions or the difference between cold start and hot start emissions, can lead to completely wrong results. Anyhow, existing inventory models use such cold start factors. Adding a set of additional correction factors for the ambient temperature, switching-off time, the driving cycle and the duration of the cycle can improve the accuracy.

In a study for Volkswagen AG a cold start emission model based on a heat balance was constructed (Hausberger, 2002) and (Nagel, 2001). This model simulates the temperature levels of the coolant and the catalytic converter and calculates the emissions and the fuel consumption of an engine not at operating temperature dependent on these temperatures.

To keep the simulation for the calculation of the fleet emissions at a reasonable state simplifications were chosen in order to have the general applicability and the accuracy for the simulation of vehicle fleets in real world traffic. The method developed was verified by making detailed measurements with three passenger cars and one light goods vehicle. It proves to have a good accuracy when simulating different driving conditions. Other models for the simulation of cold start emissions in real road traffic with comparable flexibility and accuracy are not named.

Compared to the use of cold start factors and several correction factors the model developed should give more generally valid results. It especially reduces the number of cold starts to be measured since basically one measured cold start cycle per vehicle is enough to establish the necessary model input data.

In (Hausberger, 2002) a complete data set for the simulation of passenger cars and light goods vehicles both with gasoline and Diesel engine was set up for the new method. Model input data was elaborated for EURO 0 to EURO 4 vehicles so that cold start emissions of the complete vehicle fleet can be simulated with the model. In the following the method is described in brief and results for one vehicle are shown. A comprehensive validation is given in (Hausberger, 2002). Certainly this method is applicable for HDV, too. Corresponding results are given in (Engler, 2001).

5.2.1 Methodology

The method for cold start simulation is a subroutine of the model PHEM. Additionally to the simulation of fuel consumption and emissions in hot running conditions (chapter 4.4 and 4) the cold start tool includes the following procedures:

(A) construction of "cold start emission maps"

With the simulated (or optionally measured) instantaneous engine power and the measured (or optionally simulated) temperature of the catalytic converter and the cooling water as well as the instantaneously measured emissions PHEM scans the emission values into cold start maps with the engine power (Pe/P_rated) and the relevant temperature (catalytic converter and cooling water respectively). Scan format and time intervals for the averaging of measurements can be chosen freely. Analogous to that a polygon is calculated for the warm-up behaviour of the catalytic converter and the cooling water over the cumulated "heat flow losses".

(B) simulation of cold start emissions

For the simulation of cold start emissions in a given driving cycle the temperatures of the catalytic converter and of the coolant are calculated as function of the "heat flow losses". The fuel consumption and emissions are then gained from the cold start maps as function of the simulated actual engine power and temperature levels.

The following gives an overview of this method and the results achieved so far.

5.2.2 Basics

Basic assumption is that the emissions after a cold start can be shown with the help of the relevant temperature of the components and the effective engine power:

Equation 1: general assumption of the simulation of cold start emissions

$$E_{cold} = E_{warm} + F(T_{coolant}, T_{oil}, T_{cat}, Pe)$$

with: E_{cold} ..... Emissions before the operating temperature is reached [g/h]

E_{warm} ..... Emissions at operating temperature [g/h]

T ..... Temperature of cooling water and catalytic converter [°C]

Including the temperature of the engine oil did not prove to be of any help in this given model. The engine speed has a clear influence on the emission behaviour. However, it was not included in order to get by on a 3-dimensional engine emission map.

5.2.3 Simulation of relevant temperature of the components

A detailed heat balance for the calculation of the relevant temperatures was taken as the basis for the development of the simulation method (Figure 135). Heat source is the input fuel energy (Hu, net calorific value) as well as an exothermic reaction in the catalytic converter as soon as that one is at cut-off temperature. The input heat energy is partly transported as indicated work of the

engine, as exhaust gas enthalpy as well as via the cooling water and engine oil. During the transient state a part of the energy input is used for the warm-up of the components.

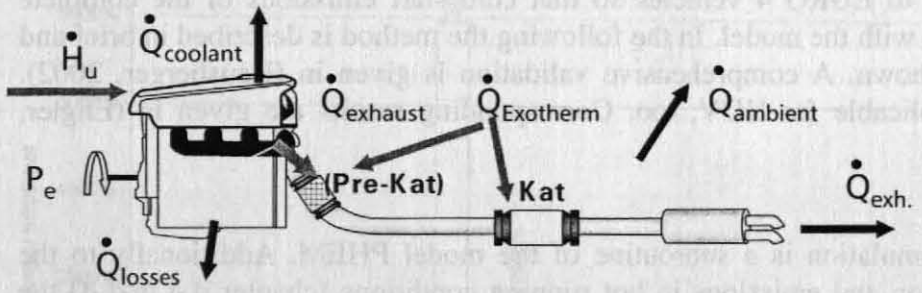

Figure 135: scheme of the heat balance of engine and exhaust gas system

The heat balance is shown in the following:

$$\dot{H}_u - Pe = \dot{Q}_{exhaust} + \dot{Q}_{coolant} + \dot{Q}_{amb} + \sum A_i \times m_i \times c_i \times \frac{dT_i}{dt}$$

with: $\dot{H}_u$ ..... net calorific value of the fuel consumption per second

P_e ..... effective engine power output

$\dot{Q}_{exhaust}$ .. heat flow of the exhaust gas

$\dot{Q}_{coolant}$ .. heat loss to the cooling water

$\dot{Q}_{amb}$ ..... heat loss to the ambiance

$\frac{dT_i}{dt}_i$ ..... differential temperature change (in this case per second) of the component i

m_i ..... mass of the component i

c_i ..... specific heat capacity of the component i

A_i..... share of the entire heat flow which is added to the part i

To be able to solve this equation a number of parameters has to be defined (specific heat capacities of the components, coefficients of heat transfer, ...). This makes a complex collection of data necessary which cannot be realized in the simulation of vehicle fleets. Additionally, the calculation of the heat flow into the cooling water, the lube oil and to the ambiance turns out to be a serious problem and includes a certain percentage of inaccurateness. Thus, a simplified method was developed which is described subsequently.

5.2.4 Simulation of the warm-up of the catalytic converter and cooling water

For the calculation of emission factors the heat balance was simplified extremely without changing the basic physical interrelations. We simplified it to the extent that the total heat which is dissipated from the combustion chamber is split to the different parts with shares being independent of the operating state of the engine.

With this simplification the warm-up of the component gets a universally valid and empirically ascertainable function of the cumulated "heat flow loss" (Hu-P_e).

equation 2: simplified heat balance

$$T_i = F_1\left(\int_{t=0}^{i}(\dot{H}u_i - Pe_i)dt\right) - F_2\left[\int_{t=0}^{i}\dot{Q}_{amb}dt\right]$$

with: T_i ..... temperature of a component i seconds after the start

$(\dot{H}u_i - Pe_i)$ .... difference of the lower heat value of the actually consumed fuel and the effective engine power ("heat flow loss", Q_{loss})

$\dot{Q}_{amb}$ ..... heat flow from the respective part to the ambiance (only relevant in case of high temperature of catalytic converter, long idle running or motoring, is not taken into account in the performed model).

Q_{amb} can be neglected in nearly all driving conditions without having to cope with any serious losses of accurateness. This enormously simplifies the algorithm calculation. However, the possible cooling of the catalytic converter can not be illustrated in case of phases of long idle running or motoring. In the subsequent figures the heat transmission to the ambiance is ignored.

Figure 136 shows the measured temperature of the exhaust gas of a EURO 3 passenger car with a catalytic converter in two different driving cycles. As was assumed the temperature curves during the duration of the different driving cycles were clearly different. But when the temperature is plotted over the cumulated heat flow loss, the temperature curves of the cycles are close to each other. This was the expected result of the idea of the simplified heat balance. Similar results were achieved with different driving cycles for other vehicles as well (Hausberger, 2002).

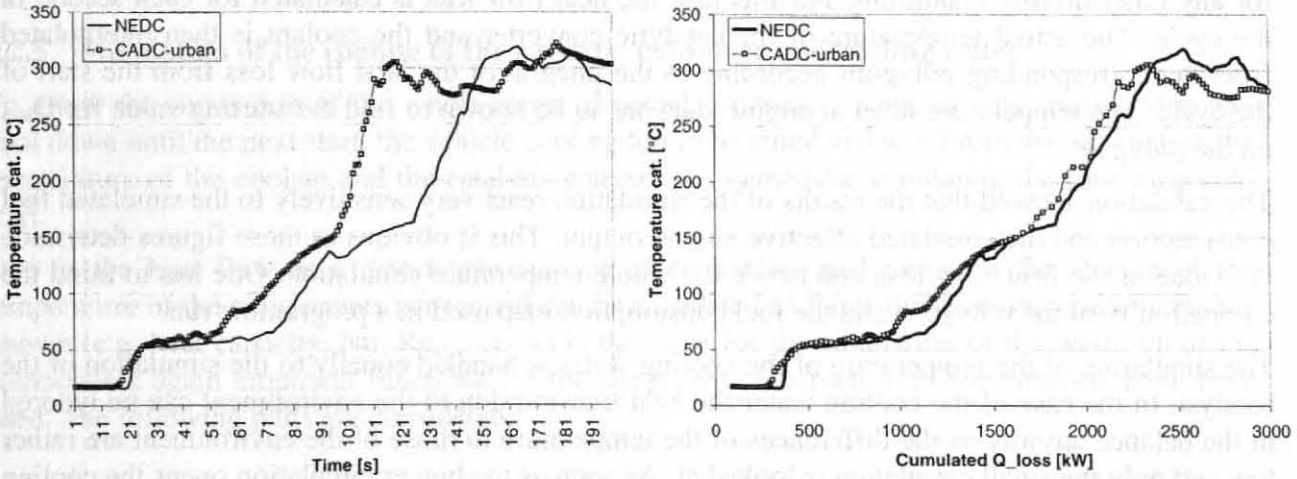

Figure 136: measured temperature curves after a catalytic converter for two driving cycles for a gasoline EURO 3 car plotted over the cycle duration and over the cumulated heat flow losses

The functionality F_1 of equation 2 is determined empirically by the measurement of a cold start on the roller test bed. F_1 simply is the average polygon for the temperature curve plotted over the cumulated heat flow losses which are shown in the right picture in Figure 136. F_1 is computed by the model from the measured fuel consumption, the measured emissions and the simulated engine power. The measurements are used with 1 Hz registered data.

The cumulated loss of heat flow on the x-axis of the polygon is rated by the division by the engine rated power of the measured vehicle. This allows to average the warm-up polygons of various passenger cars or heavy duty vehicles for assessing emission factors for vehicle fleets. Assuming that vehicles with more mass to warm up have on average proportionally higher rated engine powers and fuel consumption values this procedure is correct.

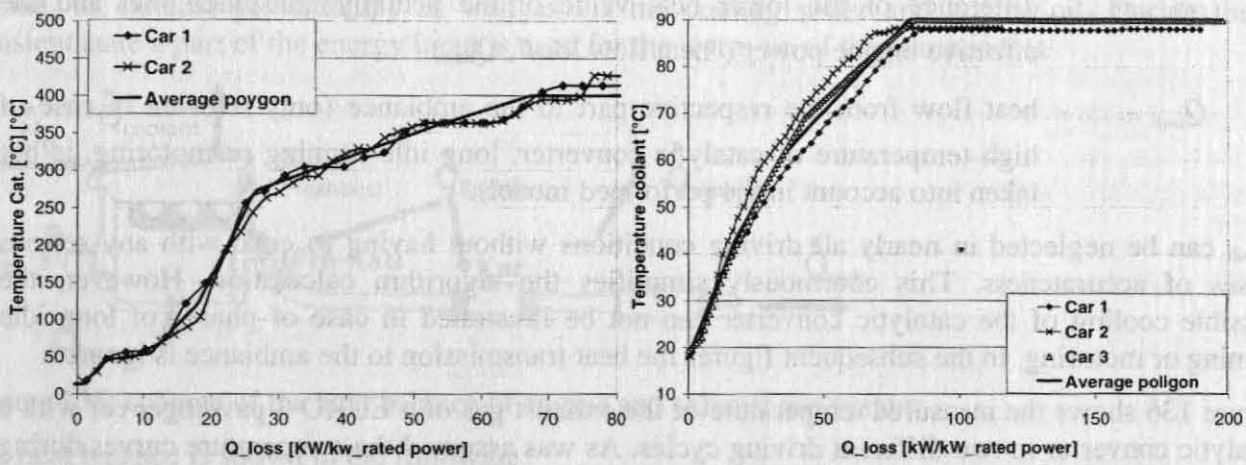

Figure 137: warm-up polygons for the catalytic converter and for the coolant computed for different cars

With these polygons the temperature of the catalytic converter and of the coolant can be calculated for any other driving conditions. For this task the heat flow loss is calculated for each second in the cycle. The actual temperature of the catalytic converter and the coolant is then interpolated from the corresponding polygons according to the integral of the heat flow loss from the start of the cycle. The temperature level at engine start has to be known to find the starting value for Q_{loss} on the polygon.

The validation showed that the results of the simulation react very sensitively to the simulated fuel consumption and the simulated effective engine output. This is obvious as these figures determine the value of the heat flow loss and hence the whole temperature simulation. One has to mind the compatibility of the polygons and the fuel consumption map used in a programme run.

The simulation of the temperature of the cooling water is handled equally to the simulation of the catalyst. In the case of the cooling water the heat transmission to the environment can be ignored in the balance anyway as the differences of the temperature to those of the environment are rather low and only the small circulation is looked at. As soon as the bigger circulation opens the cooling water is at operating temperature and the cold start is finished by definition.

Figure 138 compares the measured and simulated temperatures of the catalytic converter and of the coolant. All cycles can be simulated satisfactorily. One has to keep in mind that the demonstrated calculation only gives useful results up to the point when the catalytic converter is at operating temperature (about 300°C). When the catalytic converter reaches a higher temperature the temperature of the exhaust gas before the catalytic converter has a non-negligible influence on the heat transmission as the temperature of the catalytic converter then gets to the temperature range of the exhaust gas. E.g. there is no heat transmission to the catalytic converter in spite of the enthalpy of the gas when the temperature of the exhaust gas is lower than the one of the catalytic converter. This is not relevant at all for the simulation of the cold-start emissions as there are no cold-start emissions when the catalytic converter is at operating temperature.

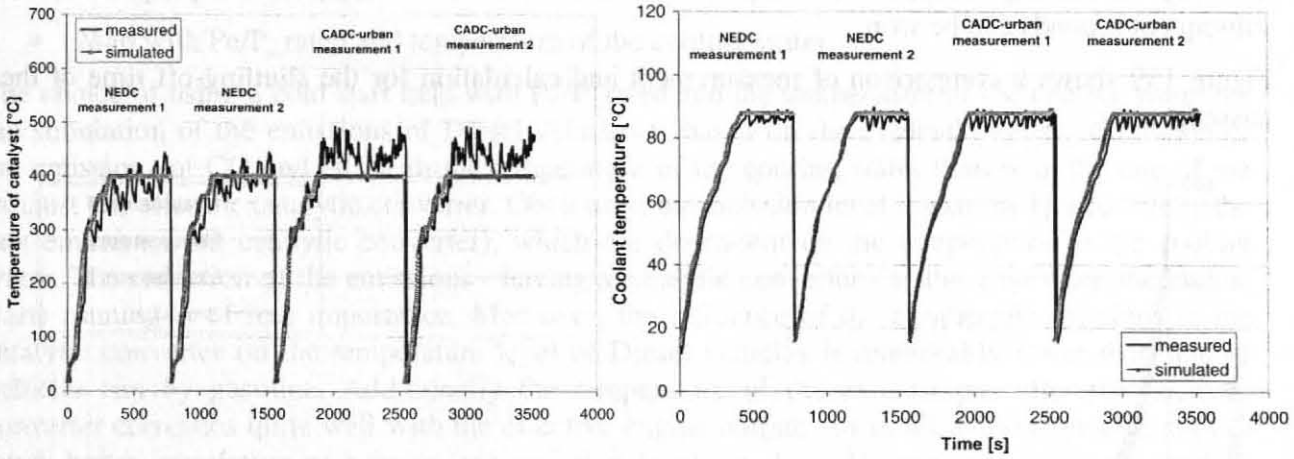

Figure 138: measured and simulated temperature curves of the exhaust gas after catalytic converter and for the coolant for an EURO 3 gasoline car for two driving cycles (2 repetitions each, only the warm-up phase is illustrated)

5.2.5 Simulation of the cooling of the catalytic converter and cooling water

To allow the simulation of the whole chain of vehicle operation, start, driving, engine stop and cool down until the next start, the vehicle cooling has to be simulated too. From this simulation the temperature of the coolant and the catalytic converter is gained for simulating the following cold start.

Due to the heat flow as a direct consequence of convection and radiation the change of the temperature of the components per second can be calculated as far as the necessary parameters are known (e.g. heat capacity, Nu, Re, ….). As is the same for the simulation of the warm-up of the components again empirical functions for the simplified construction of the function have been used. The following parts are considered:

convection: $A \times (T_i - T_{u,i})$

radiation: $B \times (T_i^4 - T^4{}_{u,i})$

with: T_i ..... temperature of the component at the second i

$T_{u,i}$ ..... ambient temperature at second i

A,B ..... factors for the adaptation of the measured values

We hence get the temperature gradient per second:

$$\Delta T_{(i)} = A \times (T_{(i-1)} - T_u) + B \times (T_{(i-1)}{}^4 - T_{u,i}{}^4)$$

with $\Delta T_{(i)}$ ..... decrease of temperature per second [°C]

$T_{n.(i)}$ ..... temperature (cooling water or catalytic converter) in second i

$T_{u,i}$ ..... ambient temperature at second i

The factors A and B are determined by means of regression analysis of measured cooling procedures.

The cooling procedure proves to be quite well ascertainable. In cases of high temperatures radiation dominates; the radiation is the fourth to the power of the current temperature. When

knowing the starting temperature (temperature when motor is shut off) the temperature for all subsequent seconds can be won.

Figure 139 shows a comparison of measurement and calculation for the shutting-off time of the passenger car.

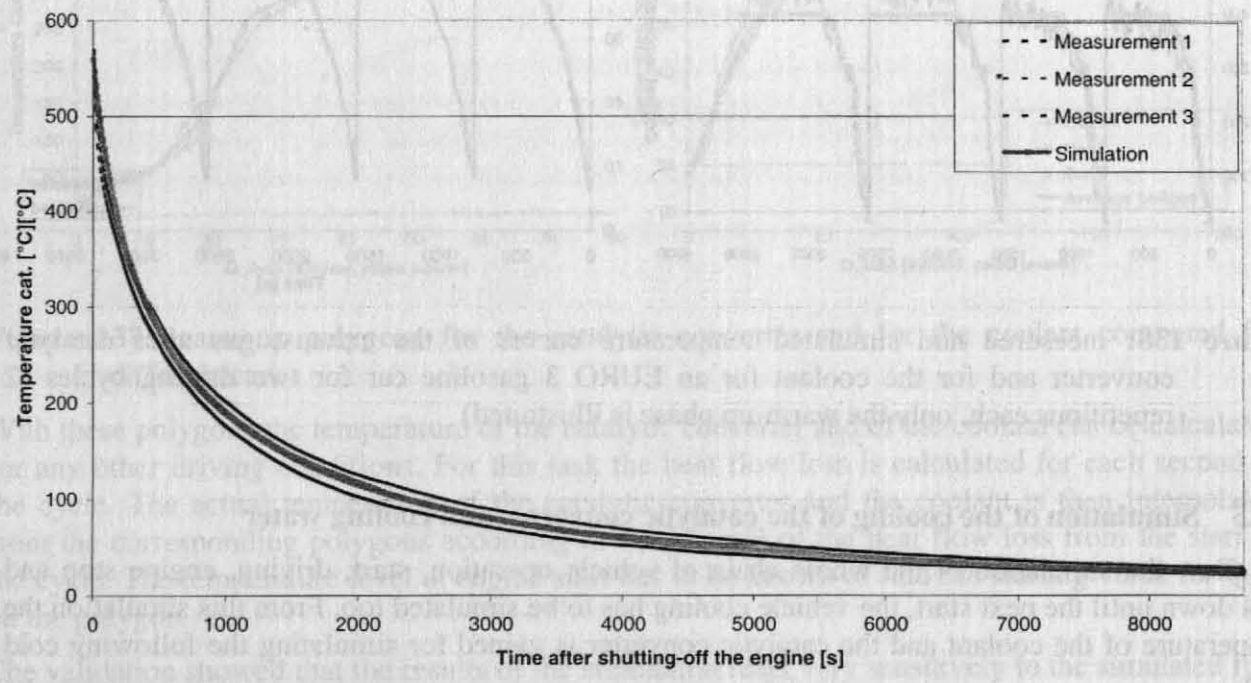

Figure 139: measured and simulated temperatures after catalytic converter when engine is shut off

As the wind velocity during the measurement campaign was rather low we cannot make a quantitative statement on the dependency on the wind velocity. The physical background however strongly implements that the convection constants adopt higher values in case of rising wind velocity and therefore induce rapid cooling.

5.2.6 Calculation of the cold-start emissions

The cohesion between the temperature of the components and the cold-start emissions is described by cold-start maps. This method proved to be efficient indeed and has the advantage that simply average cold start maps can be gained for vehicle classes.

The cold start maps are interpolated from the instantaneously measured fuel consumption and emission values after the cold start according to the actual engine power and the actual temperature of the catalytic converter and accordingly the cooling water during the cycle. The interpolation is using the modified Shepard method. This method was already described in chapter 4.4.3.1 but for cold start maps no exceptions in the routine have to be made at low engine power values.

The toxic emissions of passenger cars are relatively independent from the engine output as the homologation limits the emissions per kilometre. Thus the CO, HC, NO_x and particle emissions are left as the units [g/h] in the cold start maps for passenger cars. The fuel consumption values are rated by division by the rated engine power to make the maps of vehicles with different rated engine power comparable.

For the simulation the following kinds of cold start maps are used:

CO, HC, NO_x for gasoline passenger cars with a catalytic converter:

- Map with Pe/P_rated and temperature of the catalytic converter

Fuel consumption for Otto and Diesel as well as emissions of Diesel

- Map with Pe/P_rated and temperature of the cooling water

The choice of using a cold start map with Pe/P_rated and the temperature of the cooling water for the simulation of the emissions of Diesel-vehicles is based on the evidently better correlation of the emissions of CO and HC with the temperature of the cooling water than with the one of the exhaust gas after the catalytic converter. Obviously, the emission level is extremely affected by the raw emissions (no catalytic converter), which are dependent on the temperature of the cooling water. The reduction of the emissions - having a catalytic converter - at the time when the engine starts running is of less importance. Moreover, the influence of the exothermic reactions in the catalytic converter on the temperature level of Diesel vehicles is remarkably lower than that of vehicles run by gasoline. Additionally the temperature of the exhaust gas after the catalytic converter correlates quite well with the effective engine output. All in all, Diesel-vehicles show a much better correlation of exhaust gas emission levels in the cold start map using the cooling water than in the one using the catalytic converter. The scattering in the HC emission level in Figure 140 mainly results from the variable engine power and thus is explained by the cold start map.

Naturally, the influence of the temperature of the catalytic converter is exceedingly low in the NO_x- emissions of Diesel-vehicles.

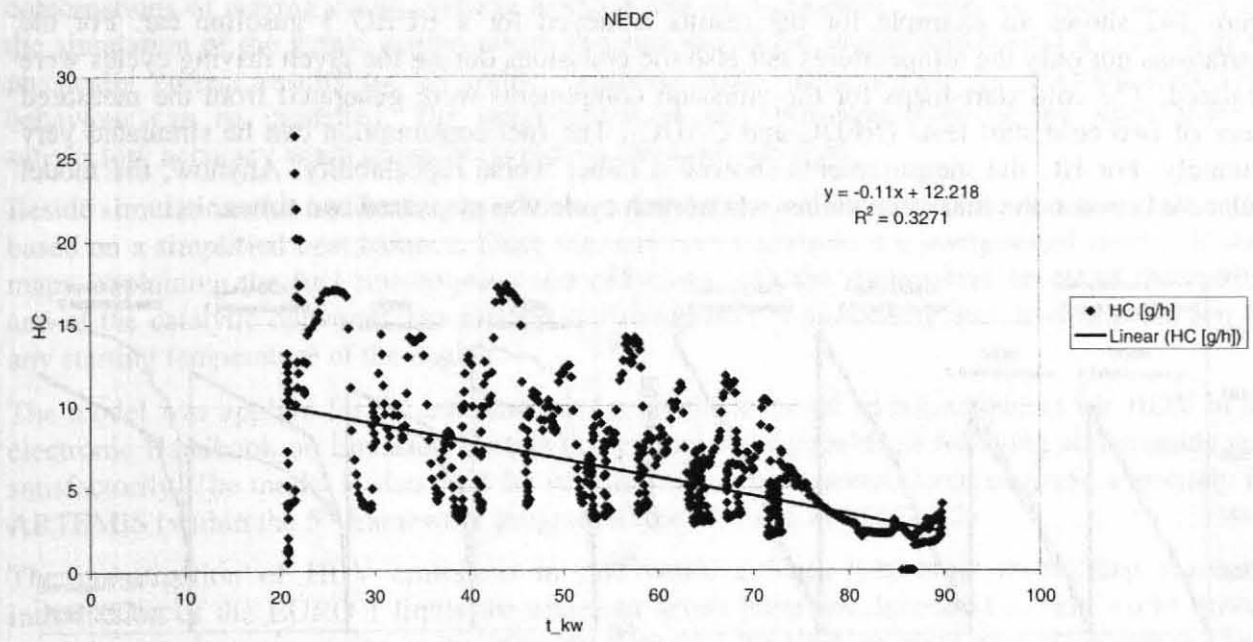

Figure 140: measured HC-emissions of a Diesel car with a catalytic converter, plotted over the actual temperature of the cooling water.

Figure 141 for example shows the cold start maps for fuel consumption and HC from a EURO 3 gasoline car. While the level of the specific fuel consumption is determined mainly by the engine power and decreases only slightly when the temperature of the coolant rises, the HC emissions are mainly a function of the temperature of the catalytic converter and drop near to zero when the operating temperature is reached.

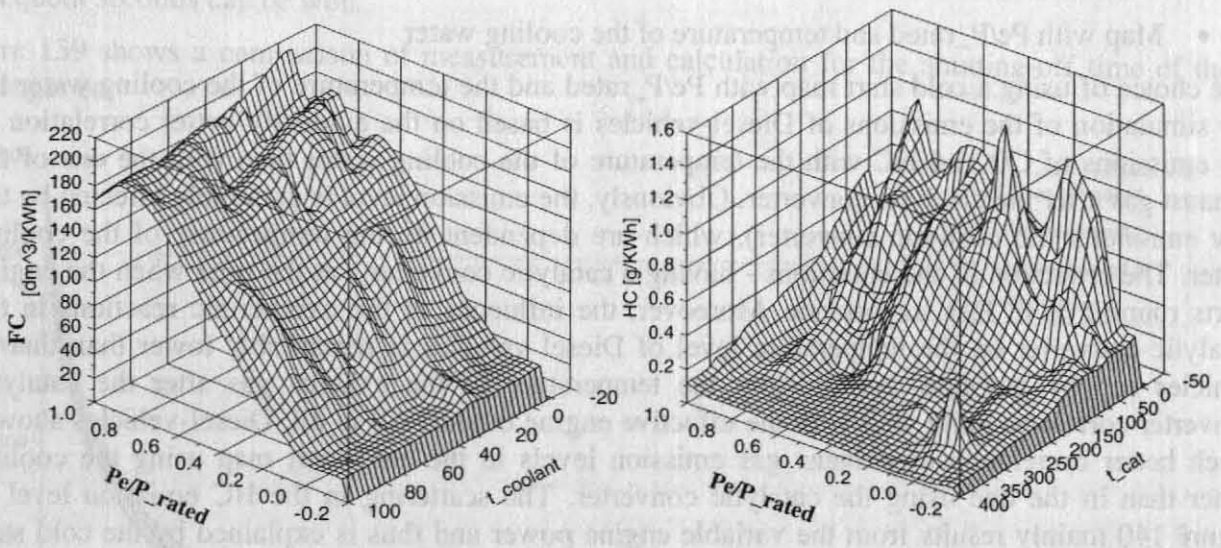

Figure 141: cold start map for the fuel consumption and for HC for a EURO 3 gasoline car

Figure 142 shows an example for the results achieved for a EURO 3 gasoline car. For the illustrations not only the temperatures but also the emissions during the given driving cycles were simulated. The cold start maps for the emission components were generated from the measured values of two cold start tests (NEDC and CADC). The fuel consumption can be simulated very accurately. For HC the measurements showed a rather worse repeatability. Anyhow, the model results are between the measured values where each cycle was measured two times.

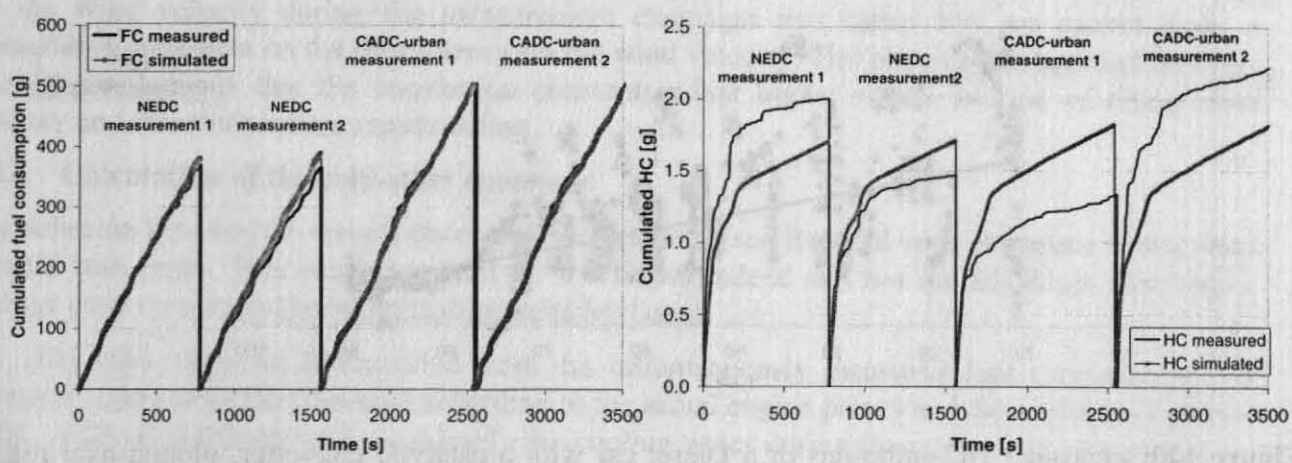

Figure 142: measured and simulated fuel consumption and HC-emissions of a EURO 3 gasoline car for two driving cycles (2 repetitions each, illustrated only in warm-up phase)

Results for NO_x and CO as well as results for other vehicles are given in (Hausberger, 2002). As a matter of principle, one can argue that the cold-start emissions of Diesel-vehicles can be more accurately simulated than of those of gasoline vehicles.

A general result is the fact that the NEDC is overvalued in the simulation when the cold start maps are won from the measured data of all cycles whereas the others are rather undervalued. When the cold start maps are only gained from the measured data of the NEDC the NEDC is reproduced very well indeed, the other cycles are however reproduced rather bad. Reasons for that may be the

different rules for gear shifts in the NEDC and real world driving cycles like the CADC[18] and the varying driving dynamics (especially concerning CO, HC) as neither the engine speed nor the cycle dynamics have been included in the model yet. To apply the method of transient correction functions (chapter 5.1.2) to the simulation of cold start emissions may be helpful. Adding the engine speed into the cold start map is no problem from the view of programming but the rather short period of cold conditions in a test cycle limits the available data of measurements. Thus, using a four dimensional cold start map may not have sufficient measured data in order to give reliable results.

6 Summary and Conclusions

The paper presented a survey of methods for measuring and simulating vehicle emissions in real world driving conditions. As a result of the increased complexity of electronic engine control systems where the application has a high influence on the emission behaviour of the vehicles the established models become increasingly inaccurate.

At our institute a new approach for modelling vehicle emissions was developed to achieve a better accuracy combined with a high flexibility of the model for simulating any driving condition with a limited demand of measurements. The resulting model PHEM (Passenger car and Heavy duty vehicle Emission Model) is capable of simulating fuel consumption and emissions for all possible combinations of driving cycles, vehicle loadings and road gradients. Since the model is based on the simulation of the actual engine power demand and of the engine speed over a cycle it gives physically correct results for all traffic situations where even effects of different gear shift behaviour can be modelled. The interpolation of the emissions from engine maps gives a satisfactory accuracy when transient correction functions are used.

Beside simulations for hot running conditions a simulation tool for cold starts was also elaborated; based on a simplified heat balance. Since the cold start emissions are interpolated from cold start maps, explaining the fuel consumption and emissions with the temperature levels of the coolant and of the catalytic converter, the method is also capable of simulating any driving condition for any starting temperature of the engine.

The model was applied for the calculation of a complete set of emission factors for HDV in the electronic Handbook on Emission Factors and proved to be capable of fulfilling all demands very satisfactorily. The model is also used for several national and international projects, especially for ARTEMIS (within the 5th framework program of the EU) and in COST 346.

The investigation of HDV emissions in real world driving behaviour shows that since the introduction of the EURO 1 limits the emission levels have not decreased in real world driving conditions to the same extent as the emission limits for the type approval have been reduced (e.g. Figure E1). Main reasons are found in the more sophisticated technologies for engine control and fuel injection. On the one hand these modern technologies are a prerequisite for reducing the environmental impacts of HDV engines, on the other hand they give freedom for different specific optimisations at different regions of the engine map. Since fuel costs are a main factor for the competitiveness of HDV engines, manufacturers optimise the engines towards high fuel efficiencies wherever possible. That affects especially the NO_x emission levels. The steady state tests at the type approval can thus not ensure low emission levels for real world driving conditions. This was mainly found for EURO 2 engines tested with the R 49 steady state cycle while the European Stationary Cycle (ESC) valid for EURO 3 engines improves the situation. But still a broad range of the engine map is not controlled sufficiently.

---

[18] The gear shift rules of the NEDC give clearly lower average engine speeds than e.g. the rules for the FTP or CADC

Additionally, the EURO 1 engines measured were on average already close to the NO_x emission limits for EURO 2 engines (Figure E1). Increased NO_x emission levels outside of the R 49 test cycle of many EURO 2 engines lead to the result that their emissions in real world driving are higher than the emissions of EURO 1 engines. For particulate matter (PM) clear reductions were achieved from pre EURO to EURO 1 and from EURO 1 to EURO 2. The EURO 3 engines tested are very close to the emission limit and thus show similar emission levels as EURO 2 engines in real world driving, although the drop of the emission limits was 33 %. Anyway, it has to be pointed out that the sample of measured EURO 3 engines covers four engines only and that these engines belong to the first generation of EURO 3 engines.

For the future technologies (EURO 4 and EURO 5 engines) the European Transient Cycle (ETC) will be mandatory. This shall further improve the agreement between the emission levels achieved in the type approval test and achieved in real world driving. For setting up the emission factors it was assumed that these engines will be driven mainly in the range of the engine map controlled by the ETC. Whether this goal will be reached without additional regulations is to be checked in future since the engine speeds tested in the ETC depend on the full load curve of the tested engine.

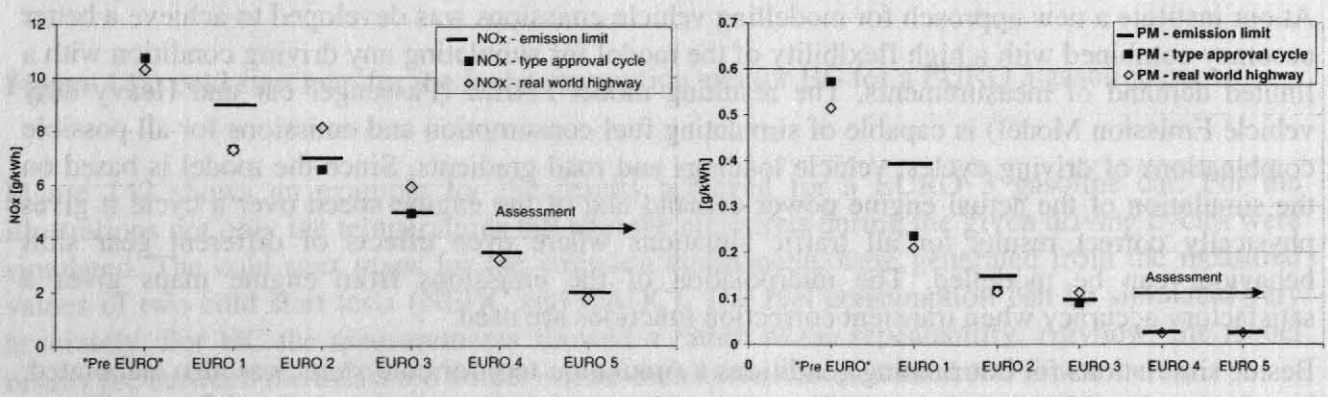

Figure E1: Development of the emission limits, the emission levels measured on average in the corresponding test cycles and the emissions simulated for real world highway driving

The work performed gave a lot of new insight into the emission behaviour of modern HDV and the technical background. The assessments are based on the broadest data base on measurements on different engines available in Europe. Beside the resulting update of the emission factors the study indicates the necessity to adapt the type approval test procedures to the technologies of actual and future HDV engines. The regulations up to EURO 3 are not suitable for the guarantee of reductions in the real world emission levels equivalent to the decrease of the type approval limits and also hindered a higher fuel efficiency of the engines. The ETC (European Transient Test Cycle), mandatory for all engines from EURO 4 onwards, shall improve the situation but leaves open gaps as well.

One of the next main steps will be to finalise the development of the methods and input data sets for the simulation of passenger cars. The results achieved so far on this task look very promising.

Most likely also this already very complex model will not be a final solution for the emission simulation of vehicles. The emission modelling will have to go in line with the increasing complexity of the engines and exhaust gas after treatment systems to keep a sufficient accuracy and to be able to give sound explanations for the results.

Literature

André M.: Design of an harmonised and common ARTEMIS test procedure; project document within the 5th EC Framework project ARTEMIS; INRETS, France 2000

Engler D., Hausberger S., Blassnegger J.: Cold start emissions of Heavy Duty Vehicles; ICE Conference proceedings; Sept. 2001

Haghofer J.: Das Digitalisierte Grazer Verfahren, Eine Methode zur Berechnung des Treibstoffverbrauches und der Schadstoffemissionen aus dem Geschwindigkeitsverlauf (*DGV, a method for the calculation of fuel consumption and emission from the vehicle speed curve*); Dissertation am Institut für Verbrennungskraftmaschinen und Thermodynamik der TU-Graz; Graz 1982

Hausberger S: Emissionen des Verkehrs im Bundesgebiet Österreich für die Bezugsjahre 1980 bis 2001 (*Emissions of the Transport Sector in Austria from 1980 to 2001*); Yearly reports to the Umweltbundesamt-Austria; Graz, Vienna; Jan. 2003

Hausberger S. et.al.: Update of the Emission Functions for Heavy Duty Vehicles in the Handbook Emission Factors for Road Traffic; Institute for Internal Combustion Engines and Thermodynamics; Graz December 2002-3

Hausberger S. et.al.: Simulation of Cold Start Emissions from Passenger Vars and Light Duty Vehicles; ; Institute for Internal Combustion Engines and Thermodynamics – VW-AG; Graz-Wolfsburg October 2002-2

Hausberger S. et.al.: Emission Factors for HDV and Validation by Tunnel Measurements; 11th International Symposium on Transport and Air Pollution; Report of the Institute for Internal Combustion Engines and Thermodynamics Volume 81; ISBN 3-901351-59-0; Conference Proceedings Volume I; page 93-100 ; Graz 2002-1

Hausberger S., Ivanisin M. Riemersma I.: Modelling transient Influences on HDV Emissions; ICE Conference proceedings; Sept. 2001

Hausberger S. et.al.: Emissionen des Off-Road-Verkehrs im Bundesgebiet Österreich für die Bezugsjahre 1990 bis 1999 (*Emissions from the off-road –sector in Austria from 1990 to 1999*); Report to the UBA; Graz; December 2000

Hausberger S: Scenarios for the Future Energy Demand and CO_2-Emissions from the Global Transport Sector; SAE Total Life Cycle Congress, Congress Manuscript; Graz, Dez. 1998 *(+ SAE Book of the Year 1998)*

Hausberger S, Pischinger R.: Cost Effectiveness Study on Measures to Reduce CO_2-Emissions in the Transport Sector in Austria; FISITA Congress Manuscript; Paris, Sept. 1998

Hausberger S.: Globale Modellbildung für Emissions- und Verbrauchsszenarien im Verkehrssektor (*Global Modelling of Scenarios Concerning Emission and Fuel Consumption in the Transport Sector*); Dissertation am Institut für Verbrennungskraftmaschinen und Thermodynamik der TU-Graz; Graz, 1997

Jungmeier G., Hausberger S.: Reduktion der Treibhausgas-Emissionen durch Biotreibstoffe und zukünftige Antriebssysteme; 3. Internationale Energiewirtschaftstagung "Die Zukunft der Energiewirtschaft im liberalisierten Markt, TU-Wien 12.-14. Februar 2003

Jungmeier G., Hausberger S.: Treibhausgas-Emissionen von Transportdienstleistungen mit Wasserstoff; Tagungsband Deutschr Wasserstoff-Energeitag vom 12 – 14. November 2002, Zeche Zollverein, Essen, Deutschland 2002

Jungmeier G., Hausberger S.: Treibhausgas-Emissionen von KFZ mit Bio-Treibstoffen - Ein Vergleich zu konventionellen Treibstoffen, 7. Symposium Energieinnovation in Europa, Schriftenreihe OVE Nr. 30, ISBN 3-85133-027-7, Graz Jänner 2002

Jungmeier G., Hausberger S.: Greenhouse Gas Emissions of Cars with Bio-fuels in Austria – A Comparison to Cars with Conventional Fuel, 12th Biomass Conference 17 - 21 June 2002, Amsterdam, proceedings in press

Keller M., Hausberger S. et.al.:: Handbuch Emissionsfaktoren für den Straßenverkehr in Österreich (*Guide on Emission Factors for the Street Traffic in Austria*); im Auftrag von Bundesministerium für Umwelt, Jugend und Familie und Umweltbundesamt Österreich; Wien 1998

Kohoutek P., Nagel C., Hausberger S. et.al.: Integrated Simulation of Traffic Demand, Traffic Flow, Traffic Emissions and Air Quality; 8th International Symposium on Transport and Air Pollution; Conference Manuscript; Report of the Institute for Internal Combustion Engines and Thermodynamics Volume 76; Graz 1999

Lambrecht U., et.al.: Bus, Bahn und PKW auf dem Umweltprüfstand; IFEU – Institut für Energie- und Umweltforschung Heidelberg GmbH; Heidelberg; Februar 2001

Molitor R., Thaler R., Hausberger S. et.al.: EST, OECD Projecte „Environmentally Sustainable Transport, Pilotstudie Österreich; BMLFUW, ISBN 3-902010-84-3; Vienna, 2000

Molitor R., Hausberger S., et.al.: Umweltbilanz Verkehr in Österreich (*Ecological Balance for the Transport in Austria*); im Auftrag des Bundesministeriums für Umwelt, Jugend und Familie Österreich; Wien 1997

Nagel C., Hausberger S., et.al.: Integrated Simulation of Traffic Demand, Traffic Flow, Conference on Traffic Emissions and Air Quality; Boulder; Sept. 2001

Ntziachristos L., Samaras Z., COPERT III, Computer programme to calculate emissions from road transport; Methodology and emission factors (Version 2.1); European Environmental Agency; Copenhagen, November 2000

Pischinger R., Hausberger S., Sammer G., Szenarios zum zukünftigen Energieverbrauch und den CO_2-Emissionen des weltweiten Verkehrs bis 2100 (*Scenarios for the Future Energy Demand and CO_2-Emissions from the Global Transport Sector up to 2100*); im Auftrag des Bundesministeriums für Umwelt, Jugend und Familie und Umweltbundesamt Österreich; Wien 1998

Pischinger R., Hausberger S., Sammer G., Schneider F. et al.: Volkswirtschaftliche Kosten-Wirksamkeisanalyse von Maßnahmen zur Reduktion der CO_2-Emissionen des Verkehrs in Österreich (*Cost-Effectiveness Study on Measures to Reduce CO_2-Emissions from Transport Sector in Austria*); im Auftrag des Bundesministeriums für Umwelt; Graz, Wien, Linz, 1997

Pischinger R., Haghofer J.: Eine Methode zur Berechnung des Kraftstoffverbrauches und der Schadstoffemissionen von Kraftfahrzeugen aus dem Geschwindigkeitsverlauf (A Method for Calculating the Fuel Consumption and Emissions of Vehicles Based on Driving Speed); Automobiltechnische Zeitschrift (ATZ); 86 – 10; page 433 to 436; 1984

Stahel W., De Haan P. Keller M. et.al.: Neues EMPA-Standard Messprogramm; Luftschadstoffemissionen des Strassenverkehrs, Folgearbeiten zum BUWAL-bericht SRU Nr. 255; Arbeitsunterlage 19; Zürich; Juni 2000

Sturm P.J., Hausberger S., Keller M., De Haan P.: Estimating real world emissions from passenger cars – use and limitations of instantaneous emission data; International Journal of Vehicle Design; Volume 24, No 1. 2000-05-26

UBA: Umweltbundesamt Österreich: Luftschadstoff-Trends in Österreich 1980-2000 (trends in toxic emissions in Austria 1980-2000); ISBN 3-85457-643-9; UBA GmbH; Wien 2002

Weilenmann M., et.al.: Describing and Compensating Gas Transport Dynamics for Accurate Instantaneous Emission Modelling; 11th International Symposium Transport and Air Pollution; June 2002 Graz; VKM-Mitteilungen, Volume 81; ISBN 3-901351-59-0; Graz 2002

WHO.: Transport, Environment and Health, WHO regional publications; European series; No 89, Copenhagen 2000, ISBN 92 890 1356 7 ISSN 0378-2255